Investigating the Role of Mitochondrial Respiratory Chain Activity and Mitochondrial DNA Damage in Skin Ageing

Amy Bowman

Submitted in Fulfilment of the Requirements for the Degree of Doctor of Philosophy in the Institute of Cellular Medicine, Newcastle University

2014

Abstract

Ageing describes the progressive functional decline of an organism over time, leading to an increase in susceptibility to age-related diseases and eventually to death, and it is a phenomenon observed across a wide range of organisms. Despite a vast repertoire of ageing studies performed over the past century, the exact causes of ageing remain unknown. For over 50 years it has been speculated that mitochondria play a key role in the ageing process, due mainly to correlative data showing an increase in mitochondrial dysfunction, mitochondrial DNA (mtDNA) damage, and reactive oxygen species (ROS) with age. Therefore, a major aim of the current project was to assess mitochondrial dysfunction, in the form of complex II activity, in the skin cells of differently aged humans. Mitochondrial complex II of the electron transport chain (ETC) was chosen to be examined, as it has recently been implicated in the generation of ROS, as well as in the ageing process of lower organisms, and is the least studied complex of the ETC. Complex II activity was found in the present study to decline in an age-dependant manner in human skin fibroblast cells, which may have been partially related to an observed decrease in the expression of specific nuclear-encoded complex II subunits with age. Further investigations into the cause of the decrease in complex II activity with age revealed that the decline was specific to senescent cells, and was not present in non-senescent cells, which was determined following sorting into subpopulations via fluorescence-activated cell sorting (FACS). The decrease in activity with age was not reflected in another mitochondrial complex examined, complex IV, for which there was no alteration in activity with age for either unsorted, senescent, or non-senescent cells. This finding could suggest the specific targeting of complex II in senescent cells only for future age-related therapeutics. Interestingly, an age-dependant decrease in complex II activity was not observed for human skin keratinocytes, despite being observed in human skin fibroblasts. In the present study, it was also observed that different cell types undergo differing rates of maximal complex II activity, which could have important consequences in terms of the rate of ageing of specific cell types.

In addition to the observed decrease in mitochondrial complex II activity with age, it was demonstrated in the present study that mtDNA damage is increased with age in the skin of both humans and a taxonomic group for which age-

related changes have not been previously studied, the whales. It was confirmed that the T414G mutation, which is a general biomarker for mtDNA mutations, was higher in human skin fibroblasts from older individuals when compared to younger individuals. Furthermore, an increase in mtDNA damage with age was also found in multiple whale species, for which mtDNA damage was measured in the form of strand breaks within a large region of the mitochondrial genome, using novel primers designed and optimised through the present study. Whales from three distinct species were chosen to be examined based on their differing levels of UV exposure, as a model for different ages. It was found that the level of mtDNA damage increased with both natural age and increased UV exposure. The three whale species studied appeared to have developed alternative mechanisms of coping with UV-induced damage. MtDNA damage was found to be lowest in those whales with the highest expression of heat shock protein 70 (Hsp70), suggesting that this UV-defensive mechanism may be useful in future studies for the prevention of age-related phenotypes. Overall, the present study provides important new insights into the potential role of mitochondria in ageing.

Acknowledgements

This PhD project was supported by the Institute of Cellular Medicine, the Faculty of Medical Sciences (Newcastle University) and the UK National Institute for Health Research (NIHR) Newcastle Biomedical Research Centre in Ageing and Chronic Disease to the Newcastle upon Tyne Hospitals NHS Foundation Trust.

I would like to thank my primary supervisor, Professor Mark Birch-Machin, for the opportunity to work on this PhD project, and for his continued support and guidance throughout. I would also like to thank my secondary supervisor, Dr Edward Okello, for his aid with the initial concept of the PhD. I would like to thank the collaborators with which the work on whale skin was performed, namely Dr Karina Acevedo-Whitehouse, Dr Laura Martinez-Levasseur, and Dr Diana Gendron. I would also like to thank Dr Alasdair Anderson for his work in collaboration with part of this project.

I would like to acknowledge the members of the Dermatology department of the Institute of Cellular Medicine, Newcastle University, for their technical advice and support, especially Ms Carole Todd, Mr Darren Johnson, Ms Laura Mottram, and Ms Martina Elias for their help with tissue culture techniques. I am grateful to Dr Ian Dimmick and Dr David McDonald for their support with the FACS machine. I would also like to thank the members of the MBM team for their continued help throughout this project, both in the laboratory and in meetings. I would like to thank Dr SarahJayne Boulton and Dr Asif Tulah for their support with photometric and pyrosequencing techniques respectively. I would also like to say thank you to Dr Jennifer Latimer for proof-reading the UV-related sections of this project, and to Dr Anne Oyewole for her laboratory guidance over the course of my PhD (as well as the sweets and chocolate).

I would like to thank my friends and family for their continued support throughout the course of this PhD, especially my parents for their encouragement. I would also like to say thank you to James Wordsworth for making the last three years an even better experience, (as well as his patience in answering my many questions on senescence!).

Declaration

This thesis is submitted to the degree of Doctor of Philosophy at Newcastle University. The research in this thesis was performed in the Department of Dermatological Sciences at the Institute of Cellular Medicine, under the supervision of Professor Mark Birch-Machin (primary supervisor), and is my own work unless stated otherwise in the text. I certify that none of the material in this thesis has been submitted previously by me for a degree or any other qualification at this or any other university.

Table of Contents

List of Figures

List of Tables

Abbreviations

$^{\cdot}OH$	Hydroxyl radical
8-oxo-dG	8-oxo-deoxyguanosine
A	Amps
a549 Parental	Human lung adenocarcinoma epithelial cells
a549 Rho-zero	Human lung adenocarcinoma epithelial cells lacking mtDNA
abs	Absorbance
ADP	Adenosine diphosphate
AMPK	AMP-activated protein kinase
ANOVA	Analysis of variance
ATP	Adenosine triphosphate
BLAST	Basic Local Alignment Search Tool
Bm	Balaenoptera musculus
Bp	Balaenoptera physalus
bp	Base pairs
BSA	Bovine serum albumin
C	Celsius
C. elegans	Caenorhabditis elegans
cDNA	Complementary DNA
CII/CS	Complex II activity/citrate synthase activity
CIV/CS	Complex IV activity/citrate synthase activity
cm	Centimetres
CO_2	Carbon dioxide

CR	Calorie restriction
Ct	Cycle threshold
DCPIP	Dichlorophenolindophenol
DDM	n-dodecyl-beta-D-maltoside
dH_2O	Deionised water
DMEM	Dulbecco's modified eagle medium
DMSO	Dimethyl sulfoxide
DNA	Deoxyribonucleic acid
dNTP	Deoxyribonucleotide triphosphate
DTNB	5,5'-dithiobis-2-nitrobenzoate
e^-	Electrons
ECL	Electrochemiluminescence
EDTA	Ethylenediaminetetraacetic acid
ETC	Electron transport chain
FACS	Fluorescence-activated cell sorting
FAD	Flavin-adenine dinucleotide
$FADH_2$	Reduced flavin-adenine dinucleotide
FCS	Foetal calf serum
ft	Foot
g	Grams
H&E stain	Hematoxylin and eosin stain
H+	Proton
H_20_2	Hydrogen peroxide
HaCaT	Immortalised human keratinocytes
HDFn	Neonatal human dermal fibroblasts

HepG2	Human hepatocellular carcinoma cells
HKGS	Human keratinocyte growth supplement
Hsp70	Heat shock protein 70
hTERT	Human telomerase reverse transcriptase
IgG	Immunoglobulin G
J	Joules
k/sec	First order rate constant
kb	Kilobases
kDa	Kilodalton
L	Litres
m	Metres
mA	Milliamps
MC1R	Melanocortin-1 receptor
MED	Minimal erythemal dose
mg	Milligrams
mJ	Millijoules
ml	Millilitres
mm	Millimetres
mM	Millimolar
MnSOD	Manganese superoxide dismutase
MRC5	Human foetal lung fibroblast cells
MRC5/hTERT	Human foetal lung fibroblast cells overexpressing telomerase
mtDNA	Mitochondrial DNA
MTS	3-(4,5-dimethylthiazol-2-yl)-5-(3-

	carboxymethoxyphenyl)-2-(4-sulfophenyl)-2H-tetrazolium
mW	Milliwatts
NAC	N-acetylcysteine
NAD	Nicotinamide adenine dinucleotide
NADH	Reduced nicotinamide adenine dinucleotide
NARP	Neuropathy, Ataxia, and Retinitis Pigmentosa
NCBI	National Centre for Biotechnology Information
nDNA	Nuclear DNA
ng	Nanograms
nm	Nanometres
nmol	Nanomoles
O_2^-	Superoxide
$p16^{INK4a}$	Cyclin-dependent kinase inhibitor 2A
p21	Cyclin-dependent kinase inhibitor 1A
p53	Tumor protein 53
PBS	Phosphate buffered saline
PCR	Polymerase chain reaction
PGC-1α	Peroxisome proliferator-activated receptor gamma co-activator alpha
PGC-1β	Peroxisome proliferator-activated receptor gamma co-activator beta
Pm	Physeter macrocephalus
PPi	Pyrophosphate
pRB	Retinoblastoma protein
PS	Penicillin-streptomycin

qPCR	Real-time quantitative polymerase chain reaction
RIPA Buffer	Radio-Immunoprecipitation Assay Buffer
RNA	Ribonucleic acid
RNAi	RNA interference
ROS	Reactive oxygen species
rpm	Rotations per minute
SASP	Senescence-associated secretory phenotype
SDHA	Succinate dehydrogenase complex subunit A
SDHB	Succinate dehydrogenase complex subunit B
SDHC	Succinate dehydrogenase complex subunit C
SDHD	Succinate dehydrogenase complex subunit D
SDS	Sodium dodecyl sulphate
SED	Standard erythemal dose
SEM	Standard error of the mean
SOD	Superoxide dismutase
SPF	Sun-protection factor
TAE	Tris acetate ethylenediaminetetraacetic acid
TBS	Tris-buffered saline
TE	Trypsin ethylenediaminetetraacetic acid
TGF-β1	Transforming growth factor beta
TR	Telomerase RNA template
TUNEL	Terminal deoxynucleotidyl transferase-mediated deoxyuridine triphosphate nick-end labelling
U	Units
UPRmt	Mitochondrial unfolded protein response

UV	Ultraviolet radiation
V	Volts
W	Watts
w/v	Weight/volume
X-gal	5-bromo-4-chloro-3-indolyl-beta-D-galactopyranoside
α-MSH	Alpha-melanocyte stimulating hormone
β-act	Beta-actin
β-gal	Beta-galactosidase
µg	Micrograms
µl	Microlitres
µm	Micrometres
µM	Micromolar

Chapter 1. Introduction

1.1 Mitochondria

Mitochondria are dynamic organelles found within the cytoplasm of eukaryotic cells, and are responsible for the production of the majority of cellular energy via oxidative phosphorylation, in the form of adenosine triphosphate (ATP) (Waterhouse, 2003; Birch-Machin, 2006). These organelles are thought to have originated from a symbiotic relationship which occurred several billion years ago between a proteobacteria and a host cell, during which a mutually beneficial relationship arose whereby the host benefitted from the additional energy-producing mechanism, and the proteobacteria was provided with a supply of nutrients and a safe environment (Berg and Kurland, 2000; Searcy, 2003). There may be up to several thousand mitochondria within a single cell depending on the specific energy requirements of the tissue (Youle and van der Bliek, 2012), with energy production taking place at the inner mitochondrial membrane, where ATP is generated from adenosine diphosphate (ADP) and phosphate obtained from the diet (Wallace, 1992). ATP is used throughout the body to power multiple processes via its conversion back to ADP plus phosphate (Wallace, 1992). Other roles of the mitochondria include the generation of reduced electron (e^-) carriers for use in the electron transport chain (ETC) (Wojtovich *et al.*, 2013), and the synthesis of metabolic precursors such as amino acids (Berg *et al.*, 2002), both of which take place at the citric acid cycle in the mitochondrial matrix. Other roles include apoptosis, or programmed cell death, which involves the release of cytochrome *c* from the degraded mitochondrial membrane, to induce the cellular death cascade (Paz *et al.*, 2008).

1.1.1 *Mitochondrial structure*

The number and structure of mitochondria within a cell varies greatly between species and tissues, and is dependent upon energy requirements (Youle and van der Bliek, 2012). Mitochondria consist of an outer membrane, and an inner membrane folded into cristae to allow for a large surface area for oxidative phosphorylation, as the inner membrane contains the ETC complexes which generate ATP (Scheffler, 2007). The inner membrane contains many copies of each of the five ETC complexes used to generate cellular energy. The centre of a mitochondrion is known as the matrix, and it is here that the multiple copies of mitochondrial DNA (mtDNA) are attached to the inner membrane (Scheffler,

2007). Ribosomes for the translation of mtDNA-encoded mitochondrial subunits are also found in the matrix (O'Brien, 2003). The area between the two membranes is known as the intermembrane space, and this area is vital for mitochondrial respiration as it allows for the generation of a proton (H+) gradient across the inner membrane which is used in the production of ATP, as discussed in more detail below. The structure of a single mitochondrion is shown in Figure 1. However, as mitochondria are dynamic, they are constantly changing their shape as they undergo fission and fusion (the joining and separation of multiple mitochondria) (Youle and van der Bliek, 2012), or when they are required at a specific location within a cell and are transported via the cytoskeleton, with which they are able to interact (Boldogh and Pon, 2006). Therefore, mitochondria form networks rather than just isolated organelles, and their shapes change continuously when viewed in live cells (Youle and van der Bliek, 2012).

Figure 1

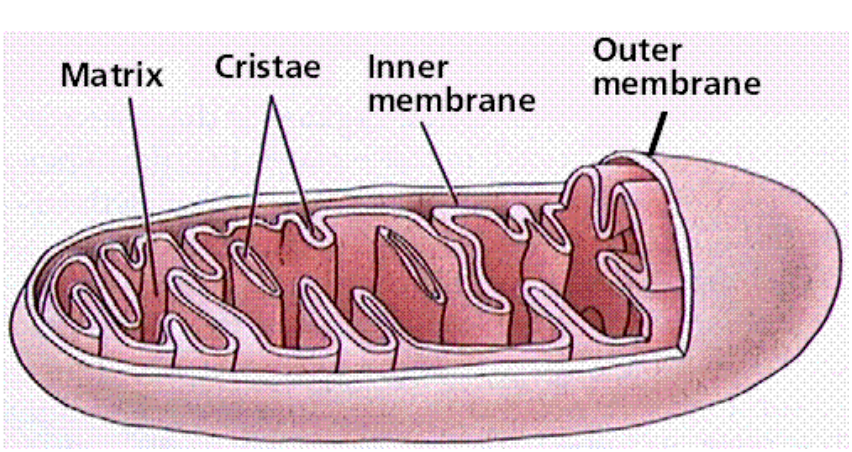

Figure 1. The structure of mitochondria. A single mitochondrion is shown, which consists of an inner membrane surrounded by an outer membrane. The inner membrane contains ETC units on folds called cristae, which increase the surface area of the inner membrane. The centre of the mitochondria is named the matrix, which contains the mtDNA attached to the inner membrane, as well as ribosomes responsible for translation of the mtDNA-encoded ETC subunits. Image from (Purves *et al.*, 1994).

1.1.2 *Mitochondrial DNA*

Human mtDNA is a double-stranded circular genome of 16,569 base pairs (bp) (Figure 2) (NCBI, 2013), which was first discovered to be present in

mitochondria in 1963 (Nass and Nass, 1963). Unlike nuclear DNA (nDNA), multiple copies of the mitochondrial genome exist within each cell. There are usually 4-10 copies of this genome per mitochondrion, and therefore may be up to thousands of copies per cell (Krutmann, 2003). MtDNA is found attached to the mitochondrial inner membrane, which is also the location of the mitochondrial respiratory complexes. As the mitochondrial genome is found in close proximity to the ETC it is particularly vulnerable to the effects of oxidative stress, exacerbated further by the fact that mtDNA has limited repair mechanisms and lacks the protective histones of nDNA (Birch-Machin and Swalwell, 2010). Reactive oxygen species (ROS) generated via the process of respiration are able to cause multiple forms of mtDNA damage, including adducts such as 8-oxo-deoxyguanosine (8-oxo-dG), which if not repaired can induce DNA strand breaks and DNA base transversions, which may result in altered mtDNA transcription and dysfunctional protein production (Efrati *et al.*, 1999). The majority of ETC subunits (~90%) are encoded by the nucleus; however, the mitochondrial genome encodes 13 subunits of the ETC, plus the machinery required to assemble these subunits (2 ribosomal RNAs and 22 transfer RNAs) (Birch-Machin and Swalwell, 2010). Therefore, alterations to mtDNA induced by ROS have the potential to alter ETC function and to decrease the efficiency of respiration and ATP production (Bandy and Davison, 1990). The presence of multiple mtDNA copies per cell allows damage to be present in some of the mtDNA copies without altering the overall mitochondrial or cellular phenotype, which is only altered once a threshold of damage is reached (Rossignol *et al.*, 2003), making mtDNA a common biomarker for cellular DNA damage (Birch-Machin and Swalwell, 2010). This mix of mutated and wild-type mtDNA within a cell is termed heteroplasmy; additionally, tissues may also be termed heteroplasmic if they contain both wild-type and phenotypically altered cells (such as senescent or apoptotic cells) (Rossignol *et al.*, 2003). Cellular or tissue function may be compromised if the level of mutated mtDNA or the number of damaged cells becomes too high (Rossignol *et al.*, 2003).

Mitochondria are under semi-autonomous control, meaning that they are encoded by both nuclear and mitochondrial DNA (Birch-Machin, 2006). The proto-mitochondrial organelles in the initial endosymbiotic relationship between

a proteobacteria and a host cell would have contained its own genes to entirely encode its own subunits (Searcy, 2003). However, over evolutionary time these genes appear to have been transferred to the nucleus, possibly to reduce the mtDNA mutational load in mitochondria which reproduce asexually (Berg and Kurland, 2000). It is important that the interaction between the nuclear and mitochondrial-encoded proteins is precise, to allow accurate control of the ETC and therefore efficient energy production and low ROS leakage (Butow and Avadhani, 2004; Rodley *et al.*, 2012).

Figure 2

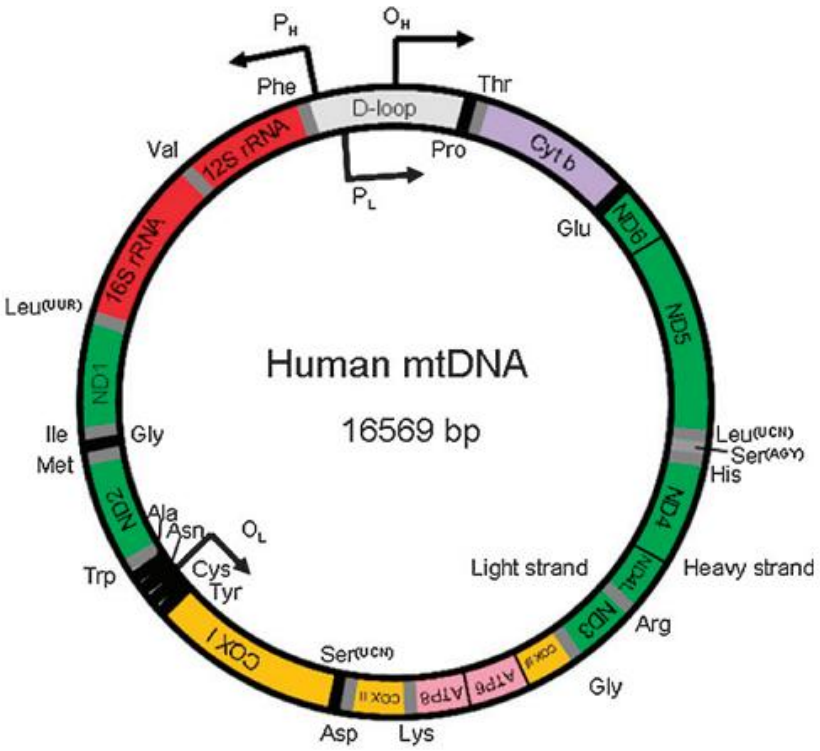

Figure 2. Human mitochondrial DNA. Human mtDNA is a circular genome of 16,569 bp, found attached to the mitochondrial inner membrane, and multiple copies are found per mitochondrion. This genome encodes 13 mitochondrial ETC subunit proteins, as well as 2 ribosomal RNAs and 22 transfer RNAs. MtDNA consists of a heavy and a light strand. The genes encoding the ETC subunit proteins are Cyt b (cytochrome *b*), ND1-6 (NADH dehydrogenase), COX1-3 (cytochrome *c* oxidase), and ATP6 and 8 (ATP synthase). Image from (Birch-Machin and Swalwell, 2010).

1.1.3 *Oxidative phosphorylation*

Human cells generate energy from fuel sources obtained from lipids, proteins, and carbohydrates from the diet (Da Poian *et al.*, 2010). These fuel sources are metabolised by cells to produce the cellular energy currency, ATP (Waterhouse,

2003; Birch-Machin, 2006), either by glycolysis in the cytoplasm or oxidative phosphorylation at the mitochondrial inner membrane (Da Poian *et al.*, 2010). Glycolysis involves the breakdown of glucose to pyruvate, and generates 2 ATP molecules per molecule of glucose (Berg *et al.*, 2006). Pyruvate is used by the citric acid cycle in the matrix to produce precursors for oxidative phosphorylation, which are 8 molecules of reduced nicotinamide adenine dinucleotide (NADH) and 2 molecules of reduced flavin-adenine dinucleotide ($FADH_2$) (Berg *et al.*, 2006), which provide e^- to the ETC. Oxidative phosphorylation generates approximately 26 ATP molecules via the ETC at the mitochondrial inner membrane (Berg *et al.*, 2006), and is therefore responsible for the production of the majority of cellular energy.

The ETC consists of 5 complexes (termed complexes I-V) which are involved in the transport of protons across the mitochondrial inner membrane from the matrix to the intermembrane space, to generate a proton gradient which is then utilised by complex V (the ATP synthase) to generate ATP (Elston *et al.*, 1998; Berg *et al.*, 2006; Birch-Machin, 2006; Scheffler, 2007; Tulah and Birch-Machin, 2013). To create this proton gradient, e^- obtained from NADH and $FADH_2$ from the citric acid cycle are transferred along the ETC through complexes I to IV via a series of redox reactions, where e^- are eventually accepted by oxygen to form water (Figure 3) (Berg *et al.*, 2006; Birch-Machin, 2006). During this series of redox reactions, energy released is used to actively pump H+ from the mitochondrial matrix to the intermembrane space between the inner and outer membranes, against an electrochemical gradient (Berg *et al.*, 2006; Tulah and Birch-Machin, 2013). The proton gradient generated acts as a reservoir of energy, with which the ATP synthase (complex V) is able to generate ATP, as the protons pass through the ATP synthase (Figure 3) (Elston *et al.*, 1998; Scheffler, 2007). At the front of the ETC, complex I receives e^- from NADH, and complex II from $FADH_2$ (Tulah and Birch-Machin, 2013), and these complexes independently transfer e^- to ubiquinone, an e^- carrier which is not covalently bound to the ETC, which becomes reduced to form ubiquinol (Figure 3) (Tulah and Birch-Machin, 2013). Ubiquinol transfers e^- to complex III, which then transfers e^- to cytochrome *c*, another non-covalently bound protein (Figure 3). Reduced cytochrome *c* is oxidised by complex IV, after which e^- are transferred to oxygen for safe removal (Tulah and Birch-Machin, 2013). Complexes I, III,

and IV are capable of pumping H+ from the matrix to the intermembrane space during this series of redox reactions, but complex II is not (Figure 3).

Figure 3

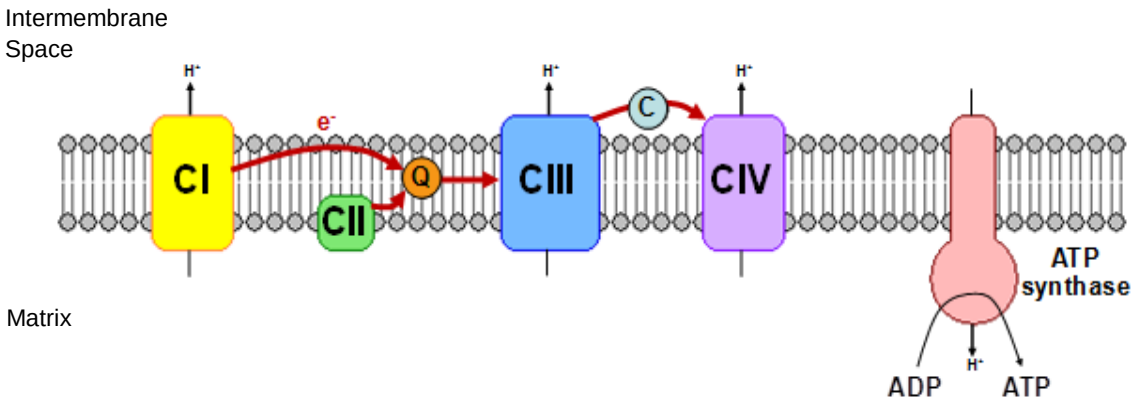

Figure 3. The mitochondrial electron transport chain. The mitochondrial inner membrane is shown in grey, which contains the 5 complexes of the ETC. The transfer of e^- occurs from complex I (CI) and complex II (CII) independently to ubiquinone (Q), which transfers e^- to complex III (CIII). CIII then transfers e^- to cytochrome *c* (C), and finally to complex IV (CIV). Electron transfer is shown by the red line. Complexes I, III, and IV are capable of pumping H+ across the inner membrane to the intermembrane space to form a proton gradient, and complex V (ATP synthase) is able to use this gradient to form ATP from ADP, as H+ re-enter the matrix down the electrochemical gradient.

1.1.4 *Electron transport chain*

The mitochondrial ETC consists of 5 complexes involved in the production of ATP as discussed above. Complexes I, III, IV, and V are encoded by both nuclear and mitochondrial DNA, and are therefore under dual control by both, whereas complex II is entirely nuclear-encoded (Smeitink *et al.*, 1998; Birch-Machin, 2006). Complex I (NADH-ubiquinone oxidoreductase) consists of 45 subunits in mammals, 7 of which are mtDNA-encoded (Scheffler, 2007). This complex is able to oxidise the substrate NADH and reduce the e^- carrier ubiquinone, to transfer e^- to complex III. During this process, e^- are transferred from NADH to a flavin mononucleotide on complex I, and then through a series of 7 iron-sulphur clusters to the e^- carrier ubiquinone (Rouault, 2012). As this complex spans the inner membrane, it is also capable of pumping protons from the matrix to the intermembrane space to contribute to the proton gradient (Tulah and Birch-Machin, 2013).

Complex II (succinate-ubiquinone oxidoreductase) of the mitochondrial ETC is the only mitochondrial complex which is entirely nuclear-encoded, rather than under dual control by both mtDNA and nDNA as for the other four complexes (Smeitink *et al.*, 1998; Birch-Machin, 2006). This complex is located on the matrix side of the inner mitochondrial membrane, and forms part of both the ETC chain for the production of ATP via electron transport, and the citric acid cycle in the matrix, which increases the ATP-producing ability of the ETC by providing reduced e^- carriers (Wojtovich *et al.*, 2013). Complex II consists of 4 nuclear-encoded subunits (Figure 4); the flavoprotein subunit, succinate dehydrogenase complex subunit A (SDHA), the iron-sulphur subunit, SDHB, and 2 membrane anchor subunits, SDHC and SDHD. SDHA is responsible for catalysing the oxidation of succinate to fumarate as part of the citric acid cycle, via the transfer of e^- to flavin-adenine dinucleotide (FAD), to generate reduced FAD ($FADH_2$) (Wojtovich *et al.*, 2013). The e^- from $FADH_2$ are then transferred through the iron-sulphur clusters of SDHB, to SDHC and SDHD which transfer e^- to a ubiquinone pool, to continue the transport of e^- to complex III and along the remainder of the ETC (Wojtovich *et al.*, 2013). Complex II was the major complex studied in the present project, and its role in the ageing process is discussed in more detail in Chapter 3.

Figure 4

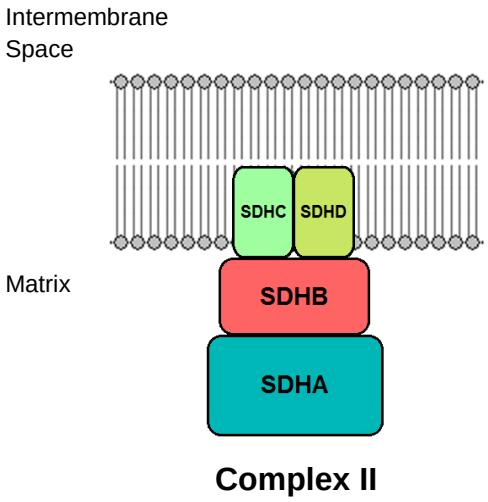

Figure 4. The subunits of mitochondrial complex II. The mitochondrial inner membrane is shown (in grey), with the individual subunits of complex II. Complex II is composed of 4 subunits, which are a flavoprotein subunit (SDHA), an iron-sulphur cluster (SDHB), and 2 membrane-anchor proteins (SDHC and SDHD).

Complex III (ubiquinone-cytochrome *c* oxidoreductase) has 1 out of 11 subunits encoded by mtDNA (Scheffler, 2007). This complex accepts e^- from reduced ubiquinone, generated by both complexes I and II (Wojtovich *et al.*, 2013). Reduced ubiquinone binds to complex III to transfer e^- through an iron-sulphur cluster to result in the reduction of cytochrome *c* (Scheffler, 2007). During this process, protons are pumped from the matrix to the intermembrane space to contribute to the proton gradient for ATP production (Scheffler, 2007).

Complex IV (cytochrome *c* oxidase) is the final e^- acceptor of the respiratory chain, and consists of 13 subunits, of which the largest 3 are mtDNA-encoded (Scheffler, 2007). Reduced cytochrome *c* transfers e^- to this complex, which are then transferred to oxygen to generate water (Berg *et al.*, 2006; Birch-Machin, 2006). Complex IV is also able to pump protons across the inner membrane to contribute to the proton gradient (Scheffler, 2007).

The final complex of the ETC, complex V (ATP synthase), is composed of 2 mitochondrial-encoded subunits and approximately 29-35 nuclear-encoded subunits (Jonckheere *et al.*, 2012). This complex is not involved in e^- transfer; however, this complex is able to utilise the proton gradient generated by the other complexes to produce ATP, as H+ pass from the intermembrane space back to the matrix. During this process, the upper section of complex V rotates as H+ enter, and this generates the energy required to produce ATP from inorganic phosphate and ADP (Elston *et al.*, 1998; Scheffler, 2007).

The organisation of the ETC complexes within the mitochondrial inner membrane has been debated previously (Barrientos and Ugalde, 2013), however, it is generally accepted that the complexes are able to move freely throughout the inner membrane (Hackenbrock *et al.*, 1986; Dudkina *et al.*, 2008), as well as being able to form supercomplexes (Cruciat *et al.*, 2000; Schagger and Pfeiffer, 2000; Barrientos and Ugalde, 2013). Complexes I, III, and IV (as well as ubiquinone and cytochrome *c*) have been shown to form different combinations of supercomplexes; however, the function of these supercomplexes has only recently begun to be elucidated (Barrientos and Ugalde, 2013). Lapuente-Brun *et al*., (2013) suggested that the formation of supercomplexes was dynamic and was used to optimise the available

substrates, by allowing multiple forms of the respiratory chain to exist simultaneously. For example, supercomplexes were suggested to be able to exist alongside free-ETC complexes (which would include complex II, as complex II is unable to form a supercomplex) (Lapuente-Brun *et al.*, 2013). This would allow supercomplexes to utilise any available NADH via complex I respiration, and the free complexes to utilise available succinate via complex II respiration (Lapuente-Brun *et al.*, 2013). An additional possible reason for supercomplex formation could be that they lower ROS formation at complex I by increasing its stability (Barrientos and Ugalde, 2013; Maranzana *et al.*, 2013).

1.1.5 *Reactive oxygen species*

During the process of oxidative phosphorylation at the ETC, e^- have been shown to leak from complexes I and III (Cadenas *et al.*, 1977; Turrens *et al.*, 1985; Hirst *et al.*, 2008; Murphy, 2009; Bleier and Dröse, 2013; Wojtovich *et al.*, 2013), and more recently from complex II (Guo and Lemire, 2003; Lemarie *et al.*, 2011; Quinlan *et al.*, 2012). Leaked e^- are able to react with oxygen to form ROS, which are therefore generated as a by-product of respiration. As e^- react with oxygen, they initially form the ROS known as superoxide (O_2^-), which is highly reactive as it contains a single unpaired electron. It is therefore capable of oxidising surrounding cellular structures such as proteins, lipids, and nucleic acids, leading to potential structural and genetic damage and altered cell homeostasis (Brand *et al.*, 2004; Cecarini *et al.*, 2007; Krishnan *et al.*, 2007).

Under normal circumstances, cells are able to decrease the level of O_2^- via the endogenous antioxidant manganese superoxide dismutase (MnSOD) found within the mitochondria (Scheffler, 2007). MnSOD causes the dismutation of O_2^- to hydrogen peroxide (H_2O_2), which is then able to be converted to water by catalase or glutathione peroxidase (Figure 5) (Berg *et al.*, 2006; Birch-Machin, 2006). However, the conversion of H_2O_2 to water is not completely efficient, and H_2O_2 may undergo the Fenton reaction to generate the extremely reactive hydroxyl radical ($^{\cdot}OH$) (Hogg *et al.*, 1992). Although H_2O_2 is not a free radical itself, it is able to pass through cellular membranes and can therefore cause damage throughout the cell where it may be converted to $^{\cdot}OH$ (Bienert *et al.*, 2006). When ROS escape antioxidant defences they are able to cause damage to cellular biological structures, an accumulation of which is thought to

contribute to the ageing process (Harman, 1956). However, ROS are not always detrimental, as they may act as important signalling molecules during processes such as apoptosis (Desler *et al.*, 2011; Fischer *et al.*, 2012).

Figure 5

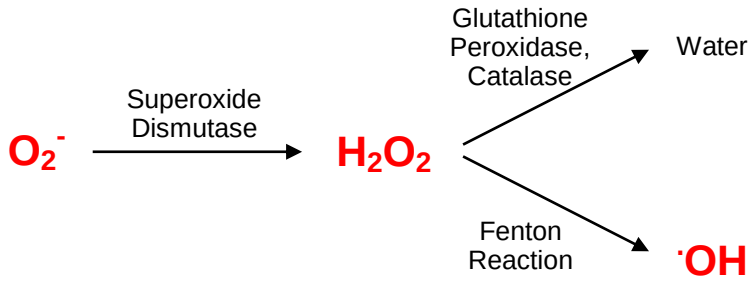

Figure 5. Mitochondrial ROS and antioxidant defences. Superoxide anions (O_2^-) generated by the mitochondria may be converted to hydrogen peroxide (H_2O_2) by superoxide dismutase within the mitochondria. H_2O_2 is able to pass through the mitochondrial membrane, and can be converted to water by the antioxidants glutathione peroxidase and catalase, to prevent it from undergoing the Fenton reaction to form the highly reactive hydroxyl radical (·OH). ROS are shown in red.

1.1.6 *Mitochondrial quality control systems*

Due to the damage inflicted upon mitochondrial macromolecules by ROS when antioxidants become overwhelmed, multiple quality control systems exist within the cell to counteract this damage, either by repair or removal. The major pathways which exist include the repair of mtDNA (Croteau *et al.*, 1999; Gredilla *et al.*, 2010; Fischer *et al.*, 2012), the mitochondrial unfolded protein response (UPRmt) (Durieux *et al.*, 2011; Fischer *et al.*, 2012), fusion and fission (Twig *et al.*, 2008; Youle and van der Bliek, 2012), lysosomal degradation of damaged mitochondrial proteins (Twig *et al.*, 2008; Youle and van der Bliek, 2012), and the removal of entire mitochondria by mitophagy (Ashrafi and Schwarz, 2013).

As mtDNA is in close proximity to ROS production from the ETC, it is especially susceptible to oxidative damage (Birch-Machin and Swalwell, 2010). Several DNA repair mechanisms exist to counteract this damage, which are base excision repair, and mismatch repair (Croteau *et al.*, 1999; Gredilla *et al.*, 2010; Fischer *et al.*, 2012); however, nucleotide excision repair has not been detected in mitochondria (Fischer *et al.*, 2012). Although these mtDNA repair

mechanisms are more limited than nDNA repair mechanisms, mtDNA exist in multiple copies within a cell and can therefore withstand high levels of damage, and therefore do not require as extensive repair mechanisms (Birch-Machin and Swalwell, 2010). Misfolded mitochondrial proteins are able to be repaired by chaperones such as the heat shock protein 70 (Hsp70) (De la Coba *et al.*, 2009). If the level of misfolded proteins becomes too great, pathways to decrease the levels of these damaged macromolecules become activated. These pathways are known as the UPRmt, and involve process such as the degradation of damaged proteins and ETC complexes via proteases, and the refolding of proteins where possible to prevent protein aggregation (Durieux *et al.*, 2011; Fischer *et al.*, 2012).

Within a cell, mitochondria constantly undergo fusion and fission, which is the joining and separating of mitochondria to decrease the levels of damage within (Twig *et al.*, 2008; Youle and van der Bliek, 2012). Fusion is the joining of a partially damaged mitochondrion with a healthy mitochondrion, via the binding of both the outer and inner membranes, during which the components of both mitochondria are mixed allowing the damage to be diluted. The healthy mitochondrial components therefore complement the damaged ones, allowing the function of the damaged mitochondria to be replenished; however, this only occurs when the damage is below 80-90% (Youle and van der Bliek, 2012). Fusion has been shown previously to result in effective redistribution of green fluorescent protein across cultured fibroblast cells (Youle and van der Bliek, 2012), demonstrating the ability of the mitochondria to dilute damage. Fission is used to remove high levels of damage from mitochondria, during which damaged components bud-off and are degraded via autophagy. This process is also used to generate new mitochondria during cellular division (Twig *et al.*, 2008; Youle and van der Bliek, 2012).

1.2 The Ageing Process

Ageing describes the functional decline of an organism over time, which occurs across all tissues of the body, leading to an increase in susceptibility to age-related diseases including cancer (Campisi, 2013), and eventually the death of the organism. It is a phenomenon observed across different organisms, with animals, plants, fungi, and even bacteria affected (Ackermann, 2008); however

the exact mechanism as to how and why we age remains unknown (Stefanatos and Sanz, 2011). In humans, average lifespan has increased dramatically over the last century due to advances in medicine, hygiene, and diet (Finch, 2012). The number of people over 60 years old is expected to increase globally from 600 million in the year 2000 to 2 billion people in 2050 (World Health Organisation, 2011), so it is therefore highly important to understand the causes and mechanisms of ageing so that the elderly may maintain their health for as long as possible. Attempts to elucidate the mechanisms of ageing have been performed throughout the 20th century, and several of the more promising theories will be discussed in detail below. However, the ageing process is still not fully understood, and therefore more work is required before attempts to slow the ageing process can be carried out. The possible role of senescence in ageing is discussed in Chapter 4, and the role of mitochondria in ageing is discussed in a subsequent section (section 1.3).

1.2.1 *The wear and tear theory of ageing*

One of the first theories of ageing to be proposed came in 1882 by August Weismann (Weismann, 1882; Goldsmith, 2004), who suggested that organisms accumulate damage over time due to general use, which could be exacerbated by unhealthy diets (such as excessive alcohol and fat), or by other environmental factors such as ultraviolet radiation (UV) (Salvi *et al.*, 2006). This was known as the 'wear and tear theory of ageing'. Although it is likely that these environmental factors contribute to the ageing process in humans (Frosch *et al.*, 2009; Voss *et al.*, 2011), a simple wear and tear theory is not likely to be the overall cause of ageing (Aldwin and Gilmer, 2013). This is due to problems with the theory, such as the vastly different rates of ageing seen across animal species (Speakman, 2005); if ageing were only due to a gradual accumulation of damage it may be expected that all species would age at the same rate. Athletes may also be expected to age at a faster rate due to higher usage of the body, but this is not the case (Paffenbarger *et al.*, 1993; Aldwin and Gilmer, 2013). Additionally, some organisms (such as the pacific salmon) show no signs of ageing before death (Morbey *et al.*, 2005), and some organisms (such as the freshwater polyp Hydra) are thought to be immortal (Boehm *et al.*, 2012).

1.2.2 *The antagonistic pleiotropy theory of ageing*

The 'antagonistic pleiotropy theory of ageing' was conceived in 1957 by George Williams (Williams, 1957), who suggested that certain genetic traits may be beneficial in early life before reproductive capacity is reached, yet detrimental in later life, during which they are unable to be selected against by natural selection. A possible example of antagonistic pleiotropy is senescence (which is where cells cease to divide yet remain viable), which is thought to be beneficial in early life as it prevents the division of potentially cancerous cells, yet detrimental in later life for which an accumulation of senescent cells is thought to contribute to a decline in tissue function and the ageing process (Campisi, 2005). One possible problematic observation with the antagonistic pleiotropy theory is that animals display different traits yet can show similar ageing phenotypes (Fabian and Flatt, 2011). It could be that aspects of antagonistic pleiotropy contribute to the ageing process; however, they are unlikely to be the overall cause of the ageing process, as differences within animals would have to occur with increasing chronological age in order for a beneficial trait to become detrimental. For example, senescence may be more detrimental with age due to a decline in antioxidant capacity (Micallef *et al.*, 2007), allowing the beneficial cancer-removing senescent cells to accumulate to the point of being damaging.

1.2.3 *The disposable soma theory of ageing*

In 1977, Tom Kirkwood (Kirkwood, 1977) proposed that because the body has a limited supply of resources available from the environment, these are therefore distributed in priority towards reproduction rather than towards maintaining somatic cells for long periods of time. The body is thought to deteriorate over time due to damage accumulation in somatic cells, whilst the germ line cells remain undamaged (Kirkwood and Austad, 2000). This theory is known as the 'disposable soma theory of ageing', and could be explained from an evolutionary perspective by the fact that resources are hard to come by in the wild. Since animals in the wild often do not live to old ages due to factors such as cold and predation, it would therefore be more beneficial for animals to put resources into reproduction rather than into attempting to maintain somatic cells, as the animals were likely to die early (Kirkwood and Austad, 2000). However this theory has been debated (Blagosklonny, 2010), as those animals

with abundant resources still age, and a higher food intake actually often results in a lower lifespan. Also, women still age after the menopause, even though after this point resources are no longer allocated to reproduction (Blagosklonny, 2010).

1.3 The Role of Mitochondria in Ageing

Many theories as to why we age have been suggested previously, and a large number of these theories involve the mitochondria. For example, the 'rate of living theory of ageing' was proposed in 1928 by Raymond Pearl (Pearl, 1928), who presented the idea that the differing metabolic rates between animal species was a determining factor in maximum lifespan potential. This theory was taken further by Denham Harman in 1956 (Harman, 1956), who proposed the 'free radical theory of ageing', which suggested that the rate of production of free radicals such as ROS, rather than the rate of metabolic activity directly, affected the ageing process of the animal. Highly reactive oxygen radicals were proposed to cause damage to biological structures which was thought to accumulate over time, eventually leading to a loss of cellular function and ageing (Harman, 1956). In support of this theory, it has been observed that pigeons have approximately 9-fold longer maximal lifespans than rats, despite similar masses and metabolic rates; however, the rate of H_2O_2 production is significantly lower in pigeons (Ku and Sohal, 1993; Barja *et al.*, 1994; Barja and Herrero, 1998). This could imply that animals which generate fewer free radicals have longer lifespans. Additionally, both mice and rats have different metabolic rates, yet a similar level of H_2O_2 production, and their maximal lifespans are the same (Herrero and Barja, 1998). Further evidence for a role of free radicals in lifespan determination is based on the observation that the level of oxidative mtDNA damage in heart tissue is lower in longer-lived mammals (Barja and Herrero, 2000; Barja, 2002). As mitochondria are responsible for the production of the majority of ROS within a cell (Berg *et al.*, 2006), the free radical theory of ageing was later refined to the 'mitochondrial theory of ageing' in 1972 (Harman, 1972).

1.3.1 *The mitochondrial theory of ageing*

The mitochondrial theory of ageing (Harman, 1972) suggested that mitochondria play a key role in the ageing process via the production of

damaging ROS molecules, and it is currently one of the most widely accepted theories of ageing (Hulbert *et al.*, 2007; Barja, 2013). Within this theory, a mechanism of ageing has been proposed called the 'vicious cycle theory of ageing' (Bandy and Davison, 1990; Zdanov *et al.*, 2006; Dlaskova *et al.*, 2008), which suggests that ROS production from the mitochondrial respiratory chain is able to cause damage to mtDNA, and because mtDNA encodes subunits of the respiratory chain, this then leads to errors in gene expression and results in dysfunctional subunits. Dysfunctional mitochondria are then thought to contribute to further ROS leakage, in a continuous vicious cycle of damage accumulation (Figure 6). However, the vicious cycle theory of ageing is disputed, as evidence both for and against this theory has been presented previously (Sanz *et al.*, 2006; Barja, 2013), which is discussed in more detail in the subsequent sections.

Figure 6

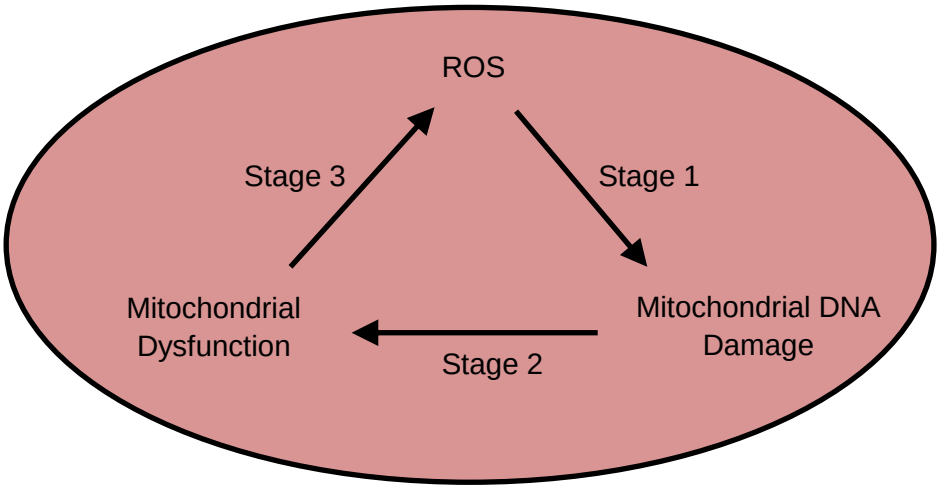

Figure 6. The vicious cycle theory of ageing. ROS generation during mitochondrial respiration is thought to cause damage to mtDNA (stage 1), which in turn is thought to result in the altered expression of ETC units (stage 2). This is thought to cause further ROS production (stage 3) in a continuing cycle of exponentially increasing damage (Bandy and Davison, 1990; Zdanov *et al.*, 2006; Dlaskova *et al.*, 2008). The mitochondrion is shown in pink.

1.3.2 *Stage one of the vicious cycle theory of ageing*

The first stage of the vicious cycle theory of ageing suggests that ROS generated predominantly by the ETC are capable of causing mtDNA damage. Evidence for this stage being able to occur comes from previous studies

demonstrating that oxidative damage (such as 8-oxo-dG lesions) is much higher in mtDNA than it is in nDNA (Richter *et al.*, 1988; Mecocci *et al.*, 1993; Shigenaga *et al.*, 1994a; Yakes and Van Houten, 1997; Hamilton *et al.*, 2001; Santos *et al.*, 2002; Cui *et al.*, 2012), due to the limited repair mechanisms of mtDNA, and especially due to its close proximity to the ETC (Birch-Machin and Swalwell, 2010). This suggests that ROS generated via respiration is able to cause damage to mtDNA. As this first stage of the vicious cycle has been demonstrated in many previous studies, it is therefore likely to be able to occur.

1.3.3 *Stage two of the vicious cycle theory of ageing*

The second stage of the vicious cycle theory of ageing proposes that mtDNA damage is able to lead to altered expression of ETC complex subunits and therefore result in dysfunctional mitochondria. Multiple studies have been presented in support of this stage; for example, Kwong *et al*. (2007) found that mtDNA mutations affecting complex V caused a decrease in the level of respiration in human osteosarcoma cells (mitochondrial dysfunction). This also led to an increase in ROS generation, which could link the second and third stages of the vicious cycle (Kwong *et al.*, 2007). Additionally, various mitochondrial diseases such as schizophrenia and NARP (Neuropathy, Ataxia, and Retinitis Pigmentosa) are characterised by mtDNA mutations, and show reduced oxidative phosphorylation capacity (Lenaz *et al.*, 2004; Wallace, 2010; Verge *et al.*, 2011; Duno *et al.*, 2013; Wu *et al.*, 2013). Further evidence for mtDNA mutations causing mitochondrial dysfunction comes from studies using knock-in mice with mutated mtDNA polymerase subunits, to increase the rate of transcriptional errors (Kujoth *et al.*, 2005; Trifunovic *et al.*, 2005). These mice accumulate mtDNA mutations at a higher rate than wild-type mice, and have dysfunctional mitochondria in the form of decreased rates of respiration and ATP production (Kujoth *et al.*, 2005; Trifunovic *et al.*, 2005). However, these mice did not show increased levels of ROS (or of antioxidants to counteract ROS), which could provide evidence against the second stage of the cycle being able to result in the third stage. It could be speculated that not all mtDNA mutations result in an increased level of ROS, so damage may increase in a manner slower than expected (Sanz *et al.*, 2006).

1.3.4 *Stage three of the vicious cycle theory of ageing*

The third stage of the vicious cycle theory of ageing suggests that mitochondrial dysfunction can lead to an increase in ROS production (Bandy and Davison, 1990). This stage has evidence against it, as demonstrated by the previously discussed studies for which mice with an accelerated accumulation of mtDNA mutations showed higher levels of mitochondrial dysfunction, yet no increase in ROS levels (Kujoth *et al.*, 2005; Trifunovic *et al.*, 2005). However, some evidence supporting this stage of the cycle comes from Esposito *et al*., (1999), who found that mice with mitochondrial dysfunction in the form of being unable to import ADP into the matrix (and therefore with inhibited oxidative phosphorylation), had significantly higher levels of H_2O_2 (Esposito *et al.*, 1999). This suggested that some forms of mitochondrial dysfunction may result in increased ROS levels, whereas other forms may not. In the study by Esposito *et al*., (1999), there was also an increase in mtDNA damage observed in the heart tissue (which showed the lowest level of antioxidant defence), which could indicate that dysfunctional mitochondria are able to cause an increase in the level of ROS, as well as an increase in mtDNA damage if the antioxidant defence is not sufficient (Esposito *et al.*, 1999). This demonstrates a link between the third and first stages of the vicious cycle theory of ageing. Lapointe *et al*., (2012) found that mice heterozygous for an enzyme involved in the synthesis of ubiquinone had lower levels of this enzyme at the mitochondrial inner membrane, and showed mitochondrial dysfunction in the form of decreased respiratory activity. These mice also had increased levels of mitochondrial oxidative stress (Lapointe *et al.*, 2012), which is in accordance with the third stage of the vicious cycle theory of ageing. In humans, ROS levels have been shown to be higher in skin fibroblast cells from older individuals, accompanied by an increase in mitochondrial dysfunction (a decrease in mitochondrial membrane potential) (Koziel *et al.*, 2011), which could suggest a link between the two factors. Therefore in conclusion, some forms of mitochondrial dysfunction may result in increased ROS production (Esposito *et al.*, 1999; Lapointe *et al.*, 2012), whereas others may not (Kujoth *et al.*, 2005; Trifunovic *et al.*, 2005).

1.3.5 *MtDNA damage and ageing*

The three stages of the vicious cycle have been shown in previous studies to be able to occur independently. The three aspects of the cycle (increased ROS, mtDNA damage, and mitochondrial dysfunction) have also all been shown separately to be correlated with increased age. For example, Hayakawa *et al*., (1992) found that the level of mtDNA damage (8-oxo-dG lesions) was higher in the human heart muscle of older people compared to younger. In the study, mtDNA damage increased exponentially from 45 years and older (Hayakawa *et al.*, 1992); this lends support to the exponential increase in damage which is thought to occur during the vicious cycle theory of ageing. Other studies have also shown an increase in oxidative mtDNA damage with age (Ames *et al.*, 1993; Mecocci *et al.*, 1993; Hudson *et al.*, 1998). Higher levels of mtDNA mutations have also been shown to be causative in terms of ageing phenotypes; Trifunovic *et al*., (2005) and Kujoth *et al*., (2005) found that mice with accelerated mtDNA mutation levels (via a mutated mtDNA polymerase) showed increased mitochondrial dysfunction, as well as reduced longevity and an accelerated onset of ageing phenotypes (Kujoth *et al.*, 2005; Trifunovic *et al.*, 2005). Additionally, mtDNA mutations and deletions have been shown to correlate with the ageing process; for example, the 4977 bp common deletion which may be used as a biomarker for general mtDNA damage (Berneburg *et al.*, 2004), has been shown to accumulate in certain human tissues with age (Arnheim and Cortopassi, 1992; Cooper *et al.*, 1992; Meissner *et al.*, 2008; Cui *et al.*, 2012). The T414G mtDNA point mutation has also been shown to be higher in the skin of older individuals (Michikawa *et al.*, 1999; Birket and Birch-Machin, 2007).

1.3.6 *Mitochondrial dysfunction and ageing*

In terms of a relationship between mitochondrial dysfunction and age, past work has shown that the individual complexes of the ETC decline with age in some tissues from different species (Trounce *et al.*, 1989; Boffoli *et al.*, 1994; Hayashi *et al.*, 1994; Rooyackers *et al.*, 1996; Lenaz *et al.*, 1997; Isobe *et al.*, 1998; Lesnefsky *et al.*, 2001; Sandhu and Kaur, 2003; Kumaran *et al.*, 2004; Cocco *et al.*, 2005; Balietti *et al.*, 2009; Braidy *et al.*, 2011; Tatarkova *et al.*, 2011; Andreollo *et al.*, 2012; Velarde *et al.*, 2012), as discussed in more detail in Chapter 3. The mitochondrial membrane potential has also been shown to be

decreased with age in specific tissues (Hagen *et al.*, 1997; Parihar and Brewer, 2007; Koziel *et al.*, 2011), as has the ATP-producing capability of mitochondria (Shigenaga *et al.*, 1994b; Drew *et al.*, 2003; Nair, 2005). However, Lapointe *et al*., (2012) demonstrated that not all forms of mitochondrial dysfunction are detrimental in terms of lifespan, as mice with lower levels of ubiquinone showed mitochondrial dysfunction in the form of decreased respiratory activity, as well as increased oxidative stress, but these mice actually had increased longevity compared to wild-type mice (Lapointe *et al.*, 2012). The study suggested that mitochondrial dysfunction can result in ROS release, yet this ROS release may not necessarily contribute to a vicious cycle and a decrease in lifespan (Lapointe *et al.*, 2012). This has also been observed for *Caenorhabditis elegans* (*C. elegans*), for which ETC activity was lowered during development using RNA interference (RNAi), which resulted in increased lifespans (Dillin *et al.*, 2002). These results suggest that the relationship between mitochondrial function and age is complicated.

1.3.7 *ROS and ageing*

Several studies have demonstrated a possible correlation between increasing ROS levels and age, whereas other studies have shown a lack of correlation. ROS production levels have been shown to be higher in human skin fibroblast cells (Koziel *et al.*, 2011) and muscle cells (Capel *et al.*, 2005) with increasing age, as well as in other species such as rats (Sawada and Carlson, 1987; Muscari *et al.*, 1990; Sawada *et al.*, 1992) and flies (Sohal and Sohal, 1991). ROS production has also been shown to be generally lower in long-lived species compared to short-lived species (Ku and Sohal, 1993; Barja *et al.*, 1994; Barja and Herrero, 1998; Lambert *et al.*, 2007). Additionally, mice overexpressing mitochondrial catalase (and therefore having lower ROS levels) show an increased lifespan (Schriner *et al.*, 2005). However, past work has shown that ROS levels are not increased in older human muscle cells (Hutter *et al.*, 2007), and other studies have shown that increasing the expression of endogenous antioxidants such as MnSOD does not result in an increase in mouse lifespan, and decreasing these endogenous antioxidants does not cause a decrease in lifespan (Jang *et al.*, 2009; Perez *et al.*, 2009; Zhang *et al.*, 2009).

In the studies using mtDNA-polymerase-mutator mice (Kujoth *et al.*, 2005; Trifunovic *et al.*, 2005), despite an acceleration of ageing and a decrease in lifespan due to increased mtDNA mutations and mitochondrial dysfunction, there was no increase in ROS detected. However, this does not necessarily imply that ROS are not involved in the natural ageing process, as multiple factors are thought to be involved in driving ageing. Therefore, if one factor is greatly increased (such as errors in polymerase function) ROS accumulation may play a negligible role, especially in the knock-in mice for which ageing was greatly accelerated by other means (Kujoth *et al.*, 2005; Trifunovic *et al.*, 2005). Additionally, this mouse model may not accurately represent natural ageing, and may just display some phenotypes similar to ageing, such as alopecia and osteoporosis (Kujoth *et al.*, 2005; Trifunovic *et al.*, 2005).

As the three aspects of the vicious cycle (ROS, mtDNA damage, and mitochondrial dysfunction) are often studied separately (Sanz *et al.*, 2006), it is difficult to reconcile the vicious cycle theory of ageing. Ageing phenotypes have been shown to occur without certain aspects of the cycle taking place (such as ROS production (Kujoth *et al.*, 2005; Trifunovic *et al.*, 2005; Hutter *et al.*, 2007)), which could suggest that each stage of the vicious cycle is able to contribute separately to the ageing process, but this does not necessarily result in a continuing vicious cycle (Sanz *et al.*, 2006). For example, it could be that not all mtDNA mutations causing mitochondrial dysfunction lead to the generation of ROS (Kujoth *et al.*, 2005; Trifunovic *et al.*, 2005); however, these mutations could still be damaging by other mechanisms, and may therefore still contribute to the ageing process without inducing a vicious cycle of damage. In accordance with this, mtDNA mutations have been shown to be capable of inducing age-related diseases independently from ROS production (Mott *et al.*, 2001; Cui *et al.*, 2012). The exact link between the stages and whether the stages are causative or correlative in terms of the ageing process remains unknown, and so the vicious cycle theory remains disputed. However, the mitochondria are still extremely likely to play a role in the ageing process (Barja, 2013), even if not necessarily via a vicious cycle of damage.

1.3.8 *Mitochondria and telomeres in ageing*

Telomeres are nucleoprotein structures found at the ends of nuclear chromosomes to protect DNA from degradation via unwinding and from undergoing unnecessary strand repair mechanisms (Rodier *et al.*, 2005; Campisi, 2013). Telomere length gradually decreases as a cell divides; if telomeres reach a critically short length they activate a process known as cellular senescence (Greider and Blackburn, 1985; Harley *et al.*, 1990; Harley *et al.*, 1992; Bodnar *et al.*, 1998), which is discussed in more detail in Chapter 4. An accumulation of senescent cells has been shown previously to occur with age (Dimri *et al.*, 1995; Mishima *et al.*, 1999; Campisi, 2005; Herbig *et al.*, 2006; Noppe *et al.*, 2009; Naylor *et al.*, 2013), and longer telomere lengths have been associated with increased longevity in humans, with a previous study demonstrating that the offspring of centenarians maintain longer telomere lengths with increasing age compared to controls, and have fewer age-related diseases (Atzmon *et al.*, 2010). Telomere shortening may be seen as a separate contributor to the ageing process from the mitochondrial theory of ageing; however, recent studies have demonstrated a link between mitochondrial dysfunction and the telomeres. Studies have demonstrated that mice deficient in the catalytic subunit (TERT) of telomerase, the enzyme which maintains telomere length (Greider and Blackburn, 1985), show an accelerated telomere shortening and development of ageing phenotypes (Jaskelioff *et al.*, 2011), as well as impaired mitochondrial function and increased ROS production (Sahin *et al.*, 2011). Sahin *et al*., (2011) found that TERT-deficient mice have a decreased expression of the peroxisome proliferator-activated receptor gamma co-activators α and β (PGC-1α and PGC-1β), which regulate mitochondrial biogenesis and metabolism, suggesting that telomerase and mitochondria are linked, and may both be involved in the ageing process. The p53-protein, which may be activated if telomeres become critically short (Campisi, 2013), was thought to link mitochondria and the telomeres, as it was shown to cause repression of PGC-1α and PGC-1β (Sahin *et al.*, 2011). Other studies have shown that telomerase is translocated to the mitochondria during stressful conditions (Santos *et al.*, 2004; Jakob and Haendeler, 2007; Haendeler *et al.*, 2009), where it possibly binds to mtDNA to improve mitochondrial function (Haendeler *et al.*, 2009). Improvements in the

mitochondrial ETC complex activities have also been observed when TERT is overexpressed (Haendeler *et al.*, 2009; Indran *et al.*, 2011).

1.4 Ageing Treatments

1.4.1 *Caloric restriction and ageing*

It has been recognised for several centuries that a reduction in dietary intake can cause an increase in lifespan (Hursting *et al.*, 2003). This is known as calorie restriction (CR), and is one of the few repeatable methods of successful lifespan extension in laboratory animals (Hursting *et al.*, 2003). The first official studies into the effects of CR came at the start of the 20th century, when it was observed that a decrease in food intake in rodents improved their lifespan (Osborne *et al.*, 1917; McCay *et al.*, 1935). This lifespan-extending effect of CR has now also been observed in a variety of other organisms, such as yeast (Fabrizio *et al.*, 2003), spiders (Austad, 1989), cows (Pinney *et al.*, 1972), and dogs (Lawler *et al.*, 2008). An on-going study has demonstrated that rhesus monkeys fed approximately 30% fewer calories than controls throughout their lives have fewer signs of ageing and age-related diseases (Kemnitz *et al.*, 1993; Colman *et al.*, 2009). The effects of CR on humans are not fully known; however, on the Japanese Island of Okinawa the average calorie intake is lower, and there are a higher than average number of centenarians and fewer cases of age-related diseases (Willcox *et al.*, 2007). CR is thought to occur via AMP-activated protein kinase (AMPK), which is a metabolic regulator capable of detecting changes in cellular energy demand (Park *et al.*, 2012). AMPK is able to cause the activation of sirtuins and therefore increase mitochondrial biogenesis and function (as well as activating other pathways such as those involved in stress resistance), resulting in an enhanced lifespan (Park *et al.*, 2012).

1.4.2 *Endogenous treatments of ageing*

Since mitochondria produce the majority of ROS within a cell (Berg *et al.*, 2006), and since the proposal of the mitochondrial theory of ageing (Harman, 1972) and the observation that many age-related diseases are linked to oxidative stress (Khansari *et al.*, 2009), there have been many attempts to modulate longevity using exogenous antioxidants from plant and food sources (Lebel *et al.*, 2012). There are conflicting results regarding the supplementation of

antioxidants, including those received from studies involving vitamin E, which is found in wheat and other food sources. Navarro *et al*., (2005) found that mice supplemented with vitamin E had a ~40% increase in median lifespan and a ~17% increase in maximum lifespan (Navarro *et al.*, 2005). In the study, it was also observed that vitamin E partially decreased the higher oxidative damage usually observed in the aged mice (Navarro *et al.*, 2005). This could suggest that vitamin E may decrease ROS levels and extend lifespan, which is in support of the mitochondrial theory of ageing. However, another study in mice undergoing lifelong vitamin E supplementation found that although longevity was enhanced, the level of oxidative damage was not altered, suggesting no change in ROS levels (Selman *et al.*, 2008). Other conflicting results regarding vitamin E supplementation come from Morley and Trainor, (2000), who found that lifelong consumption of various vitamin E concentrations in mice, did not affect lifespan (Morley and Trainor, 2001).

With regards to antioxidant supplementation, the contradictory results obtained could be because the antioxidant was unable to get to the site of ROS production in the mitochondria at a high enough level, due to the method of supplementation used (Morley and Trainor, 2001). The dose of the antioxidant is also likely to be important, as low levels of vitamin E were shown to increase the lifespan of Drosophila, yet high levels did not (Driver and Georgeou, 2003), implying possible toxicity at higher levels. Also, since ROS are important signalling molecules (Desler *et al.*, 2011; Fischer *et al.*, 2012), the dose and target of the administered antioxidant would have to be considered to prevent the alteration of cellular homeostasis.

Other supplementations include the natural plant antibiotic found in the skin of red fruits, named resveratrol. Resveratrol has been shown to have benefits to age-related health *in vitro* and in animal models, such as providing protection against diabetes, inflammation, neurodegeneration, heart disease, and cancer (Jang *et al.*, 1997; Baur and Sinclair, 2006; Li *et al.*, 2012; Tome-Carneiro *et al.*, 2013). However, studies on the effects of resveratrol on human health are limited (Tome-Carneiro *et al.*, 2013). In terms of lifespan extension, studies on yeast, flies, worms, and fish have shown that resveratrol is able to increase longevity (Howitz *et al.*, 2003; Bass *et al.*, 2007; Terzibasi *et al.*, 2007; Marchal

et al., 2013). Resveratrol has also been shown to increase the lifespan of obese mice (Baur *et al.*, 2006), but results are not conclusive in non-obese mammals (Pearson *et al.*, 2008; Miller *et al.*, 2011; Marchal *et al.*, 2013; Strong *et al.*, 2013). Also, the effects of long-term supplementation on human lifespan are not known (Marchal *et al.*, 2013). Resveratrol is thought to exert its effects via sirtuins, and is therefore thought to mimic CR (Park *et al.*, 2012; Marchal *et al.*, 2013). Because CR is one of the most repeatable methods of lifespan extension (Hursting *et al.*, 2003), it could be that resveratrol will be useful in the treatment of age-related diseases in future human studies.

1.5 Ultra-Violet Radiation and the Skin

1.5.1 *The structure of the skin*

The skin is the largest organ of the body, and it acts as a barrier to external insults, such as UV, infection, toxicity, and mechanical stress (Haake *et al.*, 2001). The skin consists of three main layers; the epidermis, the dermis, and the hypodermis (Alberts *et al.*, 2002), as shown in Figure 7. The epidermis is the outermost layer (Figure 7), responsible for protection from the environment, with the most abundant cell type in the epidermis being the keratinocyte (Haake *et al.*, 2001). Keratinocytes generate keratin, which is a structural component allowing for toughness in the outer layer of the skin (Alberts *et al.*, 2002). Keratinocytes are constantly renewed since they are under continuous insult from the environment, and they differentiate as they become closer to the surface of the skin (Alberts *et al.*, 2002). The keratinocyte cells at the base are able to actively divide (the basal cells, where the keratinocyte stem cells are located) (Figure 7) (Alberts *et al.*, 2002), and the cells gradually become more squamous as they move up through the skin to the surface (Alberts *et al.*, 2002). The top layer of the skin consists of dead cells known as the stratum corneum (Hornig-Do *et al.*, 2007), which forms a waterproof barrier and is replaced on a regular basis (every 28 days (Haake *et al.*, 2001)) due to normal skin turnover. Other cell types of the epidermis include melanocyte cells (responsible for skin pigmentation), Langerhans cells (which form part of the immune response), and Merkel cells (involved in touch responses) (Haake *et al.*, 2001). Melanocytes generate melanin, which is transferred to keratinocyte cells for UV protection (Haake *et al.*, 2001; Costin and Hearing, 2007), and are

found at higher levels in sun-exposed regions of the body such as the face (Haake *et al.*, 2001).

The dermis is found beneath the epidermis in the skin (Figure 7), and contains blood and lymph vessels, sweat glands, hair roots, connective tissues (such as collagen and elastin) and nerves (Haake *et al.*, 2001; Alberts *et al.*, 2002), and provides structural support for the skin (Haake *et al.*, 2001). The most abundant cell type found in the dermis is the fibroblast cell, which generates collagen and elastin, as well as other components of the extracellular matrix (Alberts *et al.*, 2002). Other cell types include macrophages, lymphocytes, and mast cells, all of which are involved in the immune response (Alberts *et al.*, 2002). The hypodermis is located below the dermis in the skin (Figure 7), and is composed of blood vessels and nerves, as well as adipose cells, fibroblasts, and macrophages (Haake *et al.*, 2001; Alberts *et al.*, 2002). Its function is to provide a layer of fat underneath the skin, which is involved in thermoregulation (Montagna *et al.*, 1992).

The symptoms of ageing in the skin include epidermal thinning, a decrease in dermal connective tissue resulting in wrinkles, and a general increase in skin fragility (Jenkins, 2002). The skin is often used to study human ageing, due to its easy accessibility, and the observation that the ageing process is able to be accelerated in this organ via environmental insults, such as UV (Kosmadaki and Gilchrest, 2004; Quan *et al.*, 2006; Birket and Birch-Machin, 2007; Akase *et al.*, 2012).

Figure 7

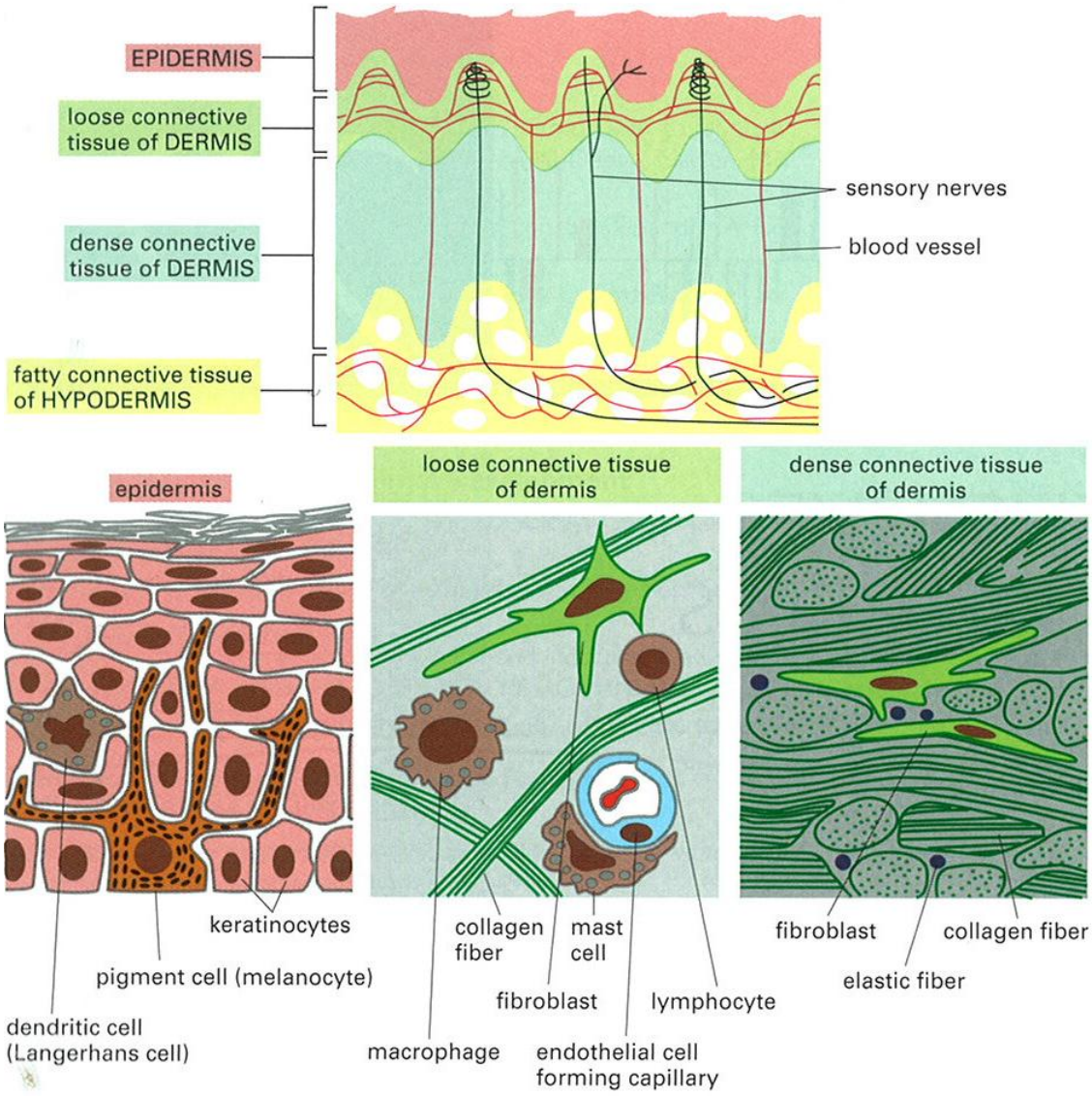

Figure 7. The structure of the skin. The skin is made up of three main layers, which are the epidermis, the dermis, and the hypodermis, shown in a simplified version in the upper image. The lower images depict close-ups of the skin layers, with the epidermis consisting of keratinocytes, melanocytes, and dendritic cells; the upper dermis consisting of loose connective tissue, with fibroblasts, mast cells, lymphocytes, and macrophages; and the lower dermis consisting of dense connective tissue and fibroblasts. Image from (Alberts *et al.*, 2002).

1.5.2 *Ultraviolet radiation and skin damage*

UV makes up approximately 9% of the radiation emitted by the sun, and is of a longer wavelength than X-rays and a shorter wavelength that visible light on the electromagnetic spectrum (Diffey, 2002). Humans are able to utilise the UV absorbed by the skin to generate vitamin D; however, the effects of excessive UV on human skin are damaging, and there is a trade-off between adequate

vitamin D synthesis and UV-induced damage (Jablonski and Chaplin, 2012). UV from the sun is the main extrinsic influence of skin ageing (De la Coba *et al.*, 2009); excessive exposure to UV can lead to cellular, molecular, and genetic changes in the skin, which if unrepaired can have deleterious effects on cellular function (Ichihashi *et al.*, 2003; Schuch and Menck, 2010). Sunburn is generally observed a few hours after acute exposure to UV; however, more serious effects of chronic UV exposure include immunosuppression, increased risk of skin cancer due to DNA mutations, and accelerated skin ageing (De la Coba *et al.*, 2009). UV is able to cause damage to cells either by the production of ROS or via direct DNA damage (Schafer *et al.*, 2010). Genetic damage to the skin from UV occurs because of the UV-absorbing properties of DNA, of which the most common genetic changes observed include pyrimidine dimers, pyrimidine monoadducts, and purine dimers (Tornaletti and Pfeifer, 1996; Sinha and Hader, 2002). If these are not repaired, they can result in DNA strand breaks and mutations, which may result in altered protein expression and reduced cellular function (Sinha and Hader, 2002), and potentially skin cancer. UV can also result in the production of ROS, which can cause oxidative damage to DNA via the formation of adducts such as 8-oxo-dG, which if not repaired can induce DNA strand breaks and base transversions (Efrati *et al.*, 1999). ROS can also cause damage to other cellular components such as lipids and proteins (De Gruijl, 1997; Finkel and Holbrook, 2000; De la Coba *et al.*, 2009). Due to this damage, UV is considered one of the largest environmental problems for human health (De la Coba *et al.*, 2009).

A possible mechanism as to how UV is able to accelerate the ageing process could be via its interaction with mitochondria, where it may contribute to a vicious cycle of increasing damage, which could potentially be involved in the ageing process (as discussed in section 1.3) (Bandy and Davison, 1990). In this scenario, UV may increase ROS levels, or cause mtDNA damage directly, which could result in an increase in mitochondrial dysfunction and a further production of ROS in a continuing vicious cycle (Figure 8) (Bandy and Davison, 1990). Even if this vicious cycle is not occurring (Sanz *et al.*, 2006), any damage to mtDNA or mitochondria directly by UV could still result in an increase in photo-ageing, as mitochondria are thought to play a prominent role in the ageing process (Birch-Machin, 2006). Many of the same symptoms and

mtDNA mutations found in photo-aged skin are also increased in chronologically aged skin; therefore, excessively UV-exposed skin may be used as a model for skin from older individuals. For example, the mtDNA 3895 bp and 4977 bp deletions, as well as the T414G mutation, are correlated more strongly with skin from sun-exposed regions and also in the skin of older individuals (Arnheim and Cortopassi, 1992; Cooper *et al.*, 1992; Yang *et al.*, 1995; Birch-Machin *et al.*, 1998; Michikawa *et al.*, 1999; Barritt *et al.*, 2000; Berneburg *et al.*, 2004; Krishnan *et al.*, 2004; Birket and Birch-Machin, 2007; Reimann *et al.*, 2007; Meissner *et al.*, 2008; Harbottle *et al.*, 2010; Cui *et al.*, 2012; Kaneko *et al.*, 2012).

Figure 8

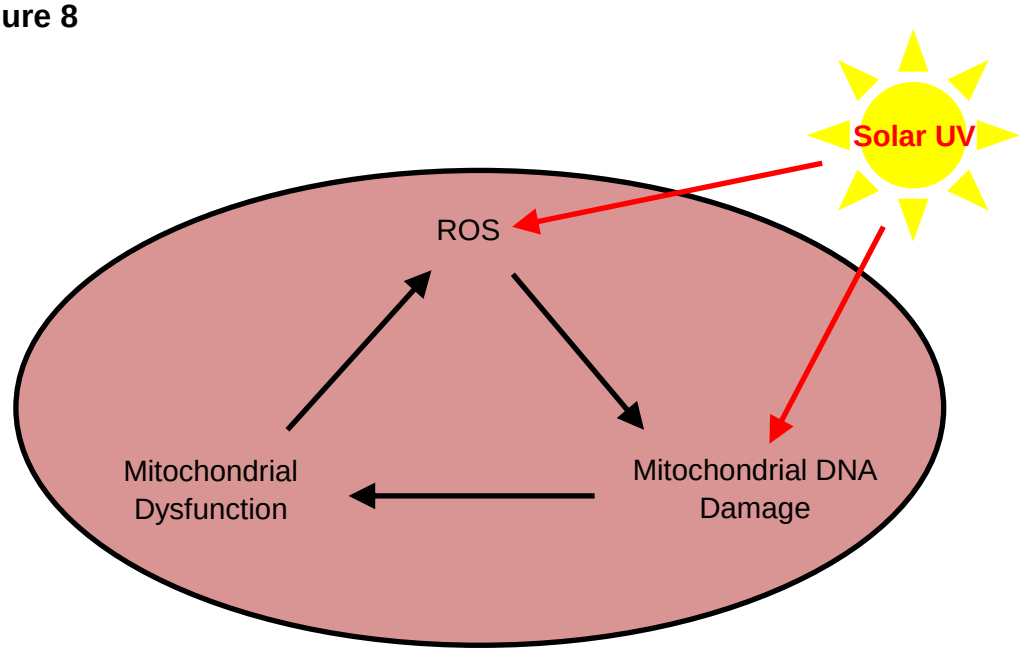

Figure 8. How UV may interact with the vicious cycle theory of ageing. UV from the sun (shown by the red arrows) is able to interact with and cause damage to mitochondria (shown in pink), either by causing direct mtDNA damage, or via an increase in ROS production. MtDNA damage may then cause an increase in mitochondrial dysfunction, and possibly a further increase of ROS, in a continuing vicious cycle resulting in accelerated ageing (Bandy and Davison, 1990).

The ozone layer provides some protection from solar radiation by absorption of damaging solar rays, such as the very harmful UVC (100 – 280 nm) (Paz *et al.*, 2008). The ozone is also capable of screening out the majority of UVB (280 – 315 nm); however, some UVB is still able to reach the earth's surface and cause damage to the skin (Paz *et al.*, 2008). UVB is only able to penetrate the

epidermal layer of the skin (Figure 9) (Birch-Machin and Swalwell, 2010), so is unable to cause damage to the deeper layers. The majority of UVA (315 – 400 nm) is not absorbed by the ozone layer, and is capable of penetration into the epidermis and the dermis of the skin (Figure 9) (Paz *et al.*, 2008; Birch-Machin and Swalwell, 2010); however, due to its longer wavelengths, it is less detrimental than UVB (Birch-Machin and Swalwell, 2010). Ozone depletion has accelerated over the last century due to man-made substances such as solvents, which contain chlorofluorocarbons and are capable of destructing the ozone layer by chemical reactions with ozone molecules (Dameris, 2010). Although the use of these man-made ozone-depleting substances was banned by the Montreal Protocol in 1987 (Dameris, 2010; Newman and McKenzie, 2011; WMO-UNEP, 2011), substances released in the last century still continue to cause damage to the ozone due to their long atmospheric half-life (Solomon, 2004).

Figure 9

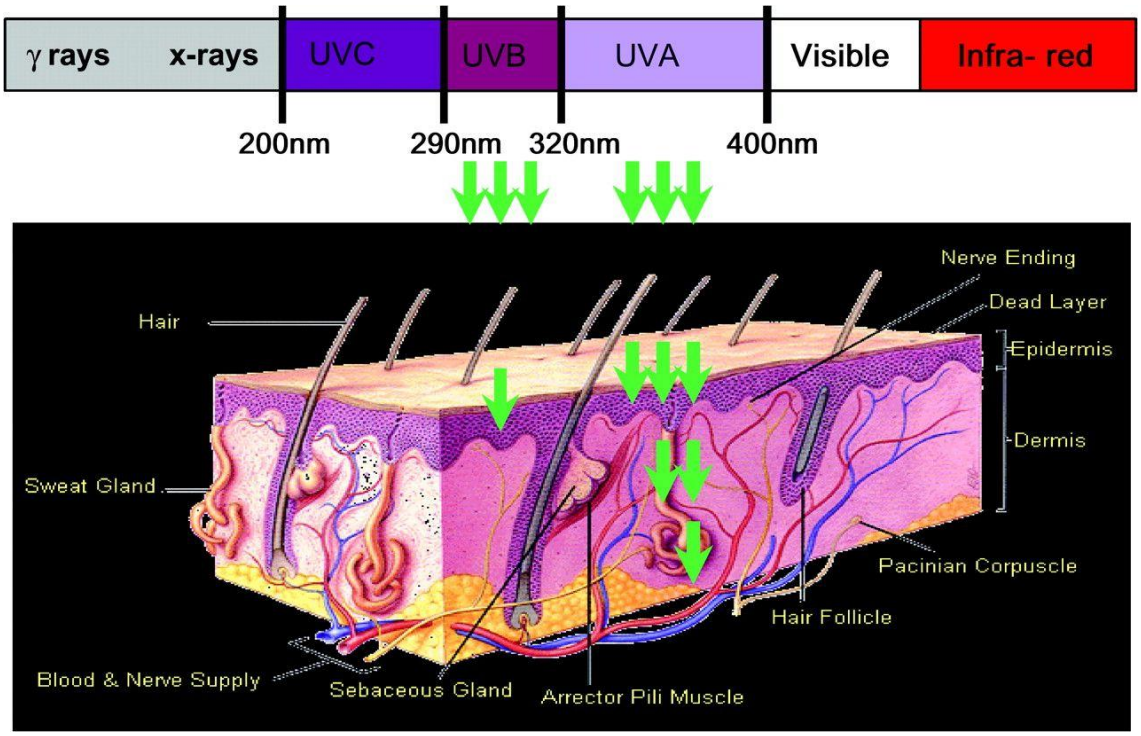

Figure 9. UV penetration of human skin. A section of human skin is shown, with the UV spectrum of light given above. The green arrows show the amount of penetration into the skin. The majority of UVB light is blocked by the ozone layer before it can reach the skin, and only penetrates the epidermis. UVA is not blocked by the ozone, and can penetrate through the epidermis into the dermis; however, UVA is less detrimental than UVB. UVC is completely blocked by the ozone. Image from (Birch-Machin and Swalwell, 2010).

1.5.3 *Cellular defence mechanisms to counteract UV-induced damage*

As the skin provides a barrier for the body from the environment, it is vital that mechanisms have evolved for its protection, especially against the main extrinsic cause of damage, the sun. Melanin is the colouration found within the skin of humans, as well as a vast array of other animals (Costin and Hearing, 2007), and is a major defensive tool against UV. Melanin is produced by melanocyte cells at the base of the epidermis, where it is transferred to the keratinocyte cells, for UV protection at the outer layer of the skin (Costin and Hearing, 2007). Melanocyte count is similar regardless of skin colour when looking at the same body region, but melanocytes from darker-skinned individuals are able to generate larger amounts of melanin with a different pattern of distribution (Haake *et al.*, 2001), meaning that lighter-skinned individuals are at a higher risk of skin cancer (Yamaguchi *et al.*, 2006). There are two types of melanin pigment found in human skin; pheomelanin which is associated with lighter skin and is red/yellow in colour (Maddodi *et al.*, 2012), and eumelanin which is associated with darker skin and is black/brown in colour (Maddodi *et al.*, 2012).

The melanocortin-1 receptor (MC1R) is a G-protein-coupled receptor responsible for skin pigmentation (Rees, 2004). It binds to the α-melanocyte stimulating hormone (α-MSH) to regulate the ratio of eumelanin to pheomelanin in the skin (Kennedy *et al.*, 2001). Polymorphisms in this receptor are associated with an increased risk of melanoma (Brudnik *et al.*, 2009), and particular variants that cause an increase in pheomelanin are more commonly associated with families with red hair, pale skin, and an increased sensitivity to UV (Rees, 2004). Variants of this gene are also found to affect the fur colour of wildlife such as foxes (Vage *et al.*, 1997), and some MC1R amino acid substitutions are associated with light-coloured animal coats such as the R67C substitution in beach-coloured mice, and some substitutions are associated with dark coats such as the Q233H substitution in melanic mice (Nachman *et al.*, 2003; Ayoub *et al.*, 2009). MC1R variants in nature may have arisen through positive selection if they produce beneficial phenotypes (Ayoub *et al.*, 2009). In humans, it is thought that as our early ancestors migrated out of Africa to cooler areas, they lost their darker skin colour to allow for more vitamin D to be absorbed from the sun in those areas with a lower UV index (Beleza *et al.*,

2013), due to genetic polymorphisms in different pigmentation genes. In animals, skin colouration caused by melanin is more likely to be due to factors such as concealment from predators and breeding competition, rather than UV protection (Ayoub *et al.*, 2009). However, the ability to tan has been observed in animals such as hammerhead sharks (Lowe and Goodman-Lowe, 1996) and seabream fish (Adachi *et al.*, 2005) under high UV conditions, which could imply that UV has played some role in the colouration of animal skin and that melanin allows for UV protection in these animals.

Cellular stress response mechanisms may also be activated to counteract UV. For example, antioxidants are able to remove UV-induced ROS. Additionally, the family of heat shock proteins known as Hsp70 are highly conserved proteins whose expression is induced in response to cellular stressors such as heat shock and infrared radiation (De la Coba *et al.*, 2009), as well as being induced in the skin of humans and laboratory animals in response to UV (Muramatsu *et al.*, 1992; Simon *et al.*, 1995; Matsuda *et al.*, 2010). These proteins are thought to be involved in cellular protection, by binding to damaged proteins to decrease the level of protein unfolding and potential aggregation (Hirsch *et al.*, 2006; Lennikov *et al.*, 2013; Morris *et al.*, 2013), and to prevent the unnecessary removal of repairable proteins.

Once UV damage has occurred, there are several defensive mechanisms which are capable of removing the damage, to prevent the likelihood of skin cancer. DNA repair mechanisms to resolve UV-induced genetic damage include excision repair mechanisms (base excision repair and nucleotide excision repair) to remove damaged DNA bases, as well as end joining (homologous and non-homologous) to repair double-strand breaks. Base excision repair is activated when a single base is damaged by UV or other toxic agents. During this process, the damaged strand is ligated, the base is cleaved and replaced using DNA polymerase, and the strand is re-sealed (Sinha and Hader, 2002). Nucleotide excision repair (which is absent in mitochondria) is activated to remove larger lesions such as pyrimidine and purine dimers. During this process, the DNA dimer is excised and the gap is filled by polymerase, after which the DNA strand is re-sealed (Sinha and Hader, 2002). If multiple single-strand breaks occur in close proximity on opposite strands, this can result in

double-strand breaks. Double-strands are repaired by either homologous or non-homologous end joining. Homologous end joining involves the use of an undamaged chromosome as a template for the synthesis of lost bases, followed by strand ligation (Shuman and Glickman, 2007). Non-homologous end joining involves the processing and sealing of the broken strands by ligase (Shuman and Glickman, 2007). The p53 tumour suppressor gene can respond to UV-induced DNA damage, causing the activation of downstream genes, and a cell cycle arrest may occur if it is possible to repair the DNA (Amundson *et al.*, 2002; Yamaguchi *et al.*, 2006). If the DNA damage is too vast, apoptosis (programmed cell death) can be initiated to prevent potentially carcinogenic mutations from being replicated (Yamaguchi *et al.*, 2006; Schafer *et al.*, 2010).

1.6 Hypotheses

Mitochondria are thought to play a key role in the ageing process; however, the exact nature of this role is undetermined. Therefore, further work is required to provide insights into the changes in the mitochondria with age. As ageing is a very broad topic, multiple aspects of the mitochondria are expected to be involved in the ageing process and are required to be examined.

The least studied mitochondrial ETC unit, complex II, has recently been implicated in the ageing process; therefore, this complex was selected to be examined in multiple areas of the study. The measurement of complex II activity in human skin from differently aged individuals has not been performed previously. It was hypothesised that there may be age-related differences in complex II activity in human skin, as well as in complex II subunit protein and expression levels. If this complex is found to be associated with age, this would provide insights into the role of complex II in human ageing.

Senescent cells are thought to play a key role in the ageing process, whereby an accumulation reduces tissue function in older individuals. It is hypothesised that senescent cells from older individuals behave differently to senescent cells from younger individuals, which has not been assessed previously. Therefore, differences in mitochondrial complex II activity between senescent cells from the skin of younger and older individuals were examined, to provide information on the causes of mitochondrial differences with age.

It was additionally hypothesised that differences in mitochondrial complex II activity exist between different cell types, which could have implications in terms of ageing rates of specific cell types. Complex II activity was therefore tested in a variety of human cell types derived from the skin, the lungs, and the liver.

MtDNA deletions and mutations have been shown to increase with both age and UV exposure in human and animal skin. As many of the same phenotypes are present for both photo-aged and chronologically-aged skin, differently UV-exposed skin may be used as a model for differently aged skin. In this context, it was hypothesised that skin under lower levels of UV (representing lower natural age) will have lower mtDNA damage, and that this damage will be decreased by

more effective cellular defensive mechanisms. MtDNA damage was therefore measured in an animal model exposed to varying levels of natural UV, as a model for different ages, to determine whether damage is increased with age in mtDNA, and to examine which aspects of cellular defence result in the lowest levels of mtDNA damage which could have possible implications for the treatment of human ageing. Whale skin was chosen for this purpose, as these animals face excessive natural UV exposure, they are long-lived so may accumulate UV damage over their lifetimes, and they lack UV protection from fur or feathers. Additionally, due to the high-levels of UV which whales are exposed to throughout their long lifetimes, it is likely that they will have strong defensive mechanisms to counteract this damage. Three whale species were chosen to be examined, as these species were likely to have undergone different levels of UV exposure, due to differences in pigmentation, apoptosis, micro-vesicles, migration patterns, dive times, and the level of Hsp70 expression.

Chapter 2. Materials and Methods

The general materials and methods described within this chapter were used throughout the project. More specific materials and methods sections are given at the beginning of each chapter, if a particular method was used only in that chapter. Green lines on graphs in results sections represent a significant correlation and show the line of best fit, and were added to graphs using the linear regression analysis feature of GraphPad Prism 6 (GraphPad Software Inc., USA).

2.1 Acquiring Primary Tissue

2.1.1 *Primary cell culture from human skin samples*

Primary skin cells (fibroblasts and keratinocytes) were cultured from foreskin samples obtained from donors from the Urology department, Royal Victoria Infirmary (Newcastle upon Tyne, UK). Whole foreskin samples were transferred immediately to DMEM following excision, then transferred to 60.1 cm^2 Petri dishes (Techno Plastic Products, Switzerland) containing 5 ml phosphate buffered saline (PBS) (Sigma-Aldrich, UK) supplemented with 5 U/ml penicillin and 5 µg/ml streptomycin (PS) (Invitrogen, UK), to wash the skin samples. Sterilised tweezers and scalpel were used to remove excess fat from the sample. The sample was then placed into a Universal tube (Greiner Bio One, UK) containing PBS plus 20 mg dispase (Roche, UK), and left for 16 hours at 4°C, during which the dispase was able to separate the epidermis from the dermis. Following incubation, the sample was placed into a Petri dish and the epidermis peeled from the dermis using sterilised tweezers. Keratinocytes were cultured from the epidermis by placing the whole epidermis into a Universal tube containing 5 ml trypsin-ethylenediaminetetraacetic acid (TE) (Lonza, UK), followed by incubation at 37°C for 5 minutes with a vigorous shake midway through the incubation to assist in the removal of cells from the tissue. The activity of TE was neutralised by the addition of an equal volume of foetal calf serum (FCS) (Invitrogen, UK), and the sample was centrifuged at 1200 rotations per minute (rpm) for 5 minutes. The cell pellet containing the keratinocyte cells was resuspended in 15 ml Epilife Medium (Life Technologies, UK) containing 10% FCS and PS (complete Epilife), after which the cell sample was transferred to a 75 cm^2 Tissue Culture Flask (Corning Inc., USA), and maintained at 37°C in a humidified atmosphere with 5% carbon dioxide (CO_2) until use. Keratinocytes were cultured from the epidermis by Professor Nick Reynolds'

research group (Newcastle University). Fibroblasts were cultured from the dermis by scoring a Petri dish with a scalpel to allow adhesion of dermal sections to the dish, and the whole dermis was cut into sections of 2-5 mm^2 and approximately 10 dermal sections were placed onto the scored regions of the dish. Sections were covered with FCS, and incubated at 37°C for 16 hours. Following incubation, 10 ml Dulbecco's Modified Eagle Medium with 4.5 g/L glucose and L-glutamine (DMEM) (Lonza, UK) containing 10% FCS and PS (complete DMEM) was added to the Petri dish, and the cells were grown for approximately 3 weeks with the media replaced every 5 days. As keratinocyte cells were able to be cultured in a much shorter time frame, these were either used before the fibroblast cells or stored at -80°C until use. Further information regarding the age, sex, race, and body site of each donor skin sample is given in the Appendix (Table 13 and Table 14).

2.2 Cell Culture

2.2.1 *Primary fibroblast, HDFn, HaCaT, HepG2, a549 Parental, MRC5, and MRC5/hTERT cells*

Primary fibroblast cells, neonatal human dermal fibroblast cells (HDFn) (Invitrogen, UK), an immortalised human keratinocyte cell line (HaCaT) (Boukamp *et al.*, 1988), a hepatocyte carcinoma cell line (HepG2), a human lung adenocarcinoma epithelial cell line (a549 Parental), a human foetal lung fibroblast cell line (MRC5), and a MRC5 cell line overexpressing a subunit of telomerase (MRC5/hTERT) were cultured in complete DMEM and maintained at 37°C in a humidified atmosphere with 5% CO_2. Cells were passaged 2-3 times a week by washing twice in PBS, then incubating with TE for 5 minutes at 37°C. Following incubation, an equal volume of complete DMEM was added to neutralise the TE, and cells were split into two new flasks with 15 ml complete DMEM. MRC5 and MRC5/hTERT cells were received from Dr Gabriele Saretzki (Newcastle University). Primary fibroblasts were used up to passage 6, HDFn cells up to passage 30, HaCaT cells up to passage 60, HepG2 cells up to passage 30, a549 Parental cells up to passage 30, MRC5 cells up to passage 35, and MRC5/hTERT cells up to passage 140 (Lawless *et al.*, 2012).

2.2.2 *Primary keratinocyte cells*

Primary keratinocyte cells were cultured at 37°C in a humidified atmosphere containing 5% CO_2, in complete Epilife supplemented with human keratinocyte growth supplement (HKGS) (Invitrogen, UK). Cells were passaged 1-2 times a week, and were not used past passage 2-3, after which cell differentiation may begin to occur.

2.2.3 *a549 Rho-zero cells*

The a549 Rho-zero cells were the same cell type as the a549 Parental cells, but were cultured in a low concentration of ethidium bromide to inhibit the synthesis of mtDNA (Hashiguchi and Zhang-Akiyama, 2009). This prevented the correct assembly of mitochondrial complexes encoded in part by mtDNA (complexes I, III, IV and V), resulting in a dysfunctional respiratory chain. Rho-zero cells were cultured in complete DMEM supplemented with 50 µM uridine (Sigma-Aldrich, UK), as these cells are unable to synthesis this amino acid (Hashiguchi and Zhang-Akiyama, 2009). Cells were obtained from Professor Ian Holt (University of Cambridge).

2.2.4 *Cell storage*

Cells which were not immediately required were frozen at -80°C, by washing cell culture flasks twice with PBS, then removing the cells from the flask using TE at 37°C for 5 minutes, followed by the addition of media to neutralise the TE. Cells were centrifuged at 1200 rpm for 5 minutes, and the pellet resuspended in 1 ml FCS containing 10% dimethyl sulfoxide (DMSO) (Fisher Scientific, UK), and transferred to a 1.6 ml CryoPure Tube (Sarstedt, Germany), and stored at -80°C. To use frozen cell samples, samples were rapidly thawed and added to 20 ml appropriate media. Cells were kept at 37°C in a humidified atmosphere with 5% CO_2, and the media replaced after 24 hours.

2.3 Photometry

Total cell count of cells to be examined photometrically was determined using a haemocytometer, with approximately 9 x 10^6 cells used for each sample in total, for the citrate synthase activity, the complex II activity, and the complex IV activity assays. To prepare cells for photometry, cell culture flasks were washed twice with PBS, and TE was added to detach cells from the flask, during a

5 minute incubation at 37°C. An equal amount of the appropriate media for each cell type was added to neutralise the TE, and cells were centrifuged at 1200 rpm for 5 minutes. The supernatant was discarded and cells were resuspended in 2 ml PBS and centrifuged at 1200 rpm for 5 minutes to remove any remaining media. The supernatant was again discarded and cells were resuspended in 200 µl complex II buffer (25 mM potassium phosphate and 5 mM magnesium chloride (Sigma-Aldrich, UK), in deionised water (dH_20), pH 7.2). Samples were snap frozen 3 times in liquid nitrogen to break open the cell membranes, and stored at -80°C until use. HaCaT, HepG2, a549 Parental cells, and a549 Rho-zero cells were maintained by Dr Alasdair Anderson (Newcastle University) until preparation for photometry was performed. To perform the photometric assays (Birch-Machin and Turnbull, 2001; Kirby *et al.*, 2007), a Cary 300 Bio UV-Visible Spectrophotometer (Varian Inc., USA) was used, with the output viewed using Cary WinUV Kinetics Application (Varian, Inc.).

2.3.1 *Protein assay*

The concentration of samples examined via photometry was approximately 7 mg/ml, as determined by a protein assay. During this process, standard protein concentrations were prepared at 2-fold dilutions from a 2 mg/ml bovine serum albumin (BSA) standard solution (Thermo Scientific, UK), to produce concentrations of 1.5 mg/ml, 0.75 mg/ml, 0.38 mg/ml, 0.19 mg/ml, 0.09 mg/ml, and 0.05 mg/ml. Cell samples were diluted either 5-fold or 2-fold. A Bio-Rad Detergent-Compatible Protein Assay (Bio-Rad, UK) was used. The alkaline copper tartrate solution (Reagent A and S at a ratio of 50:1) which reacts with the protein in the colorimetric assay, was added to each sample or standard at a ratio of 5:1, and the solution was added in triplicate to wells of a 96-Well Plate (Techno Plastic Products, Switzerland) with 30 µl per well. To each well, 200 µl Folin Reagent (Reagent B) was added to start the reaction and the plate was incubated for 15 minutes at 20°C, after which the absorbance was measured at 750 nm using a SpectraMax 250 Microplate Reader (Molecular Devices, UK) with the results viewed using SoftMax Pro V3.1.1 (Molecular Devices, UK).

2.3.2 *Citrate synthase activity assay*

Citrate synthase activity is measured to determine mitochondrial content per sample. Citrate synthase converts oxaloacetate and acetyl coenzyme A to citrate and coenzyme A respectively during the citric acid cycle (Wiegand and Remington, 1986). Photometry can be used to measure the amount of coenzyme A, and therefore the rate of the reaction, via the addition of 5,5'-dithiobis-2-nitrobenzoate (DTNB), which reacts with coenzyme A to form the 5-thio-2-nitrobenzoate ion (Itoh and Srere, 1970). The rate of citrate synthase activity can be determined by measuring the level of 5-thio-2-nitrobenzoate at 412 nm, which should increase over time. To perform the citrate synthase assay, the following reagents were added to a 1 cm^2 Plastic Cuvette (Fisher Scientific, UK): 100 µM DTNB (Sigma-Aldrich, UK), 1% w/v of the detergent Triton X (Sigma-Aldrich, UK) to break open cell membranes, 50 µM acetyl coenzyme A (Sigma-Aldrich, UK), and at least two different volumes of sample (with 20 µl used initially and either more or less used depending on the outcome) (Kwong and Sohal, 2000). This was made up to 1 ml with citrate synthase stock buffer (0.1 mM Tris-hydrochloride (Sigma-Aldrich, UK), in dH_20, pH 8.0, 30°C). The cuvette was gently mixed and added to the spectrophotometer, after which the reaction was set to zero, and the run was started and left for 30 seconds to obtain a baseline measurement. Following this time period, 250 µM of the substrate oxaloacetate was added to begin the enzymatic reaction, and citrate synthase activity was measured at 412 nm for 2 minutes.

In order to calculate the citrate synthase activity in nanomoles of 5-thio-2-nitrobenzoate produced per minute (nmol/min), the extinction coefficient of this ion had to be taken into account. This is the strength at which light is absorbed by the particular ion at the particular wavelength used, with the extension coefficient of 5-thio-2-nitrobenzoate being 13.6 mM^{-1}/cm^{-1} (Eyer *et al.*, 2003; Kirby *et al.*, 2007). The sample volume and total volume also had to be taken into account. If for example a sample gave an absorbance per minute (abs/min) of 0.087, when 20 µl of sample was added to the reaction and the total reaction volume was 1000 µl, then the citrate synthase activity would be calculated by dividing the abs/min by the extinction coefficient and multiplying by the dilution factor (Kirby *et al.*, 2007), as follows:

Citrate synthase activity = (abs/min ÷ 13.6) x (dilution factor)
= (0.087 ÷ 13.6) x (1000 ÷ 20)
= 0.32 nmol/min

2.3.3 *Complex II activity assay*

During the complex II activity assay, the other mitochondrial ETC complexes I, III, and IV were inhibited using rotenone (Sigma-Aldrich, UK), antimycin A (Sigma-Aldrich, UK), and potassium cyanide (Sigma-Aldrich, UK) respectively. The substrate sodium succinate and the e^- acceptor ubiquinone were added in excess, and the artificial e^- acceptor dichlorophenolindophenol (DCPIP) (Sigma-Aldrich, UK) was added in its oxidised form to accept e^- as ubiquinol (Sigma-Aldrich, UK) was oxidised to ubiquinone (Kirby *et al.*, 2007; Quinlan *et al.*, 2012). The decrease in oxidised DCPIP was measured at 600 nm to determine complex II activity. To perform the complex II activity assay, 20 mM sodium succinate (Sigma-Aldrich, UK), 1 ml complex II buffer (containing 3 mM potassium cyanide), and at least two different volumes of sample were added to a 1.5 ml Eppendorf tube, and incubated at 30°C for 10 minutes to activate complex II. Following incubation, the solution was added to a 1 cm^2 plastic cuvette to which 50 µM DCPIP, 3.6 µM antimycin A, and 5 µM rotenone were added. The cuvette was gently mixed and added to the spectrophotometer, after which the reaction was set to zero, and the run was performed for 30 seconds to obtain a baseline measurement. Following this time period, 65 µM of ubiquinone was added to start the reaction, and the absorbance of light at 600 nm was measured for 4-5 minutes.

In order to calculate complex II activity, in nanomoles of DCPIP reduced per minute (nmol/min), the extinction coefficient of DCPIP (19.1 mM^{-1}/cm^{-1}) was taken into account (Kirby *et al.*, 2007; Quinlan *et al.*, 2012), as well as the volume of sample added to the reaction and the total volume used. For example, if a sample gave an abs/min of 0.043, with 20 µl added to a 1000 µl reaction:

Complex II activity = (abs/min ÷ 19.1) x (dilution factor)
= (0.043 ÷ 19.1) x (1000 ÷ 20)
= 0.11 nmol/min

Once complex II activity had been determined, it was then normalised to citrate synthase activity to allow complex II activity per mitochondrial unit to be determined (Birch-Machin and Turnbull, 2001). To do this, complex II activity per unit of citrate synthase activity (CII/CS) was calculated as follows (Kirby *et al.*, 2007):

CII/CS = Complex II activity ÷ citrate synthase activity
= 0.11 ÷ 0.32
= 0.34 nmol DCPIP reduced/min/citrate synthase unit

2.3.4 *Complex IV activity assay*

During the complex IV activity assay, n-dodecyl-β-D-maltoside (DDM) (Sigma-Aldrich, UK) was used to solubilise the mitochondrial membrane (le Maire *et al.*, 2000), and the rate of complex IV was determined via the addition of the substrate reduced cytochrome *c* (Sigma-Aldrich, UK), which was oxidised by complex IV. The absorbance of reduced cytochrome *c* was measured at 550 nm to determine complex IV activity, which should decrease over time. To perform the complex IV activity assay, the following reagents were added to a 1 cm^2 plastic cuvette: 345 µM DDM, 15 µM reduced cytochrome *c*, and complex IV buffer to a final volume of 1 ml (20 mM potassium phosphate (Sigma-Aldrich, UK), in dH_20, pH 7.4, 30°C). The cuvette was gently mixed and added to the spectrophotometer with the reaction set to zero, and the run was then started for 30 seconds to obtain a baseline measurement. The mitochondrial sample was then added to the cuvette following the 30 seconds (for at least two different runs with two different volumes of sample), and the run was continued for 3.5 minutes. Following this time period, several grains of potassium ferricyanide (Sigma-Aldrich, UK) were added to fully oxidise the remaining cytochrome *c*, to allow the endpoint of the reaction to be obtained and the amount of cytochrome *c* which was available to be found.

As the oxidisation of cytochrome *c* occurs at an exponential rate, it was inappropriate to measure just the initial reaction period, which would not be a linear rate. The rate of cytochrome *c* oxidisation was therefore expressed as a first-order rate constant (Kirby *et al.*, 2007). To determine the activity of complex IV as a first-order rate constant (k/sec), the rate of the exponential phase of the reaction was determined. To do this, 6 time points (T_0 to T_5) were initially chosen during the exponential phase of the reaction, and the abs/min of each of

these time points (A_0 to A_5) were obtained (Figure 10). The overall abs/min change (X) from each time point to the end point was then determined, by subtracting the end point abs/min from each time point abs/min. For example:

X_0 = A_0 – end point
= 0.3372
X_1 = A_1 – end point
= 0.3281
X_2 = A_2 – end point
= 0.3182
X_3 = A_3 – end point
= 0.3100
X_4 = A_4 – end point
= 0.2059
X_5 = A_5 – end point
= 0.1993

Each individual X value (X_1 to X_5) was then normalised to the overall absorbance change (X_0) (e.g. $X_0 \div X_1$) to obtain the values N_0 to N_5, and were converted to log scale due to the exponentially changing absorbance ($\log N_1$ to $\log N_5$) (Kirby *et al.*, 2007). To calculate complex IV activity as a first order rate constant (k/sec), if the time period was for example 72 seconds with 40 µl sample and 1000 µl total volume, using the above X_0 to X_5 values, the following equation would be used:

Complex IV activity = $((\log N_5 - \log N_1) \div$ time period) x 2.303 x (dilution factor)
= (0.216 ÷ 72 seconds) x 2.303 x (1000 ÷ 40)
= 0.17 k/sec

Once complex IV activity was determined, it was normalised to citrate synthase activity (CIV/CS) to determine complex IV activity per unit of mitochondria:

CIV/CS = Complex IV activity ÷ citrate synthase activity
= 0.17 ÷ 0.32
= 0.53 k/sec/citrate synthase unit

Figure 10

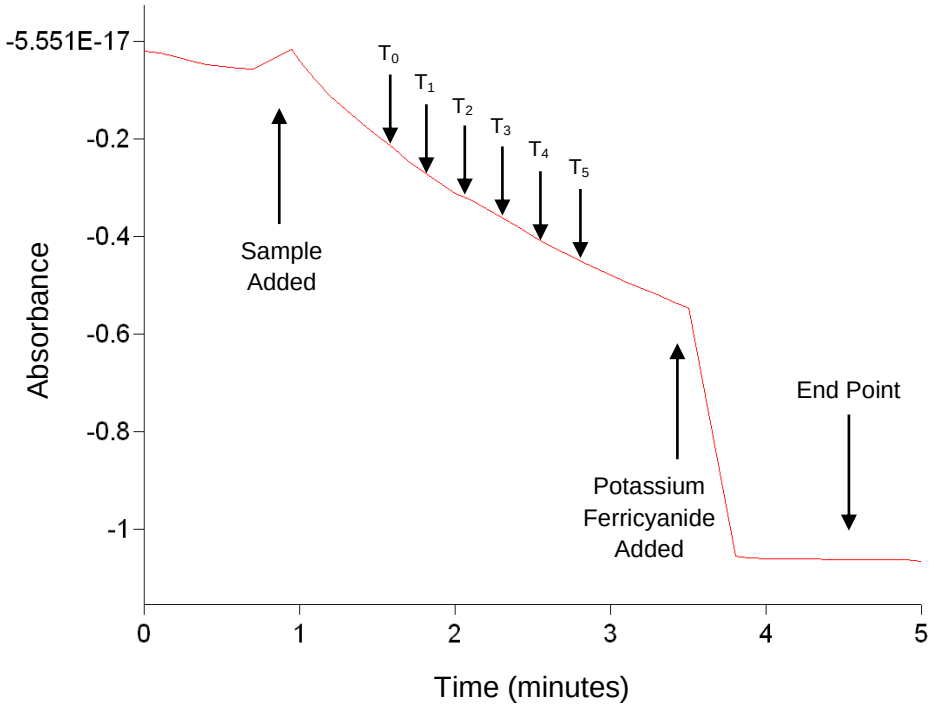

Figure 10. Mitochondrial complex IV activity assay. The graph obtained during the complex IV activity assay using photometry. The reaction was started by the addition of the cell sample, and the exponential decrease in absorbance of reduced cytochrome *c* at 550 nm was measured. Time points T_0 to T_5 were chosen to express complex IV activity as a first-order rate constant. The end point was determined following the addition of potassium ferricyanide to fully oxidise the remaining cytochrome *c*.

2.4 MtDNA Analysis

2.4.1 *DNA extraction*

Total DNA (nuclear and mitochondrial) was extracted from cells using a QIAamp DNA Mini Kit (Qiagen, UK). For cells grown in culture flasks or dishes, cells were washed twice with PBS and the cells removed from the flask using TE, which was neutralised after 5 minutes incubation at 37°C using appropriate media. Cells were placed into a 1.5 ml Eppendorf tube and centrifuged at 8000 rpm for 5 minutes, after which the supernatant was discarded. Cell pellets were resuspended in 200 µl PBS and 20 µl Proteinase K to degrade any proteins present, and 200 µl lysis buffer (Buffer AL) was added to samples. Samples were vortexed for 15 seconds and incubated at 56°C for 10 minutes, to lyse samples. Following the incubation, 200 µl ethanol was added to samples to assist in DNA purification, and the sample was vortexed for 15 seconds. The

solution was added to a QIAamp Spin Column and centrifuged at 8000 rpm for 1 minute to allow DNA to adsorb to the spin column. The flow-through was discarded and 500 µl wash buffer (Buffer AW1) was added to wash the column, and the column was centrifuged at 8000 rpm for 1 minute. The flow-through was again discarded and 500 µl of another wash buffer (Buffer AW2) was added to wash the membrane further, and the column was centrifuged at 14,000 rpm for 3 minutes. The flow-through was discarded and the column centrifuged for 1 minute at 14,000 rpm to completely remove any remaining Buffer AW2. 50-100 µl Buffer AE was added to the column, and samples were incubated at 20°C for 5 minutes, and centrifuged for 1 minute at 8000 rpm to elute the DNA from the membrane into a 1.5 ml Eppendorf tube. This was repeated using the eluted flow-through to increase DNA yield. DNA concentrations were determined using an ND-1000 Nanodrop Spectrophotometer (Thermo Scientific, UK) at a wavelength of 260 nm, and DNA was stored at 4°C until use or at -20°C for long term storage.

2.4.2 *Real-time quantitative polymerase chain reaction*

All real-time quantitative polymerase chain reaction (qPCR) assays for the analysis of either mtDNA damage or relative mtDNA amount were performed using a StepOnePlus Real-Time PCR System (Applied Biosystems, UK) with the results viewed using StepOne Software V2.1 (Applied Biosystems, UK), or using a Chromo4 Real-Time PCR Detection System (Biorad, UK) with the results viewed using MJ Opticon Monitor 3 Analysis Software (Biorad, UK). The StepOnePlus Real-Time PCR System was used unless stated otherwise in the results.

To perform the qPCR reactions using the StepOnePlus Real-Time PCR System, the following components were assembled on ice to a final volume of 20 µl to each well of a MicroAmp Fast Optical 96-Well Reaction Plate (Applied Biosystems, UK): dH_20, 1x Phusion HF Buffer (Thermo Scientific, UK), 0.1x Phusion DNA polymerase (Thermo Scientific, UK), 200 µM dNTP mix (Roche, UK), 0.5 µM each of forward and reverse primers (Eurofins MWG Operons, Germany), 0.1x SYBR Green dye (Sigma-Aldrich, UK), and 100 ng template DNA. For the UV-irradiated cells, a concentration of 30 ng was used based on the limited availability of DNA. The following conditions were used for

the qPCR run: 98°C for 30 seconds; 30 cycles of 98°C for 8 seconds, 60°C for 20 seconds, and 72°C for 135 seconds; and a final stage of 72°C for 8 minutes. A melt curve was added immediately after the reaction with the conditions of: 95°C for 15 seconds; 60°C for 1 minute, followed by a plate read at every 0.3°C temperature increase; ending at 95°C for 15 seconds.

To perform the qPCR reactions using the Chromo4 Real-Time PCR Detection System, the same components as for the StepOnePlus machine were used, and added to a final volume of 20 µl to each well of 0.2 ml 8-Tube Strips (Biorad, UK) with Optical Flat 8-Cap Strips (Biorad, UK). The qPCR conditions used were: 98°C for 30 seconds; 30 cycles of 98°C for 8 seconds, 57°C for 20 seconds (60°C for the 8.5 kb whale sections), and 72°C for 135 seconds (or 230 seconds for the 8.5 kb whale sections); and a final stage of 72°C for 8 minutes. A melt curve was added immediately after the reaction using the same conditions as above.

KAPA HiFi DNA polymerase (KAPA Biosystems, UK) was tested for qPCR efficiency with the whale mtDNA samples using the Chromo4 machine. The components for the reaction were made up to a final volume of 25 µl and added to each well of 0.2 ml 8-Tube Strips with Optical Flat 8-Cap Strips: dH_20, 1x KAPAHiFi Buffer (KAPA Biosystems, UK), 0.5 U KAPA DNA polymerase (1 U/µl) (KAPA Biosystems, UK), 200 µM dNTP mix, 0.5 µM each of the forward and reverse primers, 0.08x SYBR Green dye, and 100 ng template DNA. The qPCR conditions used were: 95°C for 2 minutes; 30 cycles of 98°C for 20 seconds, 57°C for 15 seconds, and 68°C for 135 seconds; and a final stage of 68°C for 5 minutes. A melt curve was added after the reaction with the same conditions as above.

Amplification of the short 83 bp (human) or 51 bp (whale) mtDNA sections was performed using a JumpStart SYBR Green Kit (Sigma-Aldrich, UK), with the following components assembled to a final volume of 25 µl, and added to a MicroAmp Fast Optical 96-Well Reaction Plate: dH_20; 1x JumpStart SYBR Green (Sigma-Aldrich, UK); 0.5 µM each of forward and reverse primers; and 50 ng template DNA. The cycling conditions used were: 94°C for 2 minutes; 35 cycles of 94°C for 15 seconds, 60°C for 45 seconds, and 72°C for

45 seconds; and a final stage of 72°C for 2 minutes. A melt curve followed the reaction with the same conditions as above.

2.4.3 *Agarose gel electrophoresis*

To ensure mtDNA sections of the correct size were generated following DNA amplification by qPCR, DNA was separated by size using gel electrophoresis. During this technique, an electrical charge is applied to a gel, which causes DNA movement from the negative to the positive electrode (due to the negative charge of DNA), with the agarose gel providing a matrix through which the differently-sized DNA fragments pass at different rates (Lee *et al.*, 2012). Larger fragments pass through this agarose matrix at a slower rate than shorter fragments. The agarose gel was produced using agarose at 1.5% w/v, dissolved in 50 ml 1x TAE buffer (40 mM Tris acetate (Fisher Scientific, UK), 1 mM ethylenediaminetetraacetic acid (EDTA) (Fisher Scientific, UK), pH 8.3) with 1 µg/ml ethidium bromide. Gels were set in a template and added to an electrophoresis tank containing 1x TAE buffer. DNA Loading Buffer (Bioline, UK) was added to samples at a ratio of 1:6 and 10 µl of the sample/loading buffer was added to each gel well, with 5 µl Hyperladder 1 (Bioline, UK) used as a reference for DNA lengths. Reaction conditions were 120 volts (V) and 56 milliamps (mA) for 40 minutes, and results were viewed using UV light from a FluorChem imaging system (Alpha Innotech, Germany) with AlphaEase FluorChem software (Alpha Innotech, Germany).

Chapter 3. Mitochondrial Complex II Activity in the Skin of Young and Old Human Donors

3.1 Introduction

3.1.1 *Complex II and the ageing process*

Previous studies have implicated a possible involvement of the mitochondrial ETC complexes in the ageing process, of which complex II will be focused on in the present study. Past work has demonstrated a potential role of complex II in the ageing process, by demonstrating that mutations in the SDHC subunit can cause an accelerated accumulation of ageing markers and a decreased lifespan compared to the wild-type in *C. elegans* (Hosokawa *et al.*, 1994; Adachi *et al.*, 1998; Ishii *et al.*, 1998; Pfeiffer *et al.*, 2011). This decrease in lifespan was prevented when respiration through complex II was blocked (Pfeiffer *et al.*, 2011). A decreased lifespan caused by complex II defects in SDHC has also been seen in Drosophila (Tsuda *et al.*, 2007). Mutations in another subunit, SDHB, were also found to generate a similar phenotype in terms of accelerated ageing in nematodes (Huang and Lemire, 2009; Wojtovich *et al.*, 2013), suggesting that complex II is able to affect the ageing process. The reduction in lifespan observed was thought to be due to an increase in superoxide production (Ishii *et al.*, 2004), causing free radical damage to cellular components, and accelerated ageing. Another study found that drosophila with mutated SDHB subunits had increased oxidative stress levels, accelerated ageing, and decreased lifespans, which were specific to complex II defects as none of the other complexes were affected (Walker *et al.*, 2006).

The exact role of complex II in terms of mammalian ageing remains unknown and has only recently begun to be elucidated. Complex II has been suggested to play a role in the ageing process of mammals (Velarde *et al.*, 2012), as it was found that complex II was lower in the skin of naturally aged older mice compared to younger mice, suggesting that complex II activity decreased with age in mouse skin. It was also found that when the mitochondrial antioxidant SOD was knocked-out in mice, they showed impaired complex II activity, which has also been shown previously in this mouse-type (Li *et al.*, 1995), as well as accelerated ageing, with increased senescence and nDNA damage (Velarde *et al.*, 2012). Increased ROS production was also observed in the mice, which was thought to be contributing to senescence *in vivo* and therefore to the ageing process (Velarde *et al.*, 2012); however, it is unknown whether the activity of complex II was causative or consequential in terms of natural mouse ageing.

Other studies have demonstrated that the activity of complex II is decreased with age in various rat tissues such as heart, liver, muscles, kidneys, lungs, brain, and lymphocytes (Sandhu and Kaur, 2003; Kumaran *et al.*, 2004; Cocco *et al.*, 2005; Balietti *et al.*, 2009; Braidy *et al.*, 2011); however, a lack of decrease in certain mouse tissues has also been observed (Kwong and Sohal, 2000). Additionally, studies have demonstrated that mutations in the complex II subunit SDHC in hamster and mouse cell lines can result in an increased production of steady-state superoxide and hydrogen peroxide (Ishii *et al.*, 2005; Slane *et al.*, 2006), which could potentially accelerate the ageing process.

Complex II ROS production could potentially be contributing to the ageing process. The majority of studies on ROS production by normal mitochondria have focussed on complexes I and III (Cadenas *et al.*, 1977; Turrens *et al.*, 1985; Hirst *et al.*, 2008; Murphy, 2009; Bleier and Dröse, 2013; Wojtovich *et al.*, 2013). However, other work has suggested a possible prominent role for complex II in terms of normal ROS production (Guo and Lemire, 2003; Lemarie *et al.*, 2011; Quinlan *et al.*, 2012), which could contribute to the ageing process via free radical damage (Harman, 1956). Quinlan *et al*., (2012) found that complex II was capable of producing ROS levels comparable to those of complexes I and III in mitochondria isolated from rat skeletal muscle. Complex II ROS production has also been shown to prevent cell cycle progression (Byun *et al.*, 2008), which could indicate that increased complex II ROS production contributes to the senescent phenotype of cells seen with age.

Further understanding of this important mitochondrial complex is vital to improve our knowledge of the ageing process, for which mitochondrial complex II could play a causative role. Further studies into the role of complex II in ageing are required to understand the exact role, preferentially in human tissues.

3.1.2 *The role of mitochondrial complexes I, III, and IV in ageing*

In terms of the other mitochondrial complexes in ageing (complexes I, III, and IV), previous studies have shown that complex I activity (Lenaz *et al.*, 1997; Tatarkova *et al.*, 2011), complex III activity (Lesnefsky *et al.*, 2001; Kumaran *et al.*, 2004; Tatarkova *et al.*, 2011), and complex IV activity (Trounce *et al.*, 1989;

Boffoli *et al.*, 1994; Hayashi *et al.*, 1994; Rooyackers *et al.*, 1996; Isobe *et al.*, 1998; Sandhu and Kaur, 2003; Braidy *et al.*, 2011; Andreollo *et al.*, 2012) can decrease in an age-dependant manner in both human and animal tissues. However, some studies have shown conflicting results, with complexes III and IV shown not to be altered with age in human lymphocyte cells (Drouet *et al.*, 1999). In mice, the activity of the different complexes with age has been shown to be tissue-dependant, as complex I was shown not to change with age in the brain, heart, liver, kidneys, or skeletal muscle; complex III was decreased with age in the brain but did not change in the heart, liver, or kidneys and was increased in the skeletal muscle; and complex IV was decreased in the heart and kidneys, but did not change in the brain, liver, or skeletal muscle (Kwong and Sohal, 2000). Therefore, it is inconclusive as to the exact role of the mitochondrial complexes in terms of the ageing process.

3.2 Hypotheses

The main reason for this area of my project was to further understand the role of complex II, the least studied complex of the mitochondrial respiratory chain, in human ageing. This was performed using human skin cells from differently aged donors, to allow for differences in natural age to be determined in a non-sun-exposed region of the body. The specific hypotheses of this chapter were 1) differences in complex II activity exist with age in human skin cells; 2) differences also exist with age in the specific subunits of complex II; and 3) these differences in complex II activity with age are specific to complex II, and are not observable in another complex of the respiratory chain.

3.3 Materials and Methods

The cell culture and photometric techniques used in this chapter are given in the general Materials and Methods (Chapter 2).

3.3.1 *RNA extraction from cells*

In order to study the expression of specific complex II subunit transcripts, RNA (which gives information on the level of DNA expression) had to be isolated. RNA was extracted from cell cultures using an RNeasy Mini Kit (Qiagen, UK), with approximately 1.5 x 10^6 cells used per sample. Cell culture flasks were washed twice with PBS, and cells were removed from the flask by incubating with TE for 5 minutes at 37°C, followed by TE neutralisation using appropriate media. Cells were centrifuged at 8000 rpm for 5 minutes, and the cell pellets resuspended in 350 µl lysis buffer (Buffer RLT). The lysate was homogenised by vortexing for 1 minute, and an equal volume of 70% ethanol was added to the sample to help purify the RNA. The sample was transferred to an RNeasy spin column containing a silica-based membrane to which RNA could bind, and the column was centrifuged at 10,000 rpm for 15 seconds. The flow-through was discarded and 700 µl wash buffer (Buffer RW1) added to wash the spin column and remove unwanted biomolecules, during centrifugation at 10,000 rpm for 15 seconds. The flow-through was again discarded and 500 µl of a different wash buffer (Buffer RPE) was added to further wash the membrane, during centrifugation at 10,000 rpm for 15 seconds. The second wash was repeated, and the column centrifuged for 2 minutes at 10,000 rpm, to allow any ethanol in the wash buffer to be removed. The column was re-centrifuged at 13,200 rpm for 1 minute to dry the membrane completely. Spin columns were placed in a 1.5 ml Eppendorf tube, and 30 µl RNase-free water was applied to the centre of the silica membrane, followed by centrifugation at 10,000 rpm for 1 minute to elute the RNA from the membrane for collection. The concentration of RNA was determined using an ND-1000 Nanodrop Spectrophotometer at a wavelength of 260 nm.

3.3.2 *Reverse transcription of RNA*

To measure the relative expression of a transcript, the extracted RNA was used as a template to produce complementary DNA (cDNA) for use in qPCR. Reverse transcription was performed using a High Capacity cDNA Reverse

Transcription Kit (Applied Biosystems, UK). During this process, the following components were added to a final volume of 20 µl per well, to MicroAmp Fast Reaction Tubes with MicroAmp Optical 8-Cap Strips: dH_20, 1x RT Buffer (Applied Biosystems, UK), 200 µM dNTP mix, 1x RT Random Primers (Applied Biosystems, UK), 50 U MultiScribe Reverse Transcriptase (Applied Biosystems, UK), 1 U RNase Inhibitor (Applied Biosystems, UK), and 500 ng template RNA. A GeneAmp PCR System 9700 (Applied Biosystems, UK) was used to perform the reverse transcription reaction, with the following conditions: 25°C for 10 minutes, 37°C for 120 minutes, and 85°C for 5 minutes.

3.3.3 *Real-time qPCR to determine gene expression*

QPCR was performed on the cDNA to determine the relative expression levels of the complex II subunits SDHA, SDHB, and SDHC. In order to study the complex II subunits, primers to amplify a 70 bp region of the SDHA gene (on chromosome 5), a 77 bp region of the SDHB gene (on chromosome 1), and an 86 bp region of the SDHC gene (on chromosome 1) were used (Applied Biosystems, UK). To perform the qPCR reaction, the following components were assembled to a final volume of 25 µl, and added to a MicroAmp Fast Optical 96-Well Reaction Plate: dH_20, 1x TaqMan Gene Expression Master Mix (Applied Biosystems, UK), 1x TaqMan Gene Expression Assay primer/probe set (Applied Biosystems, UK), and 20 ng template cDNA. QPCR reactions were performed on a StepOnePlus Real-Time PCR System with the results viewed using StepOne Software V2.1. The following conditions were used for the reaction: 50°C for 2 minutes; 95°C for 10 minutes; and 40 cycles of 95°C for 15 seconds and 60°C for 1 minute.

In order to normalise the amount of SDHA, SDHB, or SDHC transcript to the overall amount of nDNA present, a housekeeping gene transcript at equal levels in all cell types was used. This transcript used as an internal control for normalisation was β-actin (β-act), which has been shown to be expressed at a constant level in skin fibroblasts (Li *et al.*, 2011). QPCR was performed simultaneously for all transcripts. Relative expression levels were normalised to β-act as determined by the $2^{-\Delta\Delta Ct}$ method (Livak and Schmittgen, 2001). The $2^{-\Delta\Delta Ct}$ method calculates the relative transcript level by finding the difference between the β-act and the target transcript cycle threshold values (Ct) for each

sample (the ΔCt). This value is then normalised to a chosen control sample, and expressed to the power of 2, as each 1 Ct represents a 2-fold difference in damage:

$$2^{-\Delta\Delta Ct} = 2\text{^-}(\Delta Ct \text{ of sample} - \Delta Ct \text{ of control})$$

3.3.4 *Protein amount*

To determine the amount of complex II subunit proteins present, Western blotting was used. Prior to this, the amount of overall protein per sample was determined to allow the same amount of protein to be added per Western blot. To determine protein concentrations, a protein assay was performed. During this technique, approximately 9 x 10^6 cells grown in flasks were washed twice with PBS, and removed from the flasks via a 5 minute incubation with TE at 37°C. TE was then neutralised using complete DMEM, and the sample was transferred to a 1.5 ml Eppendorf tube and centrifuged at 1200 rpm for 5 minutes. The supernatant was discarded and the pellet resuspended in 1.5 ml PBS to wash any remaining media from the sample, after which the sample was centrifuged again at 1200 rpm for 5 minutes. The supernatant was removed, and the pellet resuspended in 200 µl Radio-Immunoprecipitation Assay Buffer (RIPA Buffer) (Sigma-Aldrich, UK) containing 1 Protease Inhibitor Cocktail Tablet (Roche, UK) per 50ml solution, to lyse the cells, and samples were sonicated for 10 seconds. A protein assay was then performed on samples as described in section 2.3.1.

3.3.5 *Western blotting*

To determine the relative levels of the complex II subunit proteins (SDHA and SDHB) within a sample, Western blotting was performed. Samples were diluted to the appropriate concentrations in dH_20 to 10 µl, based on the results of the protein assay, and an equal volume of loading buffer was added (loading buffer final concentration: 62.5 mM Tris-hydrochloride (Fisher Scientific, UK), 2% sodium dodecyl sulphate (SDS) (Sigma-Aldrich, UK), 10% glycerol (Fisher Scientific, UK), and 0.002% bromophenol blue (Sigma-Aldrich, UK), in dH_20, pH 6.8, with 10% β-mercaptoethanol (Fisher Scientific, UK)). Samples were kept at 95°C for 5 minutes to break the disulphide protein bonds. Novex 4-20% Tris-Glycine Mini Gels 1.0 mm 10 Well (Life Technologies, UK) were placed into

an XCell SureLock Mini-Cell Electrophoresis System (Life Technologies, UK), and running buffer (25 mM Tris base (Fisher Scientific, UK), 190 mM glycine (Fisher Scientific, UK), and 0.1% SDS, in dH_20, pH 8.3) was added to the tank to cover the gel. 10 µl BenchMark Pre-Stained Protein Ladder (Life Technologies, UK) or 20 µl sample was then added to each well. Gel electrophoresis was performed for 90 minutes at 75 V, 40 mA, and 5 Watts (W), using a PowerEase 500 Power Supply (Life Technologies, UK).

Following electrophoresis, gels were transferred to a Trans-Blot Turbo Transfer Pack Mini Format 0.2 µM Nitrocellulose membrane (Biorad, UK), and a Trans-Blot Turbo Transfer System (Biorad, UK) was used to perform the transfer. The settings used were 25 V and 1.3 amps for 7 minutes. Membranes were then placed into a 50 ml Centrifuge Tube (Sarstedt, Germany) and washed using Tris-buffered saline with tween (TBS-tween) (25 mM Tris-Base, 150 mM sodium chloride (Fisher Scientific, UK), 0.1% Tween 20 (Fisher Scientific, UK), in dH_20, pH 8.0) 3 times with gentle shaking. To block non-specific binding, 5% BSA (Sigma-Aldrich, UK) in TBS-tween was added to membranes for 1 hour with gentle shaking. Following blocking, the membrane was washed 3 times with TBS-tween, the primary antibody was added to the membrane at a concentration of 1 in 5000 in BSA, and the membrane was gently shaken for 1 hour. The primary antibodies used were SDHA (mouse monoclonal, clone number 2E3GC12FB2AE2, catalogue number ab14715, Abcam, UK), SDHB (mouse monoclonal, clone number 21A11AE7, catalogue number ab14714, Abcam, UK), or the control β-act (mouse monoclonal, clone number mAbcam 8226, catalogue number ab8226, Abcam, UK). Membranes were again washed 3 times with TBS-tween. The secondary antibody, peroxidase-labelled anti-mouse IgG (Vector Laboratories Inc., USA), was added at a concentration of 1 in 5000 in BSA for SDHA and SDHB, and at 1 in 10,000 in milk solution (5% Skim Milk (Fisher Scientific, UK), 0.1% sodium azide (Sigma-Aldrich, UK), in TBS-tween) for β-act. Membranes were gently shaken for 1 hour and washed 3 times in TBS-tween. Membranes were then removed from tubes and 0.75 ml SuperSignal West Dura Extended Duration Substrate (Thermo Scientific, UK) added for 5 minutes to allow later visualisation of the proteins. Membranes were placed in a Hypercassette (GE Healthcare, UK) and exposed to Hyperfilm ECL (GE Healthcare, UK) in the absence of light for varying lengths of time

depending on signal strength. Hyperfilm was placed in Developer and Replenisher (Kodak, UK) for 2 minutes, washed in water, placed in Fixer and Replenisher (Kodak, UK) for 1 minute, then washed in water and left to dry. Films were analysed using a FluorChem imaging system with reflective white light and results viewed using AlphaEase FluorChem software.

3.4 Results

3.4.1 *Mitochondrial amount per sample*

Different samples may contain different amounts of mitochondria. To ensure that any possible changes observed in mitochondrial respiratory chain activity were not confounded by differences in mitochondrial content, the activity of a common mitochondrial marker, citrate synthase (Birch-Machin and Turnbull, 2001), was measured. Citrate synthase is an enzyme which plays a key role in the citric acid cycle, during which citrate synthase converts the substrates oxaloacetate and acetyl coenzyme A to citrate and coenzyme A respectively (Wiegand and Remington, 1986). A spectrophotometer was used to measure the amount of coenzyme A, and therefore the rate of the enzymatic reaction, following the addition of DTNB, which reacts with coenzyme A to form the 5-thio-2-nitrobenzoate ion which is yellow in colour (Figure 11A) (Itoh and Srere, 1970). The rate of citrate synthase activity was determined by the rate of absorbance of 5-thio-2-nitrobenzoate at 412 nm (Figure 11B), which increases as citrate synthase activity takes place. The absorbance of 5-thio-2-nitrobenzoate did not change when no sample was added (Figure 11C). The citrate synthase activities of skin samples taken from a variety of differently aged donors were measured and later used to normalise the activities of complex II and complex IV (Birch-Machin and Turnball 2001).

Figure 11

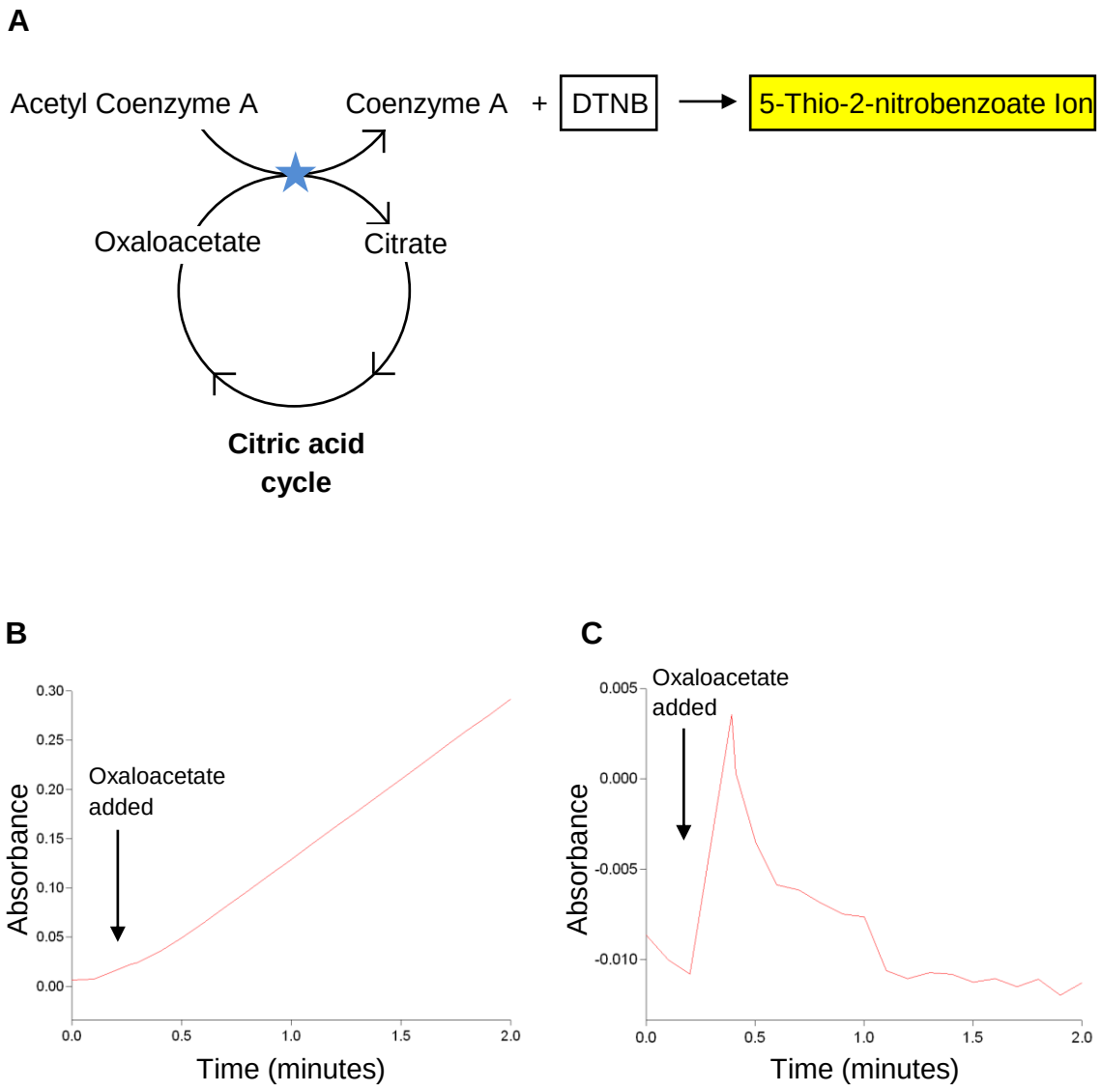

Figure 11. Citrate synthase assay to determine mitochondrial content. A) During the citric acid cycle, acetyl coenzyme A is converted to coenzyme A by citrate synthase, which then reacts with DTNB, which is a colourless solution, to form the 5-thio-2-nitrobenzoate ion which is yellow in colour. The blue star shows the area of citrate synthase activity. B) The absorbance of light at 412 nm was measured to assess the amount of 5-thio-2-nitrobenzoate ion present, from 0 to 2 minutes, with oxaloacetate added to start the reaction. C) The absorbance of light at 412 nm remained constant when no sample was added to the reaction.

3.4.2 *Complex II activity in skin cells from differently aged donors*

The activity of complex II was studied in skin cells cultured from differently aged donors, in order to determine any possible differences in this complex with age. Photometry was used to measure differences in complex II activity (Kirby *et al.*, 2007). During this process, complexes I, III, and IV of the mitochondrial

respiratory chain were inhibited, using the inhibitors rotenone, antimycin A, and potassium cyanide respectively (Figure 12A), to allow the activity of complex II alone to be studied. The complex II substrate sodium succinate was added in excess to ensure a plentiful supply of e^-, and the e^- acceptor ubiquinone was added in excess to allow maximum e^- transfer from complex II. The artificial e^- acceptor, DCPIP, was added in its oxidised form to accept e^- released as ubiquinol was oxidised to ubiquinone. As DCPIP was reduced it caused a measurable colour change from blue to colourless (Figure 12B). The absorbance of light was measured at 600 nm, the wavelength at which oxidised DCPIP absorbs light, and a decrease in the level of absorbance was observed as DCPIP was reduced (Figure 12C). The absorbance at 600 nm remained constant when no sample was added (Figure 12D).

Complex II activity was determined in fibroblasts and keratinocytes grown from the skin of a total of 46 individuals, ranging in age from 6 years old to 80 years old, from a region of sun-protected skin. Complex II activity was normalised to citrate synthase activity to determine complex II activity per unit of mitochondria. Figure 13A shows the results for the 27 fibroblast cell samples used, which gave a significant inverse correlation between the age of the donor and complex II activity ($P=0.0154$, $rho=-0.4614$, non-parametric Spearman correlation). This suggested that older individuals have a lower complex II activity per mitochondrial unit in their fibroblast cells. Figure 13B shows the complex II activity results for the 19 keratinocyte cell samples tested; no significant correlation was found between donor age and complex II activity ($P=0.7262$, $rho=-0.0860$, non-parametric Spearman correlation).

Figure 12

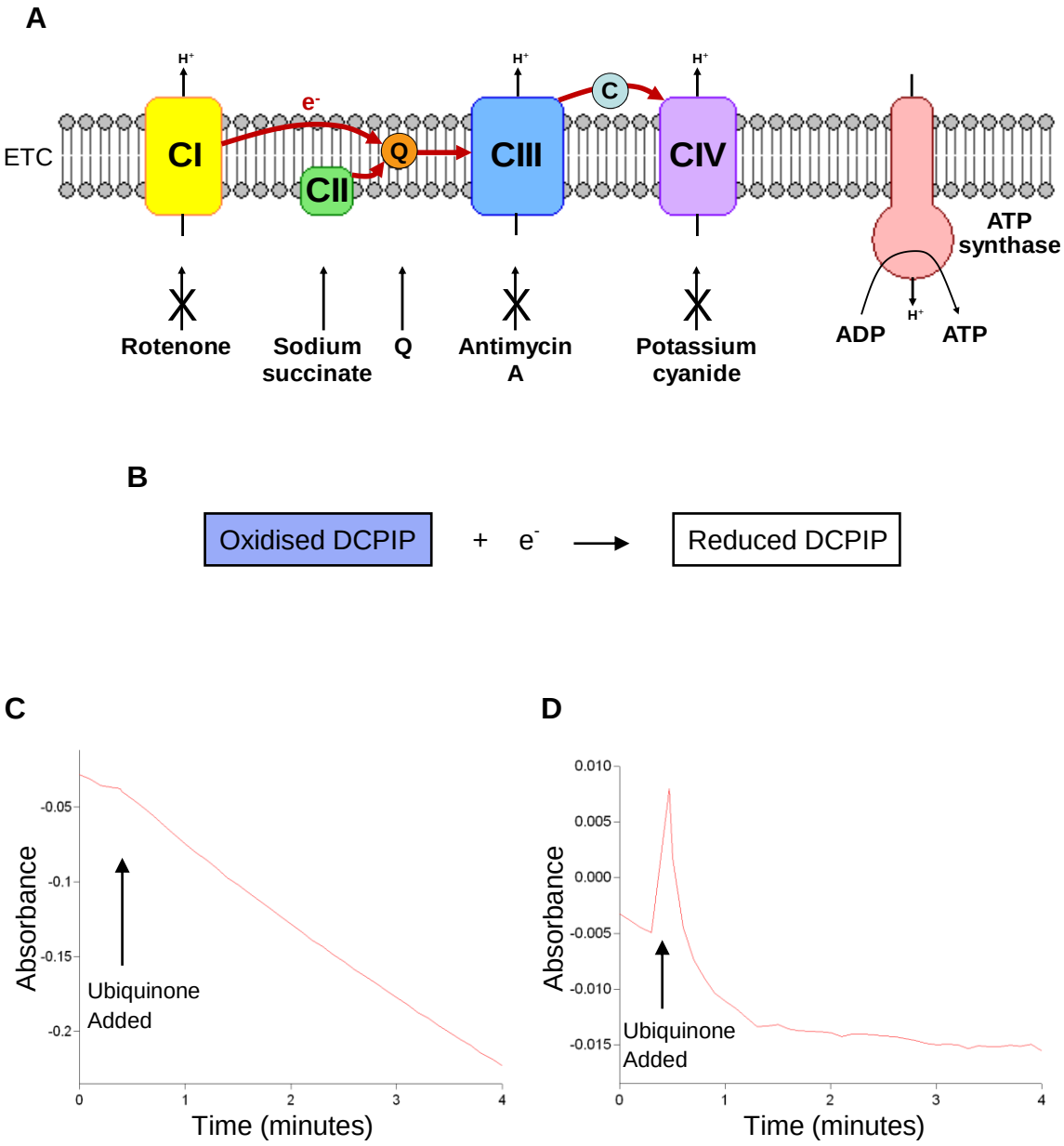

Figure 12. Mitochondrial complex II activity assay. A) During the complex II activity assay, complexes I, III, and IV were inhibited using rotenone, antimycin A, and potassium cyanide respectively (shown by the arrows with crosses). Sodium succinate and ubiquinone (Q) were added in excess to allow maximum complex II activity to be measured. B) Oxidised DCPIP was also added, to react with e^- released from ubiquinol, to form reduced DCPIP, which caused a colour change from blue to colourless. C) The absorbance of light at 600 nm was measured to assess the amount of DCPIP present, from 0 to 4 minutes, with ubiquinone added to start the reaction. D) The absorbance of light at 600 nm remained constant when no sample was added to the reaction.

Figure 13

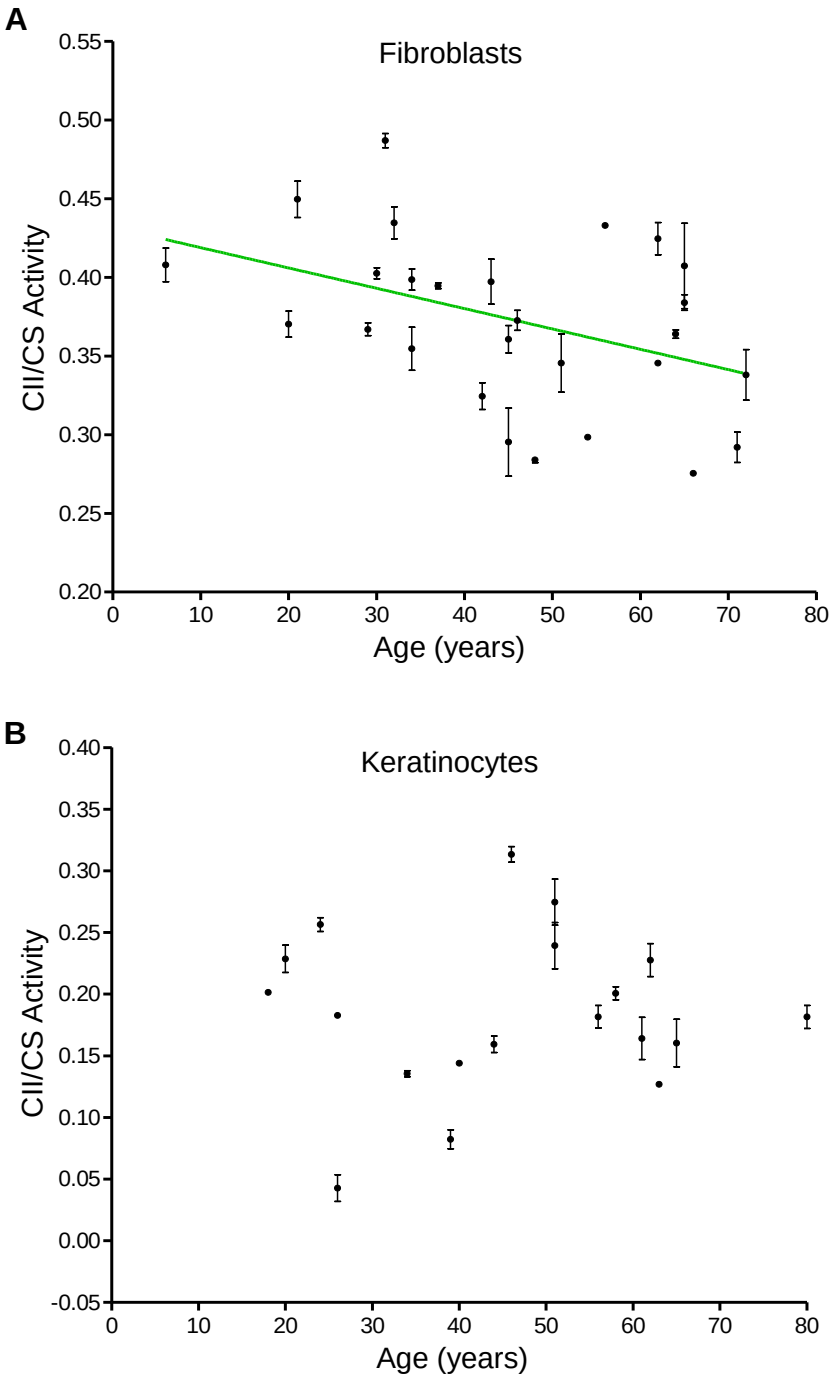

Figure 13. Complex II activity versus donor age in human skin cells. A) Complex II activity normalised to citrate synthase activity (CII/CS) of fibroblasts from 27 donors of varying ages compared to the age of the individual. Donor age correlated significantly and inversely with CII/CS activity (P=0.0154, rho=-0.4614, non-parametric Spearman correlation). The green line shows the line of best fit. B) The CII/CS activity of keratinocytes from 19 donors of varying ages compared to the age of the individual donor. Donor age did not correlate significantly with CII/CS activity (P=0.7262, rho=-0.0860, non-parametric Spearman correlation). The error bars show the standard error of the mean (SEM). Photometry was performed at least two times for the citrate synthase assay and at least two times for the complex II activity assay for each sample.

3.4.3 *Complex II subunits and age: expression levels*

To investigate the cause of the observed decrease in complex II activity with age in the fibroblast cells, the individual subunits of complex II were investigated. The DNA expression levels of 3 out of the 4 complex II subunits (SDHA, SDHB, and SDHC) were measured by qPCR in the skin fibroblasts and keratinocytes of the differently aged donors. During the qPCR reaction, a section of the subunit mRNA transcript was amplified, and the relative transcript level determined by the number of cycles it took before the level of amplified product reached a certain threshold (the Ct value), with a fewer number of cycles indicating a higher expression as more DNA was available to be amplified.

The levels of SDHA, SDHB, and SDHC expression were studied in 25 fibroblast samples and 17 keratinocyte samples, relative to β-act controls for each sample. It was found in the fibroblast samples that SDHA showed a significant decrease in expression with age (Figure 14A) (P=0.0083, rho=-0.5158, non-parametric Spearman correlation). The level of SDHB also showed a strongly significant decrease with age (Figure 14B) (P=0.0011, rho=-0.6128, non-parametric Spearman correlation). No significant correlation was seen for the SDHC subunit (Figure 14C) (P=0.1195, rho=-0.3195, non-parametric Spearman correlation). In the keratinocyte samples studied, it was found that SDHA expression did not correlate significantly with age (Figure 14D) (P=0.0600, rho=-0.4650, non-parametric Spearman correlation). However, SDHB expression in the keratinocytes did correlate significantly and inversely with age (Figure 14E) (P=0.0328, rho=-0.5190, non-parametric Spearman correlation). SDHC expression did not correlate significantly with age (Figure 14F) (P=0.1141, rho=-0.3975, non-parametric Spearman correlation).

Figure 14

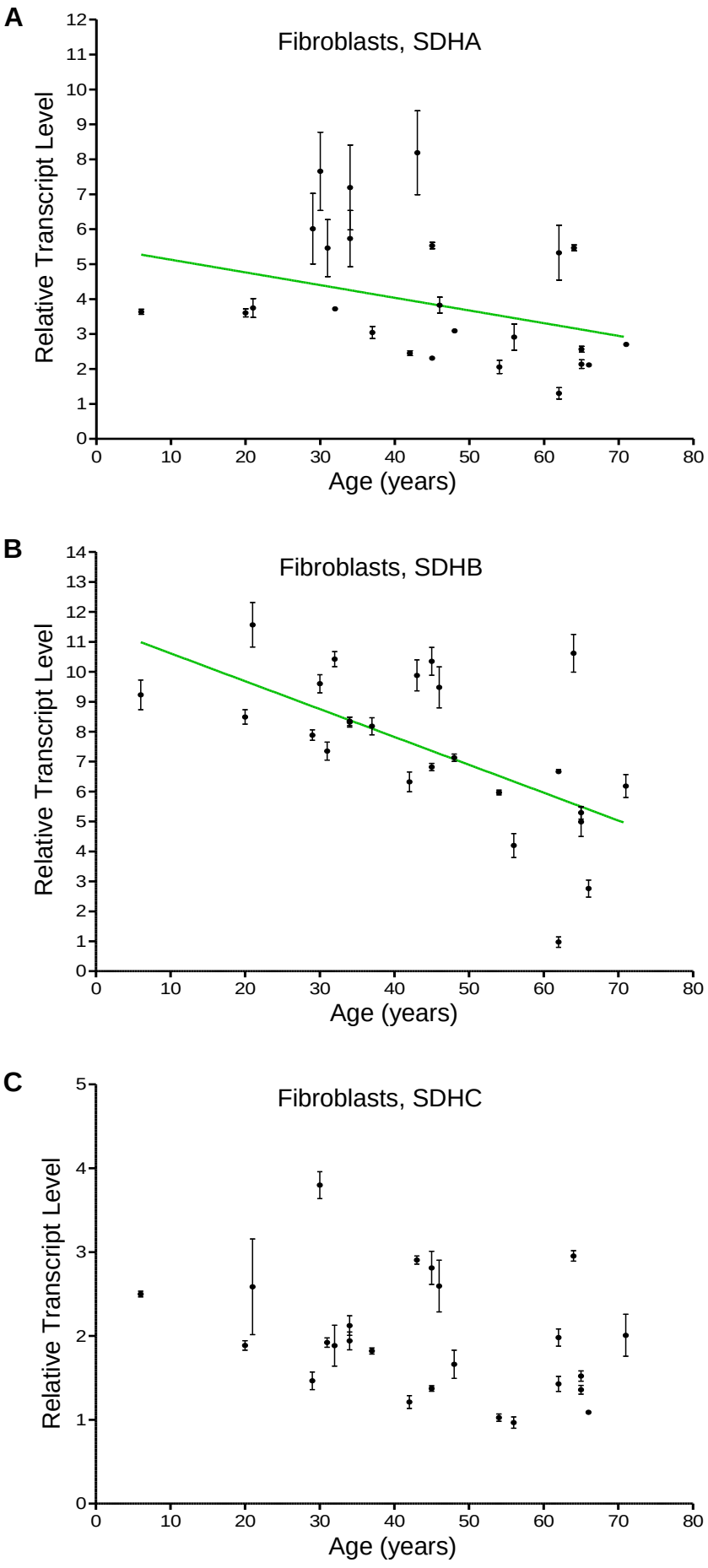
A
Fibroblasts, SDHA
Relative Transcript Level
Age (years)
B
Fibroblasts, SDHB
Relative Transcript Level
Age (years)
C
Fibroblasts, SDHC
Relative Transcript Level
Age (years)

D

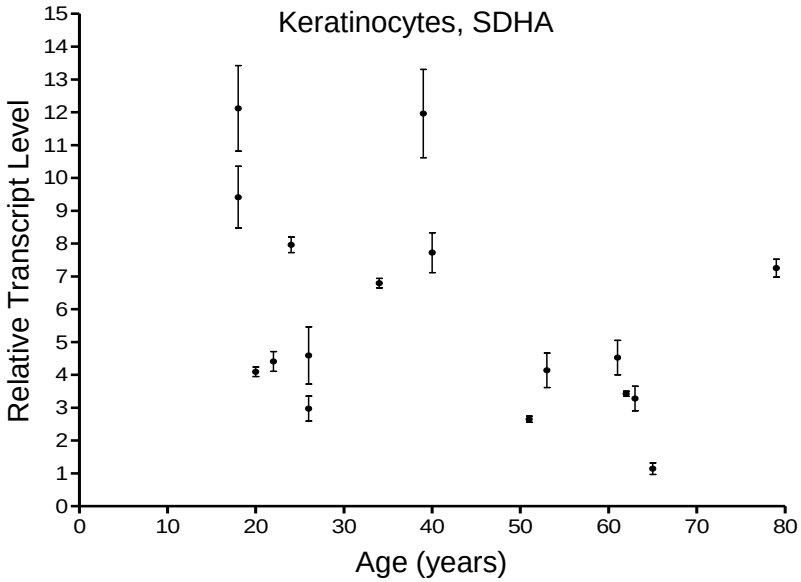
Keratinocytes, SDHA
Relative Transcript Level
Age (years)

E

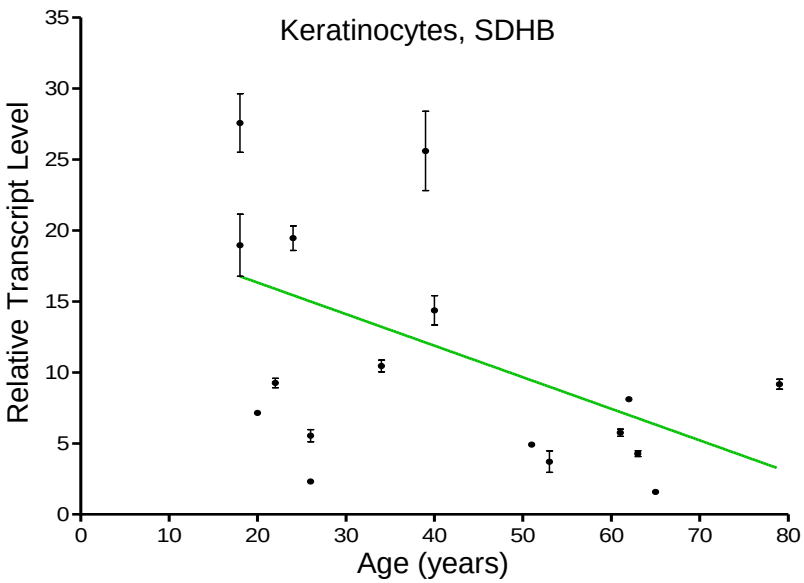
Keratinocytes, SDHB
Relative Transcript Level
Age (years)

F

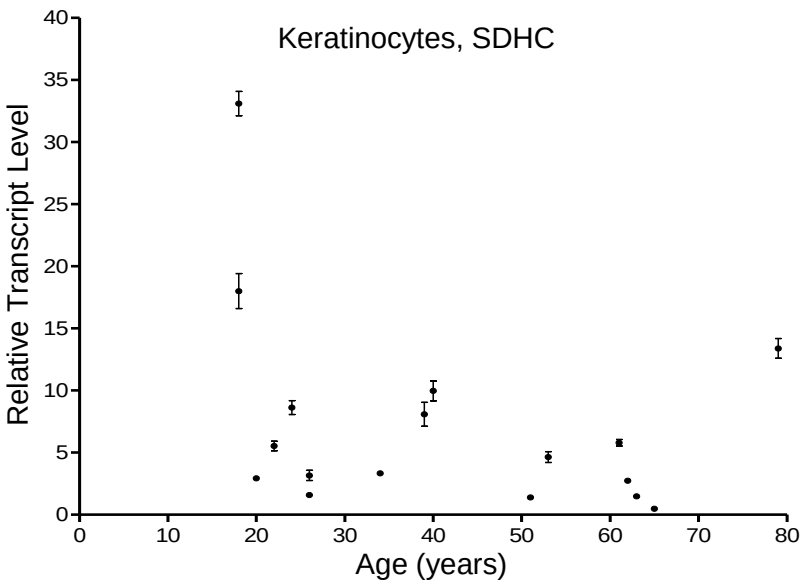
Keratinocytes, SDHC
Relative Transcript Level
Age (years)

Figure 14. Complex II subunit transcript levels in skin cells from differently aged donors. A) The relative level of SDHA expression in fibroblasts compared to the age of the donor for 25 samples, relative to the sample with the lowest transcript level. A significantly lower level of transcript expression was seen in older individuals (P=0.0083, rho=-0.5158, non-parametric Spearman correlation). B) The relative level of SDHB expression in fibroblasts compared to the age of the donor. A significant decrease in transcript level with age was observed (P=0.0011, rho=-0.6128, non-parametric Spearman correlation). C) The relative level of SDHC expression in fibroblasts compared to the age of the donor. There was no significant correlation between transcript level and age (P=0.1195, rho=-0.3195, non-parametric Spearman correlation). D) The relative level of SDHA expression in keratinocytes compared to the age of the donor for 17 samples, relative to the sample with the lowest transcript level. There was no significant correlation between SDHA level and donor age (P=0.0600, rho=-0.4650, non-parametric Spearman correlation). E) The relative level of SDHB expression in keratinocytes compared to donor age. There was a significant decrease in SDHB transcript with age (P=0.0328, rho=-0.5190, non-parametric Spearman correlation). F) The relative level of SDHC expression in keratinocytes compared to donor age. There was no significant correlation between SDHC transcript level and age (P=0.1141, rho=-0.3975, non-parametric Spearman correlation). The qPCR reactions were repeated twice for each sample, each in triplicate, for all 3 transcript types and the β-act control. The green lines show the lines of best fit. The error bars show the SEM.

When comparing the activity of CII/CS for each sample with the level of subunit expression directly, it was found that there was a significant positive correlation between the level of CII/CS activity and the expression of SDHA for the fibroblasts (P=0.0397, rho=0.4138, non-parametric Spearman correlation), suggesting that complex II activity is higher when there is more SDHA expression. Although there was also a trend towards a correlation between the level of complex II activity and the level of SDHB expression, this was not significant (P=0.0792, rho=0.3577, non-parametric Spearman correlation). This was also not significant for SDHC expression (P=0.1827, rho=0.2754, non-parametric Spearman correlation). For the keratinocyte cells it was found that there was no significant correlation between CII/CS activity for either SDHA (P=0.4262, rho=-0.2418, non-parametric Spearman correlation), SDHB (P=0.6415, rho=0.1429, non-parametric Spearman correlation), or SDHC (P=0.9432, rho=0.0220, non-parametric Spearman correlation) (results not shown).

3.4.4 *Complex II subunits and age: protein levels*

To further investigate the decrease in complex II activity seen with age, the protein levels of SDHA and SDHB were determined to see whether these also decreased with age, as measured by Western blot. The optimum protein concentration for use in the Western blots was chosen using two samples following protein quantification via protein assays. As can be seen in Figure 15,

values of higher than 20 µg appeared to show little difference in the level of protein quantified by Western blot for both samples tested, and only concentrations below 20 µg showed a linear relationship. Therefore, a value of 10 µg was chosen for Western blot analysis.

Figure 15

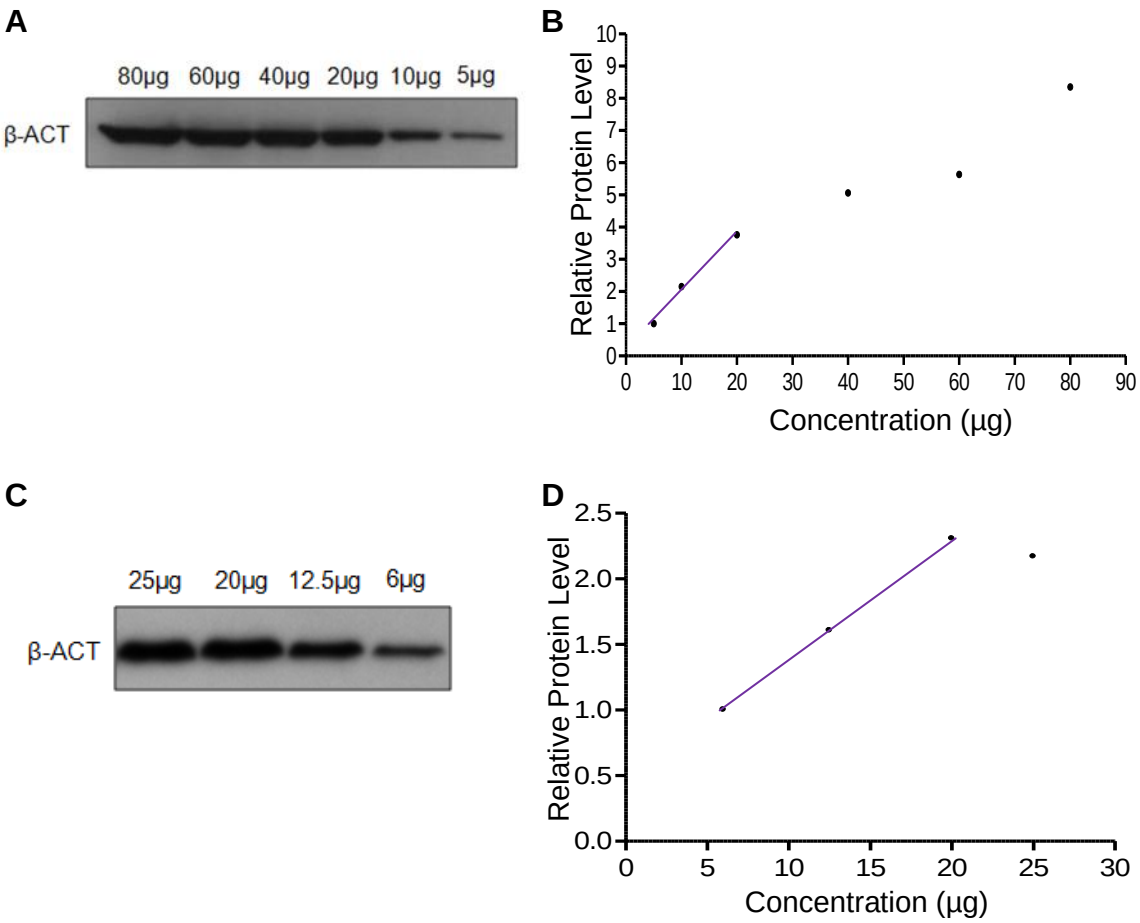

Figure 15. Optimal sample concentrations for Western blotting. A) Raw Western blot result for a sample at concentrations of 5 µg, 10 µg, 20 µg, 40 µg, 60 µg and 80 µg, for the β-act protein. B) Quantification of the Western blot bands by densitometry, normalised to the lowest concentration. The purple line shows that the reaction was linear from 5 µg to 20 µg. C) Raw Western blot result for a different sample at concentrations of 6 µg, 12.5 µg, 20 µg, and 25 µg, for the β-act protein. D) Quantification of the Western blot by densitometry, normalised to the lowest concentration. The purple line shows the reaction was linear from 6 µg to 20 µg. Western blots were repeated twice for each sample.

Due to the limited availability of keratinocytes, and since fibroblasts showed the strongest correlation between age and complex II activity, only the fibroblasts were examined in terms of subunit protein levels. It was found that in the 14

fibroblast samples tested, following normalisation to β-act, that there was a significantly lower level of the SDHA protein in older individuals (Figure 17A) (P=0.0006, rho=-0.8009, non-parametric Spearman correlation). This was also the case for the SDHB protein, which also decreased significantly with age (Figure 17B) (P=0.0049, rho=-0.7041, non-parametric Spearman correlation). Figure 16 shows the raw results for the differently aged samples. Unfortunately the level of SDHC protein with age was not able to be studied due to time constraints.

Both the SDHA and SDHB protein levels appeared to be trending towards a correlation with the level of complex II activity in the fibroblasts, however these were not significant (P=0.0694, rho=0.4989 for the SDHA protein, P=0.0694, rho=0.4989 for the SDHB protein, non-parametric Spearman correlation). This suggests that there was not a direct link between subunit protein level and complex II activity. There was also no direct link between protein level and transcript expression for either SDHA or SDHB (P=0.7593, rho=0.0901 for SDHA, P=0.1854, rho=0.3758 for SDHB, non-parametric Spearman correlation) (results not shown).

Figure 16

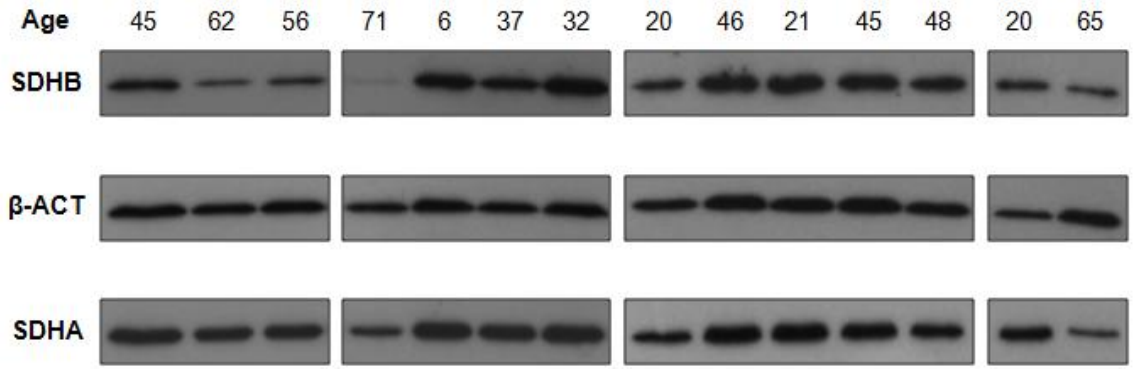

Figure 16. Raw Western blot results of fibroblast cells from differently aged donors. The Western blot results of 14 fibroblast samples, with the ages of the donors (in years) given. Protein levels of the complex II subunits SDHA and SDHB are shown, as well as the control protein β-act. The weight of SDHA is 70 kDa; SDHB is 32 kDa; and β-act is 42 kDa. Two biological repeats (cells from the same donor grown separately), each with two Western blot repeats, were performed; only one repeat is shown.

Figure 17

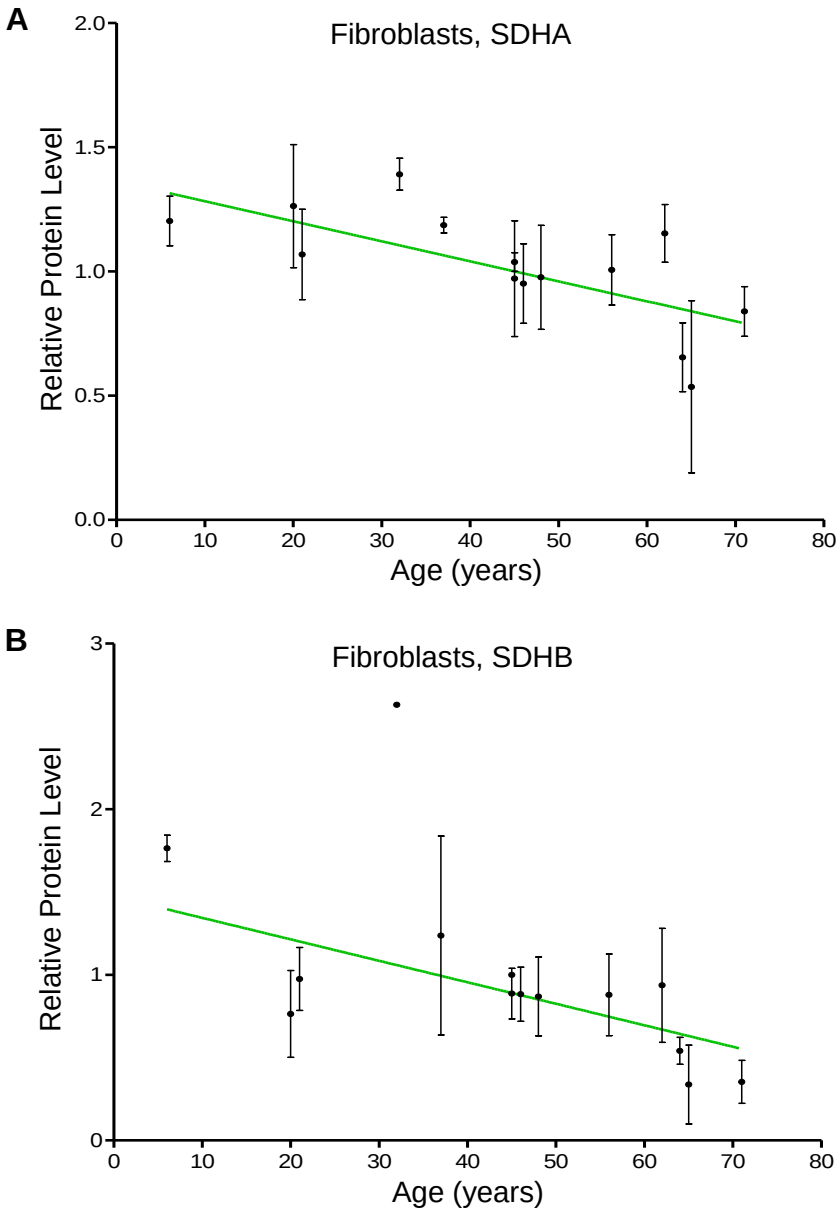

Figure 17. Complex II subunit protein levels in skin fibroblast cells from differently aged donors. A) The relative SDHA protein level normalised to β-act in 14 fibroblast samples, as determined by Western blot, relative to a control sample for each blot. There was a significantly lower level of SDHA protein in older individuals (P=0.0006, rho=-0.8009, non-parametric Spearman correlation). B) The relative SDHB protein level in 14 fibroblast samples compared to the age of the donor. There was a significantly lower level of protein in the older individuals (P=0.0049, rho=-0.7041, non-parametric Spearman correlation). The green lines show the lines of best fit. The error bars show the SEM. Two biological repeats (cells from the same donor grown separately), each with two Western blot repeats, were performed.

3.4.5 *Complex IV activity in skin cells from differently aged donors*

Complex IV is made up of 13 subunits, of which 3 are encoded by the mtDNA (Scheffler, 2007). The activity of mitochondrial complex IV was studied in skin cells from differently aged donors, to determine whether mitochondrial complexes other than complex II were decreasing with age in human skin. Photometry was used to measure differences in complex IV, by a similar method to the complex II measurement. Since complex IV is the only complex capable of oxidising the measured substrate (cytochrome *c*), it was not necessary to inhibit the other complexes (unlike for the complex II assay where e^- from other complexes could interfere). During the photometric assay, DDM was added to samples, which is a detergent capable of solubilising the mitochondrial membrane proteins whilst retaining their activity (le Maire *et al.*, 2000). Reduced cytochrome *c* was also added (Figure 18A) which is red in colour, and is oxidised by complex IV to a colourless solution (Figure 18B). The absorbance at 550 nm was measured (the absorbance of reduced cytochrome *c*) (Figure 18C), which decreases as complex IV activity occurs. The absorbance did not decrease when no sample was added to the reaction (Figure 18D).

Complex IV activity was measured in 18 fibroblast samples and 13 keratinocyte samples from the skin of individuals ranging in age from 6 to 79 years old. As can be seen in Figure 19A for the 18 fibroblast samples tested, there was no significant correlation between the age of the donor and complex IV activity (P=0.1478, rho=0.3554, non-parametric Spearman correlation). This was also the case for the 13 keratinocyte samples tested (Figure 19B) (P=0.8094, rho=-0.0743, non-parametric Spearman correlation).

It was observed that there was no significant correlation between CII/CS activity and CIV/CS activity for the individual fibroblast samples (P=0.4182, rho=-0.2034, non-parametric Spearman correlation), which could be expected since CII/CS activity was shown to decrease with age and CIV/CS activity was not. This could suggest that these two complexes have independent activities, and that only complex II is associated with age. This could not be tested for in the keratinocyte samples due to lack of matching samples.

Figure 18

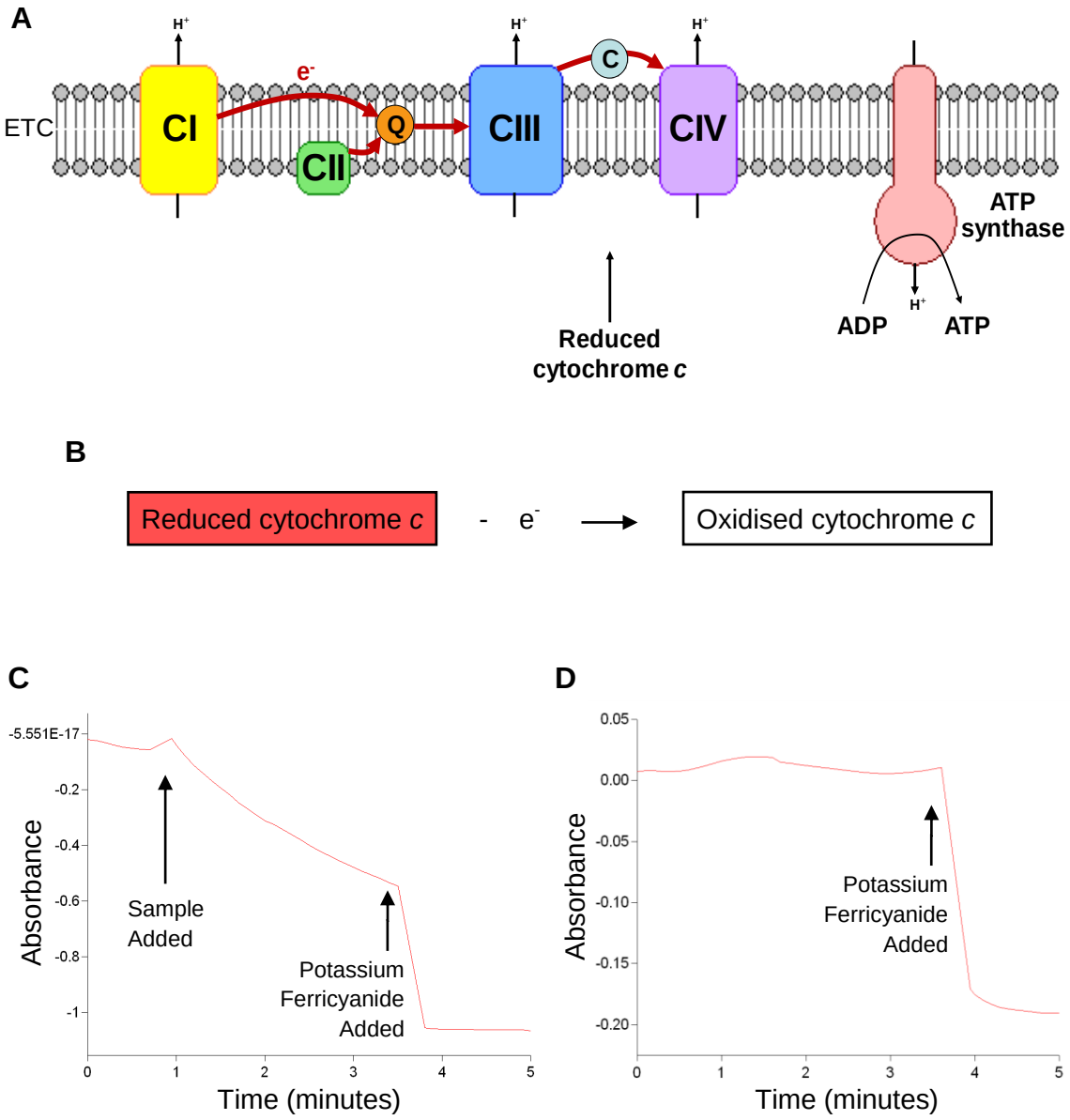

Figure 18. Mitochondrial complex IV activity assay. A) During the complex IV activity assay, reduced cytochrome *c* was added in excess to provide the substrate for complex IV. B) Complex IV activity was then measured by the oxidisation of cytochrome *c* from a red solution to a colourless solution as e^- were removed by complex IV. C) The absorbance of light at 550 nm was measured to assess the level of reduced cytochrome *c* present, which began to decrease at an exponential rate once the cell sample was added. Potassium ferricyanide was added to fully oxidise the remaining cytochrome *c* to determine the end point of the reaction. D) The absorbance of light at 550 nm remained constant and did not decrease when no sample was added to the reaction.

Figure 19

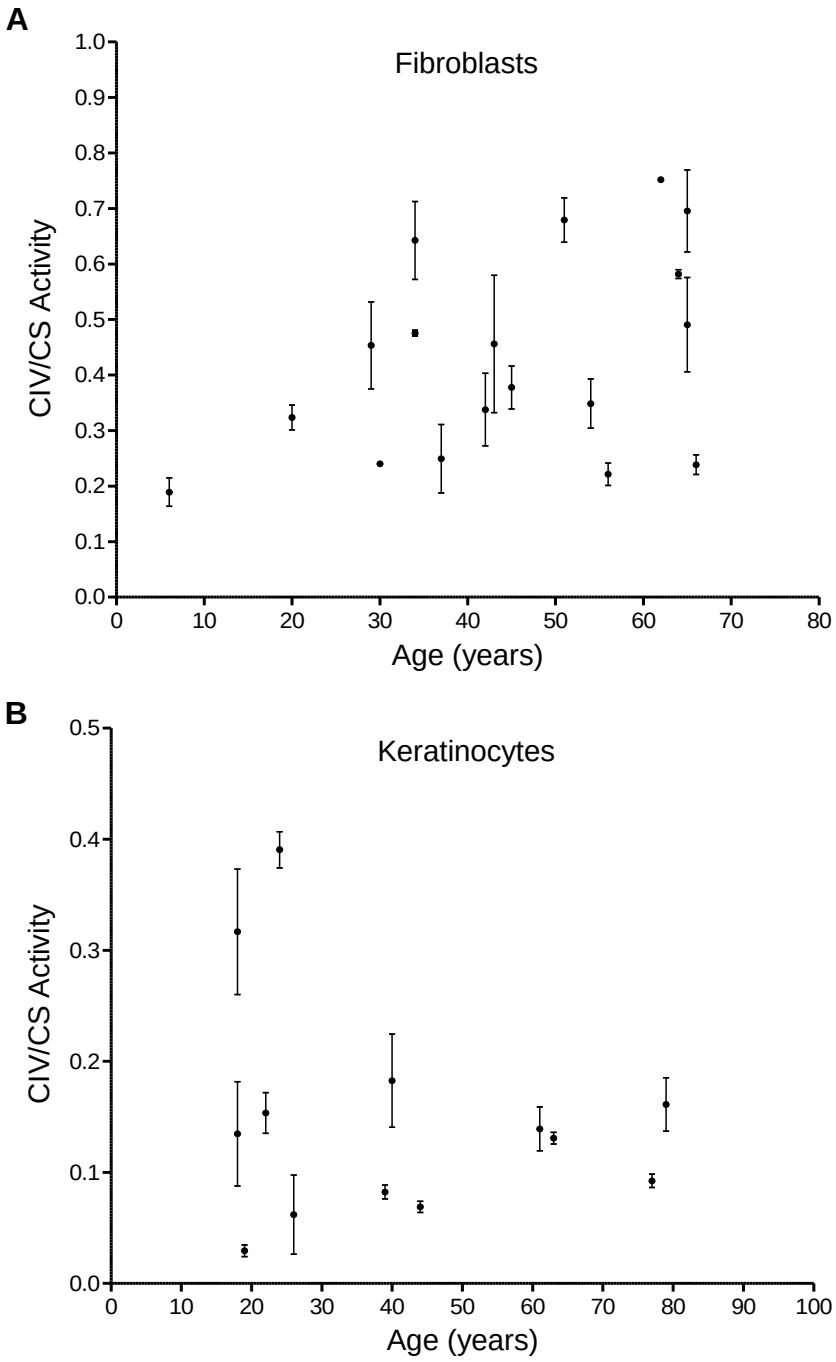

Figure 19. Complex IV activity versus donor age in human skin cells. A) The CIV/CS activities of fibroblasts from 18 donors of varying ages were compared to the age of the individual. Donor age did not correlate significantly with CIV/CS activity (P=0.1478, rho=0.3554, non-parametric Spearman correlation). B) The CIV/CS activities of keratinocytes from 13 donors of varying ages were compared to the age of the individual. Donor age did not correlate significantly with CIV/CS activity (P=0.8094, rho=-0.0743, non-parametric Spearman correlation). The error bars show the SEM. Photometry was performed at least two times for the citrate synthase assay and at least two times for the complex IV activity assay for each sample.

3.5 Discussion

3.5.1 *Complex II activity decreases with age in human skin fibroblast cells*

Photometry is a technique used in past studies to sensitively and reliably detect changes in mitochondrial complex activity (Birch-Machin *et al.*, 1994; Kirby *et al.*, 2007). Following photometry, sample complex activities were normalised to citrate synthase activities, which is a commonly used marker for mitochondrial content (Birch-Machin and Turnbull, 2001), and allows for the complex activity within the same amount of mitochondria to be determined. It was found in this project that complex II activity declined with age in human skin fibroblasts per unit of mitochondria, which to my knowledge has not been demonstrated previously. This suggested that older individuals have a lower level of complex II activity in their skin, which could be indicative of a broader complex II decrease throughout the whole body, and could potentially be causative in terms of ageing.

The age-related decrease in complex II activity observed in this project is in accordance with some previous studies, which have shown that there is a decline in complex II activity in laboratory animals with age. For example, a study using rat heart and muscle cells (Kumaran *et al.*, 2004), found that the activity of complex II (as well as complexes I, III, and IV) was significantly lower in older rats (aged the equivalent of 60 years and older in human terms) compared to younger rats (aged the equivalent of less than 18 years old in human terms (Andreollo *et al.*, 2012)), when determined photometrically by the same method as used in this study. Complex II activity has also been shown to be decreased with age in rat liver, kidneys, lungs, brain, and lymphocytes (Sandhu and Kaur, 2003; Cocco *et al.*, 2005; Braidy *et al.*, 2011). Another study in rat heart muscle also showed that complex II activity decreased with age when tested photometrically (Tatarkova *et al.*, 2011); however in the study, complex II activity did not show a significant decline until the mice were extremely old, at 26 months of age. This is equivalent to a human age of over 70 years old (Wilson *et al.*, 2010), which could explain why the correlation between age and complex II activity was not strongly significant in the present project, as there were only 2 human skin samples of over 70 years old available. Future studies could therefore include a higher number of samples from donors of over 70 years old, which could be expected to increase the

strength of the correlation between the two factors. There have been a limited number of studies performed on mitochondrial complex activity and age in terms of skin; however, a recent study on mouse skin did find that complex II activity was decreased in naturally aged mouse skin (Velarde *et al.*, 2012). Additionally, in the study by Velarde *et al*., (2012), in mice with SOD knocked-out, there was a decreased level of complex II activity and accelerated ageing; this could suggest a causative role for complex II in the ageing process. In terms of studies on human complex II activity there have been few performed. However, some previous studies on human muscle have found that complex II activity decreases with age (Trounce *et al.*, 1989; Coggan *et al.*, 1992; Boffoli *et al.*, 1994; Short *et al.*, 2005). These previous studies correlate with the results found in this project; however, studies in other human tissues are required to determine whether this is a phenomenon observed throughout the entire human body.

Since complex II has recently been shown to play a prominent role in ROS production (Quinlan *et al.*, 2012; Moreno-Sanchez *et al.*, 2013; Siebels and Drose, 2013), it could be that the observed decrease in complex II activity with age is resulting in a higher ROS leakage, which has been shown to occur when this complex is blocked by inhibitors (Byun *et al.*, 2008) or is at a lower activity level (Quinlan *et al.*, 2012). This has also been shown to occur in mice in that when complex II activity is decreased, this complex generates a higher level of superoxide (Morten *et al.*, 2006). Increased ROS with age caused by increased complex II dysfunction (lower activity) may be causing damage to mtDNA, lipids, and proteins in the mitochondria, resulting in a decreased production of ATP and of aerobic capacity, which has also been seen with age (Conley *et al.*, 2000; Petersen *et al.*, 2003; Tonkonogi *et al.*, 2003; Short *et al.*, 2005). It could also be that the level of complex II activity is decreased with age as a consequence of an increase in ROS, as it has been shown in previous *in vivo* mice studies that a decrease in complex II activity occurs when mitochondrial SOD is knocked-out to cause an increase in ROS (Li *et al.*, 1995; Melov *et al.*, 1999; Morten *et al.*, 2006; Velarde *et al.*, 2012). Increased ROS levels with age may increase mitochondrial dysfunction (as represented by a complex II activity decrease (Passos and Zglinicki, 2012)), which may be exacerbated further by a higher level of ROS leak by the dysfunctional mitochondria, as the vicious cycle

theory of ageing predicts. It has also been speculated that the reason for complex II being entirely nuclear-encoded (and therefore within the protection of the nuclear-repair mechanisms instead of the mtDNA which is under high ROS insult), is because complex II dysfunction is so detrimental that protective measures to prevent its dysfunction have been implemented by cells (Wojtovich *et al.*, 2013). Further studies on ROS production with age are required to determine whether the decrease in complex II activity is causative or consequential in terms of the increase in ROS levels seen with age.

The observed significant inverse correlation between age and complex II activity was not a direct 1:1 correlation, as determined by the Rho value (which measures the strength of the relationship between two factors (Royal Geographical Society, 2013)), which was not extremely close to 1 or -1 (it was -0.4614). This indicates that other factors may be contributing to the ageing process other than complex II alone as could be expected since ageing is a multifactorial process. Also, it could be that other factors are having an effect on complex II activity. Variations in complex II activity observed in those people of similar ages could be due to differences in lifestyle between individual donors; for example, whether or not the individual is a smoker or the level of exercise which the donor partakes in. Smoking has been shown previously to decrease the activity of specific complexes of the ETC including complex II (Miro *et al.*, 1999; Alonso *et al.*, 2004; Luo *et al.*, 2013), and therefore could be causing some variation in complex II activity. Exercise has been shown to improve mitochondrial function in muscle across the whole ETC including complex II (Menshikova *et al.*, 2006), as well as in lymphocytes and in other tissues (Cardellach *et al.*, 2003; Bouhours-Nouet *et al.*, 2005), and could therefore explain the slight variations in complex II activity seen among individuals of similar ages. However, a decrease in mitochondrial function has been shown to occur with age even in exercise-matched humans (Tonkonogi *et al.*, 2003), so it is unlikely that the decline in complex II activity with age is only due to higher exercise levels in younger individuals. As all of the samples were taken from a non-UV-exposed region of the body, differences in UV were unlikely to be affecting the complex II activity in the present study, as UV has been demonstrated previously to decrease ETC activity (Djavaheri-Mergny *et al.*, 2001).

3.5.2 *Complex II activity decreases with age in fibroblasts but not in keratinocytes*

Complex II activity was found to be decreased with age in skin fibroblasts, but not in skin keratinocytes. It was speculated that this was due to the epidermal cells in human skin being replaced on a regular basis (every 47 days (Iizuka, 1994)) due to normal skin turnover, during which the keratinocytes are shed from the outer layer of the skin and replaced by new cells. Therefore, any damage may be unable to accumulate to cause a reduction in complex II activity, as keratinocytes are being continually replaced with 'young' cells. This method of damage removal by cellular turnover has been demonstrated previously in mice *in vivo* (Stout *et al.*, 2005), whereby it was found that mice lacking nucleotide excision repair pathways (and therefore having increased levels of DNA damage), were able to remove this damage by turnover to prevent its accumulation. Other studies have found that the level of the age-related mitochondrial 3895 bp deletion did not accumulate as readily in the epidermis (which is mostly keratinocyte cells) compared to the dermis (which is mostly fibroblast cells) (Krishnan *et al.*, 2004; Harbottle and Birch-Machin, 2006), and mtDNA damage generally accumulates more readily in cells which undergo slower turnover (Cortopassi *et al.*, 1992; Harbottle and Birch-Machin, 2006). Additionally, the epidermis has been shown to have a higher activity of certain antioxidants (such as glutathione peroxidase), compared to the dermis (Shindo *et al.*, 1994; Harbottle and Birch-Machin, 2006; Hornig-Do *et al.*, 2007), which could also be decreasing the possible damage to complex II with age.

3.5.3 *The decrease in complex II activity with age may be due to a decrease in complex II subunits*

In order to better understand the cause of the observed complex II activity decrease with age, the levels of the individual complex II subunits were examined. Possible reasons for the decrease in complex II activity seen with age could be that either the actual activity of complex II is lower in older individuals per unit of mitochondria, or the amount of complex II present per unit of mitochondria is decreased (Figure 20).

Figure 20

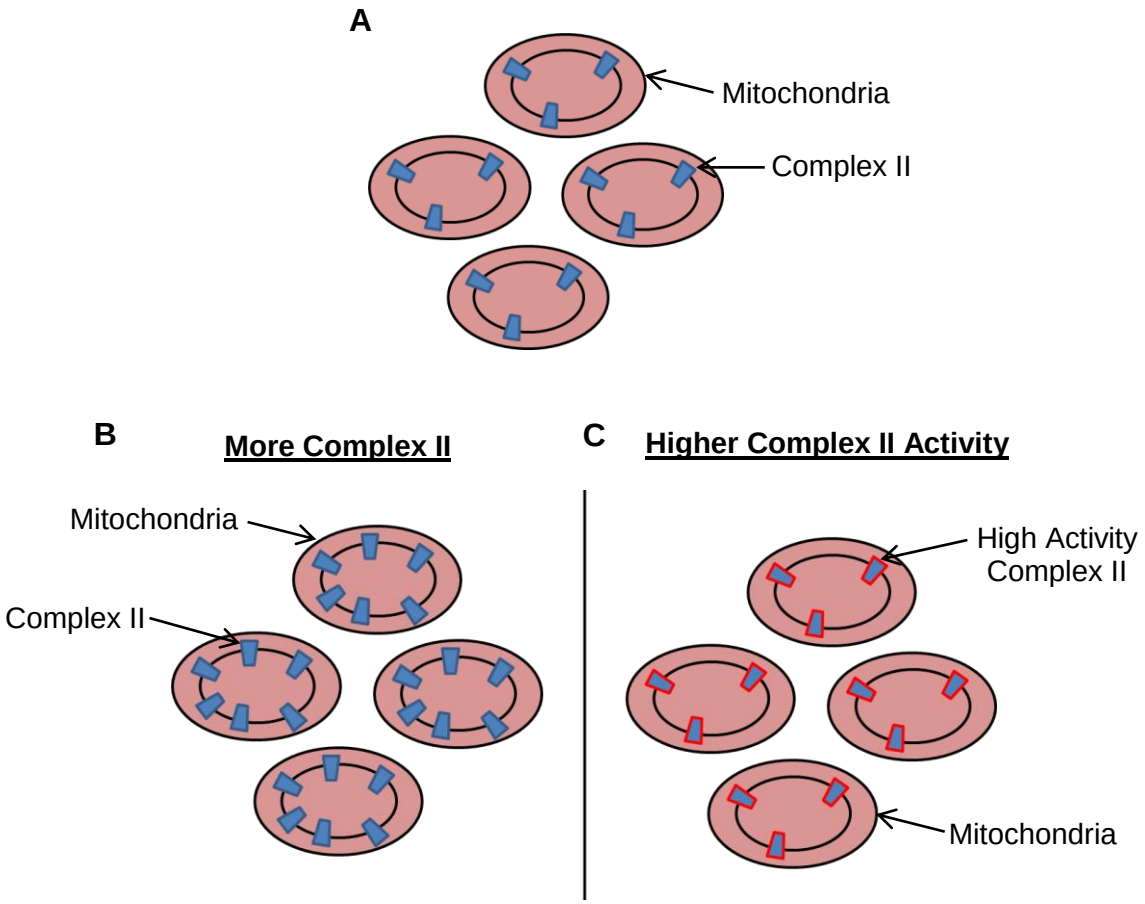

Figure 20. Possible causes of the higher complex II activity in young age. Two possible explanations as to why complex II activity was higher in the mitochondria of younger individuals. A) A simplified example of the complex II unit (shown in blue) on the mitochondria (in pink). B) A simplified example of more complex II being present per mitochondrial unit in a younger individual, which could be one of the explanations for a higher overall CII/CS activity seen with lower age. C) A simplified example of a younger individual having the same amount of complex II, but with each complex having a higher rate of activity. The red line around the complex indicates a higher level of activity.

In order to test whether the decrease in complex II activity with age was due to a lower level of complex II units or a lower activity per unit, the level of individual complex II subunits were measured. It was found that the levels of SDHA and SDHB expression and their protein levels decreased in an age-related manner in the fibroblasts, suggesting that the amount of complex II was decreasing with age per mitochondrial content. Although SDHC expression did not show a reduction with age, the level of complex II activity was still likely to be affected by the decrease in SDHA and SDHB as all 4 subunits are required for complex II ETC activity (Morten *et al.*, 2006). The decrease in these particular complex II

subunits has been shown to be associated with decreased complex II activity previously, when it was found that mice with SOD knocked-out had a reduction in both the SDHB subunit and the activity of complex II (Morten *et al.*, 2006). This could imply that an increase in mitochondrial ROS (caused by the SOD knock-out) is able to cause a decrease in complex II subunit levels which is then causing a reduction in complex II activity, which could also be occurring naturally with age. Additionally, past work has shown that when the level of SDHB protein is low due to a decrease in iron-sulphur assembly, there is a reduction in complex II activity (Yoon *et al.*, 2004), suggesting that the amount of SDHB can affect complex II activity. Increases in SDHB protein have also been associated with increased complex II activity (Dayal *et al.*, 2009).

The levels of both SDHA and SDHB were decreased with older age in the fibroblast cells; however, these subunits did not correlate directly with the level of complex II activity. This could possibly be because other factors were also contributing to the level of complex II activity, preventing a direct relationship between subunit amount and activity. For example, the amount of ROS present could be affecting complex II activity following expression and production of the complex II subunits, as ROS has been shown previously to directly target mitochondrial complexes including complex II (Kirkinezos and Moraes, 2001). A lack of direct link between SDHA expression and complex II activity has been observed previously, in which it was found that a particular protein (uncoupling protein-4) increased the activity of complex II; however, the expression of SDHA remained unchanged (Ho *et al.*, 2012). So it is possible that the decrease in complex II SDHA and SDHB subunits with age were contributing to the decrease in activity of complex II, but this may not have been significant due to other *in vivo* factors also contributing to the alteration of complex II activity.

The decrease in complex II subunits with age could have been caused by a general decrease in mitochondrial proteins and protein expression with age. Previous work has indicated that this can occur; Short *et al*., (2005) found that the abundance of 11 out of 13 mitochondrial proteins tested were decreased with age in human muscle. This included nuclear-encoded proteins, and was also shown in other studies (Rooyackers *et al.*, 1996; Balagopal *et al.*, 1997; Miller *et al.*, 2012). In terms of gene expression, it has been shown previously

that mRNA expression of both nuclear and mitochondrial-encoded genes (COX3 and COX4 respectively) were decreased with age in human muscle (Short *et al.*, 2005). However, to my knowledge there have been no other studies investigating the abundance of complex II subunits with age in human skin; therefore this project provides evidence of additional mitochondrial proteins which could be declining with age. Further work is required to determine the exact role of the decrease in SDHA and SDHB in terms of complex II activity; however, since previous studies have shown that defects in these subunits can affect the activity of complex II negatively (Hosokawa *et al.*, 1994; Adachi *et al.*, 1998; Ishii *et al.*, 1998; Tsuda *et al.*, 2007; Huang and Lemire, 2009; Wojtovich *et al.*, 2013), it is likely that they are having some effect on complex II activity rather than undergoing an independent decrease with age. Overexpression of SDHA/SDHB has also been shown to restore complex II activity in neuronal cells from the brains of Huntington's disease patients, which could suggest a possible future therapeutic potential for ageing (Benchoua *et al.*, 2006).

One possible reason as to why the level of mitochondrial subunit expression was decreased with age could be due to increased oxidative damage to both nDNA and mtDNA, as has been demonstrated previously to occur with age (Richter *et al.*, 1988; Yakes and Van Houten, 1997; Best, 2009; Haigis *et al.*, 2012). This could be lowering the expression of functional proteins such as the complex II subunits, and therefore decreasing the overall activity of complex II. This could tie-in with the mitochondrial theory of ageing (Harman, 1972; Bandy and Davison, 1990), in that genetic damage is causing decreased functional protein expression, and therefore increased mitochondrial dysfunction. Whether or not this process is resulting in an increased production of ROS in a continuing vicious cycle would remain to be established (Figure 21). If this was the case, it could be that ROS production would then affect DNA as well as complex II activity directly, as ROS has been shown previously to affect the iron-sulphur clusters of complex II (Figure 21) (Wallace, 1999; Kumaran *et al.*, 2004).

Figure 21

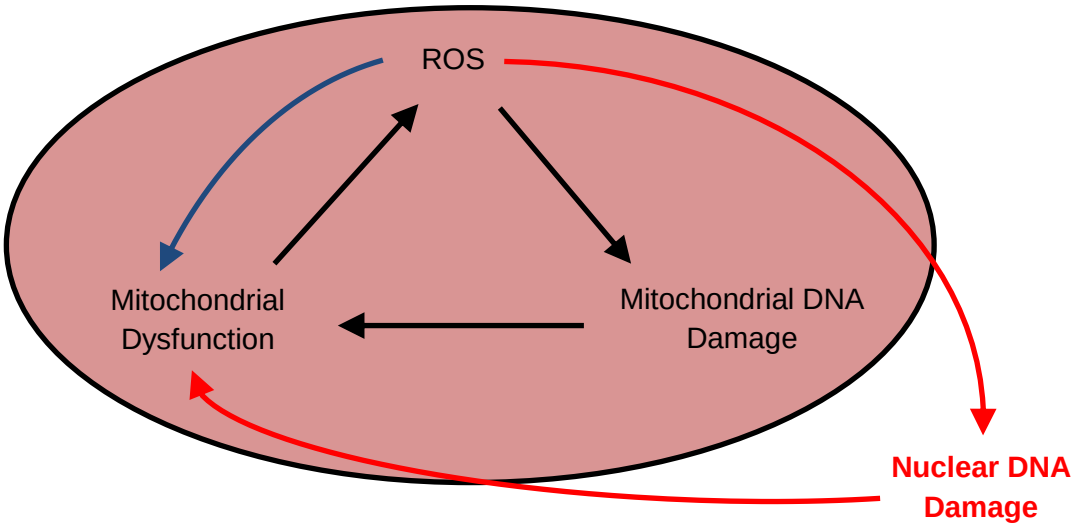

Figure 21. Potential interaction of nDNA with the vicious cycle theory of ageing. The vicious cycle theory of ageing proposes that mtDNA damage caused by ROS decreases the expression of functional mitochondrial units, resulting in an increase in ROS production in a continuing cycle (Harman, 1972; Bandy and Davison, 1990). However, it may be that mitochondrial proteins encoded by nDNA (including complex II) also contribute to the mitochondrial dysfunction observed with age. ROS production may cause damage to nDNA (shown in red) as these leak from the mitochondria (shown in pink) (Kirkinezos and Moraes, 2001). This would extend the more traditional view of the vicious cycle theory. ROS are also thought to affect mitochondrial subunits directly (shown by the blue arrow) (Wallace, 1999; Kumaran *et al.*, 2004), which could extend the theory further.

3.5.4 *Complex IV activity does not change with age in human skin*

Complex II, but not complex IV, showed an age-related decline in activity in human skin fibroblast cells. This could suggest that the age-related decline in mitochondrial complex activity is localised to complex II of the respiratory chain in human skin; however, previous studies suggest that this may not be the case, as both complex I activity (Lenaz *et al.*, 1997; Tatarkova *et al.*, 2011) and complex III activity (Lesnefsky *et al.*, 2001; Kumaran *et al.*, 2004; Tatarkova *et al.*, 2011) have been shown to decrease with age. The observed decrease in activity of complex II but not complex IV is in accordance with a previous study on human lymphocyte cells, for which it was found that the activity level of complex II, but not complexes III or IV, was lower in human subjects over 50 years old compared to those under 50 years old (Drouet *et al.*, 1999). This could imply that complex II is playing a bigger role than complex IV in the ageing process. Additionally, a study on mouse skin found that when

mitochondrial SOD was knocked-out, there was an increase in ROS and a decrease in complex II activity, as well as accelerated ageing, but the level of complex IV was not altered (Velarde *et al.*, 2012). This has also been shown in another mouse model with mitochondrial SOD knocked-out, which decreased the activity of complex II but not complex IV (Melov *et al.*, 1999), and generally complex II is more severely affected than complex IV in mouse SOD knock-out models (Morten *et al.*, 2006). However, other studies have shown opposite results regarding complex IV activity in ageing, by showing a decrease in activity in various rat organs (Sandhu and Kaur, 2003; Braidy *et al.*, 2011; Andreollo *et al.*, 2012), and human muscle (Trounce *et al.*, 1989; Boffoli *et al.*, 1994; Rooyackers *et al.*, 1996), and studies on complex IV activity in human skin fibroblasts with age have shown conflicting results (Hayashi *et al.*, 1994; Allen *et al.*, 1997; Isobe *et al.*, 1998). The present study however suggests that complex II may have a higher responsibility than complex IV in determining the rate of ageing in the skin. The possible lack of correlation between complex IV and age in the present study could be due to a higher resistance of complex IV to oxidative damage compared to complex II (Marchi *et al.*, 2012), and also due to this complex releasing the lowest levels of ROS (Kowaltowski *et al.*, 2009). Additionally, it could be that the activities of the mitochondrial complexes differ depending on the tissue type from which the cells were obtained. For example, Kwong and Sohal, (2000) directly compared the complex activities of cells from different mouse tissues and demonstrated that the activity of complex IV decreased with age in the kidneys and heart, but did not change in the brain or liver. Additionally, complex II activity actually increased with age in the heart yet decreased in the brain and skeletal muscle, and did not change in the kidneys or liver. Skin was not however tested, and it could be that for this organ the activity of complex II is decreased and the activity of complex IV remains unchanged with age.

3.6 Summary

In conclusion, the rate of complex II activity within human skin fibroblast cells was shown to be lower in older individuals in this study. This could have important consequences in terms of ageing, as it could implicate a role for complex II in the ageing process, and may lead to future studies investigating whether or not complex II plays a causative role in ageing. If so, therapeutic interventions to prevent complex II dysfunction with age could be important in lowering the rate of ageing. Complex IV activity was not decreased with age in human skin cells in this study, suggesting that the reduction in complex II activity was not just the result of a general decrease in overall ETC activity. The possible cause of complex II activity reduction with age could be because of a decreased expression of SDHA and SDHB subunits, resulting in a lower level of complex II per mitochondrial unit. Overall, this study provides important new insights into the potential role of complex II with ageing.

Chapter 4. Mitochondrial Differences in Senescent and Non-Senescent Cells from the Skin of Young and Old Human Donors

4.1 Introduction

4.1.1 *Cellular senescence*

Over 50 years ago it was recognised that cells growing in culture do not replicate indefinitely, and cease to proliferate after a certain number of population doublings, known as the 'Hayflick's limit' (Hayflick and Moorhead, 1961; Hayflick, 1965). This phenomenon is now acknowledged to be cellular senescence, and it describes the transformation of cells from a proliferating to a non-proliferating state, as a tumour suppressive mechanism to prevent cells with potentially cancerous DNA mutations from undergoing replication (Campisi and d'Adda di Fagagna, 2007). During senescence, cells lose the ability to divide yet remain viable, and are capable of releasing factors into their environment (Passos *et al.*, 2010; Nelson *et al.*, 2012). Senescence is activated by two main pathways, usually as a result of DNA damage; the p53/p21 pathway and the $p16^{INK4a}$/pRB pathway (Campisi, 2013), as shown in Figure 22. These pathways result in altered gene expression and a permanent cellular growth arrest (Campisi, 2013).

Figure 22

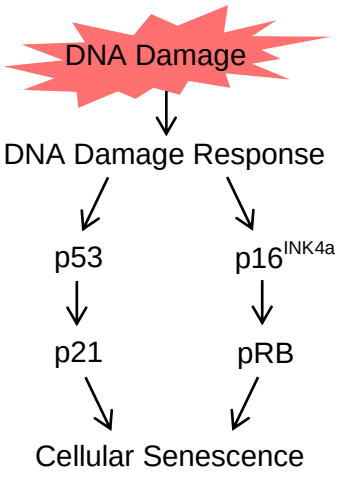

Figure 22. The major DNA damage response pathways involved in cellular senescence. A simplified version of the two major pathways resulting in cellular senescence, which occur via activation of the tumour suppressor proteins p53 or $p16^{INK4a}$, to activate the cell cycle inhibitors p21 or pRB respectively. This induces gene expression changes and a state of permanent growth arrest known as cellular senescence. Image was influenced by (Campisi, 2013).

4.1.2 *Causes of cellular senescence*

One of the first causes of cellular senescence to be described was in the 1970s, when it was discovered that the protective DNA sequences found at the ends of chromosomal DNA (the telomeres) become progressively shorter with each cellular division, due to DNA polymerase being unable to fully synthesise up to the very end of one of the strands of DNA (Watson, 1972; Olovnikov, 1973). If telomeres reach a critically short length, they risk undergoing unnecessary repair mechanisms such as non-homologous end joining, which could potentially result in genomic instability in subsequent cell divisions if chromosomes become joined (Rodier *et al.*, 2005; Campisi, 2013). To prevent this, cells were found to undergo senescence as a protective response when telomeres reach a critical length (Greider and Blackburn, 1985; Harley *et al.*, 1990; Harley *et al.*, 1992; Bodnar *et al.*, 1998). Additional causes of senescence are now known; for example, senescence can be activated by DNA damage either at the telomeres (Hewitt *et al.*, 2012), or at areas of the genome other than the telomeres when damage is severe enough (Nakamura *et al.*, 2008). Senescence can also be induced in response to oncogene activation in an attempt to reduce the risk of cancer (Serrano *et al.*, 1997), and senescence can be induced in response to epigenetic changes such as histone alterations (Rebbaa *et al.*, 2006). The mitochondrial production of ROS has also been shown to be increased prior to senescence (Moiseeva *et al.*, 2009) suggesting a causal role, which could have consequences in terms of ageing for which ROS levels are increased (Rufini *et al.*, 2013).

4.1.3 *Consequences of cellular senescence*

During senescence, cells maintain the ability to secrete a variety of factors, such as ROS (Passos *et al.*, 2010), growth factors, and pro-inflammatory cytokines and chemokines (Nelson *et al.*, 2012). This profile of released factors is known as the senescence-associated secretory phenotype (SASP), which may have both beneficial and detrimental consequences (Campisi, 2013). An example of a beneficial consequence is the recruitment of pro-inflammatory cytokines to the senescent cell, to remove not only the senescent cells themselves eventually, but also to remove the surrounding non-senescent cells which may have bypassed the senescent response and be potentially carcinogenic (Kang *et al.*, 2011; Campisi, 2013). Examples of detrimental

consequences of the SASP include accelerated ageing, due to the release of damaging factors such as ROS and inflammatory factors (Nelson *et al.*, 2012). Other consequences of senescence include its role in cancer. The process of senescence is thought to have evolved as a tumour-suppressive mechanism to prevent the incidence of cancerous cells (Campisi and d'Adda di Fagagna, 2007). However, senescence may be a double-edged sword in terms of cancer, because it can also increase ROS levels and inflammatory cytokine release, which may cause genetic mutations in adjacent cells and potentially result in a malignant transformation (Krtolica and Campisi, 2002; Nelson *et al.*, 2012; Rufini *et al.*, 2013).

4.1.4 *Senescence and ageing*

Cellular senescence may be an example of a trait which has evolved due to its benefits in early life in terms of cancer suppression, but is detrimental in later life (due to an accumulation of senescent cells) for which natural selection is no longer effective (known as antagonistic pleiotropy) (Campisi, 2005). Senescence is thought to play a prominent role in ageing, and the mechanisms by which these cells may affect ageing include: 1) depletion of the stem cell pool as stem cells senesce, resulting in a decreased capacity for repair and renewal in older individuals (Rossi *et al.*, 2008; Rufini *et al.*, 2013); 2) depletion of somatic cells, resulting in a loss of tissue function (Rufini *et al.*, 2013); and 3) the release of factors (the SASP) which can induce chronic inflammation and damage in surrounding cells (Nelson *et al.*, 2012; Naylor *et al.*, 2013). Senescent cells have been shown to be increased in an age-dependant manner in many tissues and organisms, including humans (Dimri *et al.*, 1995; Mishima *et al.*, 1999; Campisi, 2005; Herbig *et al.*, 2006; Noppe *et al.*, 2009; Naylor *et al.*, 2013). The first causative role of senescence in ageing was demonstrated by Baker *et al*., (2011), who found that if senescent cells were eliminated by drug-administration in a prematurely aged mouse model, the progression of age-related disorders such as cataracts and dermal thinning was halted (Baker *et al.*, 2011).

Mitochondrial dysfunction is thought to play a role in the increased levels of senescent cells observed with age. Previous studies have shown that mice with knocked-down MnSOD have higher levels of mitochondrial ROS production,

and an increased number of senescent cells (Treiber *et al.*, 2011; Velarde *et al.*, 2012), suggesting a causal role for mitochondrial ROS in senescence. These mice also showed accelerated ageing phenotypes and a reduced lifespan, implicating a role for both senescence and mitochondria in ageing. Other studies suggesting a causal role of mitochondria in senescence have been performed in human lung fibroblasts, for which it was found that a decrease in superoxide production by the mitochondria (via uncoupling) resulted in a decreased number of senescent cells (Passos *et al.*, 2007a). ROS production by inhibition of complex I has also been shown to lead to senescence in human skin fibroblasts (Dekker *et al.*, 2009), and mitochondrial complex III inhibition has been shown to induce senescence in a human lung fibroblast cell line (Moiseeva *et al.*, 2009).

In human lung fibroblast cells, it was found that p21 activation (which induces senescence) is able to induce mitochondrial dysfunction (decreased mitochondrial membrane potential) and increase ROS production (Passos *et al.*, 2010). This ROS production by the mitochondria following senescence was shown to be necessary for maintaining the senescent phenotype, by maintaining DNA damage and the DNA damage response (Passos *et al.*, 2010). This could potentially imply that an increase in mitochondrial dysfunction and ROS production with age are both a cause and a consequence of increased senescence levels with age. This could extend the vicious cycle theory of ageing further (Bandy and Davison, 1990) by introducing an additional interacting factor to contribute to mitochondrial dysfunction and ROS, whilst also itself being affected by ROS (Figure 23). The role of mtDNA damage in senescence remains unclear, however it has been suggested that mtDNA damage contributes to the senescent phenotype by increasing mitochondrial dysfunction and ROS (Passos *et al.*, 2007b), which ties-in with the vicious cycle theory of ageing (Figure 23). MtDNA damage has also been shown to be higher in senescent cells, by measuring the level of damage via qPCR within an 11 kb section of the mitochondrial genome (Passos *et al.*, 2007a). However, not all cells in older organisms become senescent, as the induction of senescence is a stress response which only occurs in a minority of cells exposed to unfavourable conditions, or with mutations leading to oncogenic activation.

Figure 23

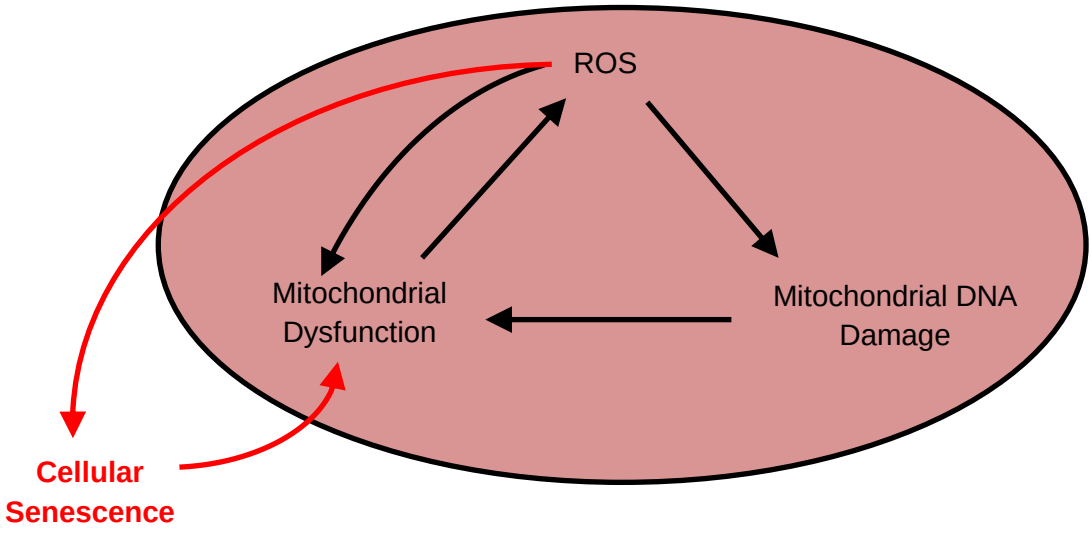

Figure 23. Potential interaction of cellular senescence with the vicious cycle theory of ageing. The vicious cycle theory of ageing proposes that mtDNA damage caused by ROS results in mitochondrial dysfunctional and further ROS release in a continuing cycle of damage (Harman, 1972; Bandy and Davison, 1990). However, it may be that additional factors interact with this cycle, such as cellular senescence (shown in red). Senescence has been shown to cause mitochondrial dysfunction and ROS release, and has also been shown to be induced and maintained by ROS caused by mitochondrial dysfunction. The mitochondrion is shown in pink.

4.1.5 *Complex II and senescence*

A possible role for complex II in promoting cellular senescence comes from the observation that mice *in vivo* have decreased complex II activity when ROS levels are increased by SOD knock-out or by natural age (Li *et al.*, 1995; Melov *et al.*, 1999; Morten *et al.*, 2006; Velarde *et al.*, 2012), and an increase in senescent cells (Velarde *et al.*, 2012). This could suggest a link between a decrease in complex II activity, an increase in ROS, and an increase in senescence; however, a causal role between complex II and senescence was not established. In humans, it has been shown that a decrease in iron in liver cells is able to cause a decrease in complexes I, II, and III (as these complexes contain iron), and also an increase in senescence (Yoon *et al.*, 2003; Yoon *et al.*, 2004). This could indicate a potential role for complex II (as well as complexes I and III) in senescence induction. As complex II has recently been shown to play a prominent role in ROS production (Quinlan *et al.*, 2012), it is possible that any disruptions in this complex will have an effect on senescence in human skin.

4.1.6 *Telomerase and ageing*

Telomeres are the repetitive DNA structures found at the ends of linear chromosomal DNA, responsible for preventing the unwinding and unnecessary repair of the DNA (Rodier *et al.*, 2005; Campisi, 2013). Due to DNA polymerase being unable to fully synthesis one strand-end of DNA during replication (Watson, 1972; Olovnikov, 1973), telomeres become gradually shorter with age both *in vitro* and *in vivo* (Harley *et al.*, 1990; Allsopp *et al.*, 1995; Cawthon *et al.*, 2003), which can induce cellular senescence. To prevent this from occurring in certain cells, such as germ line cells (Kim *et al.*, 1994), an enzyme called telomerase is present which adds DNA bases to the ends of the telomeres to decrease the rate of shortening and prevent senescence induction (Greider and Blackburn, 1985). However, telomerase is not present in the majority of somatic cells so is unable to protect these cells from senescence (Kim *et al.*, 1994; Bacchetti and Counter, 1995).

Telomerase is made up of 2 subunits, a catalytic unit (TERT), and an RNA template unit (TR) (Autexier and Lue, 2006). During telomerase activity, TERT is able to bind to the telomeres, and TR acts as a template for the addition of new bases for telomere extension (Greider and Blackburn, 1985). Previous studies have shown that TERT overexpression in cells *in vitro* is able to stably maintain the length of the telomeres, increase replicative lifespan, and reduce the number of senescent cells observed (Bodnar *et al.*, 1998; Franco *et al.*, 2001; Daniels *et al.*, 2010). In terms of *in vivo* studies, it has been found that mice lacking telomerase activity experience accelerated ageing and increased senescence, which was reversed when TERT was knocked-in (Jaskelioff *et al.*, 2011). It has also been found that treating normal mice with an adenovirus expressing TERT can cause a reduction in ageing biomarkers, and an increased lifespan (Tomás-Loba *et al.*, 2008; Bernardes de Jesus *et al.*, 2012). Due to the properties of TERT overexpression such as a decreased rate of telomere shortening, improved antioxidant defences, increased repair capacity, lower ROS levels, a higher number of population doublings, and lower senescence levels, cells overexpressing this catalytic unit can be used as a model for younger cells (Bodnar *et al.*, 1998; Zhu *et al.*, 2000; Franco *et al.*, 2001; Sharma *et al.*, 2003; Armstrong *et al.*, 2005; Masutomi *et al.*, 2005; Mondello *et al.*, 2006; Passos *et al.*, 2007b; Ahmed *et al.*, 2008; Saretzki, 2009;

Daniels *et al.*, 2010; Indran *et al.*, 2011; Bellot and Wang, 2013; Smith *et al.*, 2013). This technique was used in one area of the present chapter to confirm differences in mitochondrial complex II activity with age, in a synthetic model of ageing.

4.1.7 *Cell sorting into senescent and non-senescent populations*

In order to study differences between senescent and non-senescent cells, previous studies have sorted cells into senescent and non-senescent cell populations based on biomarkers of senescence, using fluorescence-activated cell sorting (FACS) (Martin-Ruiz *et al.*, 2004; Passos *et al.*, 2007a; Passos and von Zglinicki, 2007; Birket *et al.*, 2009). FACS is a method used to separate cells based on certain physical properties (such as size, granularity, or fluorescence), and lipofuscin has been used previously in FACS to sort cells into senescent and non-senescent populations (Martin-Ruiz *et al.*, 2004; Passos and von Zglinicki, 2007; Birket *et al.*, 2009), as this pigment is higher with age. Previous work has shown that FACS-sorted senescent populations have higher ROS levels, higher levels of mitochondrial dysfunction (in the form of increased mitochondrial superoxide production and increased mtDNA damage), shorter telomeres, and higher telomeric DNA damage (Martin-Ruiz *et al.*, 2004; Passos *et al.*, 2007a), when compared to the non-senescent cells. However, the rate of mitochondrial complex II activity has not been investigated previously in these separated cell populations, and would be useful to investigate due to the potential role of complex II in the ageing process as shown in Chapter 3.

4.2 Hypotheses

In the previous chapter (Chapter 3), it was found that complex II activity decreased with age in human skin fibroblasts. It could be hypothesised that senescent cells from older individuals are less efficient that those found in younger individuals, which has not been examined previously, resulting in a decrease in complex II activity in senescent cells with age. To address this hypothesis, fibroblasts from differently aged individuals were separated into senescent and non-senescent cell populations using FACS, with the hypotheses that 1) differences exist in complex II activity in senescent cells with age; 2) differences do not exist in complex II activity in non-senescent cells with age; and 3) senescent cells and non-senescent cells differ in terms of complex II activity. Additionally, further differences between senescent and non-senescent cells were elucidated by examining the level of an age-related mitochondrial mutation (T414G) in the two populations, to see whether there are any differences in mutation level with age in the populations, in an attempt to provide a better understanding of differences in mtDNA damage in senescent and non-senescent cells with age.

Complex II activity in a model of younger and older cells was also tested, in lung fibroblast cells either with (younger) or without (older) additional telomerase, to confirm whether the decrease in complex II activity observed in naturally aged cells (Chapter 3) is also observable in cell lines representing different ages, as it was hypothesised that complex II activity is decreased in this model of older cells.

4.3 Materials and Methods

Cell culture techniques, photometric assays, DNA extractions, qPCR reactions, and gel electrophoresis assays used within this chapter are described in the general Materials and Methods chapter (Chapter 2). MRC5 and MRC5/hTERT cells were received from Dr Gabriele Saretzki, and the overexpression of human TERT (hTERT) was achieved previously using retroviral transfection (Saretzki *et al.*, 2002; Ahmed *et al.*, 2008).

4.3.1 *Fluorescence-activated cell sorting*

FACS was used to separate human skin fibroblast cells into senescent and non-senescent populations. To perform FACS, cell culture flasks containing approximately 18 x 10^6 cells per sample were washed twice with PBS, and cells were detached from the flask using TE at 37°C for 5 minutes, followed by TE neutralisation using complete DMEM. Cell samples were placed into 15 ml Centrifuge tubes (Sarstedt, Germany) and centrifuged at 1200 rpm for 5 minutes, followed by resuspension into 2 ml PBS to wash. Cells were re-centrifuged at 1200 rpm for 5 minutes, and the pellet resuspended in 4 ml serum-free DMEM (Life Technologies, UK) with 1% FCS, and transferred to a 15 ml tube for sorting. FACS was performed using a FACS Aria II Cell Sorter (BD Biosciences, UK), by Dr Ian Dimmick (Newcastle University) and Dr David McDonald (Newcastle University). During the FACS process (Figure 24), the cell sample was added to the sorting machine, and a laser was passed through a stream of the sample to multiple detectors set to measure lipofuscin autofluorescence from 515 nm to 545 nm (Birket *et al.*, 2009). The excitation wavelength range of lipofuscin autofluorescence is 320 nm to 460 nm, and the emission wavelength range is 460 nm to 630 nm (Lois and Forrester, 2009). The stream of cells was separated into single cell droplets by vibrations, to which opposite electrical charges were applied to droplets based on the parameter of choice (lipofuscin autofluorescence) (Abcam, 2013). Cells in the lower 20% autofluorescence were given an opposite charge to those in the upper 20%, to separate non-senescent and senescent cells respectively. These percentages were chosen based on those used previously to separate human skin fibroblasts into senescent and non-senescent populations (Birket *et al.*, 2009). Following the assignment of a charge, cell droplets were passed through oppositely charged plates (Abcam, 2013) to be separated (Figure 24), ready for

future analysis. Cells in the middle 60% were discarded as they were not required for this study.

Figure 24

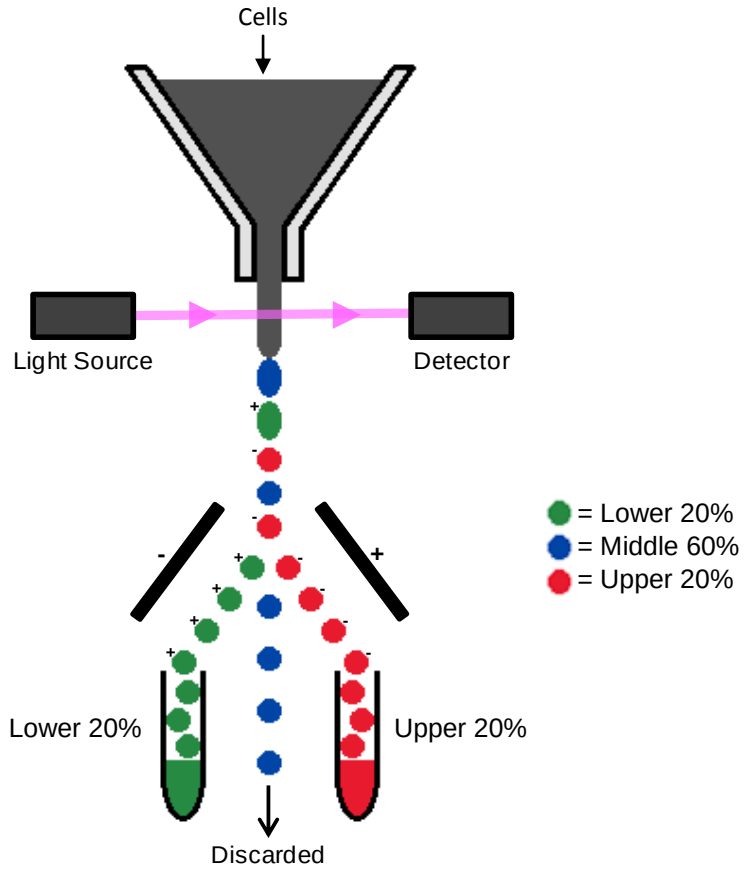

Figure 24. Fluorescence-activated cell sorting. During the FACS process, a stream of cells (shown in grey) was passed through a laser (shown in pink) to multiple detectors able to determine differences between the cells. Cells were assigned a specific charge during droplet formation, and separated based on lipofuscin autofluorescence into the lower and upper 20% (shown in green and red respectively) using oppositely-charged plates. Those cells in the middle 60% (shown in blue) were not assigned a charge and were discarded. +, positive charge; -, negative charge. Image influenced by (Abcam, 2013).

During the FACS sort, viable cells were initially selected based on the forward scatter (size) of the cells, due to cells below a certain size being non-viable or debris (Figure 25A) (Hughes *et al.*, 2009). Viable cells were sorted further into single cells based on side scatter (granularity and size), as the height and area of a single cell are generally proportional (Figure 25B) (Hughes *et al.*, 2009). Viable single cells were then sorted into senescent and non-senescent populations based on lipofuscin autofluorescence (515 nm to 545 nm) (Figure 25C and Figure 25D) (Birket *et al.*, 2009). Cells were collected into two separate 15 ml tubes and centrifuged at 1200 rpm for 10 minutes. DNA was either

extracted from the pellet, or the pellet was resuspended in 200 µl complex II buffer, snap-frozen 3 times, and stored at -80°C until use in photometry.

Figure 25

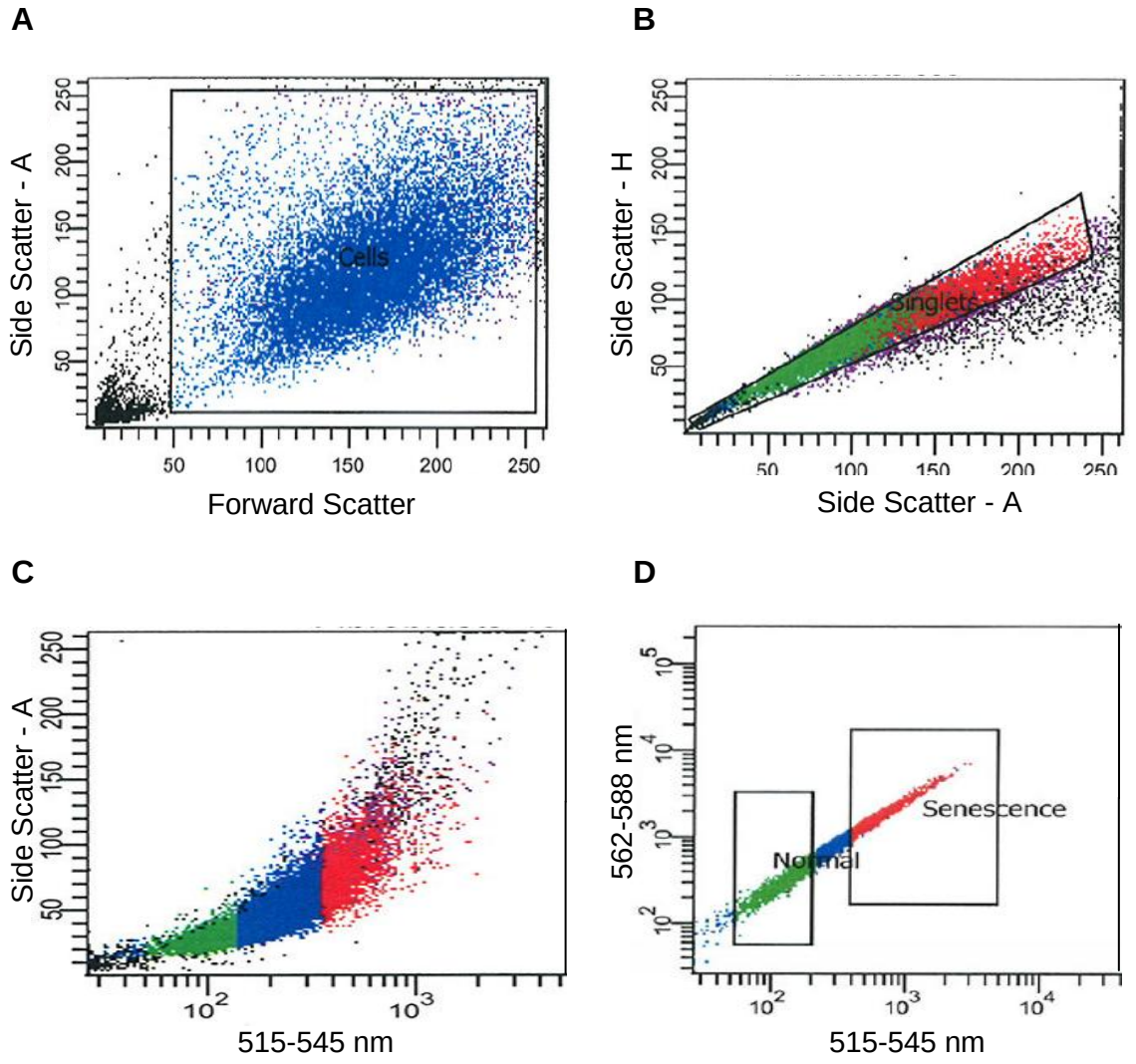

Figure 25. FACS output graphs for the separation of cells into senescent and non-senescent populations. A) Initially, viable cells were selected for based on their size (forward scatter), as shown by the black box. Those cells below a certain size were excluded from the analysis, and cells which were further sorted are shown in blue. Each dot represents a cell. B) Single cells were selected from the viable cells as shown by the black box. Side scatter-A represents cell area and side scatter-H represents cell height, which are generally proportional for single cells. C) Viable singlets were sorted into the upper and lower 20% lipofuscin autofluorescence, from 515-545 nm. Side scatter was not used to sort cells but is shown to give an approximation of the relative size of cells, which generally increases as senescence increases. The green dots show the lower 20% autofluorescence, the blue dots the middle 60% autofluorescence, and the red dots the upper 20% autofluorescence. D) The cells are shown again with a different y-axis parameter, with the lipofuscin autofluorescence wavelengths used (515-545 nm), compared to other fluorescence wavelengths of 562-588 nm. This second fluorescence was not used to sort cells, but it can be seen that cells with higher fluorescence for 515-545 nm also show higher fluorescence for 562-588 nm, as these wavelengths are included in the emission range of lipofuscin autofluorescence (Lois and Forrester, 2009). The black boxes show the senescent and non-senescent cell populations.

4.3.2 *Senescence-associated β-galactosidase staining*

To quantify the senescent and non-senescent cells in the sorted populations, senescence-associated β-galactosidase (β-gal) staining was performed using a Senescence Cells Histochemical Staining Kit (Sigma-Aldrich, UK), as β-gal has been shown to be present only in senescent cells (Dimri *et al.*, 1995; Lee *et al.*, 2006; Itahana *et al.*, 2007; Passos *et al.*, 2007a). During the staining procedure, the added substrate 5-bromo-4-chloro-3-indolyl-β-D-galactopyranoside (X-gal) is cleaved by β-gal to form galactose and 5-bromo-4-chloro-3-hydroxyindole (Norgen, 2010). The 5-bromo-4-chloro-3-hydroxyindole then forms 5,5'-dibromo-4,4'-dichloro-indigo which is blue in colour and can be visualised (Norgen, 2010). Approximately 1 x 10^5 cells were seeded per well from FACS-sorted populations into a 12-Well Plate (Corning Inc., USA). Cells were incubated at 37°C for 16 hours to allow adhesion to the plate, then washed twice with PBS, and 1.5 ml Fixation Buffer was added per well. The plate was incubated for 6 minutes at room temperature, after which cells were washed 3x with PBS, and 1 ml Staining Mixture (containing 1x Staining Solution, 12.5 µl Reagent B, 12.5 µl Reagent C, 25 µl X-Gal Solution, and 850 µl dH_20) was added per well. Plates were incubated at 37°C for 16 hours in the absence of CO_2 with Parafilm Laboratory Film (Bemis, USA), to allow staining to occur. Following incubation, the number of blue cells (senescent cells) and the number of non-blue cells (non-senescent cells) were counted under a light microscope out of 500-1000 cells (Birket *et al.*, 2009), with the percentage of cells expressing the blue β-gal expressed as a percentage of the total number of cells.

4.3.3 *T414G sequence amplification*

In order to determine the level of the T414G mtDNA mutation within samples, DNA was extracted from approximately 1.5 x 10^6 cells. The mtDNA sequence of 130 bp containing the T414G mutation was amplified using a GeneAmp PCR System 9700. One of the primers used for amplification was biotin-labelled, to generate a biotin-tagged DNA strand, and the primers were designed previously by Dr Emma Watson (Newcastle University) and produced by Eurofins MWG Operons, with the sequences shown in Table 1. To perform the PCR reaction, the following components were made up to a final volume of 25 µl per well, in MicroAmp Fast Reaction Tubes (Applied Biosystems, UK) with MicroAmp

Optical 8-Cap Strips (Applied Biosystems, UK): dH_20, 1x Colourless GoTaq Flexi Reaction Buffer (Promega, UK), 200 µM dNTP mix, 6 mM magnesium chloride (Promega, UK), 0.5 µM each of forward and reverse primers, 0.1x GoTaq Hot Start polymerase (Promega, UK), and 100 ng template DNA. The PCR conditions used were: 95°C for 10 minutes; 30 cycles of 94°C for 30 seconds, 62°C for 30 seconds, and 72°C for 30 seconds; and a final stage of 72°C for 10 minutes. Agarose gel electrophoresis was performed to confirm a product size of 130 bp.

Table 1

Primer Set		Base Sequence (5' to 3')	Length (bp)	Nucleotide Numbers (bp)
T414G Human	F	CCT AAC ACC AGC CTA ACC AGA TTT	130	370-499
	R	Bio-CGG GGG TTG TAT TGA TGA GAT TA		

Table 1. Primer sequences for the detection of the T414G mutation. The primer sequences to amplify the mtDNA region containing the T414G mutation are shown in a 5' to 3' direction, for the forward (F) and reverse (R) primers. The length of the sequence to be amplified and the nucleotide numbers showing the region of binding are given. The biotin-label (Bio) is shown on the reverse primer.

4.3.4 *Pyrosequencing*

Pyrosequencing to determine the percentage of a particular nucleotide at a particular position (T414G) was performed using a Pyromark Q24 Instrument (Qiagen, UK), with the 130 bp DNA as a single-stranded template. In order to separate single DNA strands from the PCR-amplified double-stranded DNA, 15 µl DNA sample was placed into each well of a 24-Well PCR Plate (Starlab, UK), and made up to 80 µl with dH_20, 40 µl PyroMark Binding Buffer (Qiagen, UK) and 2 µl Streptavidin Sepharose High Performance beads (GE Healthcare, UK), to allow the biotin-labelled DNA strand to bind to the sepharose beads and later become separated from the opposite DNA strand. Plates were shaken for 10 minutes to allow DNA binding to sepharose beads, and a PyroMark Q24 Workstation (Qiagen, UK) was used to separate the biotin-labelled DNA strand from the opposite strand. During this process, samples were taken-up by a vacuum pump tool, to which the sepharose beads adhered. Any impurities were then removed by placing the vacuum pump in 70% ethanol for 5 seconds with

the vacuum pump turned on. The vacuum pump was next placed into PyroMark Denaturation Solution (Qiagen, UK) for 5 seconds whilst turned on, to remove the opposite DNA strands and retain the required single-stranded DNA with the biotin-label. The vacuum pump was placed in PyroMark Wash Buffer (Qiagen, UK) for 10 seconds, after which the pump was switched off and placed into a 24-Well PyroMark Q24 Plate (Qiagen, UK), with each well containing 0.75 µl PyroMark Sequencing Primers (Qiagen, UK) and 24.25 µl PyroMark Annealing Buffer (Qiagen, UK), to allow the single-stranded DNA to enter the mix. The plate was kept at 80°C for 2 minutes then cooled to 20°C to allow primer binding (Schock, 2012), and was added to the pyrosequencing instrument along with a cartridge containing 116 µl Pyromark Enzyme Mixture (Qiagen, UK) (containing DNA polymerase, ATP-sulfurylase, luciferase, and apyrase), 116 µl PyroMark Substrate Mixture (Qiagen, UK) (containing adenosine 5' phosphosulfate and luciferin), and the 4 separate dNTPs (Qiagen, UK) (dATP, dTTP, dGTP, and dCTP). The reaction was performed, and the data analysed using PyroMark Q24 Software (Qiagen, UK). During the pyrosequencing reaction, each of the 4 dNTPs were added sequentially to the reaction, to allow complementary bases to be incorporated onto the single-stranded DNA. The successful binding of a dNTP caused the release of pyrophosphate (PPi) (Figure 26A). This PPi was converted to ATP by sulfurylase (Schock, 2012), and then ATP converted the substrate luciferin to oxyluciferin causing an emission of visible light (Figure 26A) (Schock, 2012). This light was represented in the form of a peak (Figure 26B and Figure 26C), to provide information on the level of T and G present at the 414 nucleotide location. The non-incorporated dNTPs were degraded by apyrase to prevent interference with the addition of the next nucleotide in the sequence. The cycle was repeated for each dNTP type at each DNA-strand nucleotide. The positive and negative controls containing 100% G and 0% G are shown in Figure 26B and Figure 26C respectively. Samples which gave percentages of G of over 2% were assumed to have the mutation present (Birket and Birch-Machin, 2007).

Figure 26

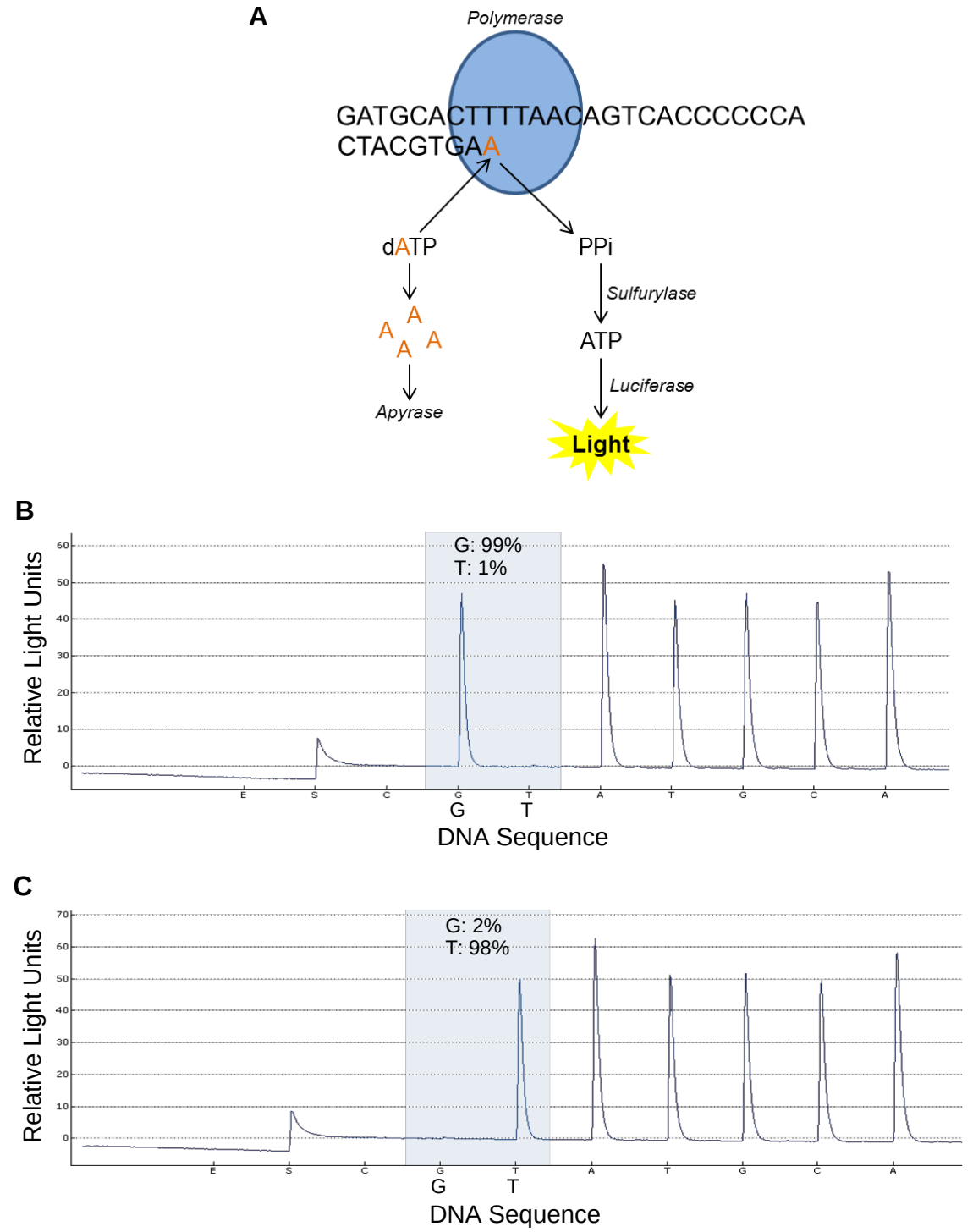

Figure 26. Pyrosequencing principle. A) During pyrosequencing, single-stranded DNA is amplified by polymerase (represented by the blue circle), with the individual dNTPs (dATP, dTTP, dCTP, and dGTP) added sequentially, and degraded by apyrase before the addition of the subsequent dNTP. In the figure above, T is the next DNA base in the single-stranded DNA sequence, so the added nucleotide (dATP) is able to bind (shown in orange). If the dNTP is able to bind it will release PPi, which is converted to ATP by sulfurylase. ATP is used to convert luciferin to oxyluciferin, causing visible light to be emitted. T: thymine; A: adenine; G: guanine; and C: cytosine. B) The positive control containing 100% G and 0% T at position 414 gave the expected peaks. C) The negative control containing 0% G and 100% T gave the expected peaks.

4.4 Results

4.4.1 *Cell sorting into senescent and non-senescent populations*

In the previous chapter (Chapter 3), it was demonstrated that complex II activity decreased with age in human skin fibroblasts. To further investigate the reason behind this decrease in activity, fibroblast cell samples from the same differently aged donors as used in the previous chapter were separated into senescent and non-senescent populations using FACS. Following cell sorting, the senescent and non-senescent cell populations were stained with a marker of senescence to confirm that the cells in the lower 20% lipofuscin autofluorescence did in fact contain mostly non-senescent cells, and the cells in the upper 20% lipofuscin autofluorescence contained mostly senescent cells. The marker β-gal was used, as this is a previously validated marker of senescence as it is found only in senescent cells (Dimri *et al.*, 1995; Lee *et al.*, 2006; Itahana *et al.*, 2007; Passos *et al.*, 2007a). Non-senescent cells appeared colourless, and senescent cells were blue in colour, as shown in Figure 27. As can be seen in Figure 28A, the cells in the lower 20% autofluorescence had significantly higher levels of non-blue cells (non-senescent cells) than blue cells (senescent cells) ($P<0.0001$, unpaired t-test). Cells in the upper 20% autofluorescence had significantly lower levels of non-senescent cells compared to senescent cells (Figure 28B) ($P<0.0001$, unpaired t-test). These significant differences confirmed successful sorting into senescent and non-senescent cell populations (Birket *et al.*, 2009). As the upper 20% lipofuscin autofluorescence had mostly senescent cells, and the lower 20% had mostly non-senescent cells, these populations are referred to senescent and non-senescent populations respectively in future sections.

Figure 27

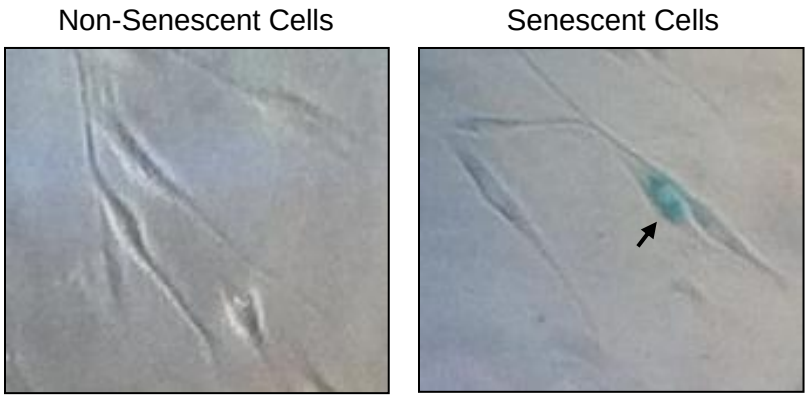

Figure 27. Senescence-associated β-gal staining. The presence of senescence in cells from FACS-sorted cell populations was examined using senescence-associated β-gal staining. β-gal activity has been shown previously to only be present in senescent cells (Dimri *et al.*, 1995), and these cells were shown by a blue colour, an example of which is given by the black arrow. The non-senescent cells remained colourless.

Figure 28

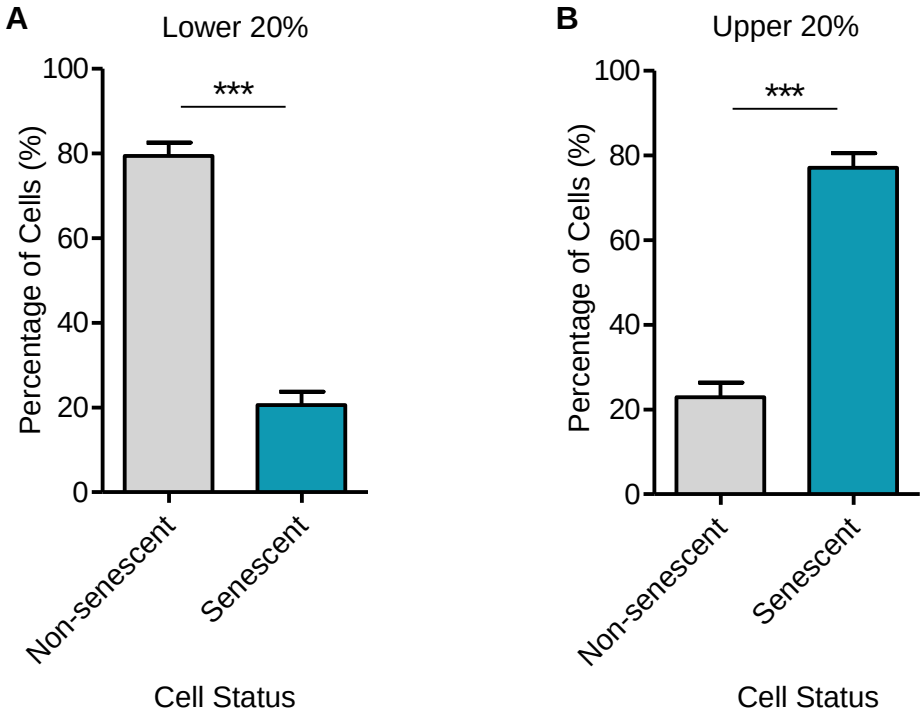

Figure 28. The percentage of senescent and non-senescent cells in the lower and upper 20% of lipofuscin autofluorescence. Senescence was determined by β-gal staining following FACS. A) The percentage of non-senescent cells (grey bar) and senescent cells (blue bar) in the lower 20% lipofuscin population for 5 donor samples. There was a significantly higher percentage of non-senescent than senescent cells (P<0.0001***, unpaired t-test). B) The percentage of non-senescent and senescent cells from the upper 20% lipofuscin population for 5 donor samples. There was a significantly higher percentage of senescent cells than non-senescent cells (P<0.0001***, unpaired t-test). The error bars show the SEM. The β-gal stain was performed at least in duplicate for each donor sample for each cell status (senescent and non-senescent), for 5 samples in total for each of the upper and lower lipofuscin groups.

4.4.2 *β-gal staining in senescent and non-senescent populations from older and younger donors*

Older individuals have been shown in previous studies to have a higher number of senescent cells than younger individuals (Dimri *et al.*, 1995; Noppe *et al.*, 2009). Therefore, it was speculated that the FACS-sorted upper 20% autofluorescence population (the senescent population) from the older individuals may possibly contain a higher number of senescent cells than the upper 20% from younger individuals, which could affect later results. To ensure that this was not the case, β-gal was used to stain the FACS-sorted cells, and it was found that both the older (>50 years old) and the younger (<50 years old) donor samples did not have significantly different percentages of senescent cells present in either the lower 20% autofluorescence (Figure 29A) (P=0.1434, unpaired t-test), or the upper 20% autofluorescence (Figure 29B) (P=0.8845, unpaired t-test). The age parameter used (younger or older than 50 years old) was chosen based on previous work (Chretien *et al.*, 1994; Micallef *et al.*, 2007; Williams *et al.*, 2010; Geng *et al.*, 2011).

Figure 29

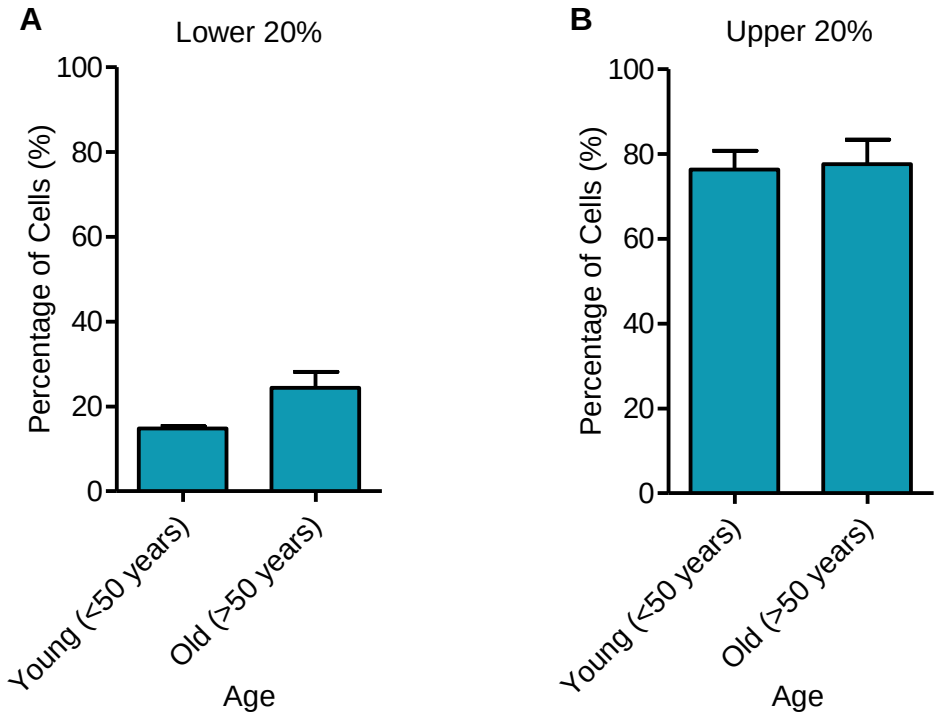

Figure 29. Percentage of senescent cells in the lower and upper 20% lipofuscin for older and younger individuals. Senescence was determined by β-gal staining following FACS. A) Percentage of blue cells in the lower 20% lipofuscin populations for young (<50 years old) and old (>50 years old) individuals, for 5 donors. There was no significant difference between age groups (P=0.1434, unpaired t-test). B) Percentage of blue cells for the upper 20% lipofuscin populations, for 5 young and old donors. There was no significant difference between age groups (P=0.8845, unpaired t-test). The error bars show the SEM. The β-gal stain was performed at least in duplicate for each sample for both the upper and lower lipofuscin populations.

4.4.3 *Complex II activity in senescent and non-senescent cells from differently aged donors*

Skin fibroblast samples from 15 donors aged from 6 to 71 years old were sorted via FACS into senescent and non-senescent populations, to determine the level of complex II activity within these two populations for each individual. It was found that within the non-senescent cells alone, there was no correlation between CII/CS activity and age (Figure 30A) (P=0.5366, rho=-0.1734, non-parametric Spearman correlation). However, within the senescent cell population, there was a significant decrease in CII/CS activity with age (Figure 30B) (P=0.0289, rho=-0.5630, non-parametric Spearman correlation).

When the CII/CS activities of the 15 senescent and 15 non-senescent cell populations were compared, it was found that complex II activity was

unexpectedly higher in the senescent cells (Figure 31A) (P=0.0086, unpaired t-test). This may seem unusual as older people are thought to have a higher number of senescent cells (Dimri *et al.*, 1995; Noppe *et al.*, 2009), yet the complex II activity for the older individuals was not higher than for the younger individuals (Chapter 3). However, it was found that senescent cells from older individuals have a lower complex II activity than senescent cells from younger individuals (Figure 30B), which could explain the overall lower CII/CS activity with age (Chapter 3). Upon further investigation, it was found that the non-senescent cells from younger individuals showed no difference in CII/CS activity compared to the senescent cells from older individuals (Figure 31B) (P=0.5470, unpaired t-test), indicating that the senescent cells from older individuals would not be likely to cause a higher CII/CS activity in overall cell samples. Additionally, younger individuals showed significantly higher levels of CII/CS activity in their senescent cells compared to their non-senescent cells (Figure 31C) (P=0.0311, unpaired t-test), whereas although a trend was present, there was no significant difference in CII/CS activity between the senescent and non-senescent cells of the older individuals (Figure 31D) (P=0.0708, unpaired t-test).

Figure 30

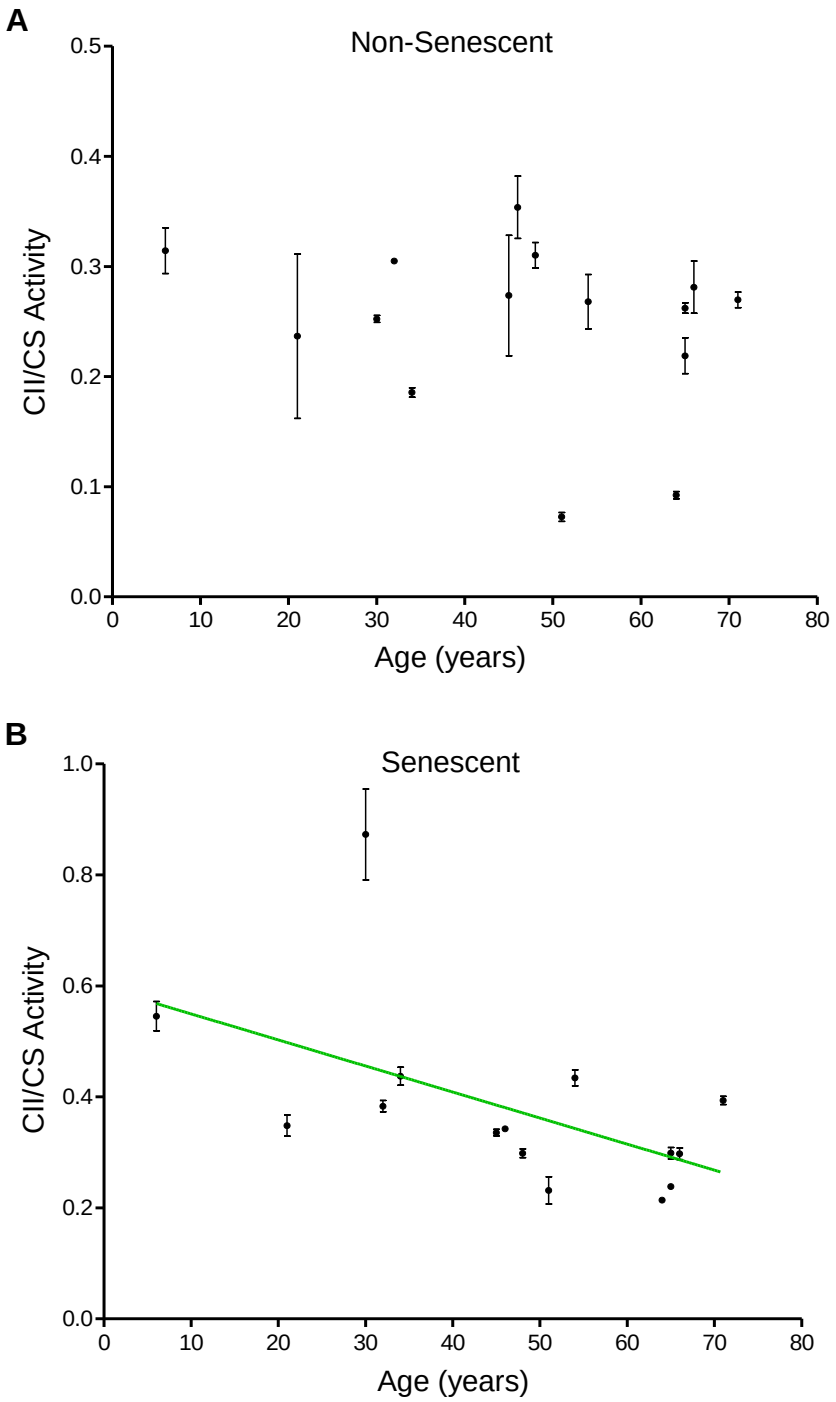

Figure 30. Complex II activity compared to donor age for non-senescent and senescent human skin fibroblasts. A) CII/CS activity for the FACS-sorted non-senescent populations of fibroblasts from 15 donors was compared to the age of each donor. There was no significant correlation between CII/CS activity and age for the non-senescent cells (P=0.5366, rho=-0.1734, non-parametric Spearman correlation). B) CII/CS activity for the FACS-sorted senescent populations of fibroblasts from 15 donors, compared to the age of each donor. There was a significant decrease in CII/CS activity with age for the senescent cells (P=0.0289, rho=-0.5630, non-parametric Spearman correlation). The green line shows the line of best fit. The error bars show the SEM. Photometry was performed at least twice for the citrate synthase assay and at least twice for the complex II activity assay for each cell population of each sample.

Figure 31

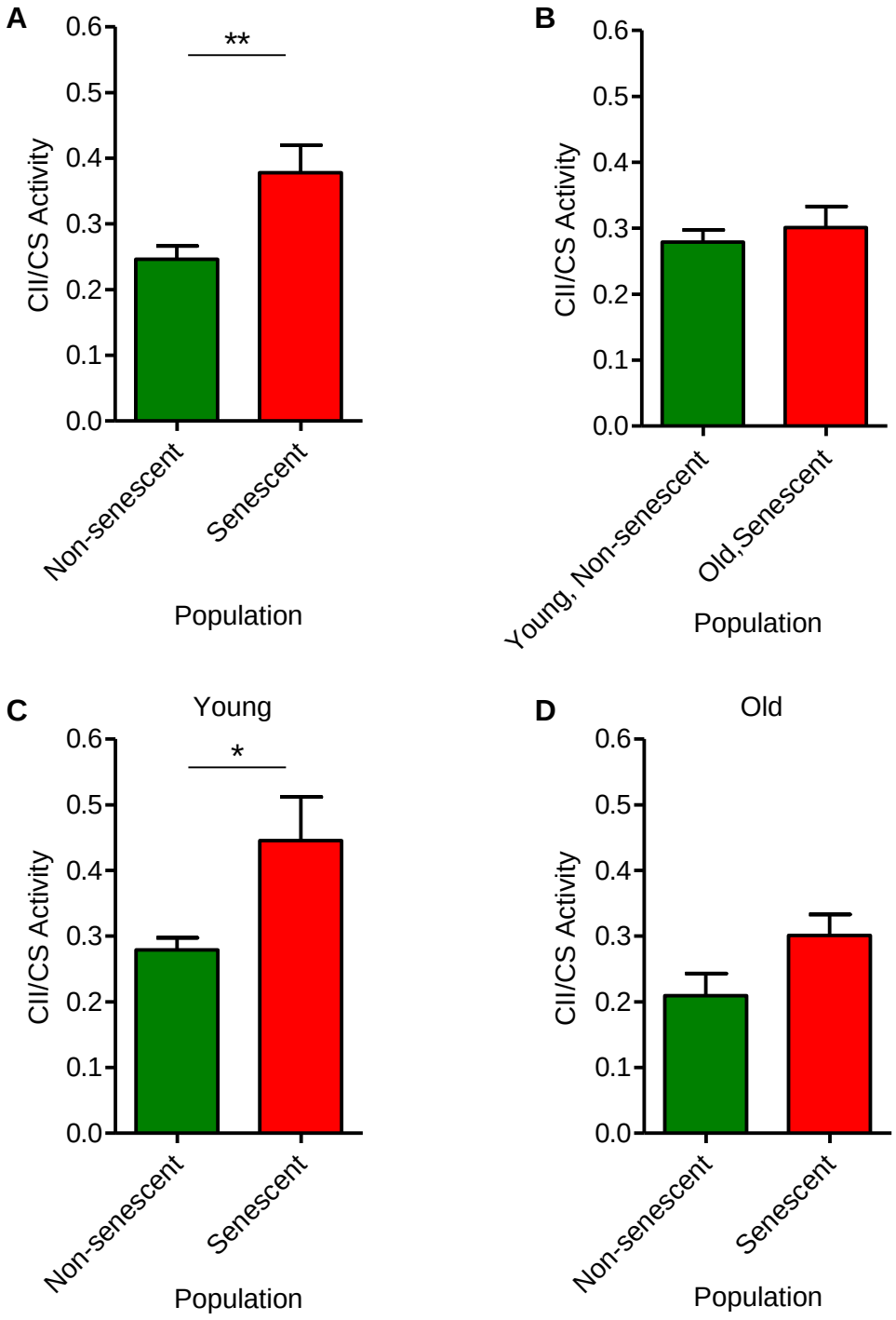

Figure 31. Complex II activity in senescent and non-senescent cell populations. A) CII/CS activity of fibroblasts from 15 donors was determined following FACS, in senescent and non-senescent cell populations. CII/CS activity was significantly higher in senescent cells than in non-senescent cells (P=0.0086**, unpaired t-test). B) CII/CS activity was not significantly different in non-senescent cells from younger donors (<50 years old) compared to senescent cells from older donors (>50 years old) (P=0.5470, unpaired t-test). C) Younger donors had significantly higher levels of CII/CS activity in their senescent cells compared to their non-senescent cells (P=0.0311*, unpaired t-test). D) Older donors had no significant difference in CII/CS activity between their senescent and non-senescent cells (P=0.0708, unpaired t-test). The error bars show the SEM. Photometry was performed at least twice for the citrate synthase assay and at least twice for the complex II activity assay for each cell population of each sample, and the average value was used for each sample.

4.4.4 *Complex IV activity in senescent and non-senescent cells from differently aged donors*

To determine whether the decrease in complex II activity seen in senescent cells with age was also occurring in other mitochondrial complexes, the level of complex IV activity was measured in the FACS-sorted cell populations. It was found that there was no significant correlation in CIV/CS activity with age for the non-senescent population (Figure 32A) (P=0.5560, rho=-0.2857, non-parametric Spearman correlation) or for the senescent population (Figure 32B) (P=0.4976, rho=0.3214, non-parametric Spearman correlation). This suggested that complex II activity, but not complex IV activity, decreases with age in senescent cells. It also suggested that neither complex is affected by age in the non-senescent cell population. Despite fewer samples available for complex IV activity analysis, there did not appear to be any trend present between complex IV activity and age in either the senescent or the non-senescent populations. There was also no correlation between complex IV activity and age in unsorted cells (Chapter 3), which suggested that the rate of complex IV activity does not decrease with age.

There was no significant difference in complex IV activity between the senescent and non-senescent cells when directly compared (Figure 33) (P=0.8175, unpaired t-test).

Figure 32

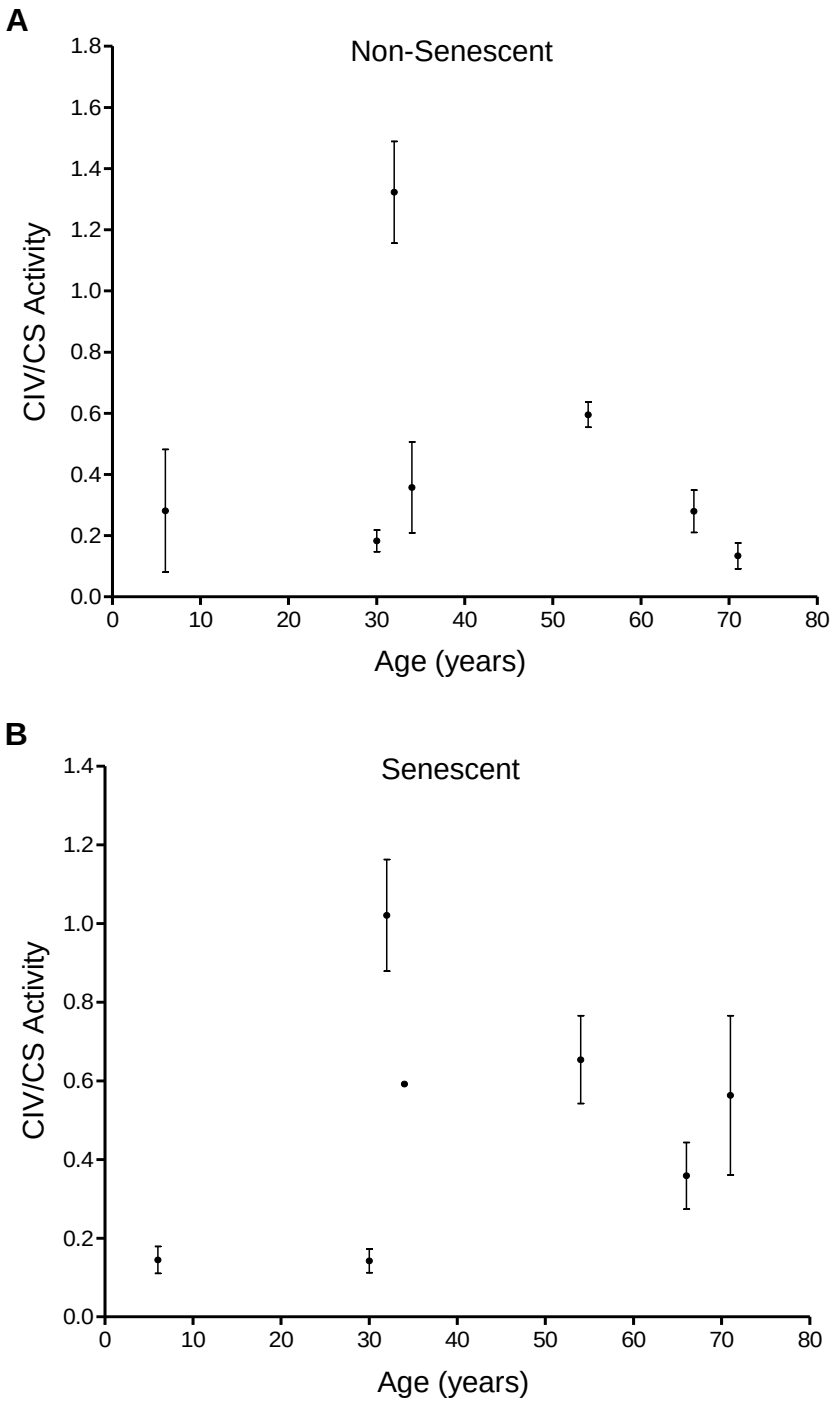

Figure 32. Complex IV activity compared to donor age for non-senescent and senescent human skin fibroblasts. A) CIV/CS activity for the FACS-sorted non-senescent populations of fibroblasts from 7 donors, compared to the age of each donor. There was no significant correlation between CIV/CS activity and age (P=0.5560, rho=-0.2857, non-parametric Spearman correlation). B) CIV/CS activity for the FACS-sorted senescent populations of fibroblasts from 7 donors, compared to the age of each donor. There was no significant correlation between CIV/CS activity and age (P=0.4976, rho=0.3214, non-parametric Spearman correlation). The error bars show the SEM. Photometry was performed at least twice for the citrate synthase assay and at least twice for the complex IV activity assay for each cell population of each sample.

Figure 33

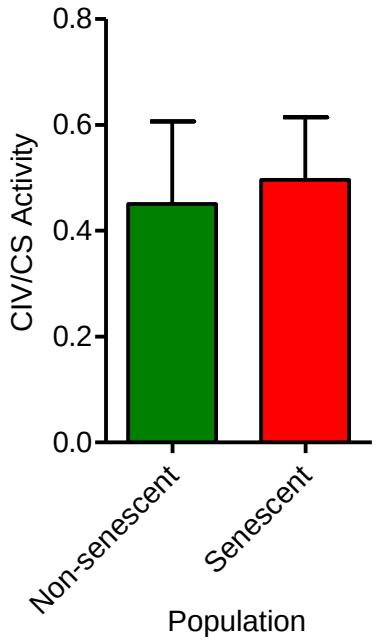

Figure 33. Complex IV activity in non-senescent and senescent cell populations. CIV/CS activity of fibroblasts from 7 donors was determined following FACS. There was no significant difference in CIV/CS activity between the non-senescent and senescent cell populations (P=0.8175, unpaired t-test). The error bars show the SEM. Photometry was performed at least twice for the citrate synthase assay and at least twice for the complex IV activity assay for each population of each sample, and the average value was used for each sample.

4.4.5 *T414G mutation level in senescent and non-senescent cells from differently aged donors*

To further understand the possible differences between senescent and non-senescent cells with age, the level of an age-related mtDNA mutation, T414G (Birket and Birch-Machin, 2007), was measured using pyrosequencing. Initially, to confirm an age-related increase in this mutation, unsorted fibroblast samples from 21 individuals aged between 6 and 72 years old were tested. It was found that the T414G mutation was detectable in 9 of the 21 samples, and a significant increase in the level of mutation was observed with age (Figure 34) (P=0.0291, rho=0.4762, non-parametric Spearman correlation). However, this was not the case for the FACS-sorted cells, for which the T414G mutation was not detected in any of the 13 senescent or 13 non-senescent sample populations tested (despite being present in 5 of the same unsorted samples) (results not shown). This could imply that the mutation was present only in those cells which were discarded (the middle 60% lipofuscin autofluorescence), or that the mutation was present throughout the cell sample regardless of

senescence status, and was therefore not detectable when only the upper or lower 20% of the sample was examined due to its dilution to low levels. Additionally, it is worth noting that the T414G mutation was not able to be detected in primary unsorted keratinocyte cells which were also tested.

Figure 34

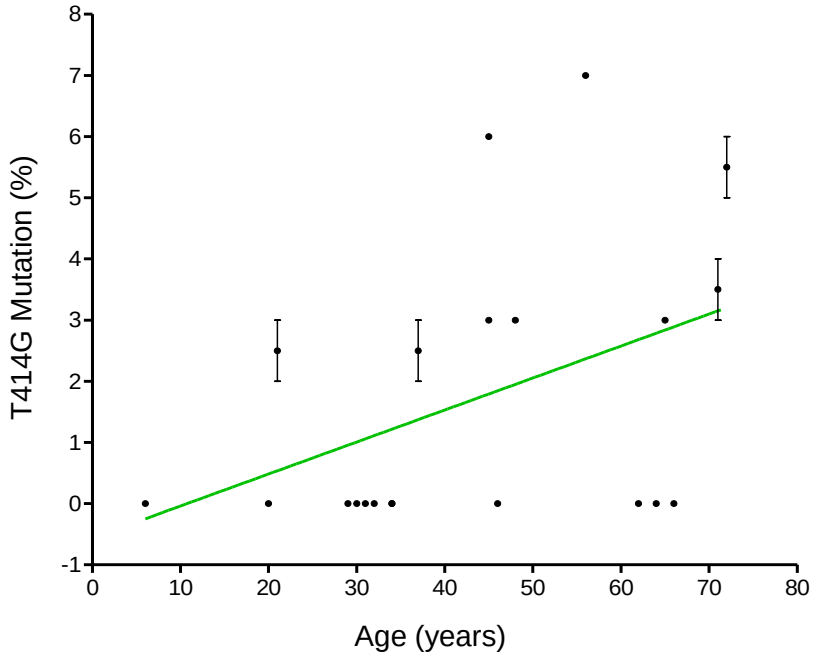

Figure 34. The level of T414G mutation compared to the age of the donor in unsorted fibroblast cells. A) The percentage of T414G mutation in 21 unsorted fibroblast samples compared to the age of the donor. There was a significantly higher level of mutation with age (P=0.0291, rho=0.4762, non-parametric Spearman correlation). The green line shows the line of best fit. The error bars show the SEM. Results were obtained from two pyrosequencing repeats for 21 samples.

4.4.6 *Mitochondrial activity in a model of younger and older cells*

Finally, to further confirm the decrease in complex II activity observed with age in human skin fibroblasts (Chapter 3), a model for older and younger cells was used. The model used was human lung fibroblast cells (MRC5 cells), and human lung fibroblast cells with increased expression of the catalytic subunit of telomerase (MRC5/hTERT cells). The cells overexpressing hTERT were used to represent the younger cells, as the additional telomerase activity should result in similar phenotypes to those found in cells from younger individuals. To demonstrate the reliability of hTERT overexpression in preventing cellular senescence, the MRC5/hTERT and the MRC5 cells were tested for β-gal

activity. It was found that the MRC5/hTERT cells had a significantly lower level of senescent cells than the MRC5 cells (Figure 35) (P=0.0026, unpaired t-test), as expected.

Complex II activity was measured in the MRC5 and MRC5/hTERT cells, and it was found that the MRC5/hTERT cells had a significantly higher level of activity than the MRC5 cells (Figure 36) (P=0.0012, unpaired t-test). This correlated with the work using differently aged skin fibroblasts where it was found that the younger individuals had faster complex II activity than the older individuals (Chapter 3). Contradictory to the complex IV activity results found in the naturally aged human skin (Chapter 3) for which there was no difference with age, the MRC5/hTERT cells overexpressing telomerase showed a significantly higher level of complex IV activity than the MRC5 cells (Figure 37) (P=0.0209, unpaired t-test). This suggested that in the lung cells, the level of complex IV activity is higher in cells with additional telomerase.

Figure 35

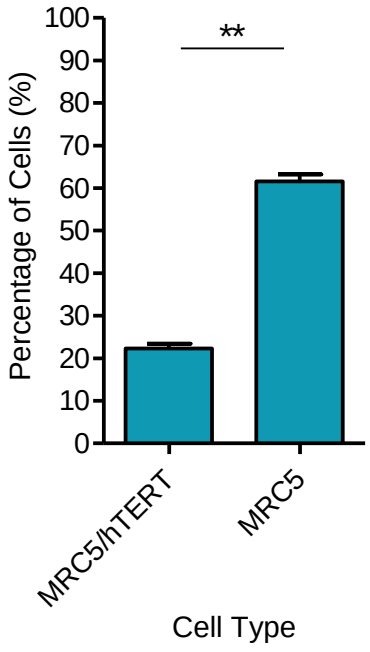

Figure 35. The percentage of senescent cells for MRC5 and MRC5/hTERT cells. The percentage of senescent cells for the MRC5 and MRC5/hTERT cells as determined by β-gal staining. The level of β-gal-stained cells was significantly higher in the MRC5 cells than in the MRC5/hTERT cells (P=0.0026**, unpaired t-test). The error bars show the SEM. The β-gal staining was performed at least in triplicate for each cell type.

Figure 36

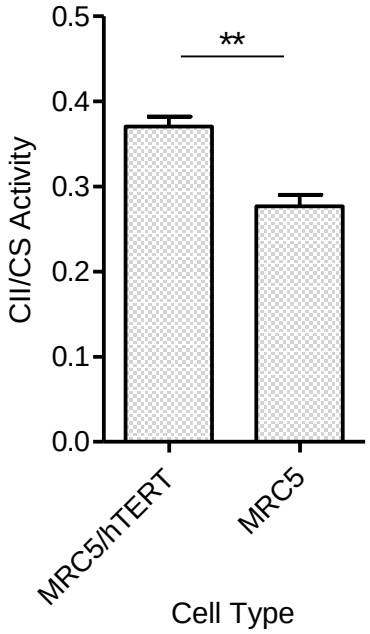

Figure 36. Complex II activity in MRC5 and MRC5/hTERT cells. CII/CS activity of MRC5 and MRC5/hTERT cells as determined by photometry. CII/CS activity was significantly higher in the MRC5/hTERT cells than in the MRC5 cells (P=0.0012**, unpaired t-test). The error bars show the SEM. Photometry was performed at least twice for the citrate synthase assay and at least four times for the complex II activity assay.

Figure 37

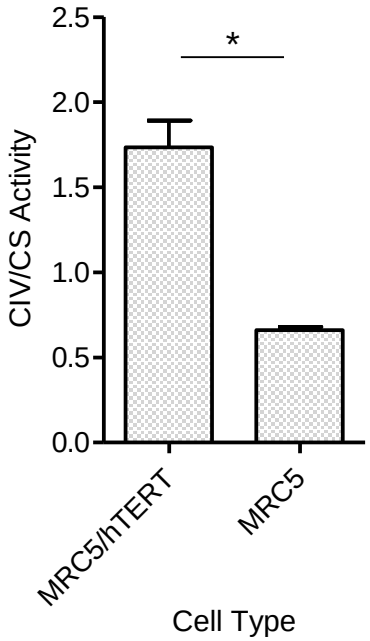

Figure 37. Complex IV activity in MRC5 and MRC5/hTERT cells. CIV/CS activity of MRC5 and MRC5/hTERT cells as determined by photometry. CIV/CS activity was significantly higher in the MRC5/hTERT cells than in the MRC5 cells (P=0.0209*, unpaired t-test). The error bars show the SEM. Photometry was performed at least twice for the citrate synthase assay and at least twice for the complex IV activity assay.

4.5 Discussion

4.5.1 *Cells were successfully sorted into senescent and non-senescent populations*

Cells from differently aged donors were successfully sorted into senescent and non-senescent populations using FACS, as confirmed by the previously well-established biomarkers of senescence, lipofuscin autofluorescence (Martin-Ruiz *et al.*, 2004; Passos *et al.*, 2007a; Passos and von Zglinicki, 2007; Birket *et al.*, 2009) and β-gal staining (Dimri *et al.*, 1995; Lee *et al.*, 2006; Itahana *et al.*, 2007; Passos *et al.*, 2007a).

Following FACS sorting, it was initially speculated that the upper 20% autofluorescence for the older individuals may contain a higher number of senescent cells than the upper 20% autofluorescence for the younger individuals, since senescence has been shown to increase with age, both *in vivo* and in culture (Dimri *et al.*, 1995; Mishima *et al.*, 1999; Campisi, 2005; Herbig *et al.*, 2006; Noppe *et al.*, 2009; Naylor *et al.*, 2013). If this was the case, it would have been difficult to decipher whether any changes observed in complex II activity with age were due differences in senescent cell numbers or in senescent cell activity. However, this was not the case, because β-gal staining of the senescent and non-senescent cell populations of older and younger individuals (over and under 50 years old respectively, based on previous work (Drouet *et al.*, 1999; Micallef *et al.*, 2007; Williams *et al.*, 2010; Geng *et al.*, 2011)) revealed no differences in the levels of β-gal-stained cells.

4.5.2 *Complex II activity declines with age in senescent but not in non-senescent cells*

Based on the observations made in the previous chapter (Chapter 3), and observed previously in the literature (Coggan *et al.*, 1992; Boffoli *et al.*, 1994; Sandhu and Kaur, 2003; Kumaran *et al.*, 2004; Cocco *et al.*, 2005; Short *et al.*, 2005; Braidy *et al.*, 2011; Tatarkova *et al.*, 2011; Velarde *et al.*, 2012), complex II activity appears to decrease in an age-dependant manner in various organisms and tissues. To further understand the reasons behind this decrease with age, the level of complex II activity was examined in senescent and non-senescent skin fibroblast cell populations, as senescent cells are thought to play a prominent role in the ageing process, potentially via mitochondrial dysfunction

(Passos *et al.*, 2007a; Dekker *et al.*, 2009; Moiseeva *et al.*, 2009; Passos *et al.*, 2010; Treiber *et al.*, 2011; Velarde *et al.*, 2012). It was found in the present study that the activity of complex II decreased in an age-dependant manner in senescent cells, but not in non-senescent cells. This could suggest that the overall decrease in complex II activity observed in Chapter 3 was due to the senescent cells only. The Rho value (measuring the strength of the relationship between two factors) observed in Chapter 3 for the age versus the complex II activity of donors was -0.4614. For the senescent cell populations only, the strength of the relationship was -0.5630. This demonstrates a slightly stronger relationship between age and complex II activity for the senescent cells alone, possibly due to the removal of the non-senescent cells. However, as the Rho value was still not close to -1, it suggested that factors other than ageing may also be affecting complex II activity in the senescent cells, such as differences between the lifestyles of individuals and the interactions of the other mitochondrial complexes, as discussed in Chapter 3 section 3.5.1. However, it did appear that senescent cells had a higher influence than non-senescent cells in determining complex II activity with age.

To my knowledge, no previous studies have been performed comparing the differences in mitochondrial complex activity between senescent cells from older and senescent cells from younger individuals. Therefore, this study provides the first evidence that senescent cells from older individuals are less efficient in terms of mitochondrial complex II activity than senescent cells from younger individuals, which could have important implications in terms of deciphering the causes of the overall decrease in cellular efficiency observed with age (Lopez-Lluch *et al.*, 2006; Gómez and Hagen, 2012). Reasons behind this decrease in complex II activity in senescent cells with age remain unknown. Future studies measuring complex II subunit levels in these cells could be performed, as it was found in Chapter 3 that the expression and protein levels of both SDHA and SDHB were decreased with age, which could be potentially causative in terms of the decrease in complex II activity. It is therefore possible that these subunits were decreased only in the senescent cells with age and not in the non-senescent cells; however, this would need to be verified. A possible cause of the decrease in complex II activity (and potentially the complex II subunit levels) with age in senescent cells, could be due to senescent cells

having higher levels of ROS production than non-senescent cells (Passos *et al.*, 2007a), resulting in an increase in mtDNA/nDNA damage and mitochondrial dysfunction (Passos *et al.*, 2007a), which could result in a decrease in complex II activity if the damage is high enough. ROS leakage from senescent cells (Nelson *et al.*, 2012) could exacerbate the decrease in complex II activity with age by causing damage to surrounding cells. This damage may be higher in the senescent cells of older individuals due to the lower levels of antioxidants found with age (Micallef *et al.*, 2007), and the decline in senescence removal systems such as the immune system (Krizhanovsky *et al.*, 2008; Rodier and Campisi, 2011) and the autophagy/lysosomal pathway (Dutta *et al.*, 2012; Baker and Sedivy, 2013; Viiri *et al.*, 2013). This could result in a lower complex II activity in the senescent cells of older individuals. However, to confirm whether other aspects of senescent cells are less efficient with increasing age, other features of the senescent cells would need to be studied, such as the activity of complexes I and III, as well as DNA damage and ROS production changes in senescent cells with age.

4.5.3 *Complex II activity is higher in senescent cells than in non-senescent cells in younger individuals*

Complex II activity was found to be significantly higher overall in the senescent cells compared to the non-senescent cells. Therefore, it might have been expected that older individuals would have a higher level of complex II activity due to the higher number of senescent cells present in these individuals (Dimri *et al.*, 1995); however, this was found not to be the case in the previous chapter (Chapter 3). The level of complex II activity was found to be significantly higher in the senescent cells of younger compared to the senescent cells of older individuals. This could suggest that the higher number of senescent cells present in the older donors (Dimri *et al.*, 1995) would not result in a higher complex II activity compared to the younger donors. In addition to this, it was found that the complex II activity in senescent cells from older individuals was not significantly different from the activity in non-senescent cells from younger individuals, and senescent and non-senescent cells from the older donors alone showed no significant difference in activity, suggesting that a higher number of senescent cells in older donors would not be sufficient to increase complex II activity.

Younger individuals showed a higher complex II activity in their senescent cells compared to their non-senescent cells. However, the reason for this higher complex II activity in the senescent cells (which could then decrease with age due to an accumulation of unrepaired damage) was not tested. It could be speculated that senescent cells increase their complex II activity compared to non-senescent cells as a compensatory mechanism, due to the increase in mitochondrial dysfunction in senescence (Passos *et al.*, 2010). Compensatory mechanisms similar to this have been shown to occur previously in the blood cells of patients with Leber's hereditary optic neuropathy (an inherited degenerative disease of the retinal cells), for which complex I is dysfunctional due to mtDNA point mutations, and complex II activity is increased to compensate (Yen *et al.*, 1996; Baracca *et al.*, 2005). Other work has shown a compensatory increase in complex III activity when complex IV is decreased in a model of Alzheimer's disease (Rhein *et al.*, 2009), and alterations in ATP levels can cause changes in mitochondrial complex activities (Ostojic *et al.*, 2013). Additionally, it has been demonstrated that in mouse heart tissue there is a decrease in complex IV activity with age, yet an increase in complex II activity, which could be an age-related compensatory mechanism (Kwong and Sohal, 2000). Alternatively, it could be that complex II activity is increased in senescent cells in an attempt to maintain ROS levels and therefore DNA damage and the senescent phenotype (Passos *et al.*, 2010). This ROS production could be more damaging in older individuals, due to a lower efficiency of cellular defences (Micallef *et al.*, 2007; Rodier and Campisi, 2011; Dutta *et al.*, 2012; Viiri *et al.*, 2013), resulting in damage to complex II and eventually a lower complex II activity, potentially with ROS release. This may seem paradoxical, however, increased ROS production has been correlated with both a higher (Redout *et al.*, 2007; Seidlmayer *et al.*, 2011; Dröse, 2013; Moreno-Sanchez *et al.*, 2013; Siebels and Drose, 2013) and a lower (Li *et al.*, 1995; Melov *et al.*, 1999; Ishii *et al.*, 2005; Morten *et al.*, 2006; Byun *et al.*, 2008; Quinlan *et al.*, 2012; Velarde *et al.*, 2012; Dröse, 2013; Luo *et al.*, 2013) level of complex II activity. Future studies investigating the levels of ROS in senescent cells from older and younger individuals would be required to confirm this theory, however ROS has been shown to be higher in senescent cells than in non-senescent cells (Passos *et al.*, 2007a; Birket *et al.*, 2009; Nelson *et al.*, 2012).

4.5.4 *Complex IV activity is not associated with age in senescent or non-senescent cells*

As observed in the previous chapter (Chapter 3), the level of complex IV activity was not associated with the age of the individual in human skin cells. However, to ensure that a change in complex IV activity with age was not masked in senescent cells by the presence of non-senescent cells, complex IV activity was measured in FACS-sorted cells. No correlation was found between complex IV activity and age in either the senescent or the non-senescent cell populations. This is in accordance with the results found in Chapter 3, as the overall activity of complex IV did not decrease with age. These results suggested that mitochondrial dysfunction occurs at complex II but not at complex IV in senescent cells with age; however, to confirm whether the decrease in activity at the ETC in senescent cells with age was localised to complex II, the activities of complexes I and III in senescent cells from differently aged individuals would also need to be studied.

The present study demonstrated a lack of difference in complex IV activity between senescent and non-senescent cells. Previous work is somewhat contradictory in terms of complex IV activity in senescent cells, with some studies showing increased and some showing decreased complex IV activity. In a recently published study, senescent late-passage human lung fibroblasts and early-passage lung fibroblasts induced to senescence by a component of cigarette smoke (as confirmed by β-gal and other senescence markers), were compared to early-passage non-senescent fibroblasts (Luo *et al.*, 2013). It was found that the senescent cells had decreased expression of complexes I, II, III, and V, but an increase in complex IV expression (Luo *et al.*, 2013). However, other previous studies have shown lower complex IV activity in senescent cells compared to non-senescent cells; for example, complex IV has been shown to be lower in mink lung epithelial cells induced to senescence by transforming growth factor β (TGF-β1), for which ROS levels were increased (Yoon *et al.*, 2005). Also, complex IV has been shown to be lower in porcine pulmonary artery cells following serial culture to senescence (Zhang *et al.*, 2002). It could be speculated that these differences in complex IV activity are due to different mechanisms of ROS production in senescent cells, required to maintain the senescent cell phenotype (Passos *et al.*, 2010). For example, if complex IV

activity is increased in senescence to increase ROS levels, it could be that high activities of complexes I, II, and III are not required for ROS generation to maintain senescence. In the present study, it could be that sufficient ROS levels were generated by the higher complex II activity in senescent skin fibroblasts, so interaction from complex IV was not necessary.

In conclusion, the role of complex IV in senescence is not fully understood, and could show differences depending on the cell type. However, the results of the present study suggest that complex IV does not decrease with age in either the non-senescent or the senescent cells in human skin fibroblasts, and does not show a senescence-associated change in activity.

4.5.5 *The T414G mutation increases with age in unsorted samples but not in sorted samples*

Senescent cells have been shown in previous studies to have high ROS levels (Passos *et al.*, 2007a; Birket *et al.*, 2009; Nelson *et al.*, 2012); therefore, it was thought that these cells may accumulate higher levels of mtDNA mutations, and that these may be at a higher or lower level depending on the age of the donor from which the senescent cells were derived. The level of T414G mutation was measured in unsorted skin fibroblast cell samples as well as in senescent and non-senescent FACS-sorted fibroblast populations. The results obtained in the present study are in accordance with previous work (Michikawa *et al.*, 1999; Birket and Birch-Machin, 2007), in that the T414G mutation was present in a higher proportion of skin cell samples from older individuals than from younger individuals. This increase in T414G mtDNA mutation could have implications for the ageing process, as despite this mutation not thought to contribute to the ageing process directly, due to it not being selected either for or against in culture (Michikawa *et al.*, 1999; Seibel *et al.*, 2008; Birket *et al.*, 2009), it has been shown to be associated with mutations that are bioenergetically damaging (Birket and Birch-Machin, 2007; Seibel *et al.*, 2008).

Previous work has shown that mtDNA damage in the form of strand breaks is higher in senescent cells compared to non-senescent cells (Passos *et al.*, 2007a; Birket *et al.*, 2009); however, this was not the case for the T414G mutation in the present study, which was not detectable in either the senescent

or the non-senescent cell populations. This is somewhat in accordance with the only previous study on the T414G mutation in senescent and non-senescent cells, for which this mutation was not associated more strongly with either senescence or non-senescence (Birket *et al.*, 2009). However, in the previous study, the mutation was still detected in several of the sorted samples. The ability to detect this mutation in the past study may have been due to all of the samples being from very old individuals (with an average age of 81 years old for the five samples tested) (Birket *et al.*, 2009), which was not the case for the present study. In conclusion, the T414G mutation does not appear to be associated with senescence, possibly due to its lack of correlation with ROS as shown previously (Birket *et al.*, 2009).

4.5.6 *Complex II activity and complex IV activity are higher in a model of younger cells*

In order to further confirm the decrease in complex II activity observed with age in the fibroblast samples from older and younger donors (Chapter 3), a model for older and younger cells was used. This model was based on the observation that overexpression of the telomerase catalytic unit in cells allows for a decreased rate of telomere shortening, improved antioxidant defences, increased repair capacity, lower ROS levels, a higher number of population doublings, and lower senescence levels (Bodnar *et al.*, 1998; Zhu *et al.*, 2000; Franco *et al.*, 2001; Sharma *et al.*, 2003; Armstrong *et al.*, 2005; Masutomi *et al.*, 2005; Mondello *et al.*, 2006; Passos *et al.*, 2007b; Ahmed *et al.*, 2008; Saretzki, 2009; Daniels *et al.*, 2010; Indran *et al.*, 2011; Bellot and Wang, 2013; Smith *et al.*, 2013). These are features also present in younger individuals (Harley *et al.*, 1990; Allsopp *et al.*, 1995; Dimri *et al.*, 1995; Mishima *et al.*, 1999; Cawthon *et al.*, 2003; Campisi, 2005; Herbig *et al.*, 2006; Micallef *et al.*, 2007; Noppe *et al.*, 2009; Naylor *et al.*, 2013; Shi *et al.*, 2013), allowing for the hTERT-overexpressing cells to be used as a model for young age.

It was found in the present study that the activities of both complexes II and IV were higher in the MRC5/hTERT cells than in the MRC5 cells. This was in accordance with the results obtained in Chapter 3 for complex II activity, in that cells representing younger individuals (MRC5/hTERT) had higher complex II activity, as did the cells from younger donors. This provided further evidence

that a decrease in complex II activity is occurring with age, and could also indicate that this phenomenon occurs across different tissue types (lung and skin, although future tests on naturally aged lungs would be required to confirm this). To my knowledge, the present study provides the first evidence that a higher level of complex II activity is occurring in cells with increased expression of hTERT compared to those without. Previous studies have shown increased activity in complex I when hTERT is overexpressed (Haendeler *et al.*, 2009), and in complex IV (Indran *et al.*, 2011), as well as overall increases in ETC respiration (Haendeler *et al.*, 2009), which could suggest that complex II is also increased. This would be in accordance with the present study.

The higher complex IV activity in MRC5/hTERT cells found in the present study is in accordance with previous work showing higher complex IV activity in this cell type (Indran *et al.*, 2011). However, this higher activity of complex IV in the 'younger' MRC5/hTERT cells compared to the 'older' MRC5 cells is different to the results received in Chapter 3 in naturally aged cells, which showed no difference in complex IV activity with age. A possible reason for this could be due to hTERT translocation to the mitochondrial matrix under stressful conditions (Santos *et al.*, 2004; Jakob and Haendeler, 2007; Haendeler *et al.*, 2009), after which hTERT has been proposed to bind to mtDNA to improve its function (Haendeler *et al.*, 2009). In the study by Haendeler *et al*., (2009), hTERT was found to bind to the mtDNA coding regions of complex I (ND1 and ND2), which resulted in a higher complex I activity. This could potentially also be the case for complex IV, which is partially encoded by mtDNA; however this has not been tested. Since complex II is entirely nuclear-encoded, it could be that this complex in the MRC5/hTERT cells is more representative of complex II in natural cells, unlike complex IV which could be affected by hTERT at the mtDNA. Overall, the use of MRC5/hTERT cells and MRC5 cells as a model for different ages may be effective in confirming some aspects of natural ageing, but not others.

4.6 Summary

In conclusion, it was found that the level of complex II activity decreased with age in senescent cells but not in non-senescent cells, suggesting that senescent cells are more influential than non-senescent cells in determining the overall complex II activity with age. This decrease could have been partially due to a reduction in complex II subunit expression with age as observed in the previous chapter, which may have been the result of a lower antioxidant and repair capacity with age (Micallef *et al.*, 2007; Rodier and Campisi, 2011; Dutta *et al.*, 2012; Viiri *et al.*, 2013); however, any changes in complex II subunits would need to be examined in future studies. The level of complex IV activity did not change with age in senescent or in non-senescent cells, which is in accordance with results in the previous chapter.

The mtDNA T414G mutation was found in the present study to be more prevalent in older individuals than in younger, but was not detected in senescent or in non-senescent populations, suggesting that this mutation accumulates with age due to factors independent of senescence.

The model used to represent older and younger cells, the MRC5 and MRC5/hTERT cells respectively, showed higher activity for both complexes II and IV in the cells overexpressing telomerase. As complex II activity was lower in both the model for older cells and the naturally older cells, it possibly further confirms that complex II activity does in fact decrease with age or with phenotypes of age such as higher ROS levels. The reason for the higher complex IV activity in the MRC5/hTERT cells but not in the cells from young donors could be due to the hTERT in the MRC5/hTERT cells translocating to the mtDNA to enhance the expression of mtDNA-encoded complex IV subunits, which has been shown to happen previously for complex I (Haendeler *et al.*, 2009).

Chapter 5. Mitochondrial Complex II Activity in Different Human Cell Types

5.1 Introduction

5.1.1 *Mitochondrial activity in different cell types*

Cells from different tissues of the body undergo different rates of respiration depending on the energy demand of the specific tissue; for example, heart and brain cells require higher levels of ATP production than the cells of the spleen and kidneys, and are therefore capable of increased rates of mitochondrial respiration (Weber and Piersma, 1996; Goffart *et al.*, 2004; Benard *et al.*, 2006; Scheffler, 2007; Fernández-Vizarra *et al.*, 2011). This higher rate of respiration is generated either by an increased number of mitochondria, or an increased surface area and altered composition of the mitochondrial inner membrane (Scheffler, 2007; Fernández-Vizarra *et al.*, 2011). Evidence for differences in the ETC complexes between tissues comes from observations that tissue-specific phenotypes can result from general mitochondrial defects. For example, this is the case for patients with Leber's hereditary optic neuropathy, for which complex I is impaired systemically (Yen *et al.*, 1996; Baracca *et al.*, 2005), yet the disorder involves the specific degeneration of retinal cells only (Kunz, 2003). Cells from different tissues of the body have also been shown to respond differently to mitochondrial complex substrates and inhibitors, providing further evidence for tissue-specific differences in mitochondria. For example, Kwong and Sohal, (1998) demonstrated that cells from mice hearts generate high levels of ROS in the presence of the complex III inhibitor antimycin, whereas the mice brains generate high ROS levels in the presence of the complex I inhibitor rotenone (Kwong and Sohal, 1998). This could suggest that different mitochondrial complexes are of more importance in different tissues in terms of ROS generation, and illustrates the differences in the mitochondrial ETC between tissues.

Previous studies have demonstrated directly that the activity of the individual mitochondrial ETC complexes can differ depending on the tissue-type (Chretien *et al.*, 1994; Kwong and Sohal, 2000; Benard *et al.*, 2006; Fernández-Vizarra *et al.*, 2011). Kwong and Sohal, (2000) observed that the rate of activity of complexes I, II, III, and IV varied depending upon the tissue type in mice, when measured photometrically and normalised to citrate synthase activity. It was found that the activity of complex II was highest in the mouse heart cells compared to liver, kidneys, brain, and skeletal muscle cells, whereas complexes

I, III, and IV were highest in the brain and skeletal muscle. All 4 complexes were shown to have the lowest activity in the liver and kidneys, and differences were also observed in the ratio of complexes within the different tissues (Kwong and Sohal, 2000). However, a study by Fernandez-Vizarra *et al*., (2011) found contradicting results to Kwong and Sohal, (2000) in rat tissue, for which it was observed that the activity of complex IV (normalised to citrate synthase activity) was highest in the liver yet lowest in the brain. Benard *et al*., (2006) found similar results in rat tissue, by demonstrating that complexes II, III, and IV activities were higher in the liver and kidneys than in the heart and skeletal muscle. However, it was found in that particular study that the actual protein levels of the complexes were lowest in the liver and kidneys and highest in the heart and skeletal muscle (Benard *et al.*, 2006), which suggests that heart and skeletal muscle show an overall higher ATP generation due to the higher number of ETC units present, and would therefore be able to accommodate for their high bioenergetics requirements via this mechanism. Therefore, those tissues with high energy demands may show either high rates of complex activity (Kwong and Sohal, 2000) or increased complex amount (Benard *et al.*, 2006).

In humans, previous work has demonstrated that per total cellular protein amount (rather than mitochondrial amount as determined by citrate synthase activity), there was a higher activity of complexes II and IV in the heart compared to skin fibroblasts and lymphocytes (Chretien *et al.*, 1994), possibly due to the high energetic demands of the heart. For complex IV (which was the only complex normalised to citrate synthase activity), the activity was highest in the skeletal muscle and liver, and lowest in the heart, lymphocytes, and skin fibroblasts (Chretien *et al.*, 1994). Differences in mitochondrial complex activity have also been observed in various cell lines (Dayal *et al.*, 2009; Zheng, 2012; Claus *et al.*, 2013); however, the specific cell lines used in the present study have not been directly compared previously.

5.1.2 *Age-related changes in mitochondrial activity in different cell types*

Ageing is a process which takes place across all tissues of the body, for which decreases in mitochondrial complex activities have been observed in a variety of tissues from human and laboratory animals (Coggan *et al.*, 1992; Boffoli *et*

al., 1994; Sandhu and Kaur, 2003; Kumaran *et al.*, 2004; Cocco *et al.*, 2005; Short *et al.*, 2005; Balietti *et al.*, 2009; Braidy *et al.*, 2011; Tatarkova *et al.*, 2011; Velarde *et al.*, 2012). The rate of ageing may occur at different rates depending on the tissue type, as cells with slower rates of respiration have been shown to accumulate damage more readily than cells with higher rates (Kwong and Sohal, 2000). For example, the age-related 4977 bp mtDNA common deletion, which is a potential biomarker of general mtDNA damage (Berneburg *et al.*, 2004), has been shown to accumulate more readily with age in the high-energy-demanding post-mitotic heart and brain tissues of humans than in other tissues including the liver, kidneys, lungs, and skin (Arnheim and Cortopassi, 1992; Cooper *et al.*, 1992; Meissner *et al.*, 2008; Cui *et al.*, 2012). Kwong and Sohal, (2000) measured the activities of mitochondrial complexes I, II, III, IV, and V in various mouse tissues in differently aged mice, and found that differences existed between the different tissues directly, as well as in the changes in the complexes in different tissues with age. For example, a decrease in complex II activity (normalised to citrate synthase activity) was observed with age in the brain of the mice, but not in the liver or kidneys (Kwong and Sohal, 2000). Complex I showed no difference with age in any of the tissues (kidneys, liver, heart, brain, skeletal muscle), yet complex III decreased in the brain and increased in the skeletal muscle, and complex IV decreased in the kidneys (Kwong and Sohal, 2000). In general in the previous study by Kwong and Sohal, (2000), those tissues with higher overall ETC activity also had a higher overall number of complexes which were decreased with age (Kwong and Sohal, 2000). Choksi *et al*., (2011) measured mitochondrial complex activity in two mouse muscle types: the pectoralis (aerobic with lots of mitochondria), and the quadriceps (anaerobic with few mitochondria). They found that complex II (as well as complexes I, III, IV, and V) decreased in an age-dependent manner in the aerobic muscle with high ETC activity, but only complexes I and II decreased with age in the anaerobic tissue with low ETC activity (Choksi *et al.*, 2011). The results could suggest that generally, those tissues with higher ETC activity are more affected during ageing in terms of complex activity.

5.2 Hypotheses

As complex II activity was shown to decrease in an age-dependant manner in human skin fibroblasts but not in skin keratinocytes earlier in the project (Chapter 3), and as differences in mitochondrial complex activities have been observed between cell types in previous studies, it was hypothesised that differences in mitochondrial complex II activity may exist between a variety of human cell types. These differences could potentially correlate with or directly affect the rate of ageing of the specific cell type. Differences in mitochondrial complex activities have been detected previously between cell types in humans and laboratory animals (Chretien *et al.*, 1994; Kwong and Sohal, 2000; Benard *et al.*, 2006; Fernández-Vizarra *et al.*, 2011), and tissue-specific differences in complex activities have been observed with ageing in laboratory animals (Kwong and Sohal, 2000; Choksi *et al.*, 2011). Since complex II is thought to play a prominent role in ROS production (Quinlan *et al.*, 2012), it could be speculated that differences in complex II activity between different cell types could potentially affect the rate of tissue-specific ageing. Therefore, in this area of the project differences in complex II activity were examined in a range of human cell lines not previously directly compared; cells derived from the skin (HDFn, HaCaT, primary fibroblast, and primary keratinocyte cells), the liver (HepG2 cells), and the lungs (a549 Parental and a549 Rho-zero cells). In addition, differences in complex II activity between primary keratinocytes and primary fibroblasts were examined further by directly comparing activity in epidermal and dermal tissue sections, as well as in cell samples. Some work in this chapter was performed in collaboration with Dr Alasdair Anderson.

5.3 Materials and Methods

Primary fibroblast cells, primary keratinocyte cells, HDFn cells (a neonatal human dermal fibroblast cell line), HaCaT cells (a spontaneously immortalised keratinocyte cell line) (Boukamp *et al.*, 1988), HepG2 cells (a liver carcinoma cell line), a549 Parental cells (a lung adenocarcinoma epithelial cell line), a549 Rho-zero cells (a lung adenocarcinoma epithelial cell line with the synthesis of mtDNA inhibited), MRC5 cells (a lung fibroblast cell line), and MRC5/hTERT cells (a lung fibroblast cell line overexpressing telomerase) were cultured as described in the general Materials and Methods chapter (Chapter 2). Photometric assays are also described in Chapter 2. The HDFn, HaCaT, HepG2, a549 Parental and a549 Rho-zero cells were cultured and prepared for photometry in collaboration with Dr Alasdair Anderson. Further details on the cell lines used are given in the Appendix in Table 15.

5.3.1 *Preparation of skin tissue sections for photometry*

In order to measure complex II activity and citrate synthase activity in epidermal and dermal skin tissue sections via photometry, to confirm complex II activity differences between fibroblasts and keratinocytes, the epidermis and dermis were initially separated as described in Chapter 2 section 2.1.1. The separated skin sections were then sliced into sections of approximately 3 mm^2 using a scalpel and each tissue-type was prepared separately by freezing with liquid nitrogen in a mortar, and grinding to a fine powder using a pestle. To this powder, 200 µl complex II buffer was added, and the solution was transferred to a 1.5 ml Eppendorf tube and centrifuged for 5 minutes at 8000 rpm. The pellet containing the insoluble matter was discarded, and the supernatant containing the mitochondria was snap-frozen in liquid nitrogen 3 times, and stored at -80°C until use.

5.4 Results

5.4.1 *Complex II activity in different human cell types*

The activity of complex II was determined photometrically in various human cell types, then normalised to citrate synthase activity for each cell type to allow the activity of complex II per mitochondrial unit to be determined (Birch-Machin and Turnbull, 2001). The cell types used were primary fibroblast cells, primary keratinocyte cells, HDFn cells, HaCaT cells, HepG2 cells, a549 Parental cells, a549 Rho-zero cells, MRC5 cells, and MRC5/hTERT cells. The results for the primary fibroblasts, keratinocytes, MRC5 cells, and MRC5/hTERT cells were obtained in previous chapters (Chapter 3 and Chapter 4), and used in the present chapter for further comparison between cell types.

The CII/CS activity results for the different cell types are shown in Figure 38. As can be seen, the primary fibroblasts showed a significantly higher CII/CS activity than the other cell lines, except for the MRC5/hTERT cells ($P<0.0001$ for the keratinocyte, HDFn, HaCaT, HepG2, a549 Parental, a549 Rho-zero, and MRC5 cells, one-way analysis of variance, ANOVA, with Bonferroni correction to compare all columns). This activity was approximately 2-fold higher than that of the primary keratinocytes. The CII/CS activity of the primary keratinocyte cells was also significantly lower than the HaCaT, a549 Rho-zero, MRC5, and MRC5/hTERT cells ($P<0.01$ for the HaCat, a549 Rho-zero, and MRC5 cells, and $P<0.0001$ for the MRC5/hTERT cells, one-way ANOVA with Bonferroni correction). As for the other two cell lines from the skin, both the HDFn and the HaCaT cells had a significantly higher CII/CS activity than the HepG2 and the a549 Parental cells ($P<0.0001$ for the HepG2 cells, and $P<0.01$ for the a549 Parental cells, one-way ANOVA with Bonferroni correction), and a significantly lower activity than the skin fibroblasts and the MRC5/hTERT cells ($P<0.05$ for the MRC5/hTERT cells, $P<0.0001$ for the skin fibroblasts, one-way ANOVA with Bonferroni correction). The HepG2 liver cells had significantly lower CII/CS activity than all of the cell lines except for the primary keratinocytes and the a549 Parental cells ($P<0.0001$, one-way ANOVA with Bonferroni correction). The a549 Parental lung cells also had a lower CII/CS activity than the other cell types except for the keratinocytes and the HepG2 cells ($P<0.0001$ for the primary fibroblast, MRC5, and MRC5/hTERT cells, and $P<0.01$ for the HDFn, HaCaT, and a549 Rho-zero cells, one-way ANOVA with Bonferroni correction).

Therefore, when mtDNA was absent (a549 Rho-zero cells) the activity of complex II was higher. The MRC5/hTERT cells had a high CII/CS activity similar to the primary fibroblast cells, which was significantly higher than most of the other cell lines ($P<0.0001$ for the primary keratinocyte, HepG2, and a549 Parental cells, and $P<0.05$ for the HDFn and HaCaT cells, one-way ANOVA with Bonferroni correction).

Figure 38

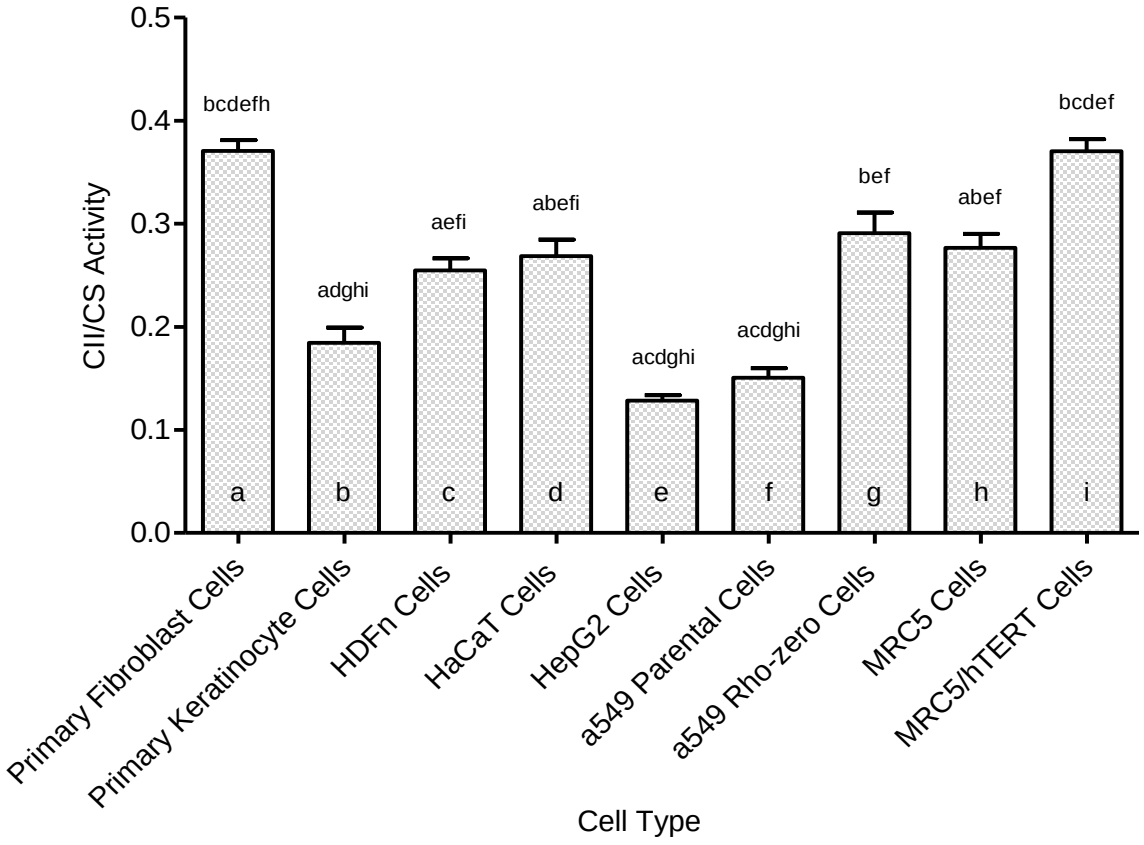

Figure 38. Complex II activity in a range of cell types. The level of complex II activity was normalised to citrate synthase activity for each cell type. The cell types used were primary fibroblast cells (a), primary keratinocyte cells (b), HDFn cells (c), HaCaT cells (d), HepG2 cells (e), a549 Parental cells (f), a549 Rho-zero cells (g), MRC5 cells (h), and MRC5/hTERT cells (i). The letters above the bars indicate significant differences from the cell type represented by that letter. The error bars show the SEM. Photometry was performed at least two times for the citrate synthase assay and at least four times for the complex II activity assay for each cell type. For the primary fibroblasts 27 donors were used, and for the primary keratinocytes 19 donors were used.

5.4.2 *Complex II activity within skin tissues*

As demonstrated in the section above, the CII/CS activity of the primary skin fibroblasts was approximately twice as fast as the CII/CS activity of the primary

skin keratinocytes. To ensure that this difference was not due to variations in the particular donors used, since the majority of fibroblast samples were from different donors to the keratinocyte samples, the activities of primary fibroblasts and keratinocytes from the same individuals were compared. As can be seen in Figure 39A, the fibroblasts still showed a significantly higher level of activity in the 5 fibroblast samples and 5 keratinocyte samples, taken from the same 5 donors (P=0.0001, unpaired t-test). To further confirm that this difference in activity between the primary skin cells was genuine, and not just an artefact of the different media in which the two cell types were cultured, the complex II activity in epidermal and dermal tissue sections directly was investigated. The epidermis is mostly made up of keratinocyte cells (Lulevich *et al.*, 2010), and the fibroblasts are the most numerous cell type within the dermis (Chen *et al.*, 2007). As can be seen in Figure 39B, the dermis showed an approximately 2-fold higher CII/CS activity than the epidermis, which was significantly different (P=0.0006, unpaired t-test), and confirms the difference observed between the cultured fibroblast and keratinocyte cells in the previous section. These results suggested that the keratinocytes do indeed have a much lower complex II activity per unit of mitochondria than the fibroblasts.

Due to time limitations, the activity of complex IV was not able to be measured in the various cell types used in the above section; however, complex IV was measured in Chapter 3 in both fibroblasts and keratinocytes from donors of different ages. Therefore, the activity of complex IV was able to be compared in these two skin cell types. As can be seen in Figure 39C, the CIV/CS activity was over twice as fast for the fibroblasts as for the keratinocytes (P<0.0001, unpaired t-test), in a similar manner to the CII/CS activity.

Figure 39

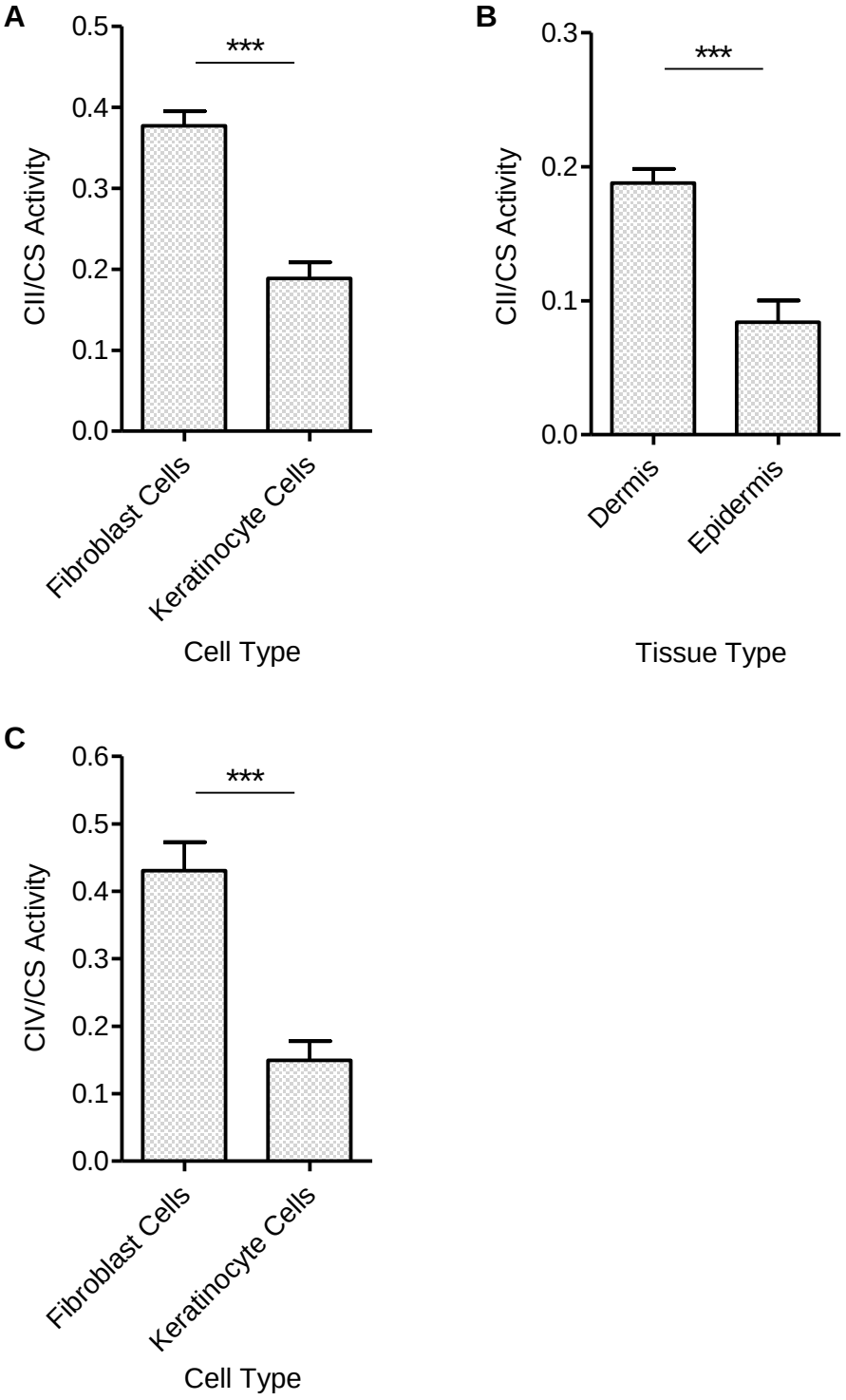

Figure 39. Mitochondrial complex activities in different skin cells and tissues. A) Complex II activity normalised to citrate synthase activity for primary fibroblasts and primary keratinocytes, with cell samples obtained from the same 5 donors. There was a significantly higher activity in the fibroblasts than the keratinocytes (P=0.0001***, unpaired t-test). B) CII/CS activity for dermal and epidermal tissue sections from 5 donors. The dermis showed a significantly higher level of activity than the epidermis (P=0.0006***, unpaired t-test). C) Complex IV activity normalised to citrate synthase activity for 18 fibroblast samples and 13 keratinocyte samples. CIV/CS activity was significantly higher in the fibroblasts compared to the keratinocytes (P<0.0001***, unpaired t-test). The error bars show the SEM. Photometry was performed at least two times for the citrate synthase assay and at least two times for the complex II activity assay for each cell sample or tissue type, and the average value was used for each sample.

5.5 Discussion

5.5.1 *The rate of complex II activity varies depending on cell type*

The rate of complex II activity was found in the present study to vary depending on the cell line as well as the tissue from which the cells were obtained, which is in accordance with previous studies demonstrating a difference in complex II activity between tissues and cell lines (Chretien *et al.*, 1994; Kwong and Sohal, 2000; Benard *et al.*, 2006; Dayal *et al.*, 2009; Fernández-Vizarra *et al.*, 2011; Zheng, 2012; Claus *et al.*, 2013). In the present study, for the non-immortal cell lines of the different tissues (the primary fibroblast, primary keratinocyte, HDFn, and MRC5 cells), the lung MRC5 cells had a significantly lower complex II activity than the skin fibroblasts, and a significantly higher activity than the skin keratinocytes, yet no difference in activity from the skin HDFn cells. This demonstrated that variations in complex II activity exist both between and within organ types. Since different tissues and cell types undergo different rates of respiration (Weber and Piersma, 1996; Goffart *et al.*, 2004; Benard *et al.*, 2006; Scheffler, 2007; Fernández-Vizarra *et al.*, 2011), it may be expected that they would show variations in complex II activity, as was seen.

The immortal cell lines used in this study (the HaCaT, HepG2, a549 Parental, and MRC5/hTERT cells) did not consistently correlate with either a higher or a lower complex II activity compared to the non-immortal cell types. The MRC5/hTERT cells showed a very high rate of complex II activity, the HaCaT cells an intermediate rate of activity, and the HepG2 and a549 Parental cells showed a low rate of activity. This is in accordance with previous work which has demonstrated that cancer cells can have either high or low mitochondrial complex activity. For example, human breast cancer epithelial cells have been shown to have a higher rate of complex II and complex IV activity than adjacent non-cancerous cells (Whitaker-Menezes *et al.*, 2011) in order to generate high ATP levels, yet other cancers such as gastrointestinal stromal tumours have been shown to have low complex II activity (Janeway *et al.*, 2011), as cancer cells can generate high energy levels via aerobic glycolysis (Vander Heiden *et al.*, 2009; Levine and Puzio-Kuter, 2010; Whitaker-Menezes *et al.*, 2011). These past studies suggest that immortal cell lines are not necessarily faster or slower in terms of complex II activity, which is in accordance with the present study.

The level of complex II activity per overall cellular protein amount was not studied in the present study. It could be that despite differences in complex II activity per mitochondrial amount in different cell types, certain cell types may have higher overall levels of mitochondria per cell (Benard *et al.*, 2006), which could be explored in future studies.

5.5.2 *Complex II activity in the liver-derived cell line*

The present project demonstrated that complex II activity in the cell line derived from the liver (the HepG2 cells) was the lowest of the cell lines tested. Primary fibroblasts from the skin have been compared previously to cells from the liver in humans, for which it was shown that complex IV activity was higher in liver cells than in skin fibroblasts (complex II activity was not tested) (Chretien *et al.*, 1994). It could be speculated that because the activity of complex IV may be higher in liver cells (Chretien *et al.*, 1994), that the activity of complex II is lower in this cell type due to a reduced demand for this complex. This potential compensatory mechanism has been demonstrated previously, whereby a decrease in activity in one complex has led to an increase in another (Yen *et al.*, 1996; Kwong and Sohal, 2000; Baracca *et al.*, 2005; Rhein *et al.*, 2009; Ostojic *et al.*, 2013). Kwong and Sohal, (2000) also showed that when comparing the ratio between complexes II and IV in mice, the kidneys and heart showed a decrease in the complex IV activity ratio with age, and the liver and skeletal muscle showed an increase, suggesting that as one complex decreases the other increases and vice versa. However, it has to be taken into account that the HepG2 cells used in the present study are an immortal cell line, which could show different results to the primary liver cells used previously (Chretien *et al.*, 1994). Additionally, only one cell line derived from the liver was tested, so it remains unknown whether liver cells in general have a lower complex II activity. Variations in ETC activity have been shown to occur even within the same organ type, as shown in the present project within the skin and the lungs, as well as in adipose tissue in a previous study (Kraunsoe *et al.*, 2010).

5.5.3 *Complex II activity in the lung-derived cell lines*

The level of complex II activity observed in the lung cells (the a549 Parental, a549 Rho-zero, MRC5, and MRC5/hTERT cells) varied depending on the specific cell type. The immortal cell lines showed opposite effects to one

another in terms of complex II activity, with the MRC5/hTERT cells showing a high activity and the a549 Parental cells showing a low activity.

To further investigate differences in complex II activity between different cells, two cell types with differences in their mitochondrial ETC were tested. The a549 Parental cells have a fully functional ETC, whereas the a549 Rho-zero cells were cultured in a low level of ethidium bromide and therefore lack mtDNA and have a dysfunctional ETC (Hashiguchi and Zhang-Akiyama, 2009). Since the ETC complexes, except complex II, are under dual control from both nDNA and mtDNA, these cells still undergo oxidative phosphorylation, yet at an altered rate (Hashiguchi and Zhang-Akiyama, 2009). When comparing the a549 Parental cells to the a549 Rho-zero cells, it was observed that the activity of complex II was approximately twice as high in the Rho-zero cells. The structure of complex II should be the same in each of these two cell types as it is nuclear-encoded; however, it is possible that the activity of complex II in the Rho-zero cells was faster due to dysfunction in the other mitochondrial complexes which are partially mtDNA-encoded, and therefore have a lower activity resulting in a lower ATP generation. Complex II activity may be increased in an attempt to compensate for the lower activity in the other complexes.

5.5.4 *Complex II activity in the skin-derived cell lines*

For the skin-derived cell types (the primary fibroblast, primary keratinocyte, HDFn, and HaCaT cells), the fibroblasts showed a high complex II activity, the keratinocytes a low, and the two non-primary cell lines showed an intermediate activity level. This again demonstrated differences in activity between cell types from the same organ.

The levels of activity of both complexes II and IV were significantly higher in the primary fibroblasts than in the primary keratinocytes. Keratinocytes have been shown to accumulate damage less readily than fibroblasts; for example the 3895 bp deletion accumulates less readily in the epidermis than the dermis (Krishnan *et al.*, 2004; Harbottle and Birch-Machin, 2006), and the T414G mutation was not detected in the keratinocytes in this project but was in the fibroblasts (Chapter 4). It was therefore initially thought before testing that the keratinocytes may show a faster rate of complex II activity due to the lower

levels of damage, yet this was not the case. However, previous work is in accordance with the present study; Hornig-Do *et al*., (2007) found that the maximal activity of complexes II, III, and IV were significantly higher in fibroblasts than in keratinocytes, despite the same rate of respiration in both cell types. This suggested that *in vivo* both cell types respire at the same rate, as there were found to be similar levels of mitochondria per overall cellular protein, but the fibroblasts have the potential for faster respiration (Hornig-Do *et al.*, 2007). The authors of the previous study also measured the level of superoxide and found this to be much higher in the keratinocytes, due to lower levels of SOD (Hornig-Do *et al.*, 2007). It was suggested that these superoxide anions are required for differentiation of the keratinocytes into the stratum corneum which occurs *in vivo* in the skin (Hornig-Do *et al.*, 2007). This could explain why the maximal activities of the complexes were lower in the keratinocytes, as they are likely to lack the reserve functional capacity for increased ETC activity when ATP generation is necessary, as they are required to use the ETC for both energy production and superoxide anion accumulation (Hornig-Do *et al.*, 2007). It is worth noting that antioxidants to counteract H_2O_2 such as glutathione peroxidase were higher in the keratinocytes than the fibroblasts, to protect the cells against the necessarily higher ROS levels, and from the accumulation of oxidative damage caused by H_2O_2 and $^{\cdot}OH$ (Hornig-Do *et al.*, 2007). This could explain why the accumulation of mtDNA damage does not occur as readily in this cell type (Krishnan *et al.*, 2004; Harbottle and Birch-Machin, 2006). An additional reason as to the lower activity of the complexes in the keratinocytes could be because keratinocytes also generate energy via glycolysis (Ronquist *et al.*, 2003). The present study further demonstrated the differences between the keratinocytes and fibroblasts as compared to previous studies, by comparing the complex II activity in epidermal and dermal tissue directly, to remove any possible artefacts induced by cell culture of keratinocytes and fibroblasts in different media. It was found that the same results were obtained using these tissue samples. Additionally, the lifestyles of individual donors can differ, and factors such as smoking and exercise have been shown to affect complex II activity (Miro *et al.*, 1999; Cardellach *et al.*, 2003; Alonso *et al.*, 2004; Bouhours-Nouet *et al.*, 2005; Menshikova *et al.*, 2006; Luo *et al.*, 2013); therefore, fibroblasts and keratinocytes obtained from the same donors were

compared and the same results were found, suggesting that the difference was not due to variations in lifestyle between donors.

In the previous chapter (Chapter 3) it was shown that the activity of complex II decreased with age in the fibroblasts but not in the keratinocytes. It could be suggested that those cell types with faster complex II activity show noticeable decreases in complex II activity with age. Similar results were seen in a previous study which showed that tissues with overall higher ETC complex activities had the highest number of complexes which decreased in activity with age (Kwong and Sohal, 2000). Additionally, aerobic tissue has been shown previously to have more complexes decreased with age than anaerobic tissue (Choksi *et al.*, 2011). Therefore, the measurement of complex II activity could be predictive in terms of the rate of ageing of different cell types, but the activities of the other complexes as well as any changes in activity with age in the different cell types would also have to be studied for further information.

5.6 Summary

In conclusion, it was found that cell types from various tissues undergo different rates of complex II activity; however, further work would be required to establish the physiological relevance of these differences, especially in relation to the rate of ageing between tissues and cell types. These differences in mitochondrial complex activity between cell types are in accordance with previous work (Chretien *et al.*, 1994; Kwong and Sohal, 2000; Benard *et al.*, 2006; Choksi *et al.*, 2011; Fernández-Vizarra *et al.*, 2011), however the specific cell lines used in the present study have not been directly compared previously, and therefore allow further insights into the differences between different cells, including between immortal and non-immortal cells. Differences within tissues were also observed, in skin and lung cell lines.

It was found in the present study that immortal cell types were neither consistency higher or lower in terms of complex II activity compared to the non-immortal cell types. This is in accordance with previous work, for which cancer cells have been shown to have higher ETC activity to generate increased ATP levels (Whitaker-Menezes *et al.*, 2011), or lower ETC activity when energy is generated via glycolysis (Janeway *et al.*, 2011). Another noticeable difference between cell types was the difference between the a549 Parental lung cells and the a549 Rho-zero cells without mtDNA, for which the Rho-zero cells showed a significantly higher complex II activity, possibly due to an increase in nuclear-encoded complex II activity as a compensatory mechanism for dysfunction in the other complexes which are partially mtDNA-encoded. The present study also confirmed previous work on human cells showing that fibroblasts have faster complex II and IV activities than keratinocytes, which may be due to the ROS-producing ability of the keratinocytes, at the expense of maximal complex activities (Hornig-Do *et al.*, 2007). It was speculated that the activity of complex II decreased with age in the fibroblasts but not in the keratinocytes (Chapter 3), due to the higher activity of complex II in the fibroblasts. This decrease in mitochondrial complex activity with age in cells with higher maximum ETC complex activities has also been observed previously (Kwong and Sohal, 2000; Choksi *et al.*, 2011).

Chapter 6. UV-Induced MtDNA Damage Detection in Human Skin Cells

6.1 Introduction

6.1.1 *MtDNA damage as a biomarker of UV-induced genetic damage*

Due to the similarities between UV damage and chronological age in skin, different UV exposures are able to be used as a model for differently aged skin as discussed in more detail in Chapter 7. In Chapter 7, whale skin exposed to varying degrees of UV was used as a model for different ages. To measure this UV damage in the subsequent chapter (Chapter 7), the qPCR amplification of a large section of mtDNA was used, for which the current chapter serves as a proof-of-concept for UV-induced damage detection in a similar-sized region. The use of mtDNA as a biomarker of damage, as analysed by qPCR, has been utilised previously to reliably and sensitively detect UV-induced genetic damage in humans and laboratory animals, usually within a large 11 kb segment (Kalinowski *et al.*, 1992; Ray *et al.*, 2000; Santos *et al.*, 2002; Durham *et al.*, 2003; Eischeid *et al.*, 2009; Hunter *et al.*, 2010; Swalwell *et al.*, 2012). This mitochondrial genome, unlike nDNA, is present in many copies within a cell and can therefore withstand a high level of mutation before cellular alterations occur; this means that damage is able to accumulate (Birch-Machin and Swalwell, 2010). It also has a limited number of repair mechanisms, for example it lacks the nucleotide excision repair pathway for removal of UV damage and also lacks protective histones (Birch-Machin and Swalwell, 2010). Therefore, mtDNA is an excellent biomarker for the measurement of UV-induced changes throughout the lifetime of an individual (Birch-Machin and Swalwell, 2010). UV-induced mtDNA damage has been measured in previous studies using qPCR to amplify a long section of mtDNA, which is based on the observation that UV-induced damage can cause strand breaks in the mtDNA and therefore block the amplifying ability of DNA polymerase (Kalinowski *et al.*, 1992). This principle is shown in Figure 40A, which also demonstrates how the relative copy number can be determined using primers to amplify a short region which is unlikely to contain damage (Koch *et al.*, 2001; Jung *et al.*, 2009; Hunter *et al.*, 2010; Swalwell *et al.*, 2012). Using qPCR, the level of amplified double-stranded mtDNA product is detectable at each qPCR cycle via the binding of a dye which displays fluorescence once bound, and the relative level of damage can therefore be determined by the number of cycles it takes before the level of amplified product reaches a certain threshold (the Ct value) (Figure 40B). Therefore, those samples with a higher number of intact mitochondrial genomes

(i.e. less damage) undergo more efficient amplification, and have a lower Ct value.

Figure 40

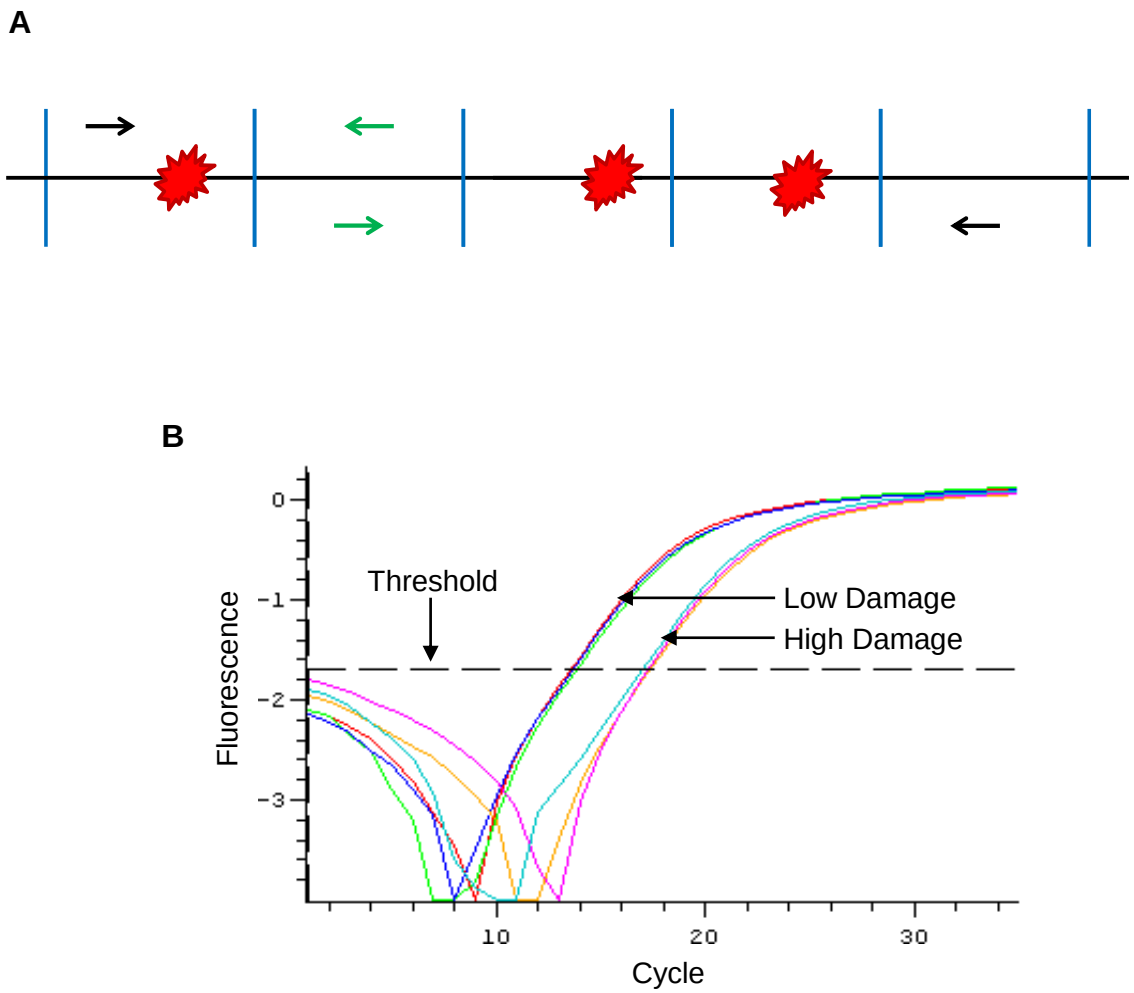

Figure 40. The principle of quantitative real-time PCR. A) The principle behind the detection of UV-induced damage using qPCR. The horizontal black line shows the mtDNA strand, with the blue vertical lines marking spaces of 1 kb apart. The red stars show areas of damage. The primers to amplify a large region are capable of detecting this damage (shown by the black arrows), and the primers to amplify a short region are to determine the relative copy number (shown by the green arrows). B) The qPCR amplification plot shows two samples run in triplicate, as shown by the coloured lines, one with low mtDNA damage and one with high mtDNA damage. A threshold is set, and the number of cycles it takes before the level of amplified DNA crosses this threshold is known as the Ct, with a low value indicating low damage (or a high copy number) and a high value indicating high damage (or a low copy number).

6.2 Hypotheses

The hypotheses of this area of the project were 1) the long-fragment qPCR assay is capable of detecting UV-induced damage in human skin cells *in vitro* as shown previously, and areas of 4.4 kb of the mtDNA are usable to detect damage for the whale skin study in Chapter 7; 2) damage detected is prevented by a UV-blocking agent, which would imply that the observed damage is due to UV; and 3) the long-fragment qPCR assay is capable of detecting UV-induced damage in human skin *in vivo*, taken by epidermal skin swabs, to confirm the appropriate use of the long-fragment qPCR assay for the analysis of whale skin sections in Chapter 7.

6.3 Materials and Methods

The cell culture, qPCR, cellular DNA extractions, and gel electrophoresis methods used within this chapter are given in the general Materials and Methods, in Chapter 2.

6.3.1 *Lamp calibration*

The two lamp types used to irradiate the HDFn cells *in vitro* were either seven 6 foot (ft) iSOLde Cleo performance 100 W-R lamps (Cleo) (iSOLde, Germany), or two 6 ft Arimed B 100 W lamps (Arimed B) (Cosmedico, Germany). The spectral irradiance of the lamps was calibrated previously by Dr Jim Lloyd (Newcastle University).

6.3.2 *UV irradiation* in vitro

HDFn cells to be used for *in vitro* irradiation were washed twice in PBS, and removed from flasks using TE at 37°C for 5 minutes. Following TE incubation, complete DMEM was added to neutralise TE activity. Approximately 1.5×10^5 cells in 3 ml complete DMEM media were seeded per 9.2 cm^2 Petri dish. Cells were grown at 37°C for 16 hours to allow adhesion to the dish, then washed once in PBS, and 1.5 ml serum-free DMEM (plus PS) was added to the dishes. The Cleo lamps or the Arimed B lamps were fitted into a custom built irradiation unit prior to use. UV irradiation levels were measured using a DMc150 Monochromator (Bentham Instruments Ltd., UK), and 6 readings for each lamp type were taken to find the average output for each. Irradiation values for multiple time points were derived from these readings, as shown in Table 2. The standard erythemal dose (SED) measured for the Cleo lamps was 23.8 after 20 minutes irradiation, and for the Arimed B lamps was 2.9 after 25 minutes irradiation, which were the chosen time points for optimum damage. To irradiate cells, lids were removed and the cells were placed under the lamps for various time points. For control cells, either lids were not removed and cells were completely wrapped in foil to prevent UV from reaching the cells, or lids were removed and foil was placed on top. Following irradiation, cells were washed once with PBS, and TE was added for 5 minutes at 37°C to detach cells. Following incubation, media was added to neutralise TE and the cells were removed from the dish using a Cell Scraper (Techno Plastic Products, Switzerland). Cells were placed into a 1.5 ml Eppendorf tube and centrifuged at

8000 rpm for 3 minutes, after which the cell pellet was resuspended in 200 µl PBS and the DNA extracted using a QIAamp DNA Mini Kit as described in section 2.4.1. The 4.4 kb and 83 bp qPCRs were performed as described in section 2.4.2.

Table 2

Lamp Type	Irradiation Time	UVA Energy	UVB Energy	SEDs
Cleo	5	43505.05	290.44	5.95
	10	87010.09	580.89	11.90
	15	130515.14	871.33	17.84
	20	**174020.19**	**1161.77**	**23.79**
	25	217525.23	1452.22	29.74
	30	261030.28	1742.66	35.69
	35	304535.33	2033.10	41.64
	40	348040.38	2323.55	47.59
	45	391545.42	2613.99	53.53
	50	435050.47	2904.43	59.48
	55	478555.52	3194.88	65.43
	60	522060.56	3485.32	71.38
Arimed B	5	987.02	39.02	0.57
	10	1974.04	78.04	1.15
	15	2961.05	117.06	1.72
	20	3948.07	156.08	2.29
	25	**4935.09**	**195.10**	**2.87**
	30	5922.11	234.12	3.44
	35	6909.12	273.15	4.02
	40	7896.14	312.17	4.59
	45	8883.16	351.19	5.16
	50	9870.18	390.21	5.74
	55	10857.19	429.23	6.31
	60	11844.21	468.25	6.88

Table 2. UV outputs for the Cleo and Arimed B lamps. The UV energy emitted from the Cleo and Arimed B lamps is shown in mJ/cm^2 for each time point for the Cleo and Arimed B lamps, as well as the SEDs. The irradiation time is given in minutes, and the underlined numbers show the chosen irradiation times for the Cleo and Arimed B lamps for optimal mtDNA damage.

6.3.3 *UV irradiation with SPF cream protection*

To ensure that any mtDNA damage detected was due to UV, a cream containing sun-protection factor (SPF) was used, which should decrease the level of mtDNA damage, as well as a sham cream containing no SPF protection. The creams used were L'Oréal Revitalift Day Cream with SPF30 protection (L'Oréal, Paris) and Revitalift Day Cream (L'Oréal, Paris). Cells were irradiated for 20 minutes with the Cleo lamps, and for 25 minutes with the Arimed B lamps, based on the results from irradiation at different time points to determine maximum DNA damage. The tape used was Transpore Clear tape (3M, UK), and cream was applied to the surface of this by adhering a 5 cm^2 section of tape to the top of cell Petri dishes with lids removed, and applying 2 mg/cm^2 cream to the top of the tape by finger using a Disposable Nitrile Powder-free Glove (Sempermed, UK). Following irradiation, cells were collected and the DNA was extracted as described in section 2.4.1, and qPCR performed as described in section 2.4.2.

6.3.4 *Cell viability following UV irradiation*

To test for cell viability following UV irradiation, a 3-(4,5-dimethylthiazol-2-yl)-5-(3-carboxymethoxyphenyl)-2-(4-sulfophenyl)-2H-tetrazolium (MTS) assay was used. This required cells to be analysed in a clear 96-well plate. Initially, 5×10^3 cells were added in 100 µl complete DMEM per well to the plate, and incubated at 37°C for 16 hours. Following incubation, the media was replaced with 100 µl serum-free DMEM (plus PS) per well, and cells were either covered with foil, Transpore Clear tape alone, Transpore Clear tape with 2 mg/cm^2 Revitalift Day Cream, or Transpore Clear tape with 2 mg/cm^2 Revitalift Day Cream with SPF30 protection. Cells were irradiated for 20 minutes with the Cleo lamps or 25 minutes with the Arimed B lamps, after which the media was replaced with 100 µl complete DMEM, 20 µl MTS (Promega, UK) was added per well, and the cells were incubated at 37°C for 4.5 hours. After the incubation, the absorbance at 490 nm was measured using a SpectraMax 250 Microplate Reader and the results viewed using SoftMax Pro V3.1.1.

6.3.5 *UV irradiation* in vivo

The backs of volunteers were irradiated in an area of approximately 7 cm^2, as performed by Boots (Nottingham, UK) under their standard *in vivo* ethically

approved program. Epidermal samples were taken using skin swabs before and after irradiation, by brushing back and forth several times on the specific areas of the back. The specific areas of the back were irradiated with solar simulated light once a day for 5 days with a single exposure of 0.8 minimal erythemal doses (MED) on each day, resulting in a cumulative dose of 4 MEDs over the 5 days. MED represents the minimal amount of UV required to produce erythema which will differ depending on skin colour, for use *in vivo* (Heckman *et al.*, 2013), whereas SED represents a standard dose equivalent to 100 J/m^2, and is independent of skin colour (Lucas *et al.*, 2006).

6.3.6 *DNA extraction from human skin swabs*

DNA from skin swabs taken from areas of human backs was extracted using a QIAamp DNA Mini Kit (Qiagen, UK), using the Buccal Swabs protocol. Skin swabs were taken by Boots, UK. This was achieved as described previously (Harbottle *et al.*, 2010), by washing the specific area of the back with 70% ethanol to remove dead skin cells and potential microbes, and allowing to dry. Cell samples were obtained by rubbing firmly with dry cotton swabs against the back 15 times, to obtain the top layers of the skin, and stored in sterile tubes until DNA extraction. Upon receiving samples, swabs were placed into 1.5 ml Eppendorf tubes, and 400 µl PBS, 20 µl proteinase K, and 400 µl lysis buffer (Buffer AL) were added. Samples were vortexed for 15 seconds and incubated at 56°C for 10 minutes, after which the extraction was performed as described in section 2.4.1 from the 56°C incubation onwards.

6.3.7 *QPCR primers*

Primers for the amplification of human mtDNA sections of approximately 500 bp or 4.4 kb to study the damage within were designed by Dr Helen Swalwell (Newcastle University), and primers for the amplification of a short section of 83 bp to check the relative mtDNA amount were chosen from the literature (Koch *et al.*, 2001). Human primer positions are shown in Figure 41, and the sequences are shown in Table 3. All primers were produced by Eurofins MWG Operon.

Figure 41

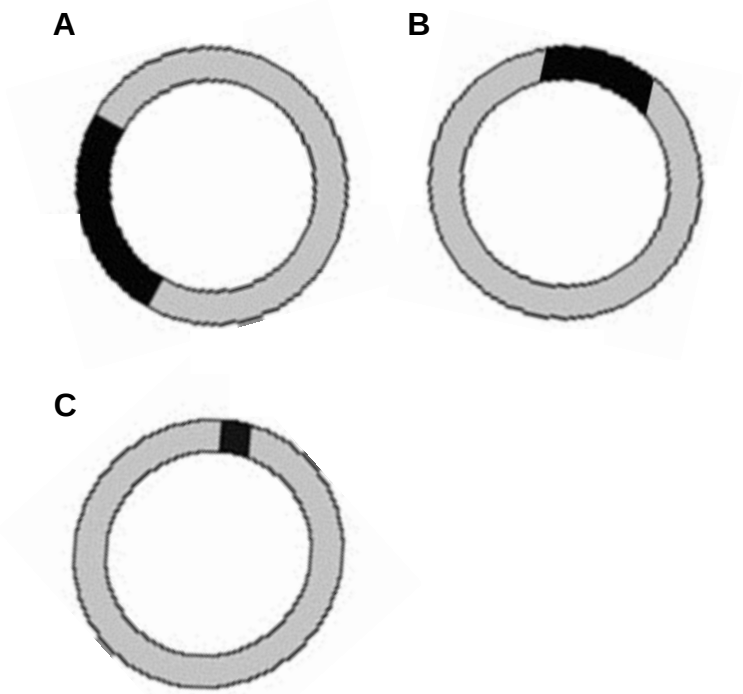

Figure 41. Positions of the designed primers on human mtDNA for use in qPCR. A) The approximate position and size of the 4.4 kb-product primer pair for use in amplifying human mtDNA to determine damage within. B) The 500 bp-product primer pair for use in amplifying human mtDNA to determine damage within. C) The 83 bp-product primer pair for use in amplifying human mtDNA to determine the relative copy number. The top of the circle is the position of the D-loop.

Table 3

Primer Set		Base Sequence (5' to 3')	Length (bp)	Nucleotide Numbers (bp)
4.4 kb Human	F	CCC GGT AAT CGC ATA AAA CT	4355	3245-7599
	R	GCT GCA TGT GCC ATT AAG AT		
500 bp Human	F	ATC GGA GGA CAA CCA GTA AG	538	15758-16295
	R	CGT GGG TAG GTT TGT TGG TAT C		
83 bp Human	F	GAT TTG GGT ACC ACC CAA GTA TTG	83	16042-16124
	R	AAT ATT CAT GGT GGC TGG CAG TA		

Table 3. Primer sequences for qPCR with human mtDNA. The primer sets specific for human mtDNA, with product sizes of approximately 4.4 kb, 500 bp, and 83 bp. The base sequences from 5' to 3' are shown for the forward (F) and reverse (R) primers, as well as the exact product length in bp, and the nucleotide numbers in bp which give the positions of the products to be amplified within the mtDNA.

6.4 Results

6.4.1 *MtDNA damage following UV exposure* in vitro

In order to show that UV radiation can cause an increase in mtDNA damage which is detectable in a 4.4 kb region of the mitochondrial genome by qPCR, two different lamp types were used to irradiate the cells for a selection of time points. The Cleo lamps and the Arimed B lamps were chosen as they provide both UVA (315-400 nm) and UVB (280-315 nm) (Figure 42), similar to the sunlight reaching the earth's surface, with the Arimed B lamps being the most similar to natural sunlight (Cosmedico, 2013). HDFn cells were used as these are derived from the skin, and are therefore susceptible to UV damage (Al-Baker *et al.*, 2005; Schroeder *et al.*, 2008). Cells were exposed to both lamp types for 5 to 60 minutes, with time points taken every 5 minutes, to determine an optimum level of mtDNA damage. It was found that significant mtDNA damage within the 4.4 kb region begins to occur after only 5 minutes exposure for both lamp types ($P<0.0001$, one-way ANOVA with Dunnett's test to compare columns to the control which was foil around for 5 minutes), despite the same number of mtDNA copies being present due to no differences in Ct values when using the 83 bp-product primers. After 20 minutes of exposure for the Cleo lamps (Figure 43A) and 25 minutes of exposure for the Arimed B lamps (Figure 43B) a level of damage was reached which was not exceeded if the cells were irradiated for longer. These results suggest that the 4.4 kb-product primers are able to detect damage caused by UV radiation.

Figure 42

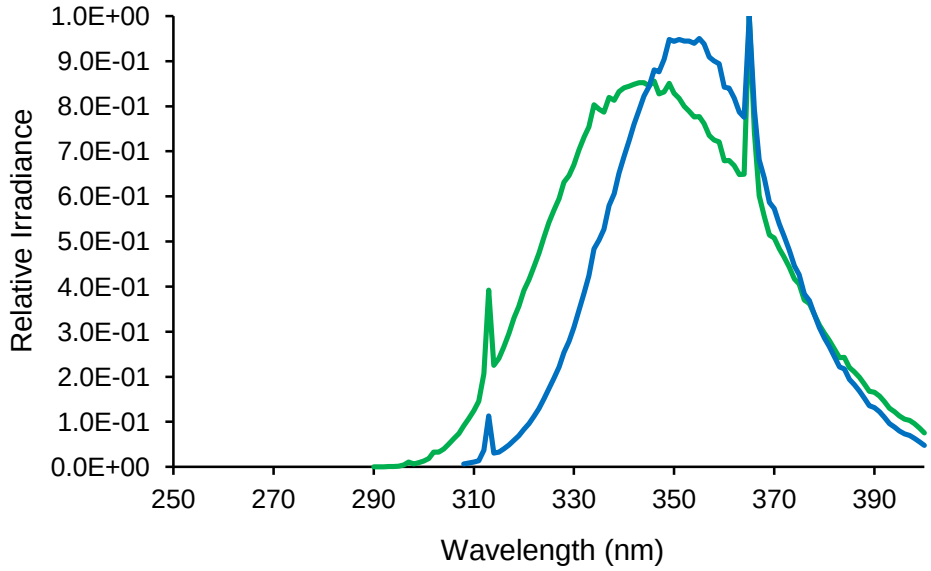

Figure 42. Spectral irradiance charts for the Cleo and Arimed B lamps. The spectral wavelengths for the Cleo (blue) and Arimed B (Green) lamps are shown, which shows the levels of irradiance at various wavelengths. The peaks in the charts at around 313 nm and 365 nm are caused by the mercury in the lamps. The approximate wavelength range for the Cleo lamps is 310 nm to 400 nm, and for the Arimed B lamps is 300 nm to 400 nm. The wavelength ranges were determined and the original graph was produced by Dr Jim Lloyd and Dr Jennifer Latimer (Newcastle University).

Figure 43

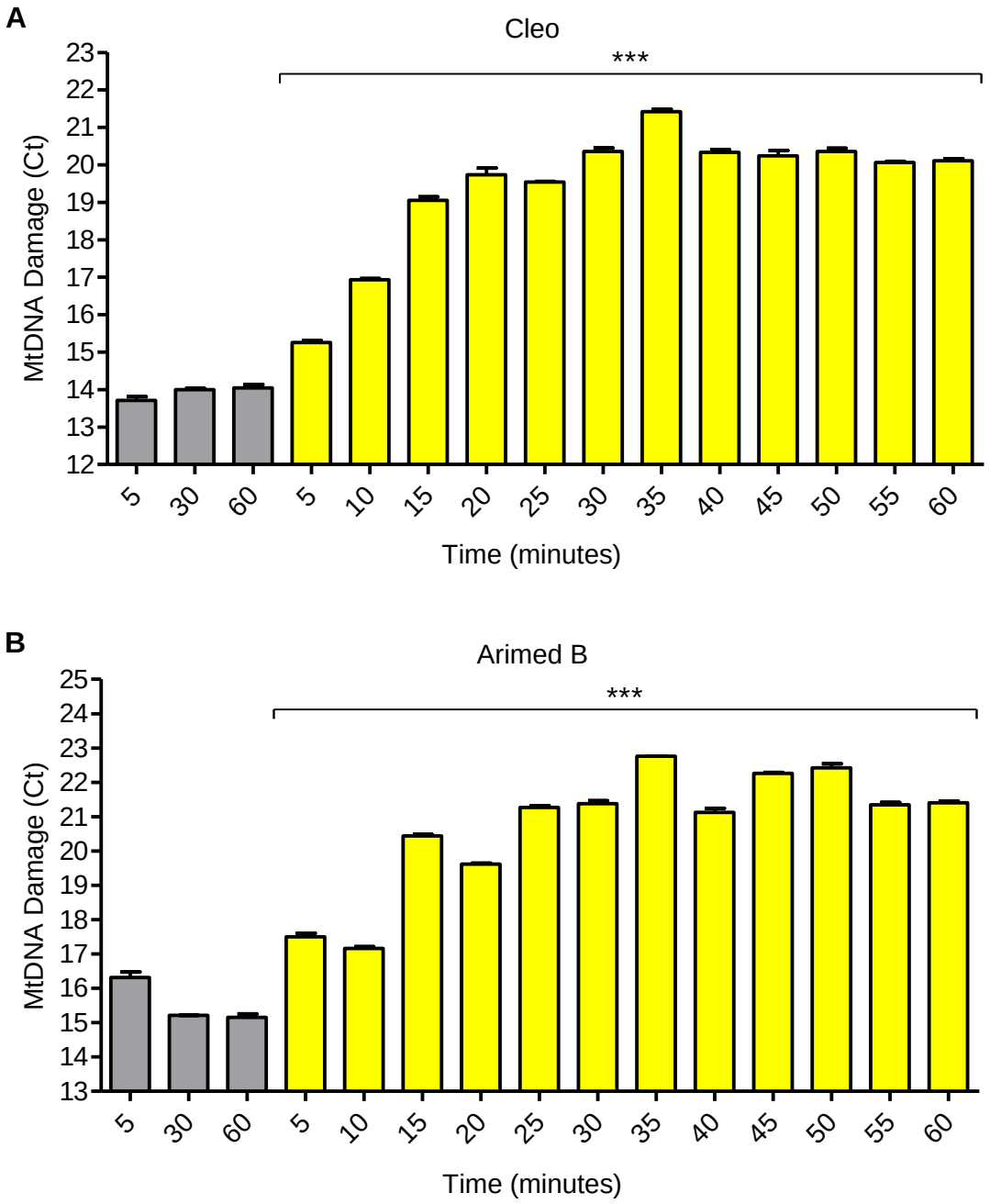

Figure 43. MtDNA damage in HDFn cells exposed to UV for various time points. A) HDFn cells were irradiated with Cleo lamps for various time points. Cells were covered in foil for 5 minutes, 30 minutes or 60 minutes as controls. Cells were irradiated without foil for 5 to 60 minutes at 5 minute time point intervals. MtDNA was extracted from cells and the level of damage was determined within a 4.4 kb region using qPCR. The Ct values obtained from the qPCR reaction represent the level of mtDNA damage within a sample. A significant difference in damage from the control (foil around 5 minutes) was seen after only 5 minutes ($P<0.0001$***, one-way ANOVA with Dunnett's test). B) HDFn cells were irradiated with Arimed B lamps under the same conditions. A significant increase in damage compared to the control (foil around 5 minutes) was seen after only 5 minutes ($P<0.0001$***, one-way ANOVA with Dunnett's test). The grey bars show the UV-protected cells (foil-covered), and the yellow bars show the cells exposed to UV radiation. The error bars show the SEM. There were two biological repeats (two different dishes) each ran in duplicate for the qPCR for each irradiation time and lamp type.

6.4.2 *MtDNA damage following UV exposure in the presence of cream containing SPF30*

In order to test whether the observed mtDNA damage was due to UV as opposed to other factors such as heat (Purschke *et al.*, 2010; Chan *et al.*, 2013), a cream containing SPF30 was tested compared to a cream without SPF protection (sham cream). For these irradiations, a control dish with foil placed on top and the lid removed was used, to mimic the conditions of the dishes with their sides exposed more closely. Tape capable of permitting UV light through was used as a positive control, to ensure that any potential decrease in mtDNA damage by the cream was not due to the tape blocking the UV. The cells irradiated using this tape did not give a significantly different level of damage than the cells fully exposed for both lamp types (Figure 44A and Figure 44B) ($P>0.05$, one-way ANOVA with Bonferroni correction). For the Cleo lamps (Figure 44A), it was found that the cream with SPF significantly reduced the mtDNA damage compared to the sham cream without SPF ($P<0.01$, one-way ANOVA with Bonferroni correction). However, the cream with SPF still gave a significantly higher level of damage than the foil on top ($P<0.01$, one-way ANOVA with Bonferroni correction), suggesting that the cream containing SPF30 was able to significantly reduce the level of damage compared to non-SPF-containing cream, but was unable to fully protect the cells as effectively as foil.

For the same experiment performed with the Arimed B lamps (Figure 44B), there was no significant difference seen between the cells with SPF cream and the cells with sham cream ($P>0.05$, one-way ANOVA with Bonferroni correction). However, this did become significant when only these two conditions were taken into account ($P=0.0472$, unpaired t-test). Additionally, there was no difference in damage between those cells with foil on top or those cells with SPF cream ($P>0.05$, one-way ANOVA with Bonferroni correction), yet there was between the sham cream and the foil ($P<0.0001$, one-way ANOVA with Bonferroni correction). This suggests that the SPF had prevented the majority of the damage caused by UV in a manner similar to the foil for this lamp type.

The level of damage within an 83 bp region of the mitochondrial genome was also studied for all samples, as this small region which is unlikely to contain damage gives information on the amount of mtDNA present in the sample (Koch *et al.*, 2001). It was found that all samples gave Ct values within 1 Ct of the average for the 83 bp qPCR, suggesting that the differences seen in the 4.4 kb reactions were not due to differences in mtDNA content (Berdal and Holst-Jensen, 2001; Niemitz *et al.*, 2004; Mraz *et al.*, 2009).

Figure 44

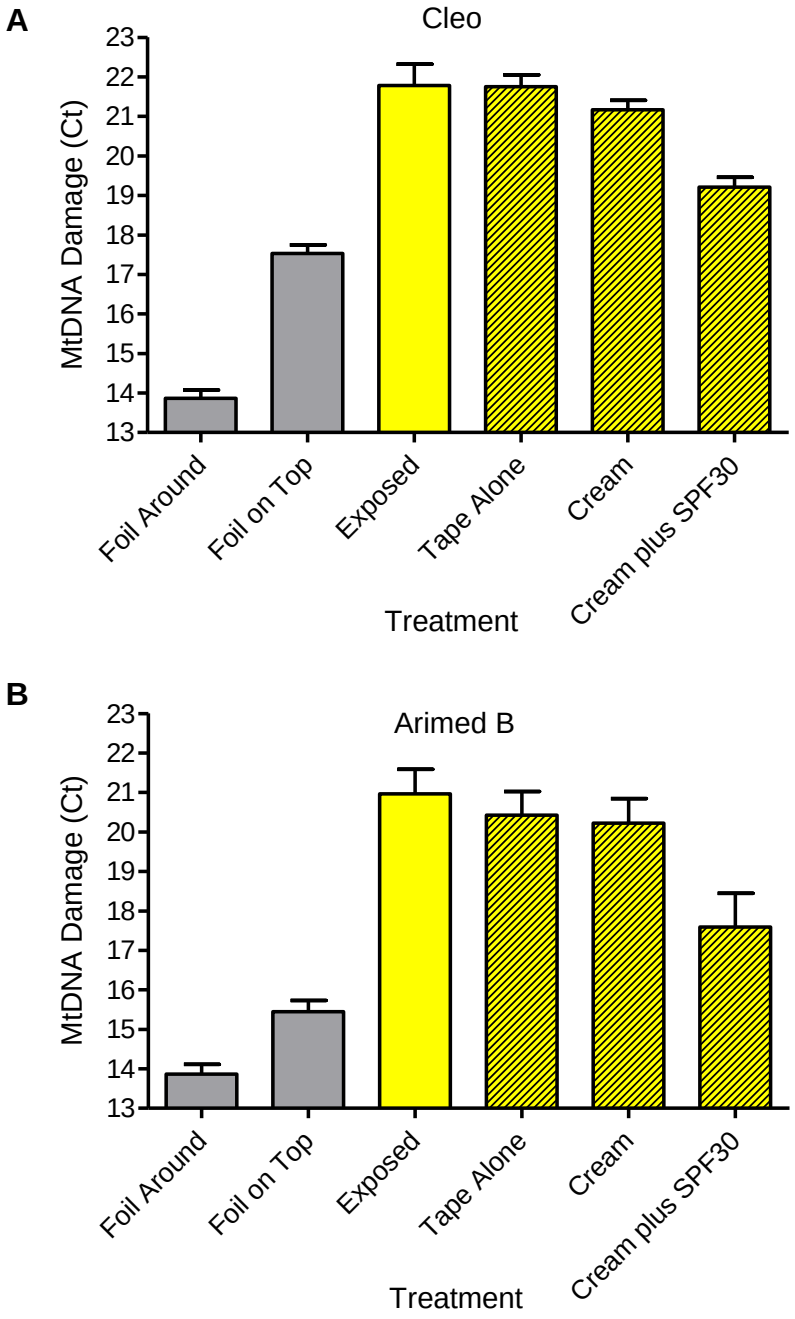

Figure 44. MtDNA damage in cells in the presence of cream with or without SPF protection. A) HDFn cells were irradiated with Cleo lamps for 20 minutes, with either foil around, foil on top, no foil (exposed), tape alone, cream without SPF, or cream plus SPF. There was a significantly higher level of damage in the cells with sham cream compared to the cells with cream and SPF ($P<0.01$, one-way ANOVA with Bonferroni correction). B) HDFn cells were irradiated with Arimed B lamps for 25 minutes under the same conditions. The cream with SPF was not significantly different from the sham cream ($P>0.05$, one-way ANOVA with Bonferroni correction), but the cream with SPF was also not significantly different than the foil on top ($P>0.05$, one-way ANOVA with Bonferroni correction), whereas the sham cream was ($P<0.0001$, one-way ANOVA with Bonferroni correction). The error bars show the SEM. For each lamp type, two dishes of cells were used per treatment. Two qPCRs were performed for each dish, each in duplicate.

6.4.3 *Cell viability following UV exposure in the presence of cream containing SPF30*

To determine whether the reduced mtDNA damage of cells with cream containing SPF, as opposed to cream without, was either due to a decrease in mtDNA damage in viable cells or due to higher cell viability, cell viability assays were performed. As can be seen in Figure 45A, for cells irradiated with the Cleo lamps, all cells which were exposed to UV had a significantly lower level of viability than the foil-covered cells ($P<0.0001$ for the exposed cells, $P<0.01$ for the cells with tape, and $P<0.05$ for the cells with SPF or sham cream, one-way ANOVA with Bonferroni correction). However, none of the exposed cells showed any significant difference from one another ($P>0.05$, one-way ANOVA with Bonferroni correction), which implies that despite there being a difference in mtDNA damage between the two cream types there was no difference in viability.

For the Arimed B lamps, it can be seen in Figure 45B that those cells which had foil on top had a significantly higher viability than those cells which were exposed ($P<0.0001$ for the exposed cells and the cells with tape, $P<0.01$ for the cells with sham cream, $P<0.05$ for the cells with SPF, one-way ANOVA with Bonferroni correction). There was again no significant difference between cells with the two different cream types ($P>0.05$, one-way ANOVA with Bonferroni correction).

Figure 45

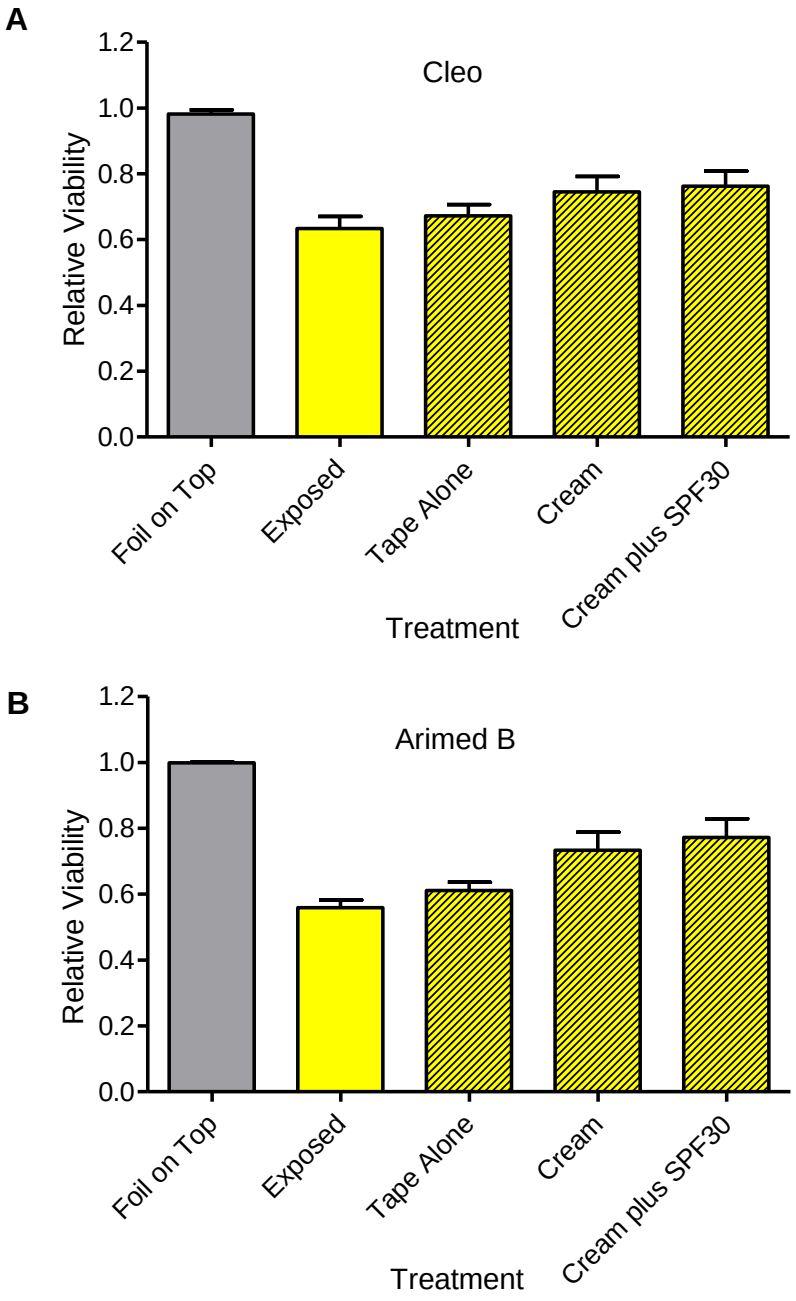

Figure 45. Cell viability in the presence of cream either with or without SPF protection. A) HDFn cells were irradiated with Cleo lamps for 20 minutes, either with foil on top, exposed, with tape, with tape and sham cream, or with tape and cream plus SPF30. The cells with foil had significantly higher viability than the cells which were fully exposed ($P<0.0001$, one-way ANOVA with Bonferroni correction), the cells with tape ($P<0.01$, one-way ANOVA with Bonferroni correction), and the cells with sham cream or cream plus SPF ($P<0.05$, one-way ANOVA with Bonferroni correction). There was no difference in viability between the cells with sham cream and the cells with cream plus SPF ($P>0.05$, one-way ANOVA with Bonferroni correction). B) HDFn cells were irradiated with Arimed B lamps for 25 minutes under the same conditions as above. The cells with foil had significantly higher viability than the cells which were fully exposed or exposed with tape ($P<0.0001$, one-way ANOVA with Bonferroni correction), the cells with sham cream ($P<0.01$, one-way ANOVA with Bonferroni correction), and the cells with cream plus SPF ($P<0.05$, one-way ANOVA with Bonferroni correction). There was no difference in viability between the cells with sham cream and the cells with cream plus SPF ($P>0.05$, one-way ANOVA with Bonferroni correction). Cell viabilities were normalised to the control (with foil on top) for each lamp type. The error bars show the SEM. For each lamp type, cell viability assays were performed with three biological repeats, each with eight technical replicates.

6.4.4 *MtDNA damage in UV-exposed human skin* in vivo

To confirm whether UV damage is detectable *in vivo* in mammalian skin, human skin swab samples were received from differently irradiated skin of human backs and the DNA was extracted. These samples were taken from the same donors both before irradiation and after irradiation with solar simulated light for 5 days with a single exposure of 0.8 MEDs on each day, resulting in a cumulative dose of 4 MEDs. MEDs were used instead of SEDs as differently pigmented skin *in vivo* responds to UV to different extents (Sachdeva, 2009), and MED represents the minimal amount of UV required to produce erythema (Heckman *et al.*, 2013).

Primers to amplify a region of 500 bp were used to check the *in vivo* samples for mtDNA damage. To ensure that the 500 bp primers were capable of damage detection within mtDNA, as regions this small have not been used previously in the literature, qPCR results for this primer set were compared to results using the 4.4 kb-primers, for which primers to amplify regions smaller than this have been used previously to attempt to detect differences (Kalinowski *et al.*, 1992; Ray *et al.*, 2000; Durham *et al.*, 2003; Eischeid *et al.*, 2009; Hunter *et al.*, 2010). It was found that the qPCR results for the 500 bp-product primers correlated directly with the damage for the 4.4 kb-product primers using human skin fibroblast cells (Figure 46) ($P<0.0001$, rho=1.0000, non-parametric Spearman correlation).

Figure 46

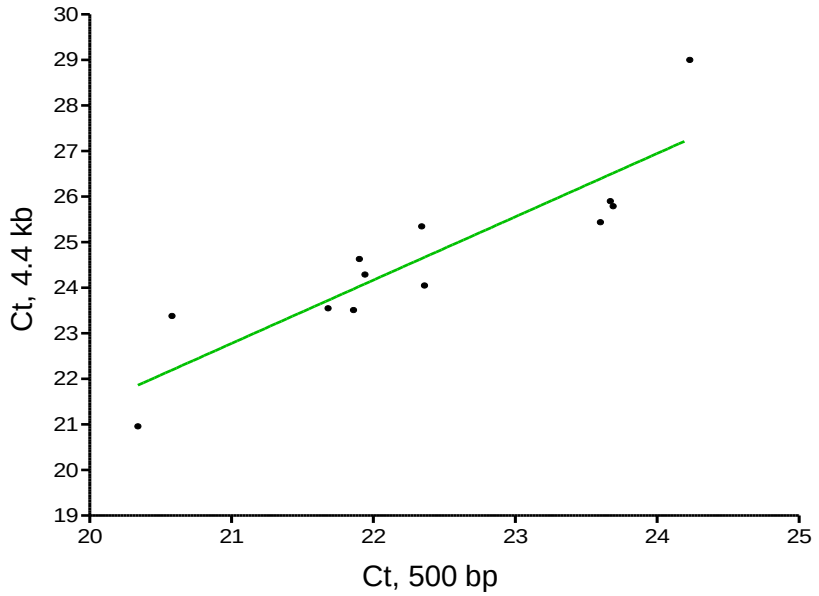

Figure 46. Comparison of the 4.4 kb and 500 bp-product primers. QPCR was performed on 12 human fibroblast samples using the 4.4 kb and the 500 bp-product primer sets, and a highly significant correlation was seen between the Ct values for the two primer sets (P<0.0001, rho=1.0000, non-parametric Spearman correlation). The green line shows the line of best fit. Results were obtained from two qPCR reactions each performed in duplicate for 12 samples.

The level of mtDNA damage within a region of 500bp was measured by qPCR, and it was found that there was a significantly higher level of mtDNA damage in samples from the same individuals following exposure with 4 MEDs, as shown in Figure 47A (P=0.0216, unpaired t-test). The difference of approximately 1.57 Cts between the non-irradiated and irradiated samples equates to an actual fold difference of approximately $2^{\wedge 1.57}$, or 3-fold more damage in the irradiated samples. To ensure that this increase in damage was not due to a natural increase in mtDNA damage over the 5 days, swabs were also taken from a different area of the back of each person before and after the 5 days of irradiation, without exposure. It was found that those areas which were not exposed did not have any significant change in damage over the course of the 5 days (Figure 47B) (P=0.4038, unpaired t-test). To ensure that an equal amount of mtDNA was added to the 500 bp qPCR, an 83 bp short section qPCR was performed, and it was found that all of the samples had similar Ct values suggesting the same amount of mtDNA. As the preliminary data found here suggested that UV damage is detectable using skin swabs of the back, the study was continued by Dr Asif Tulah (Newcastle University).

Figure 47

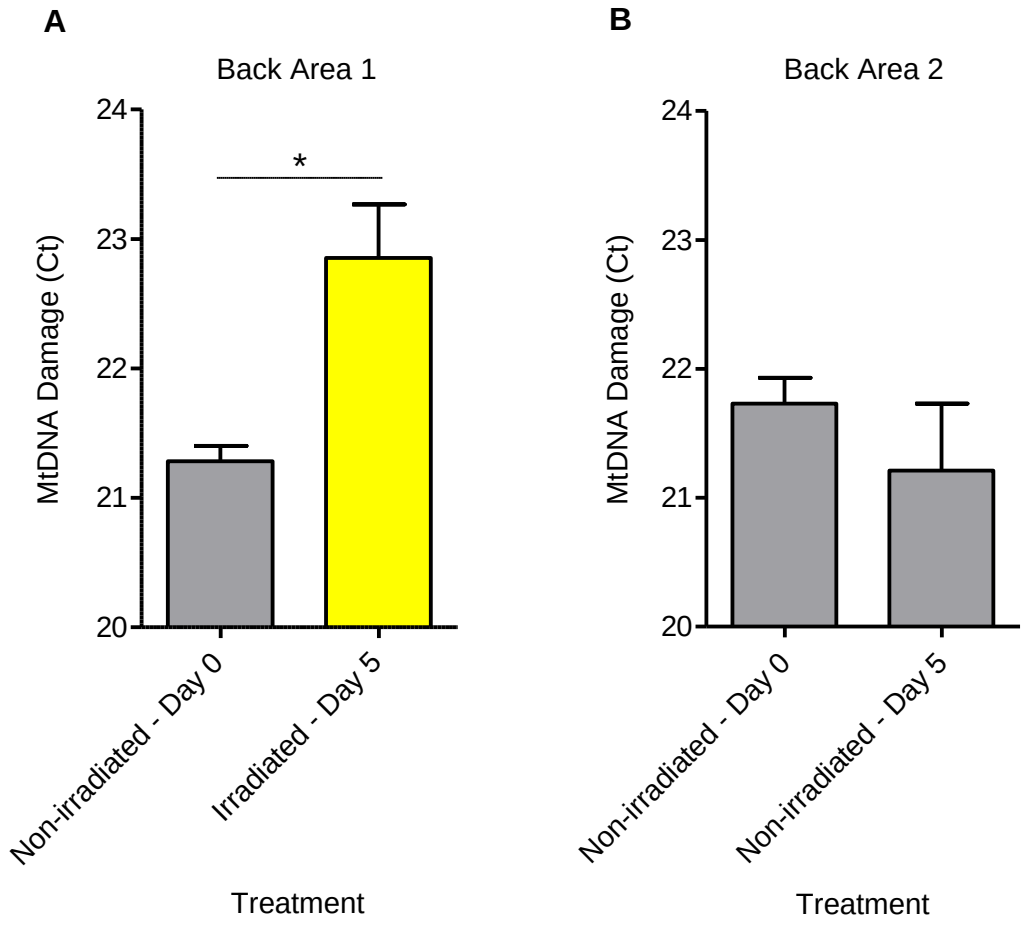

Figure 47. MtDNA damage following irradiation *in vivo*. A) Samples were taken by skin swabs from one area (area 1) of the backs of three people (non-irradiated, day 0), then the same area was irradiated every day for 5 days and a sample was taken from the same area (irradiated, day 5). There was a significant increase in the level of mtDNA damage following the 5 days of irradiation (P=0.0216*, unpaired t-test). MtDNA damage is represented by the Ct value. B) Samples were taken from another area of the back (area 2) of the same three people (non-irradiated, day 0), and a sample from the same area was taken 5 days later without any irradiation (non-irradiated, day 5). There was no significant difference in mtDNA damage (P=0.4038, unpaired t-test). The error bars show the SEM. Two qPCR reactions were performed for each sample, each in duplicate, for three donors.

6.5 Discussion

6.5.1 *MtDNA damage is detectable in a 4.4 kb mtDNA section* in vitro

Real-time qPCR is a technique used previously and reliably to detect UV-induced genetic damage in mtDNA in both cells and tissues (Kalinowski *et al.*, 1992; Birch-Machin *et al.*, 1998; Ayala-Torres *et al.*, 2000; Ray *et al.*, 2000; Durham *et al.*, 2003; Santos *et al.*, 2006; Hunter *et al.*, 2010; Meyer, 2010; Swalwell *et al.*, 2012). To confirm the ability of qPCR to detect mtDNA damage within a smaller mtDNA region (4.4 kb) using previously unpublished primers, skin cells were irradiated with both UVA and UVB simultaneously to simulate natural sunlight. The Arimed B lamps were used as these lamps give a UVA and UVB ratio similar to that of natural daylight to represent natural UV conditions, which is approximately 4% UVB and 96% UVA for the lamps (Cosmedico, 2013), with natural sunlight being 6% UVB and 94% UVA (Diffey, 2002). The Cleo lamps were chosen as they contain very little UVB (0.7% (Das *et al.*, 2002)), to allow information on UVA alone to be determined. Damage was detected with both lamp types, from as little as 0.57 SEDs. This represents approximately 4 hours of exposure to a weak sun with a UV index of 1, and only 12 minutes of exposure when the UV index is extremely high at 11 (World Health Organisation, 2006). This suggests that mtDNA damage can be detected using this technique within a 4.4 kb region, even at low levels of UV, for natural sunlight.

The damage detected using this qPCR method was most likely to be due to UV damage because the cream containing SPF30 was able to reduce the level of mtDNA damage compared to the cream without SPF, suggesting damage was not due to other factors such as heat which has been shown to induce mtDNA damage previously in some studies (Purschke *et al.*, 2010; Chan *et al.*, 2013), (however not in others (Swalwell *et al.*, 2012)). SPF represents the extent to which a sunscreen can protect against UV damage (Bech-Thomsen and Wulf, 1992), with SPF30 considered high protection (Bendová *et al.*, 2007). Since the cells in the presence of the cream containing the SPF had lower mtDNA damage than the cells with sham cream, it suggested that at least some of the mtDNA damage observed in exposed cells was caused by UV which was blocked by SPF cream. For the Arimed B lamps, the SPF cream prevented mtDNA damage to the same extent as the foil, suggesting that for this lamp type

(which is the most similar to natural sunlight) the UV is completely blocked; therefore the damage detected for the exposed cells without SPF was likely due to UV. For the Cleo lamp, the SPF was unable to block all of the UV-induced mtDNA damage, possibly due to the much higher level of SEDs compared to the Arimed B lamps (23.79 versus 2.87).

6.5.2 *MtDNA damage is detectable in an mtDNA section* in vivo

To further confirm the ability of the long qPCR assay in the detection of UV-induced damage, skin was irradiated *in vivo*, and an increase in mtDNA damage was observed. MtDNA damage induced by UV has been detected previously *in vivo* in the form of deletions and mutations. For example, the 4977 bp common deletion has been shown to be more highly induced in sun-exposed human skin (Yang *et al.*, 1995; Birch-Machin *et al.*, 1998; Berneburg *et al.*, 2004; Reimann *et al.*, 2007; Kaneko *et al.*, 2012), including via repeated artificial irradiations as used in the present study (Berneburg *et al.*, 2004; Reimann *et al.*, 2007). Other mtDNA deletions have been shown to be higher in sun-exposed skin, such as the 3895 bp deletion (Krishnan *et al.*, 2004; Harbottle *et al.*, 2010). Other mutations include the T414G mutation, which has been shown to be higher in sun-exposed human skin than in sun-protected (Birket and Birch-Machin, 2007). MtDNA damage in the form of strand breaks has also been detected in human skin tissue using the long-region amplification qPCR technique as used in the present study (Ray *et al.*, 2000; Durham *et al.*, 2003); however, in this project the level of mtDNA damage was measured within an even smaller region of 500 bp, to see whether damage could still be detected. This region appeared to be capable of detecting UV damage, and because this region was shown to correlate with the 4.4 kb primer set, it further confirmed the use of the 4.4 kb-product primer set in detection of UV-induced mtDNA damage, which provides additional confidence that UV damage is detectable in whale skin in a region of this size (for Chapter 7). This project also demonstrated that mtDNA damage is able to be detected in very few skin cells as taken by a swab; therefore, whole tissue sections may not be required which is useful to know for possible future studies on human skin for which the taking of tissue sections may not be practical.

6.6 Summary

This Chapter provided a proof-of-concept study for the following Chapter (Chapter 7), for which a 4.4 kb region was used to detect UV-induced mtDNA damage in whale skin from differently UV-exposed whales as a model for different ages. The 4.4 kb region tested in this chapter was able to show differences in mtDNA damage *in vitro*, for which the damage was shown to be preventable when using a UV-blocking cream. Damage in the 4.4 kb region also correlated with results from another primer set (500 bp) used *in vivo*. Therefore, a region of this size should be capable of demonstrating mtDNA damage in whale skin; additionally, in previous studies regions from 1 kb up to 15 kb have been capable of UV-induced damage detection (Kalinowski *et al.*, 1992; Ray *et al.*, 2000; Durham *et al.*, 2003; Eischeid *et al.*, 2009; Hunter *et al.*, 2010). In the following chapter (Chapter 7), the level of mtDNA damage was measured in whale skin taken from the Gulf of California, Mexico, where the UV index is approximately 11 during the summer (Martinez-Levasseur *et al.*, 2013). This represents an extremely high level of solar UV, and in this climate 0.57 SEDs can be achieved in only 12 minutes of exposure (World Health Organisation, 2006). As damage could be measured *in vitro* in HDFn cells at only 0.57 SEDs, and the whales spend many hours a day under UV exposure (Whitehead, 2003), it is likely that a 4.4 kb qPCR assay will be able to detect mtDNA damage induced by UV in whales.

Chapter 7. Mitochondrial DNA Damage in UV-Exposed Whale Skin

7.1 Introduction

7.1.1 *The similarities between UV exposure and chronological ageing*

The genetic changes observed in UV-irradiated (photo-aged) skin have been shown to be similar to those found in chronologically-aged skin, and it is observed that UV radiation can accelerate skin ageing (Kosmadaki and Gilchrest, 2004; Quan *et al.*, 2006; Birket and Birch-Machin, 2007; Akase *et al.*, 2012). The similarities between UV-exposed and chronologically-aged skin are demonstrated by examples of the same type of damage found in both, which include mtDNA damage such as the 3895 bp mtDNA deletion, which is correlated more strongly with skin from sun-exposed regions of the body as well as in the skin of older individuals (Krishnan *et al.*, 2004; Harbottle *et al.*, 2010). Other genetic examples include the T414G mtDNA mutation, which has been shown in previous studies (Michikawa *et al.*, 1999; Barritt *et al.*, 2000) as well as throughout this project (Chapter 4) to be more commonly associated with the skin of older individuals, as well as being higher in sun-exposed skin (Birket and Birch-Machin, 2007). Other changes in the skin with age include wrinkling, loss of elastic fibres and of collagen (Naylor *et al.*, 2011), and an increased risk of skin cancers such as malignant melanoma (Cancer Research, 2012), which are a phenomenon also observed in photo-aged skin (Nishimori *et al.*, 2001; Imokawa, 2008; Rass and Reichrath, 2008). As the effects of UV and of intrinsic ageing have very similar patterns, animal models of skin which have been differentially exposed to UV can be used as a model for differently aged skin (Seo *et al.*, 2009; Flores *et al.*, 2010; Akase *et al.*, 2012). This is useful for when it is not practical to study chronological ageing in animals due to their long lifespans.

7.1.2 *Whale skin as a model for ageing*

Skin exposed to different levels of UV is able to be used as a model for differently chronically-aged skin, due to the similarities observed for each. The effects of UV are well-documented for humans and laboratory animals (Spradbrow *et al.*, 1987; Noonan *et al.*, 2003; Hunter *et al.*, 2010); however, laboratory animals may not be the ideal model for human skin as these animals are generally small, fur-covered, and short-lived, and are irradiated in the laboratory rather than naturally. Some of the damaging effects of UV on wildlife have been documented, but these are mainly restricted to fish, amphibians, and

other aquatic invertebrates (Kiesecker *et al.*, 2001; Blaustein *et al.*, 2003; Tedetti and Sempere, 2006; Dahms and Lee, 2010). Large, wild-living mammals, which are rarely studied in terms of UV damage, may represent an ideal model for UV exposure, as they are exposed to natural UV from the sun throughout their long-lives. Due to the physiological traits of whales, such as the need to breathe air, or the long hours spent socialising at the ocean surface (Whitehead, 2003; Martinez-Levasseur *et al.*, 2011), whales are forced to undergo long periods of continuous exposure to UV, making them an ideal model for the study of UV-induced skin damage as a model for ageing. Whales also lack UV-protective fur or feathers on their skin, similar to humans, allowing the direct penetration of UV rays onto the skin, and they are also likely to have differences in UV exposure due to differences in pigmentation levels and UV exposure times (Martinez-Levasseur *et al.*, 2011). Figure 48 shows the microanatomy of whale skin in comparison to human skin. Previous research has indicated that whale skin is indeed susceptible to the damaging effects of UV, in the form of skin blisters and other skin damage such as oedema and apoptosis (Martinez-Levasseur *et al.*, 2011). However, the level of genetic damage has not been studied previously in these animals. An additional reason as to why whale skin could make a good model, is that it has been observed that whales in captivity, which are subjected to long periods at the surface of the water, are susceptible to sunburn and skin damage, and have to be regularly applied with the sun-protector zinc-oxide to protect against sunburn (Kirby, 2012), further confirming that whales are indeed susceptible to the effects of UV. Whales are also long-lived, and can live to over 100 years in the wild (Dobson, 2003), which could be useful for documenting the effects of cumulative genetic damage over many years. Therefore, whales with different UV exposures were chosen for use in this study, as a model to represent differently aged skin, to determine whether genetic damage is increased with age and what possible factors can influence the level of this damage.

Figure 48

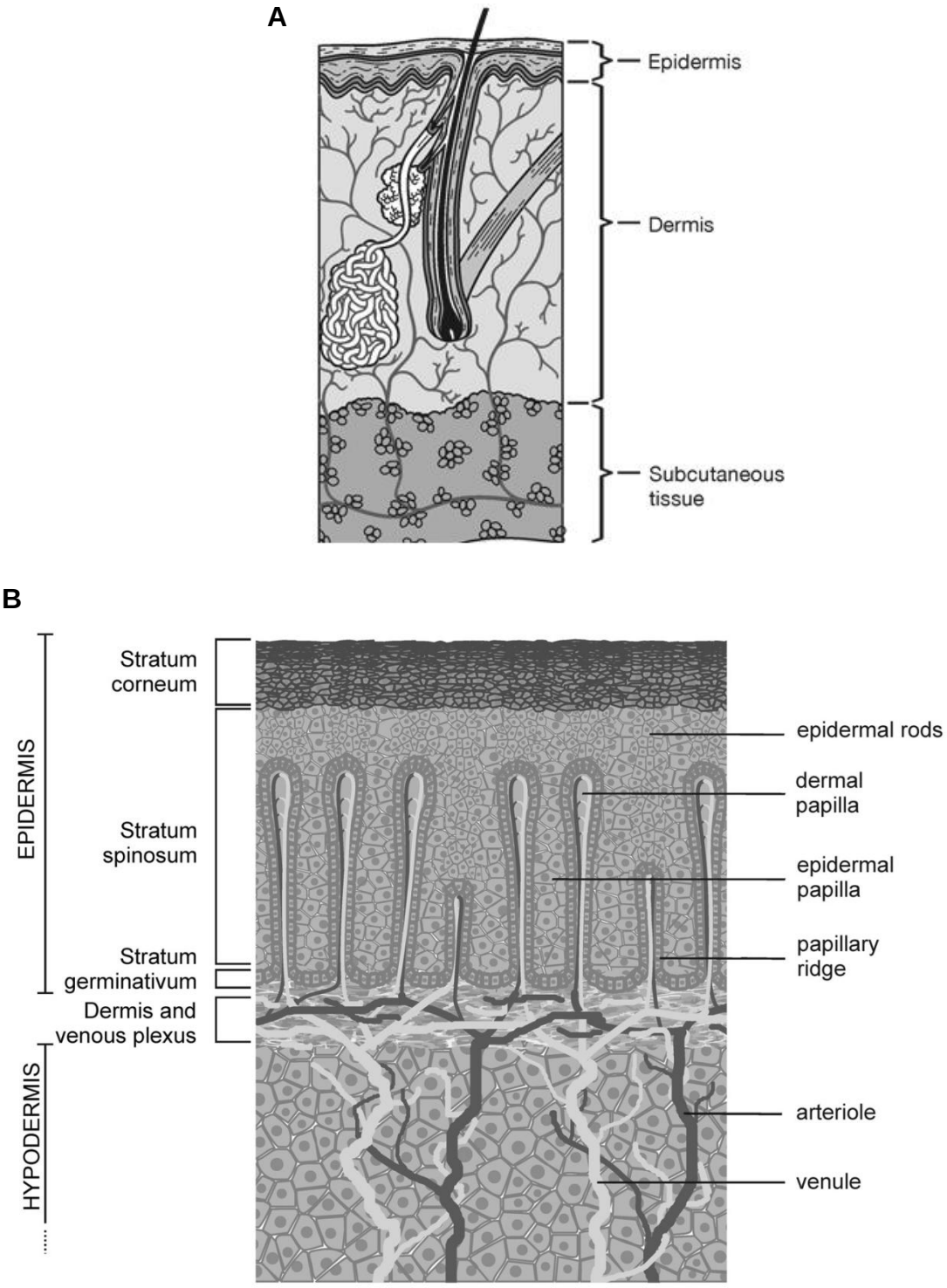

Figure 48. The microanatomy of human and whale skin. Both human and whale skin are composed of three main layers, which are the epidermis, the dermis, and the hypodermis/subcutaneous tissue. A) The epidermis of human skin is approximately 0.1 mm thick, the dermis is 1-4 mm thick, and the hypodermis is 1-6mm thick (Bashkatov *et al.*, 2005). B) Whale skin epidermis consists of a thin pigmented layer of <1 mm thick, with the total thickness of the epidermis approximately 5 mm, but can be lower or higher depending on the whale species. The dermal layer is thin and is <1 mm. The hypodermis can be up to 60 cm in thickness depending on the whale species and area of the body (Tinker, 1988). Images edited from (Berardi *et al.*, 2006; Mouton and Botha, 2012).

7.1.3 *Differences in the skin of blue whales, fin whales, and sperm whales*

In a previous study performed by Martinez-Levasseur *et al.* (2011), whale skin samples from blue whales, fin whales, and sperm whales were collected from the Gulf of California, Mexico, which has an extremely high UV index as shown in Figure 49 (Bournay and UNEP/GRID-Arendal, 2007). Samples were taken from the UV-exposed backs of these cetaceans, to obtain information regarding skin lesions such as sun-induced blistering in these differently pigmented whale species (Figure 50A) (Martinez-Levasseur *et al.*, 2011). The results indicated that the lighter-skinned blue whales and sperm whales appeared to accumulate a higher number of blisters than the darker-skinned fin whales (Figure 50B) (Martinez-Levasseur *et al.*, 2011). This pigmentation level in the whales appeared to have a higher influence than the time spent at the surface for the determination of cellular skin damage, as sperm whales spend longer periods of time at the surface during breathing (7 to 10 minutes for the sperm whales and only 2 minutes or less for the blue and fin whales (Croll *et al.*, 2001)), and they can also spend up to 6 hours longer than the blue and fin whales at the surface during socialisation (Whitehead, 2003). Due to the differences in surface times and pigmentation, these three species were chosen to determine the level of mtDNA damage within for the current project. The cellular defence mechanisms against UV such as pigmentation are discussed in more detail in the general Introduction, section 1.5.3.

Through this chapter, mtDNA from whales under various levels of UV stress was examined using qPCR to check for differences in damage, which would allow insights into mtDNA damage levels with age, as well as the ability to study differences in mtDNA damage protection mechanisms between species. These protection mechanisms may have evolved differently to counteract damage. Studying whale mtDNA also provided the chance to study for the first time in the literature the mitochondrial effects caused by UV radiation and therefore age on the skin of whales.

Figure 49

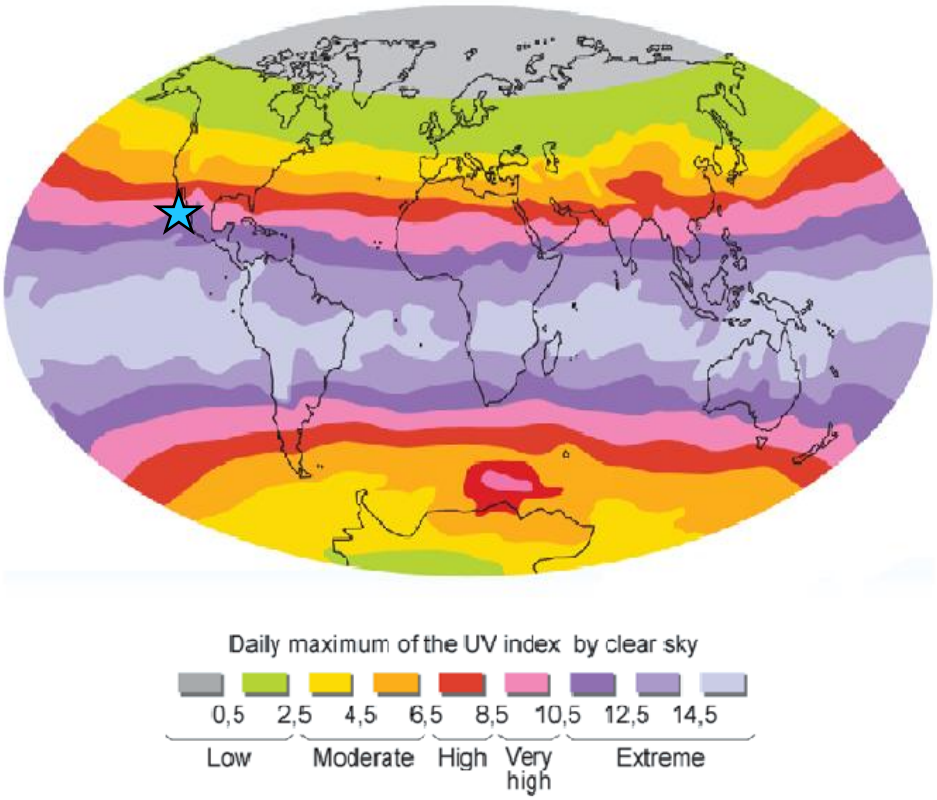

Figure 49. Global UV index map showing the area from which whale samples were taken. The UV index represents a standard measurement of UV strength reaching the earth's surface (World Health Organisation, 2013). The blue star shows where the whale skin samples from blue whales, fin whales, and sperm whales were taken (the Gulf of California, Mexico), where the UV index is very high to extreme. Image was edited from (Bournay and UNEP/GRID-Arendal, 2007).

Figure 50

A

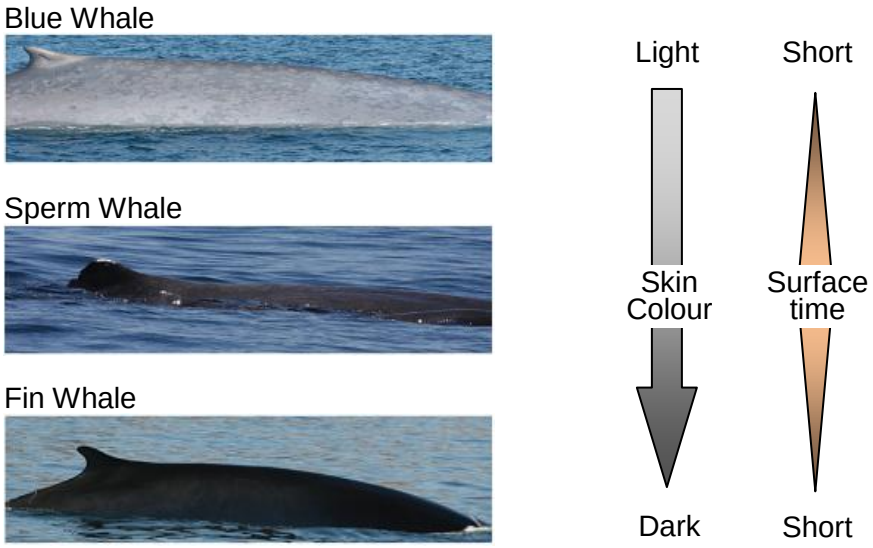

B

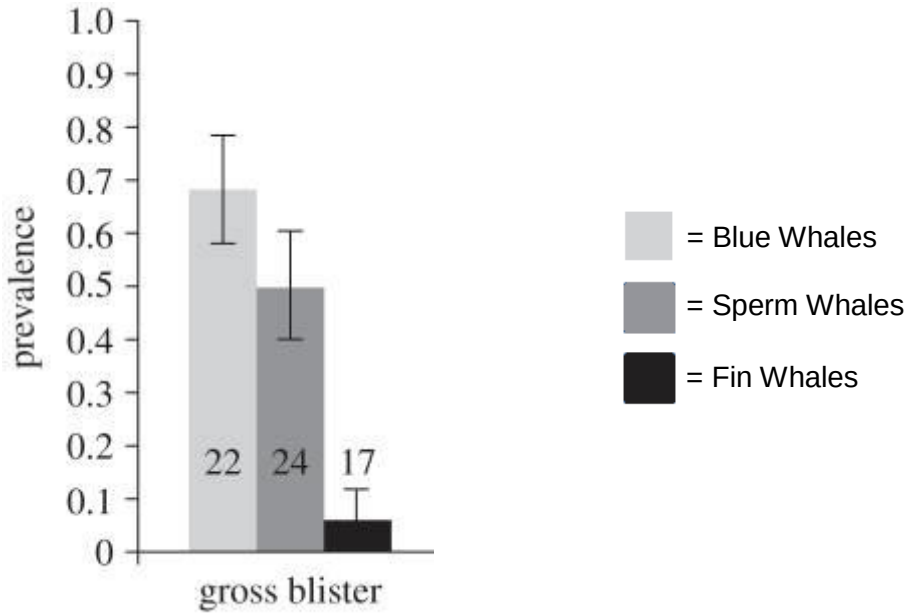

Figure 50. Whale skin colouration and surface time and the level of UV-induced skin blisters. A) Blue whales in general have the lightest skin colour, followed by sperm whales, and then the fin whales (Martinez-Levasseur *et al.*, 2011). Blue and fin whales spend similar lengths of time at the surface of the ocean, whereas sperm whales spend longer at the surface between dives and during socialisation (Whitehead, 2003; Martinez-Levasseur *et al.*, 2011). The image was highly edited from (Martinez-Levasseur *et al.*, 2011). B) The level of sun-induced gross skin blisters in blue whales, fin whales, and sperm whales. Blue whales, the lightest species, had the highest number of blisters. Pigmentation was more important in the study in determining the level of skin blisters when compared to surface time. The numbers in the bars show the sample sizes, and the image was taken and edited from (Martinez-Levasseur *et al.*, 2011).

7.2 Hypotheses

The hypotheses of this area of my project were 1) differences in UV-induced mtDNA damage can be detected simultaneously in three different whale species using qPCR; 2) this mtDNA damage is correlated with factors related to UV, such as pigmentation, apoptosis, micro-vesicles, migration patterns, surface times, and the level of Hsp70 expression; and 3) this damage differs between species, due to possible differences in evolutionary responses to UV-induced damage. Any differences observed between differently UV-exposed whales would be used as a model for differences in differently aged skin. Additionally, the defence mechanisms providing the most effective protection against mtDNA damage could have possible implications for the treatment of human ageing.

7.3 Materials and Methods

The qPCR and gel electrophoresis methods used within this chapter are given in the general Materials and Methods, in Chapter 2.

7.3.1 *Whale skin sample collection*

Epidermal whale skin samples were collected from 15 blue whales *(Balaenoptera musculus*, abbreviated Bm*)*, 10 fin whales *(Balaenoptera physalus*, abbreviated Bp*)*, and 18 sperm whales *(Physeter macrocephalus,* abbreviated Pm*)* from the Gulf of California, Mexico, during the time period from January to June (2007-2009) by Dr Laura Martinez-Levasseur (University of London), Dr Karina Acevedo-Whitehouse (University of London), and Dr Diane Gendron (Instituto Politécnico Nacional), using a 7 mm stainless steel dart (Martinez-Levasseur *et al.*, 2011). Samples were stored in ethanol at 4°C until DNA extraction was performed. The age of the whales was taken into account, and only those whales with a minimum age of 1 year old were used in the study. Only one sample was taken per whale.

7.3.2 *DNA extraction from whale skin tissue*

Total DNA was extracted from epidermal whale skin samples using a QIAamp DNeasy Blood and Tissue kit (Qiagen, UK). During this technique, whale skin samples of approximately 25 mg were sliced into smaller sections of approximately 1 mm^2 and placed into a 1.5 ml Eppendorf tube. To these tissue sections, 180 µl lysis buffer (Buffer ATL) and 20 µl proteinase K were added. The tube was vortexed and incubated at 56°C for 1 hour to lyse the sample, after which 200 µl of another lysis buffer (Buffer AL) was added to further lyse the cells. Samples were vortexed for 15 seconds, and incubated at 70°C for 10 minutes. Following incubation, 200 µl ethanol was added to purify the DNA and samples were vortexed again for 15 seconds. The sample was then transferred to a QIAamp Spin Column, and the remaining DNA extraction was performed as described in section 2.4.1 from the point of sample transfer to a QIAamp Spin Column. DNA was stored at 4°C or -20°C until use. The DNA from blue and fin whales, and several of the sperm whales was extracted by Dr Laura Martinez-Levasseur.

7.3.3 *QPCR primer design*

Primers for use in qPCR for the amplification of whale mtDNA to analyse the level of damage had to be designed in this project, as whale mtDNA has not been analysed previously using this method. The mtDNA of the blue, sperm, and fin whales are 16,402 bp, 16,428 bp, and 16,398 bp respectively. Therefore, two sections of approximately 8.5 kb or four sections of approximately 4.4 kb were initially designed to specifically amplify the mtDNA to ensure the entire mitochondrial genome could be checked for damage (primer positions are shown in Figure 51A and Figure 51B). The primer sets were designed to overlap to ensure the whole genome could be checked. The 4.4 kb and 8.5 kb-product primers were specific for the blue and fin whale samples only. Following the success of these primers and the acquisition of DNA from an additional species, the sperm whale, a universal primer set of approximately 4.3 kb was designed to bind specifically to all three species (Figure 51C), to allow direct comparisons between species in the same qPCR reaction. In order to find the relative amount of mtDNA within a sample, primers to amplify a region of 51 bp specific to all three species were also designed (Figure 51D), as a region this small is unlikely to contain high levels of damage and can therefore be used to quantify mtDNA amount (Koch *et al.*, 2001; Hunter *et al.*, 2010). The mitochondrial genome sequences of the blue whales, sperm whales, and fin whales were downloaded from the National Centre for Biotechnology Information (NCBI) database (NCBI, 2013), and primers of 20-21 bp in length were designed using Primer3 (Rozen and Skaletsky, 2000). A Basic Local Alignment Search Tool (BLAST) (NCBI, 2013) was used to ensure primers would only bind to the intended regions, and not elsewhere to potential pseudogenes within the whale nDNA (Bensasson *et al.*, 2001), or within any possible contaminating human DNA. The qPCR annealing temperature of all the primers was also checked to ensure their simultaneous use under the same qPCR conditions. The final whale primer sequences are shown in Table 4. All primers were produced by Eurofins MWG Operon.

Figure 51

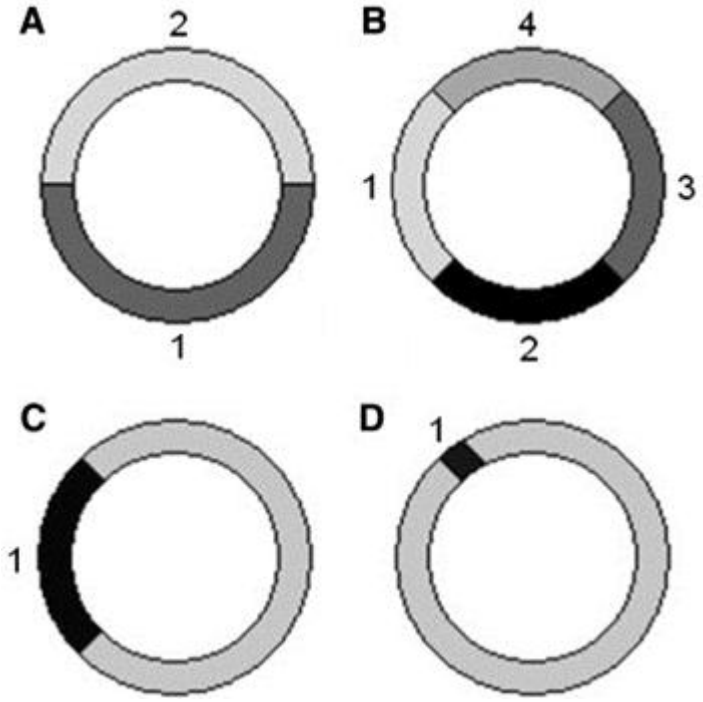

Figure 51. Positions of the designed primers on whale mtDNA for use in qPCR. A) The two 8.5 kb-product primer pairs for use in amplifying whale mtDNA to determine damage within. These primers were capable of amplifying the mtDNA from blue and fin whales only. B) The four 4.4 kb-product primer pairs for use in amplifying whale mtDNA to determine damage. These primers were capable of amplifying the mtDNA from blue and fin whales only. C) The universal 4.3 kb-product primer set for use in amplifying whale mtDNA to determine damage. These primers were capable of amplifying mtDNA from blue, fin and sperm whales. D) The 51 bp-product primers for use in determining the relative copy number of whale mtDNA. These primers were capable of amplifying the mtDNA from blue, fin, and sperm whales.

Table 4

Primer Set		Base Sequence (5' to 3')	Length (bp)	Nucleotide Numbers (bp)
8.5 kb Whale	1F	TTA ACC CAA CAG CAT CCA CA	8295; 8295	4620-12914; 4623-12917
	1R	ATT GCT GAT GGG AGT CAA GG		
	2F	CGA CCC CTA CAT CAA CCA AT	8738; 8734	12534-4869; 12537-4872
	2R	GTT TGG TTT AGT CCG CCT CA		
4.4 kb Whale	1F	GAA CTC GGC AAA CAC AAA CC	4489; 4489	2345-6833; 2348-6836
	1R	CCG CCT ACT GTG AAA AGG AA		
	2F	TCA AAC TCC CCT TTT CGT ATG	4400; 4400	6315-10714; 6318-10717
	2R	TGG GCT GTG GAG TTA ATT CAG		
	3F	TCC CAC CTA ATA TCC GCA TT	4329; 4329	10405-14733; 10408-14736
	3R	TTA AGC AGA GGC CGA GTA GG		
	4F	TTT GAA GAA ACC CCC ACA AA	4405; 4401	14469-2471; 14472-2474
	4R	CTA CCT TTG CAC GGT CAG GA		
4.3 kb Whale	F	GAA CTC GGC AAA CAC AAA CC	4302; 4302; 4306	2345-6646; 2348-6649; 1931-6236
	R	GGG CTC ATA CGA TAA AGC CTA		
51 bp Whale	F	AAC CTC ACC AAC CCT TGC TA	51; 51; 51	1077-1127; 1079-1129; 653-703
	R	TTT GCT GAA GAT GGC GGT AT		

Table 4. Primer sequences for qPCR with whale mtDNA. The primer sets specific for whale mtDNA, with product sizes of approximately 8.5 kb, 4.4 kb, 4.3 kb, and 51 bp. The two 8.5 kb and four 4.4 kb sets were specific for blue whales and fin whales, and the 4.3 kb and 51 bp sets were specific for blue whales, fin whales, and sperm whales. The base sequences from 5' to 3' are shown for the forward (F) and reverse (R) primers, as well as the exact product length in bp, and the nucleotide numbers in bp which give the positions of the products to be amplified within the mtDNA. For primer product length and nucleotide numbers, the order in the table is given as blue whale; fin whale, or blue whale; fin whale; sperm whale.

7.3.4 *Whale skin colour*

The skin colour of the whale samples was determined previously by Dr Laura Martinez-Levasseur (Martinez-Levasseur *et al.*, 2011). To do this, digital photographs of haematoxylin and eosin stained (H&E stained) sections were viewed, and a standardised area was chosen on the deepest layer of the epidermis, the epidermal ridges, as the number of melanocytes is most abundant here. Melanin pigment count was performed using the image-processing software Image J (Schneider *et al.*, 2012), by converting the photograph into greyscale and counting the areas of melanin. An example of an

H&E stained whale skin section is shown in Figure 52, with human skin shown in Figure 53 for comparison.

Figure 52

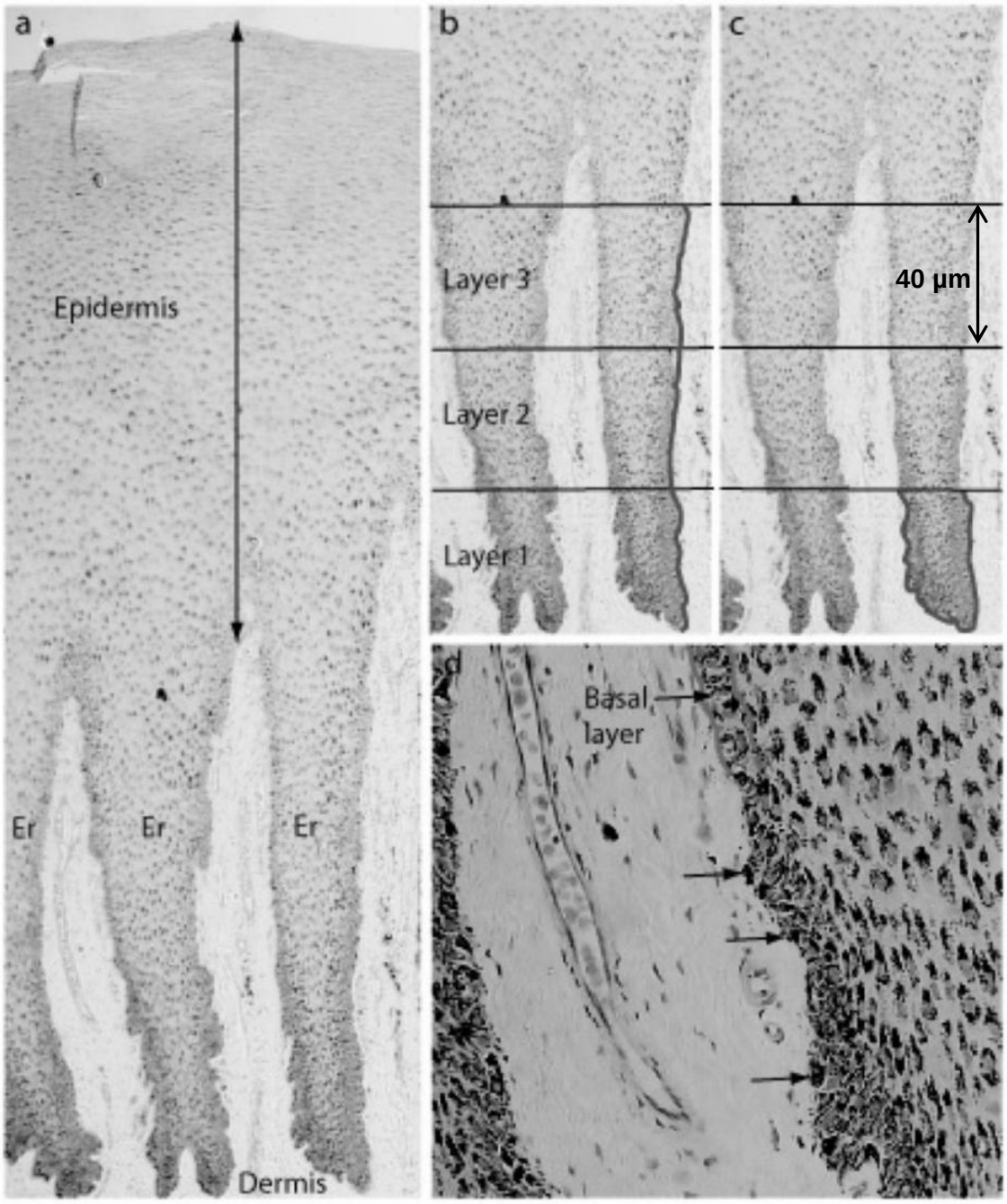

Figure 52. H&E stained section of fin whale skin. A) An H&E stained section of fin whale skin showing the epidermis, the dermis, and the epidermal ridges (Er) where the melanocytes are most abundant (Martinez-Levasseur *et al.*, 2011). B) The epidermal ridges were selected to determine whale skin colour, for which three layers were defined of 100 arbitrary units each (100 arbitrary units is equal to 40 µm). C) The deepest of the three layers was used to quantify melanocytes. D) Melanocytes are located at the basal layer of the epidermis, as shown by the black arrows. The black areas within cells (as opposed to the dark grey areas) show melanin. Image used with permission from the doctoral thesis of Dr Laura Martinez-Levasseur.

Figure 53

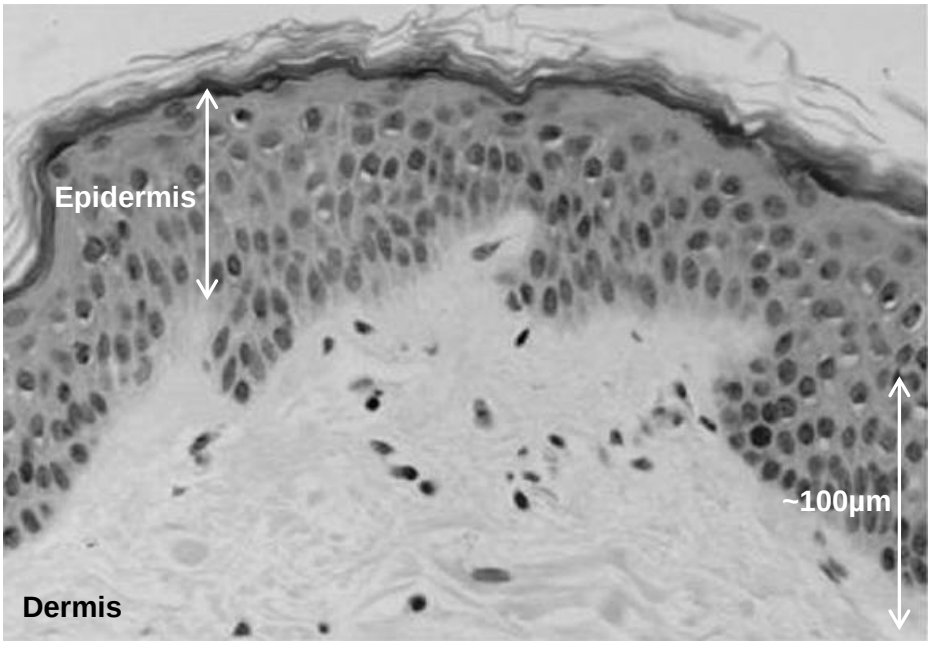

Figure 53. H&E stained section of human skin. An H&E stained section of human skin showing the epidermis and the dermis. An approximate scale bar is given to allow comparison to whale skin. Image edited from (Bernerd *et al.*, 2012).

7.3.5 *Whale apoptotic cell and micro-vesicle quantification*

Apoptosis and micro-vesicle quantification were determined as described previously (Martinez-Levasseur *et al.*, 2011) and performed by Dr Laura Martinez-Levasseur. The presence or absence of apoptosis was determined by the terminal deoxynucleotidyl transferase-mediated deoxyuridine triphosphate nick-end labelling (TUNEL) method, which detects double-strand breaks in DNA which occur in the end-stages of apoptosis (Nakaseko *et al.*, 2003; Yamaguchi *et al.*, 2008). To quantify apoptotic cells, a standardised area was determined on the dorsal area of the whales (the back), taking body length into account, by examining the dorsal fin length of each whale, which is proportional to body length (Martinez-Levasseur *et al.*, 2011). The number of apoptotic cells per individual whale was counted per 100 arbitrary units, by digital photography. Samples were considered to have apoptosis present if there was a large amount and wide distribution of apoptotic cells detected, and absent if there were few or no apoptotic cells observed (Martinez-Levasseur *et al.*, 2011). Micro-vesicles are skin lesions produced in response to UV exposure, to aid in the repair of sun-damaged tissue (Ulrich *et al.*, 2009). To quantify the level of

micro-vesicles present, a standardised area was determined on the dorsal area of the whales, taking body length into account. The number of micro-vesicles per individual whale was counted per 100 arbitrary units, by digital photography, following H&E staining. To confirm the presence of the micro-vesicles, slides were also examined by dermopathologists as described by Martinez-Levasseur *et al*. (2011).

7.3.6 *Age of individual whales*

The minimum age of the blue whales was calculated following long-term observation of the north-east Pacific Ocean population of whales. Information on the minimum age of the whales was available for 8 of the blue whale samples used in this study, as documented in the Centro Interdisciplinario de Ciencias Marinas (CICIMAR) data set, and provided by Dr Laura Martinez-Levasseur. The minimum age was estimated based on the initial sighting of the whale in the Gulf of California, and future observations of the same whale following photo identification.

7.3.7 *Whale Hsp70 expression*

The gene expression level of Hsp70 was determined by Dr Laura Martinez-Levasseur. To do this, RNA was extracted from tissue samples using an RNeasy Mini kit, and the cDNA was generated using a QuantiTect Reverse Transcription kit (Qiagen, UK). QPCR was performed using a 7300 Real-Time PCR System (Applied Biosystems) to determine the expression of Hsp70 based on the level of amplification of this protein using specific primers, as compared to two internal controls (ribosomal proteins S18 and L4).

7.4 Results

7.4.1 *Sample DNA quantification*

Total DNA (nuclear and mitochondrial) was extracted from epidermal skin sections from 15 blue whales, 10 fin whales, and 18 sperm whales and the DNA concentrations were determined. These concentrations were used as a guide as to the amount of total DNA to be added to the qPCR reaction, with the short fragment qPCR later used to determine the relative level of mtDNA per sample.

7.4.2 *QPCR optimisation: 8.5 kb sections*

Whale samples received for mtDNA analysis were originally from blue whales and fin whales only, as a preliminary test to see whether differences in damage could be determined in whale skin. Initial primers sets for qPCR optimisation were therefore specific for these two species only. QPCR was first attempted with two pairs of primers to amplify two mtDNA sections of approximately 8.5 kb each to cover both halves of the approximately 16.4 kb whale mitochondrial genome.

One blue whale sample and one fin whale sample were used to test the two 8.5 kb-product primers, using the enzyme Phusion DNA Polymerase and a Chromo4 machine. As can be seen in Table 5 and Figure 54A, the 8.5 kb-product primers were able to amplify the two samples from different species; however, the qPCR efficiencies were low. QPCR efficiencies represent the amount of sample replication at each cycle, with 100% representing a perfect doubling (Agilent Technologies, 2012). The blank negative control contained no DNA, and gave no fluorescent signal as expected. To ensure the designed primers were producing a single product, the dissociation curve (melt curve) was examined and a single product length seemed to be produced based on the presence of a single peak (Figure 54B). This is based on the observation that DNA strands of similar lengths become separated (melt) at similar temperatures, at which point the fluorescent dye becomes dissociated. This was confirmed by gel electrophoresis, for which a single band of between 8000-10,000 bp was present for both samples (Figure 54C), suggesting the qPCR amplification was successful.

Optimisation of the 8.5 kb-product qPCR reaction was attempted by using a lower level of fluorescent dye in the reaction (0.075x SYBR Green concentrate instead of the previously used 0.1x SYBR Green), as higher levels of this dye may be inhibiting the DNA polymerase (Eischeid, 2011). The efficiency however did not appear to change with a lower SYBR Green concentration (Table 6). A lower dye concentration appeared to increase the Ct values implying a lower fluorescent signal, so the original concentration was maintained. Instead, new primers were designed to amplify four sections of approximately 4.4 kb each in length, as mtDNA fragments of close to this size have been amplified previously to test for UV-induced damage (Kalinowski *et al.*, 1992; Ray *et al.*, 2000; Durham *et al.*, 2003; Eischeid *et al.*, 2009; Hunter *et al.*, 2010), as well as in Chapter 6 of this project.

Table 5

Sample	Primer Set	Average Efficiency	Average Ct Value
Blue Whale	8.5 kb Set 1	12%	14.87
	8.5 kb Set 2	14%	14.25
Fin Whale	8.5 kb Set 1	35%	20.59
	8.5 kb Set 2	46%	19.22

Table 5. QPCR results with the 8.5 kb-product primers. One blue whale and one fin whale sample were used to test the amplification ability of the 8.5 kb-product primers. Each sample was run in triplicate for each of two qPCR reactions using a Chromo4 machine, Phusion polymerase, and SYBR Green dye with a primer annealing temperature of 60°C, and the average qPCR efficiency and Ct values of the replicates are shown. Blanks showed no amplification product.

Figure 54

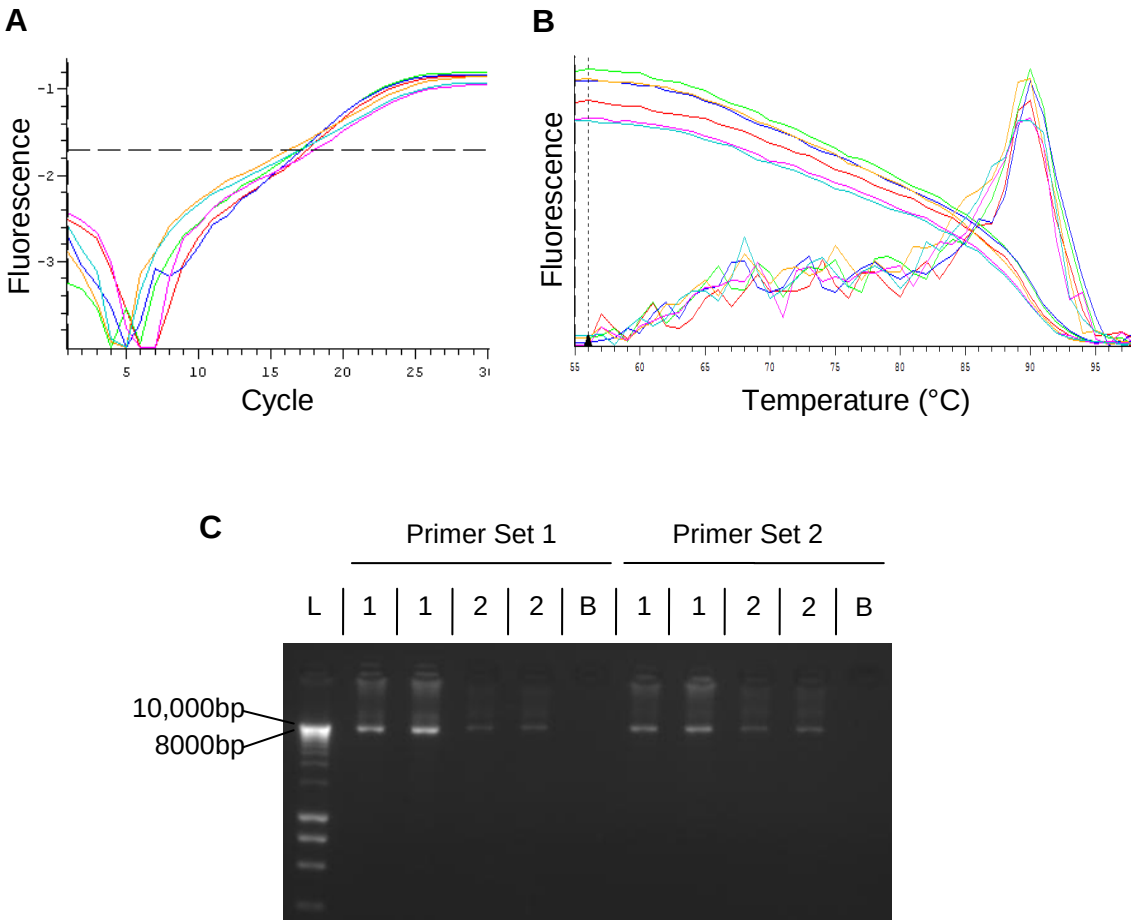

Figure 54. QPCR results with 8.5 kb-product primers. A) The amplification plot for one blue whale and one fin whale sample with the 8.5 kb-product primers. The plot shows the fluorescence versus the qPCR cycle number. Each colour represents a different sample replicate, with each sample performed in triplicate. B) The melt curve showing the fluorescence at different temperatures, and the derivative plot of the melt curve which shows a single peak at approximately 90°C. C) Two out of the three triplicates for each sample were tested for DNA length using gel electrophoresis. HyperLadder 1 (Bioline, UK) was used to determine band sizes, as shown to the left. L: ladder; 1: blue whale; 2: fin whale; B: blank.

Table 6

Sample	Primer Set	Dye Concentration	Average Efficiency	Average Ct Value
Fin Whale	8.5 kb Set 1	0.1x	41%	19.91
		0.075x	40%	20.28

Table 6. QPCR results with different fluorescent dye concentrations. QPCR using a fin whale sample was performed using either 0.1x or 0.075x concentration of SYBR Green dye, with the 8.5 kb primer set 1. Each SYBR Green dye concentration was run in triplicate for each of two qPCR reactions using a Chromo4 machine and Phusion polymerase.

7.4.3 *QPCR optimisation: 4.4 kb sections*

Primers to amplify four mtDNA sections of approximately 4.4 kb each to check the entire 16.4 kb mitochondrial genome for damage were tested, and were again specific for the blue and fin whales only. One blue whale sample and one fin whale sample were used to test the efficiency of the four 4.4 kb-product primers. The whale samples were able to be successfully amplified using these designed primers, as shown in Table 7, with higher qPCR efficiencies than for the 8.5 kb-product primers. To optimise the reaction further and improve the qPCR efficiencies, the primer-annealing temperature was lowered from 60°C to 57°C. This improved the efficiency of the qPCR reaction from approximately 66% to approximately 77% (Table 8), so an annealing temperature of 57°C was used for future experiments.

Potential differences in mtDNA damage were able to be detected at this length, as shown by the variation in Ct values between samples, which are visible in Figure 55A. All four primer sets gave similar values for the same sample. Figure 55B shows the melt curve for the 4.4 kb primer sets 1, 2, and 4, all of which gave a single peak suggesting a single product was generated. However, primer set 3 gave a slight second peak (Figure 55C). To further investigate the primers, gel electrophoresis was performed and the results are shown in Figure 55D. It can be seen that a band of approximately 4.4 kb was generated for each sample with each of the four primer sets. However, primer set 4 showed a second band of lower intensity at approximately 2 kb despite showing a single peak on the melt curve. Because of these factors, primer sets 3 and 4 were chosen not to be continued with to determine mtDNA damage. As differences in damage were able to be detected at this length of approximately 4.4 kb with a high efficiency, this length was continued with.

Table 7

Sample	Primer Set	Average Efficiency	Average Ct Value
Blue Whale	4.4 kb Set 1	76%	16.31
	4.4 kb Set 2	53%	14.57
	4.4 kb Set 3	67%	15.84
	4.4 kb Set 4	79%	16.51
Fin Whale	4.4 kb Set 1	70%	13.91
	4.4 kb Set 2	47%	13.17
	4.4 kb Set 3	68%	13.58
	4.4 kb Set 4	65%	14.28

Table 7. QPCR results with the 4.4 kb-product primers. One blue whale and one fin whale sample were used to test the amplification ability of the 4.4 kb-product primers. Each sample was run in triplicate for each of two qPCR reactions using a Chromo4 machine, Phusion polymerase, and SYBR Green dye with a primer annealing temperature of 60°C, and the average qPCR efficiency and Ct value of the replicates are shown. Blanks showed no amplification product.

Table 8

Sample	Primer Set	Average Efficiency	Average Ct Value
Blue Whale	4.4 kb Set 1	73%	17.55
	4.4 kb Set 2	70%	17.15
	4.4 kb Set 3	73%	17.43
	4.4 kb Set 4	77%	18.45
Fin Whale	4.4 kb Set 1	83%	14.83
	4.4 kb Set 2	75%	15.02
	4.4 kb Set 3	87%	14.90
	4.4 kb Set 4	76%	15.61

Table 8. QPCR results with the 4.4 kb-product primers with a lower primer-annealing temperature. One blue whale and one fin whale sample were used to test the amplification ability of the 4.4 kb-product primers following a reduction in primer-annealing temperature from 60°C to 57°C. Each sample was run in triplicate for each of two qPCR reactions using a Chromo4 machine, Phusion polymerase, and SYBR Green dye with a primer annealing temperature of 57°C. The average qPCR efficiency and Ct value of the replicates are shown. Blanks showed no amplification product.

Figure 55

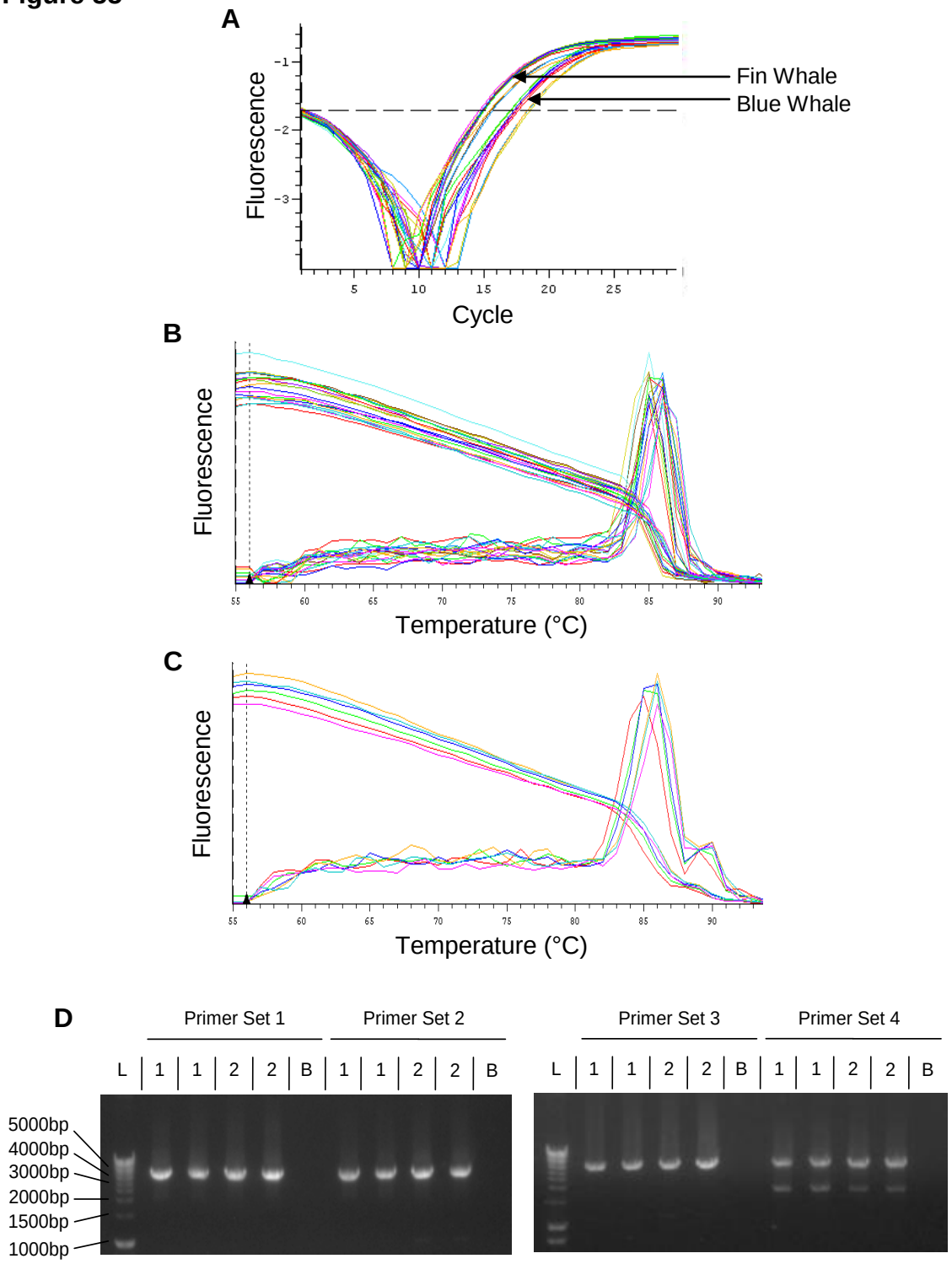

Figure 55. QPCR results with 4.4 kb-product primers. A) The amplification plot for one blue and one fin whale sample with the four 4.4 kb-product primers, showing the fluorescence versus the qPCR cycle number. Each colour represents a different sample replicate, with each sample performed in triplicate. The fin whale sample had a lower level of damage in this example, as it crossed the threshold in a lower number of cycles. B) The melt curve showing the fluorescence at different temperatures for primer sets 1, 2, and 4, with a peak at approximately 86°C. C) The melt curve for primer set 3, with two peaks at approximately 86°C and at 90°C. D) Two out of the three triplicates for each sample were tested for DNA length using gel electrophoresis. HyperLadder 1 was used to determine band sizes, as shown to the left. L: ladder; 1: blue whale; 2: fin whale; B: blank.

7.4.4 *QPCR optimisation: alternative DNA polymerase*

In an attempt to optimise the qPCR reaction further, an alternative enzyme to Phusion DNA polymerase was tested. The enzyme KAPA HiFi DNA polymerase was chosen as this enzyme is thought to have lower error rates than Phusion, to increase the sensitivity of the qPCR (Kapa Biosystems, 2013). The enzyme KAPA HiFi DNA polymerase was tested with a blue whale sample using the 4.4 kb-product primer set 1. However, with this enzyme, the efficiencies were much lower and the Ct values much higher than with Phusion polymerase (Table 9), suggesting less efficient product formation. Further analysis by gel electrophoresis showed a strong band at approximately 4.4 kb for the Phusion enzyme, but a low intensity band with the KAPA HiFi polymerase (Figure 56). As Phusion DNA polymerase provided the most efficient results, this enzyme was used in all further experiments.

Table 9

DNA Polymerase	Sample	Primer Set	Average Efficiency	Average Ct Value
Phusion DNA Polymerase	Blue Whale	4.4 kb Set 1	58%	18.00
KAPA HiFi Polymerase			37%	22.17

Table 9. QPCR results with the 4.4 kb-product primers and different DNA polymerases. QPCR using a blue whale sample was performed using either Phusion DNA polymerase or KAPA HiFi polymerase with the 4.4 kb-product primer set 1. Each polymerase was run in triplicate for each of two qPCR reactions using a Chromo4 machine and SYBR Green dye.

Figure 56

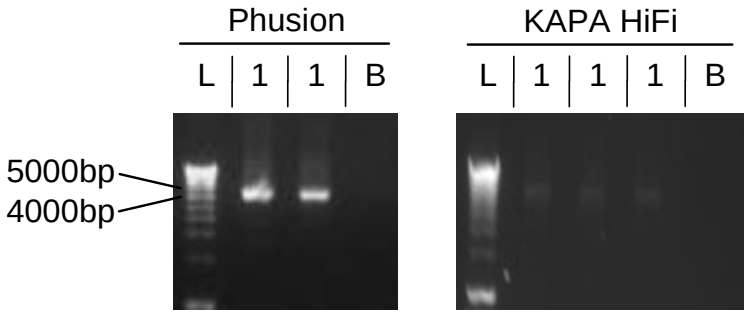

Figure 56. Gel electrophoresis with Phusion polymerase or KAPA HiFi DNA polymerase. The product lengths of the 4.4 kb-product primer set 1 qPCR reaction with a blue whale sample and different polymerases were tested using gel electrophoresis. Two out of three replicates were tested for the Phusion DNA polymerase. All three replicates were tested for the KAPA HiFi polymerase. HyperLadder 1 was used to determine band sizes, as shown to the left. L: ladder; 1: blue whale; B: blank.

7.4.5 *QPCR optimisation: alternative fluorescent dye*

An alternative fluorescent dye to SYBR Green was tested with the 4.4 kb-product primers to determine whether the reaction could be made more sensitive to double-stranded DNA detection. EvaGreen dye (Biotium, UK) was chosen to test as this dye is more stable in storage so will not degrade as quickly as SYBR Green (Khan *et al.*, 2011), which may be less effective if degraded. Various concentrations of the dye were tested with a blue whale sample and the 4.4 kb-product primer set 4, with the qPCR reaction run simultaneously with SYBR Green dye at its chosen optimised concentration. SYBR Green was used at a final concentration of 0.1x, and as EvaGreen is less inhibitory towards qPCR as it degrades more slowly than SYBR Green, it was used at higher concentrations of 0.4x, 0.7x, and 1x. As can be seen in Table 10, the efficiency of the reaction was higher with 0.4x EvaGreen dye compared to 0.1x SYBR Green dye, despite the higher average Ct value which would imply that EvaGreen has a weaker fluorescent signal. Although increasing concentrations of EvaGreen reduced the Ct value (due to more dye and a brighter fluorescent signal), it also reduced the efficiency of the reaction. It was expected that increasing the dye concentration further may provide a more detectable signal but may also reduce the reaction efficiency. Gel electrophoresis revealed a strong band at approximately 4.4 kb for SYBR Green dye and a weak band at approximately 4.4 kb for EvaGreen dye (Figure 57). Therefore, this dye was not used to replace SYBR Green. This reaction also confirmed that the 4.4 kb-product primer set 4 is not suitable for use in the strand break assay, as this primer set produced an additional brighter band between 1.5 kb and 2 kb.

Table 10

Fluorescent Dye	Sample	Primer Set	Average Efficiency	Average Ct Value
0.1x SYBR Green	Blue Whale	4.4 kb Set 4	60%	16.77
0.4x EvaGreen			82%	19.66
0.7x EvaGreen			61%	18.19
1x EvaGreen			49%	17.48

Table 10. QPCR results with the 4.4 kb-product primers and different fluorescent dyes. QPCR using a blue whale sample was performed using various concentrations of EvaGreen dye, with the previously optimised concentration of SYBR Green for comparison. Phusion DNA polymerase was used with the 4.4 kb-product primer set 4, and each concentration was run in triplicate for two qPCR reactions using a Chromo4 machine.

Figure 57

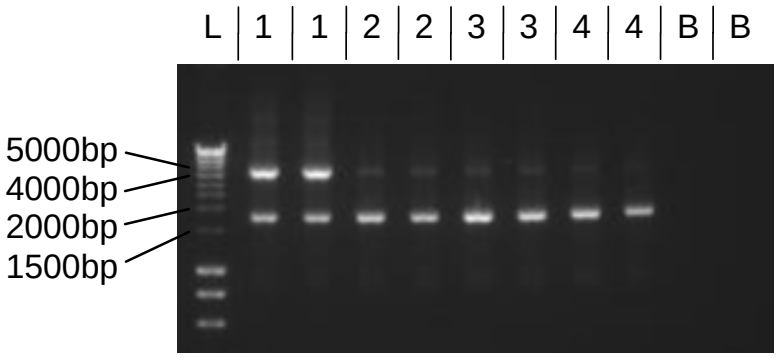

Figure 57. Gel electrophoresis with different fluorescent dyes and concentrations. The products of the 4.4 kb-product primer set 4 qPCR reactions with a blue whale sample and different dye concentrations were tested using gel electrophoresis. Two out of three replicates were tested for 0.1x SYBR Green, 0.4x EvaGreen, 0.7x EvaGreen, and 1x EvaGreen. HyperLadder 1 was used to determine band sizes, as shown to the left. L: ladder; 1: 0.1x SYBR Green; 2: 0.4x EvaGreen; 3: 0.7x EvaGreen; 4: 1x EvaGreen; B: blank.

The 4.4 kb-product primers were also tested with multiple other blue whale and fin whale samples for primer sets 1 and 2, which were able to be successfully amplified. This suggests that the length of 4.4 kb and the optimised conditions could be taken further and used to study mtDNA damage levels within and between different whale species, and to determine any correlations between genetic damage and UV exposure.

7.4.6 *QPCR optimisation: 4.3 kb section*

Based on the successful optimisation of the qPCR assay to amplify and detect differences in damage between the mtDNA of blue and fin whale samples, skin samples from an additional species, the sperm whale, were acquired. As the previously designed 4.4 kb-product primers could not bind with 100% specificity to the sperm whale mtDNA, alternative primers capable of binding to all three species were designed, to allow simultaneous analysis in a qPCR reaction. The 4.4 kb-product primer sets all showed similar Ct values within each sample, indicating that the mtDNA had similar levels of damage throughout the genome and there was not one region of the genome that was preferentially damaged. Therefore, only one region was chosen to be designed to bind to all three species with 100% specificity. The designed primer set to amplify a region of approximately 4.3 kb appeared to be successful in amplifying blue whale, fin whale, and sperm whale mtDNA, simultaneously in a single qPCR reaction with high qPCR efficiencies (Table 11 and Figure 58A). A single peak was also generated for all three samples on a melt curve (Figure 58B) and a single gel electrophoresis product of the correct length (Figure 58C).

Table 11

Sample	Primer Set	Average Efficiency	Average Ct Value
Blue Whale	4.3 kb	89%	13.62
Fin Whale		84%	16.87
Sperm Whale 1		84%	16.00
Sperm Whale 2		96%	13.98

Table 11. QPCR results with the 4.3 kb-product primers. One blue whale, one fin whale, and two sperm whale samples were used to test the amplification ability of the universal 4.3 kb-product primers. Each sample was run in triplicate for two qPCR reactions using a Chromo4 machine, Phusion polymerase, and SYBR Green dye with a primer annealing temperature of 57°C. The average qPCR efficiency and Ct values of the replicates are shown. Blanks showed no amplification product.

Figure 58

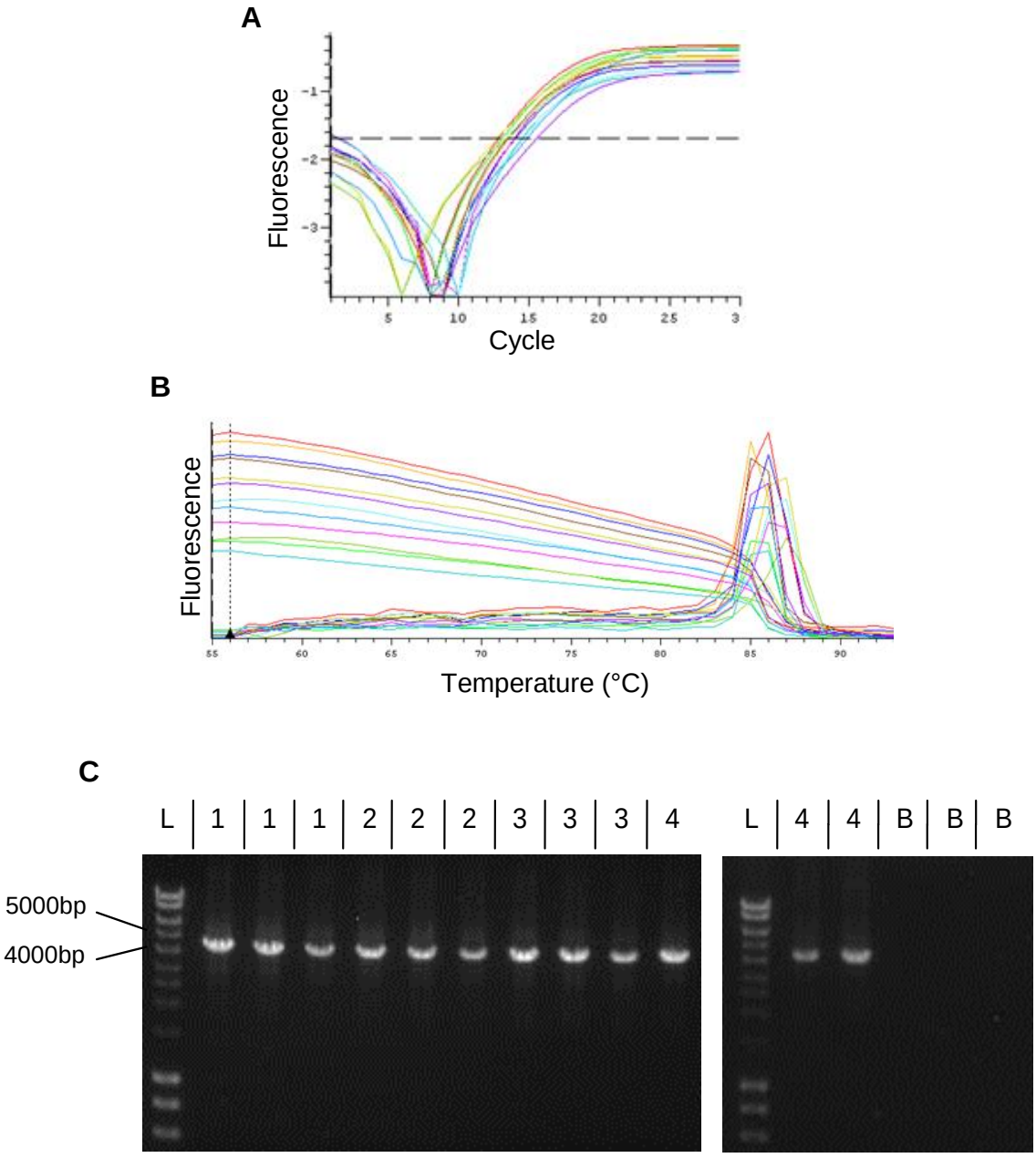

Figure 58. QPCR results with the 4.3 kb-product primer set. A) The amplification plot of one blue whale, one fin whale, and two sperm whale samples with the 4.3 kb-product primer set, showing the fluorescence versus the qPCR cycle number. Each colour represents a different sample replicate, with each sample performed in triplicate. B) The melt curve showing the fluorescence at different temperatures with a peak at approximately 86°C. C) All three triplicates for each sample were tested for DNA length using gel electrophoresis. HyperLadder 1 was used to determine band sizes, as shown to the left. L: ladder; 1: sperm whale 1; 2: sperm whale 2; 3: fin whale; 4: blue whale; B: blank.

To confirm the ability of these 4.3 kb-product primers to detect differences in mtDNA damage between samples, the Ct values obtained using the 4.4 kb-product primer set 1 and the universal 4.3 kb-product set were compared using two representative blue whale and fin whale samples. The results showed that both primer sets gave similar levels of damage for each sample, with those samples with higher Ct values for the 4.4 kb-product set also showing higher Ct values with the universal 4.3 kb-product set (Table 12). These two primer sets were also tested using two different qPCR machines (a Chromo4 machine for the 4.4 kb-product primer set, and a StepOnePlus machine for the 4.3 kb-product primer set), showing the reproducibility of the assay across multiple qPCR machines.

Table 12

Sample	Primer Set	Average Ct Value
Blue Whale 1	4.4 kb Set 1	13.83
	4.3 kb	13.94
Blue Whale 2	4.4 kb Set 1	15.83
	4.3 kb	15.85
Fin Whale 1	4.4 kb Set 1	15.43
	4.3 kb	15.27
Fin Whale 2	4.4 kb Set 1	15.84
	4.3 kb	15.70

Table 12. QPCR results with the 4.3 kb-product and 4.4 kb-product primers. Two blue whale and two fin whale samples were used to compare the Ct values received for the universal 4.3 kb-product primers and the 4.4 kb-product primers. Each sample was run in triplicate for two qPCR reactions using either a Chromo4 machine (for the 4.4 kb-product primers) or a StepOnePlus machine (for the 4.3 kb-product primers), using Phusion polymerase, SYBR Green, and a primer annealing temperature of 57°C. The average Ct values of the replicates are shown. Blanks showed no amplification product.

The concentration of mtDNA to be used in future qPCR assays to determine mtDNA damage was chosen based on results from a concentration curve for the 4.3 kb-product primers (Figure 59). Results showed that the reaction was linear from 25 ng to 200 ng (for every 2-fold increase in concentration there is expected to be a Ct decrease of 1); therefore, a concentration of 100 ng was

chosen for analysis based upon linearity of the concentration curve and the availability of DNA material.

Figure 59

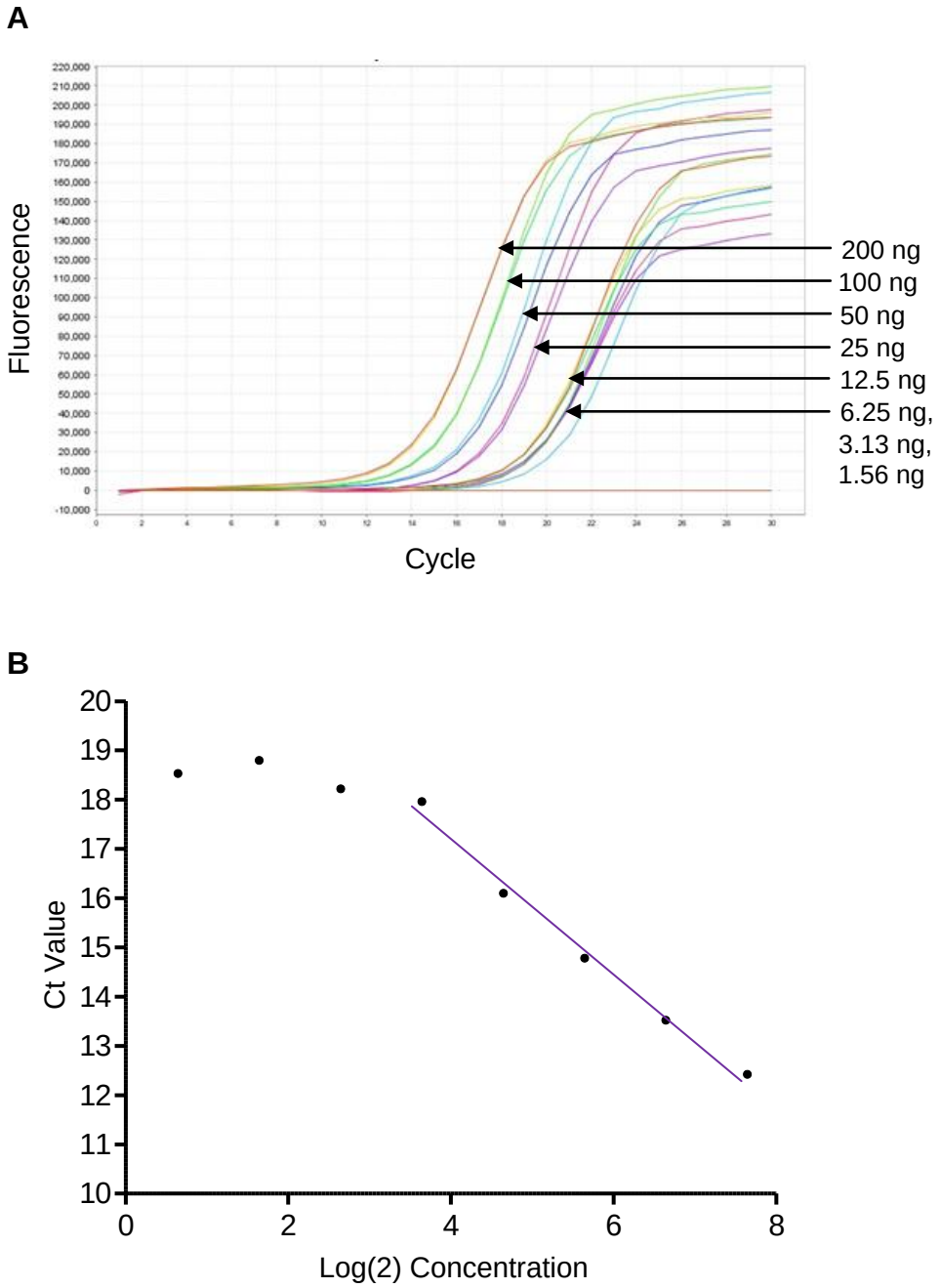

Figure 59. QPCR dilution curve for the 4.3 kb-product primers. A sperm whale sample was used to determine the optimum concentration for qPCR with the 4.3 kb-product primers, with the concentrations of 200 ng, 100 ng, 50 ng, 25 ng, 12.5 ng, 6.25 ng, 3.13 ng, and 1.56 ng used. A) The amplification plot for each concentration. B) Individual Ct values were plotted for the log(2) of each concentration, as each 2-fold increase in concentration should decrease the Ct value by 1. The reaction was linear from 25 ng to 200 ng, as indicated by the purple line. Each sample was run in duplicate for two qPCR reactions using a StepOnePlus machine, Phusion polymerase, SYBR Green, and a primer annealing temperature of 57°C.

7.4.7 *MtDNA relative copy number*

DNA extracted from whale skin samples contained both nDNA and mtDNA, as the DNA extraction technique used was not specific for either DNA type. Therefore, measurements of DNA concentrations to be used in the qPCR assays represented the total amount of nucleic acid present rather than the mtDNA concentration alone. It was therefore important to find the relative copy number of each sample to ensure that an approximately equal amount of mtDNA was added to the 4.3 kb-product primer assays for all samples. To do this, a short region of below 200 bp is amplified by qPCR and the Ct determined; from this the relative mtDNA copy number is found and the total amount of DNA added to the long qPCR altered accordingly. This approach uses the same principle as has been used previously in humans to determine the relative mtDNA copy number whereby a region of 83 bp is amplified (Koch *et al.*, 2001; Swalwell *et al.*, 2012). A set of primers to amplify a region of 51 bp were designed through this study to be specific for all three whale species used. If the samples have similar Ct values when amplified by qPCR using this short region, it ensures that they contain similar amounts of mtDNA, as this short region of mtDNA is unlikely to contain high levels of damage (Koch *et al.*, 2001; Hunter *et al.*, 2010). A higher Ct represents a lower mtDNA copy number, as a higher number of cycles are required for amplification. If this were the case, more of this sample would have to be added to the 4.3 kb-product reaction to ensure an equal mtDNA amount. To test the designed primers, a concentration curve using a sperm whale sample was performed to ensure that for each 2-fold increase in DNA added to the reaction, there was a Ct decrease of 1, and to determine an appropriate concentration to be used. The results in Figure 60A show that these primers were suitable for determining the relative amount of mtDNA in the whale samples, and as the reaction was linear from 1.56 ng to 200 ng (Figure 60B), a concentration of 50 ng was chosen for future 51 bp assays.

The relative copy number qPCR was performed with the 51 bp-product primers for the 15 blue whale, 10 fin whale, and 18 sperm whale samples to be used for the 4.3 kb assay. All of the Ct values were very similar (within 1 Ct of the average), suggesting a similar level of mtDNA per 50 ng of total DNA in each sample. As the Ct values were very close, the concentration added to the later

4.3 kb qPCR reactions was not altered (Berdal and Holst-Jensen, 2001; Niemitz *et al.*, 2004; Mraz *et al.*, 2009). Single peaks were also seen on the melt curves suggesting the formation of a single product.

Figure 60

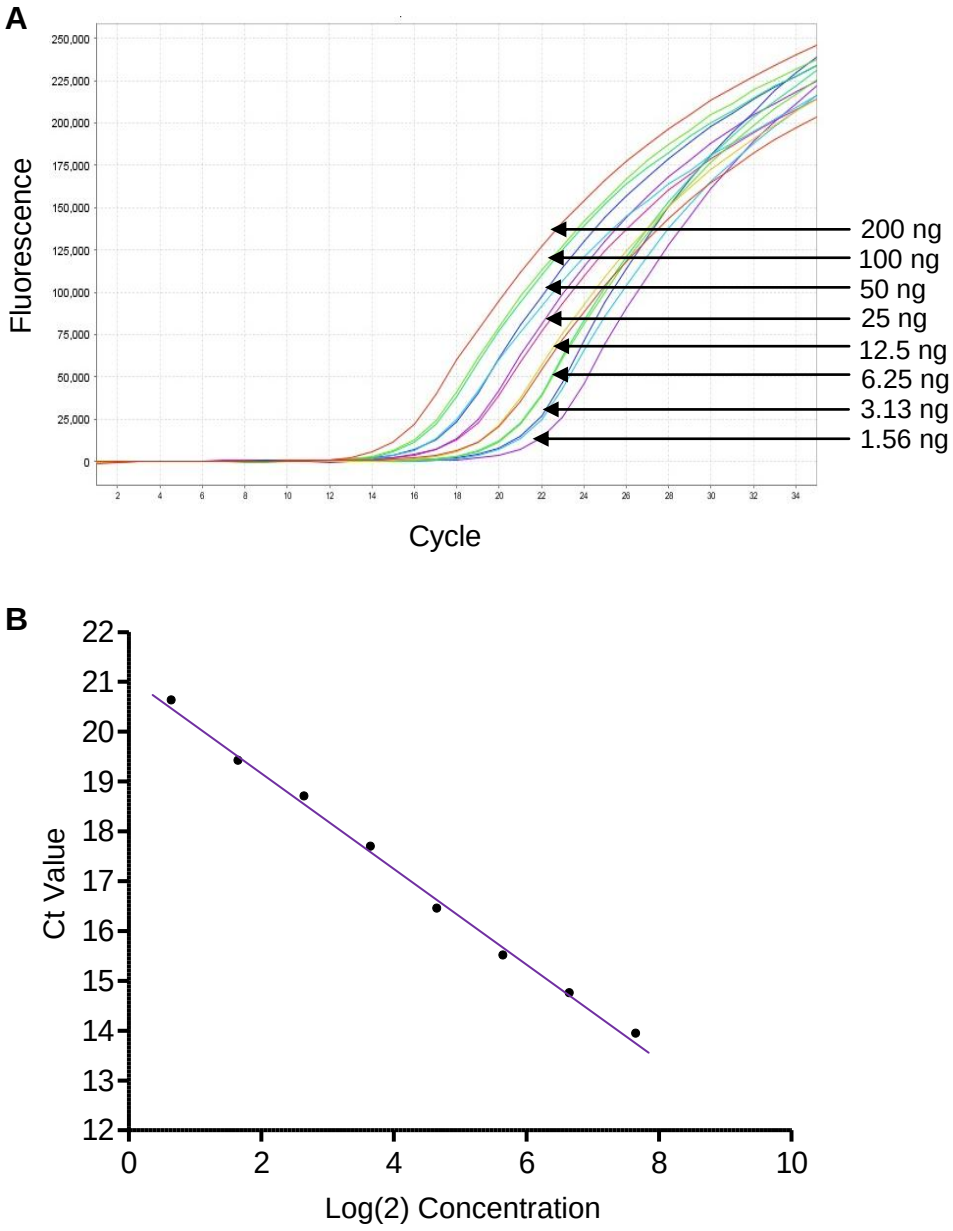

Figure 60. QPCR dilution curve for the 51 bp-product primers. One sperm whale sample was used to determine the optimum concentration for qPCR with the 51 bp-product primers, with the concentrations of 200 ng, 100 ng, 50 ng, 25 ng, 12.5 ng, 6.25 ng, 3.13 ng, and 1.56 ng used. A) The amplification plot for each concentration. B) Individual Ct values were plotted for the log(2) of each concentration, as each 2-fold increase in concentration should decrease the Ct value by 1. The reaction was linear from 1.56 ng to 200 ng, as indicated by the purple line. Each sample was run in duplicate for two qPCR reactions using a StepOnePlus machine, Phusion polymerase, SYBR Green, and a primer annealing temperature of 60°C.

7.4.8 *MtDNA damage levels within three whale species*

Once it was determined that the samples contained similar mtDNA amounts per total DNA concentration, 15 blue whale, 10 fin whale, and 18 sperm whale samples were assayed with the 4.3 kb-product primers using the previously established optimal conditions, to determine their individual levels of mtDNA damage. Figure 61 shows the results for each individual sample of the three species used, with the average raw Ct values given. It was not possible to acquire a completely undamaged sample of whale skin for use as an undamaged control; therefore the sample with the lowest level of mtDNA damage was used as a representative for an undamaged control, to compare any increases in damage (Durham *et al.*, 2003; Harbottle and Birch-Machin, 2006; Hunter *et al.*, 2010). A significantly higher level of damage was found in the majority of samples compared to the undamaged control for each species ($P<0.0001$, one-way ANOVA with Dunnett's test). This difference in damage observed between whale skin samples would be even more pronounced if the absolute fold difference in damage were to be plotted, as each 1 Ct difference from the control represents a 2-fold increase in damage. For example, the Ct difference of 5.04 between Bm754 and Bm675 actually represents a difference in damage of 32.90 ($2^{5.04}$), where Bm675 has approximately 33-fold higher damage. Results were not plotted in this manner as using this method would give bias to those samples which were much higher than the undamaged control, and make any possible differences in the less damaged samples harder to detect. For example, using the blue whale species, it was found that significant differences were present between 8 of the samples compared to the lowest sample when the fold difference in damage was plotted (Figure 62A). However, if the most highly damaged sample were to be removed (sample Bm675), 2 more of the samples become significant (Bm690 and Bm753), and the level of significance rises in others (Bm663, Bm701, Bm716, and Bm731) (Figure 62B). Therefore, the plotting of fold differences directly could alter the results if there is a massively damaged sample present within a species. If the most damaged sample were to be removed from the graph which shows the Ct value rather than the fold difference, all of the samples retain the same significance. MtDNA damage was therefore expressed as raw Ct values in this project, as used previously when examining differences in mtDNA damage (Sood *et al.*, 2011).

Figure 61

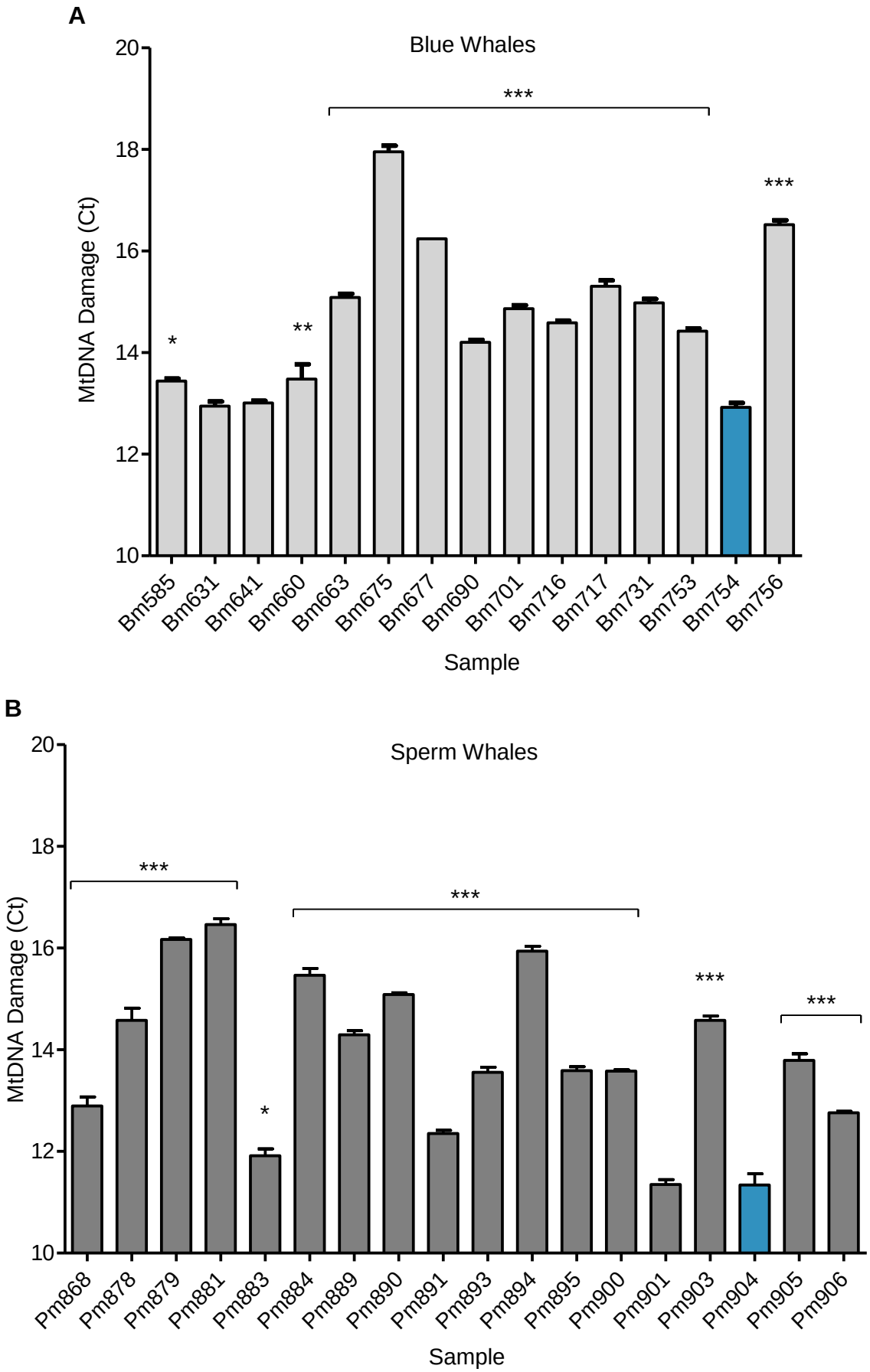
A
Blue Whales
MtDNA Damage (Ct)
20
18
16
14
12
10
***
*
**
***
Bm585
Bm631
Bm641
Bm660
Bm663
Bm675
Bm677
Bm690
Bm701
Bm716
Bm717
Bm731
Bm753
Bm754
Bm756
Sample
B
Sperm Whales
MtDNA Damage (Ct)
20
18
16
14
12
10
***
***
*
***
***
Pm868
Pm878
Pm879
Pm881
Pm883
Pm884
Pm889
Pm890
Pm891
Pm893
Pm894
Pm895
Pm900
Pm901
Pm903
Pm904
Pm905
Pm906
Sample

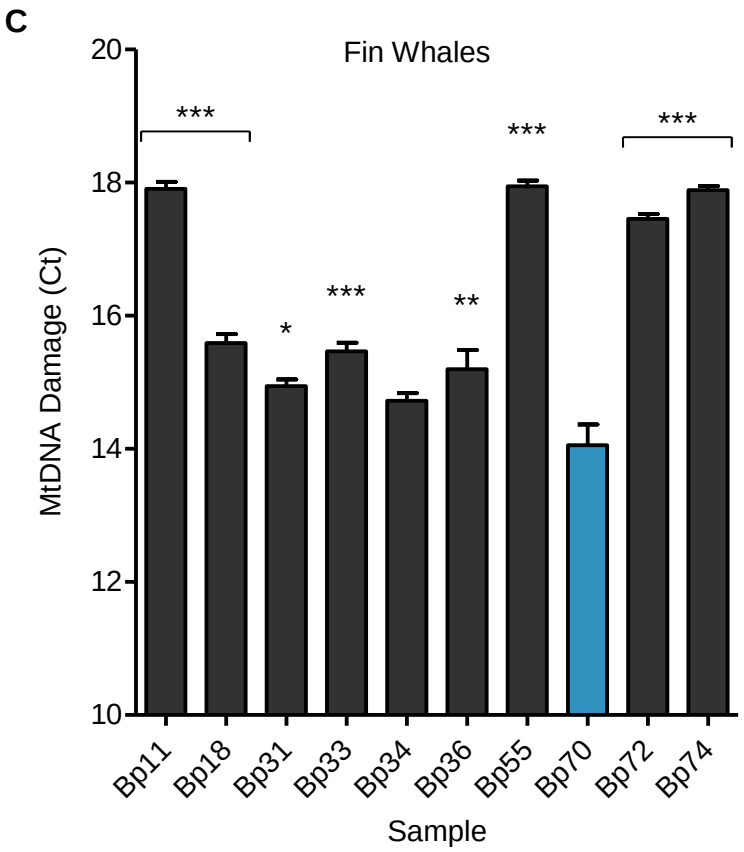

Figure 61. Graphical representation of mtDNA damage in three whale species. A) The qPCR results for the 4.3 kb-product primer set with samples from 15 blue whales. B) The qPCR results for the 4.3 kb-product primer set with samples from 18 sperm whales. C) The qPCR results for the 4.3 kb-product primer set for 10 fin whales. Each bar represents the average from at least two qPCR repeats each performed in triplicate. The Ct values show the level of mtDNA damage, and the blue bars show the least damaged sample for each species, which was used as a control to perform the statistical analysis. The error bars show the SEM. Significant differences in mtDNA damage were observed in all three species compared to the control for each ($P<0.05$*, $P<0.01$**, $P<0.0001$***, one-way ANOVA with Dunnett's test).

Figure 62

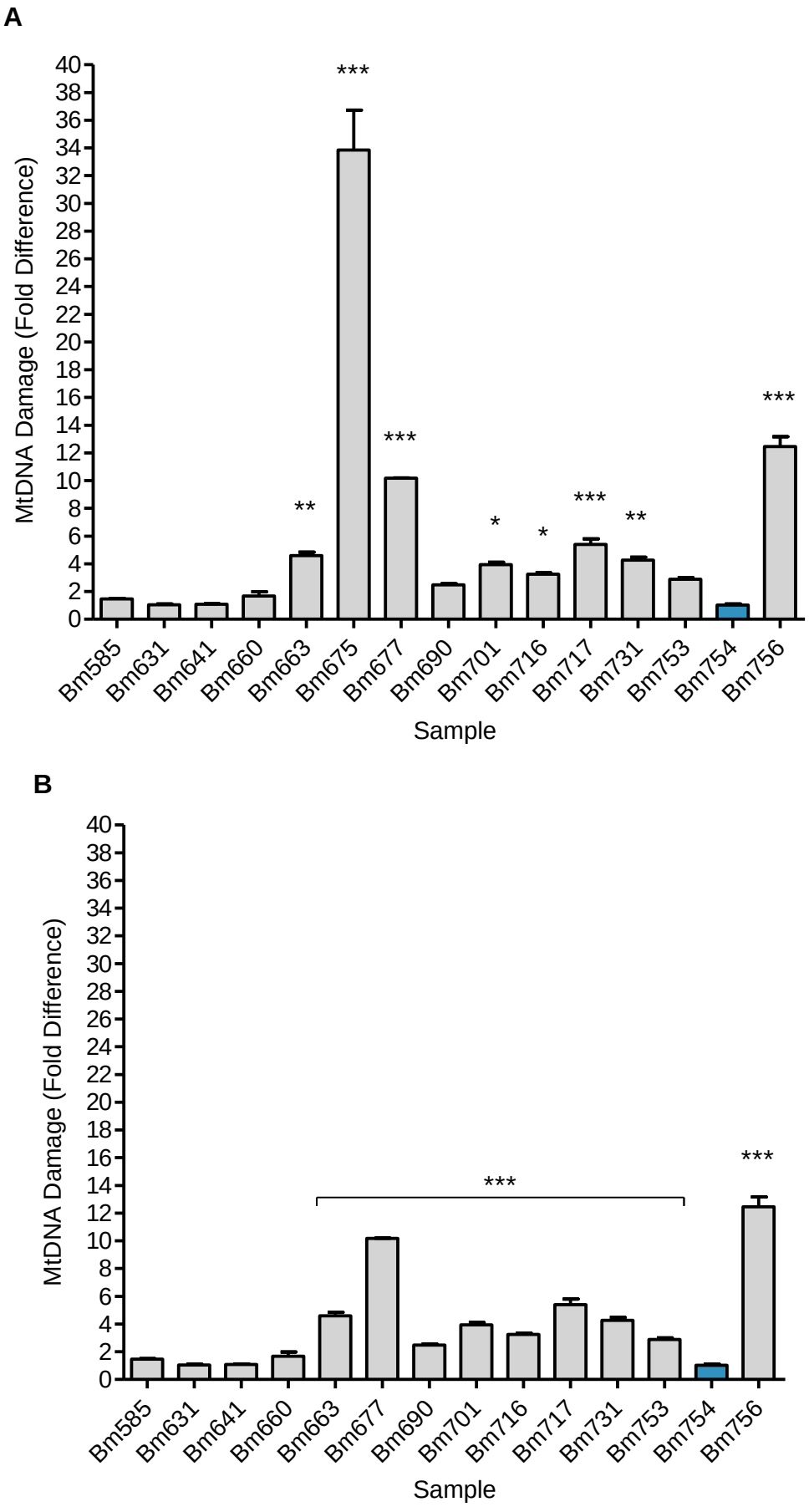
A
MtDNA Damage (Fold Difference)
Sample
Bm585
Bm631
Bm641
Bm660
Bm663
Bm675
Bm677
Bm690
Bm701
Bm716
Bm717
Bm731
Bm753
Bm754
Bm756
B
MtDNA Damage (Fold Difference)
Sample

Figure 62. Graphical representation of the fold difference in mtDNA damage for blue whale samples. A) The qPCR results for the 4.3 kb-product primer set with samples from 15 blue whales, showing the fold difference in damage compared to the least damaged sample, which is represented by the blue bar. B) The qPCR results for the 4.3 kb-product primer set with samples from 15 blue whales showing the fold difference in damage compared to the least damaged sample, represented by the blue bar. The sample showing an extremely high level fold difference in damage (sample Bm675) was removed from this graph to demonstrate its bias in reducing the significance of several of the other samples. The fold difference in damage was determined by finding the difference from the least damaged sample, and performing 2 to the power of this value. The error bars show the SEM. Significant differences in mtDNA damage were observed compared to the control sample ($P<0.05$*, $P<0.01$**, $P<0.0001$***, one-way ANOVA with Dunnett's test).

7.4.9 *MtDNA damage correlation with other markers of UV damage*

The principle of the 4 kb-product primer assay to detect UV-induced mtDNA damage has been demonstrated previously in humans (Birch-Machin *et al.*, 1998; Ayala-Torres *et al.*, 2000; Ray *et al.*, 2000; Durham *et al.*, 2003; Santos *et al.*, 2006; Swalwell *et al.*, 2012), as well as in the present project (Chapter 6). To confirm that the mtDNA damage observed in whale skin was likely to be due to UV damage instead of other factors, the mtDNA damage was correlated with other known markers of UV damage, namely the presence or absence of micro-vesicles, or the presence or absence of apoptosis. Micro-vesicles are a morphological change in response to acute sun damage (Ulrich *et al.*, 2009; Martinez-Levasseur *et al.*, 2011). The presence of micro-vesicles correlated significantly with mtDNA damage, suggesting that those whales with micro-vesicles present have increased mtDNA damage (Figure 63A) ($P=0.0047$, unpaired t-test). Apoptosis is increased in response to UV exposure to remove damage (Yamaguchi *et al.*, 2008), which is the method by which the body removes damaged cells, and is thought to be a protective mechanism against potentially carcinogenic cells (Yamaguchi *et al.*, 2008). Apoptosis levels correlated inversely with mtDNA damage in those whale samples for which information was available (Figure 63B) ($P=0.0495$, unpaired t-test). This suggests that those whales with apoptosis present have lower mtDNA damage levels. These correlations further confirm the effectiveness of the qPCR method used in this study in detecting damage principally caused by UV.

Figure 63

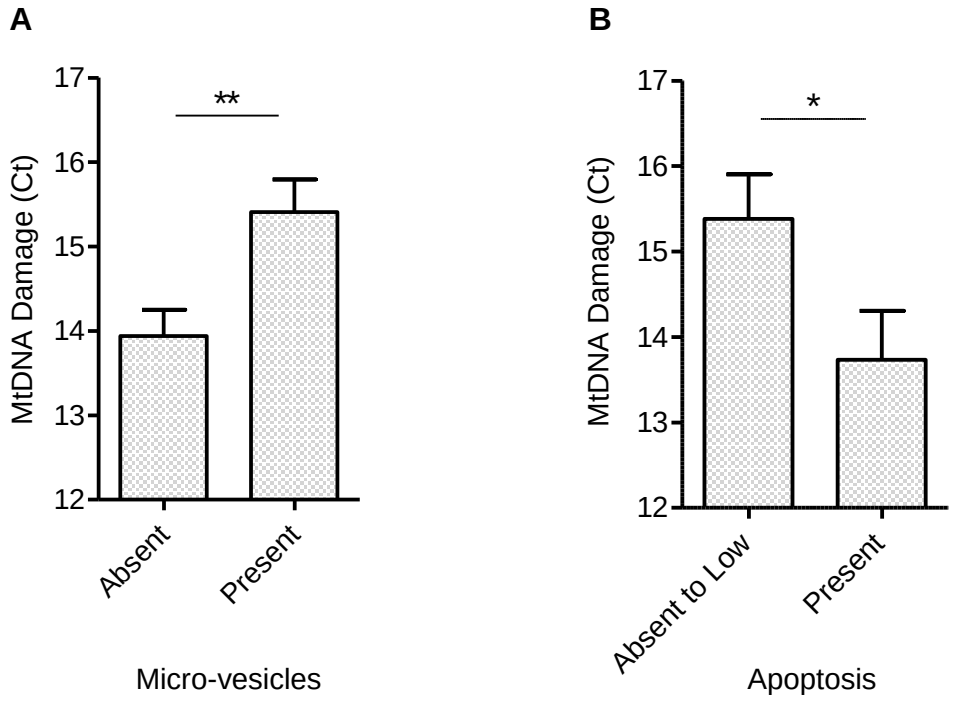

Figure 63. MtDNA damage of whales compared to the presence or absence of micro-vesicles or apoptosis. A) The qPCR results for mtDNA damage with the 4.3 kb-product primer set compared to the presence or absence of micro-vesicles, for 15 blue whale, 10 fin whale, and 17 sperm whale samples. A significantly higher level of mtDNA damage was observed for samples with micro-vesicles present (P=0.0047**, unpaired t-test). B) The qPCR results for mtDNA damage with the 4.3 kb-product primer set compared to the absence or presence of apoptosis, for 5 blue whale, 2 fin whale, and 11 sperm whale samples. A significantly lower level of mtDNA damage was observed for samples with apoptosis present (P=0.0495*, unpaired t-test). The error bars show the SEM. The averages of at least two qPCR reactions each performed in triplicate were used for each sample.

7.4.10 *MtDNA damage levels between different whale species*

The average mtDNA damage level for each species was compared to determine whether differences in damage were present between different species, to see if certain characteristics can affect the level of mtDNA damage within their skin. No significant differences in average mtDNA damage were seen for the blue whales versus the sperm whales, or the blue whales versus the fin whales (Figure 64A) ($P>0.05$, one-way ANOVA with Bonferroni correction). However, the fin whales showed a significantly higher level of mtDNA damage than the sperm whales (Figure 64A) ($P<0.01$, one-way ANOVA with Bonferroni correction). This was despite the fact that the fin whale samples used had significantly higher skin pigmentation than the blue whales and sperm whales (Figure 64B) ($P<0.01$, one-way ANOVA with Bonferroni correction), and so may have been expected to have less damage. The level of micro-vesicles was found to be significantly lower in the sperm whales compared to the blue whales and fin whales (Figure 64C) ($P<0.0001$, one-way ANOVA with Bonferroni correction), and the level of apoptosis was found to be significantly lower in the blue whales and fin whales compared to the sperm whales (Figure 64D) ($P<0.01$ for the blue whales and $P<0.05$ for the fin whales, one-way ANOVA with Bonferroni correction). These results implied that the sperm whales, which had significantly lower mtDNA damage than the fin whales, had the lowest level of micro-vesicles and the highest level of apoptosis.

Figure 64

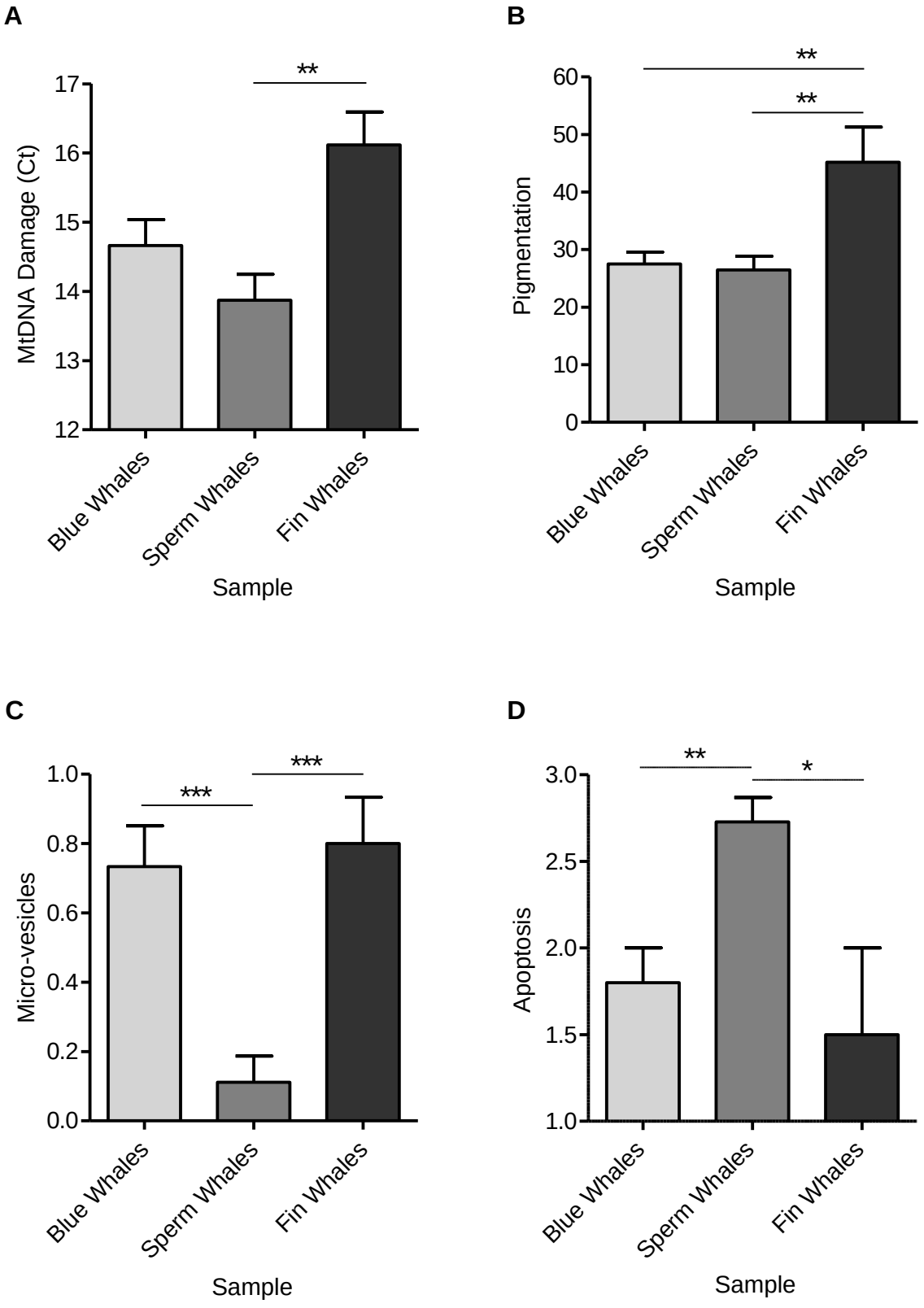
A
MtDNA Damage (Ct)
17
16
15
14
13
12
**
Blue Whales
Sperm Whales
Fin Whales
Sample
B
Pigmentation
60
50
40
30
20
10
0
**
**
Blue Whales
Sperm Whales
Fin Whales
Sample
C
Micro-vesicles
1.0
0.8
0.6
0.4
0.2
0.0
***
***
Blue Whales
Sperm Whales
Fin Whales
Sample
D
Apoptosis
3.0
2.5
2.0
1.5
1.0
**
*
Blue Whales
Sperm Whales
Fin Whales
Sample

Figure 64. Differences in mtDNA damage, pigmentation, micro-vesicles, and apoptosis between three different whale species. A) The qPCR results for the 4.3 kb-product primers to determine mtDNA damage (expressed in Ct) for 15 blue whale, 18 sperm whale, and 10 fin whale samples. There was a significantly higher level of mtDNA damage in the fin whales compared to the sperm whales (P<0.01**, one-way ANOVA with Bonferroni correction). The averages of at least two qPCR reactions each performed in triplicate were used for each sample. B) The average level of pigmentation for each species for 15 blue whale, 15 sperm whale, and 10 fin whale samples. There was a significantly higher level of pigmentation in the fin whale samples compared to the blue whale samples and the sperm whale samples (P<0.01**, one-way ANOVA with Bonferroni correction). C) The presence or absence of micro-vesicles for each species for 15 blue whale, 18 sperm whale, and 10 fin whale samples. There was a significantly lower level of micro-vesicles in the sperm whales compared to the blue whales and the fin whales (P<0.0001***, one-way ANOVA with Bonferroni correction). The presence of micro-vesicles was represented by 1, and the absence as 0. D) The presence or absence of apoptosis for each species for 5 blue whale, 11 sperm whale, and 2 fin whale samples. There was a significantly higher level of apoptosis in the sperm whales compared to the blue whales (P<0.01**, one-way ANOVA with Bonferroni correction) and fin whales (P<0.05*, one-way ANOVA with Bonferroni correction). The level of apoptosis was scaled from 0 to 3, with 0 to 2 absent to a few apoptotic cells, and 3 being high levels and widely distributed, as done previously (Martinez-Levasseur *et al.*, 2011). The error bars show the SEM.

7.4.11 *MtDNA damage and Hsp70*

The family of heat shock proteins known as Hsp70 are proteins whose expression is induced in response to cellular stressors such as heat shock, infrared radiation and UV radiation (De la Coba *et al.*, 2009). The level of Hsp70 was compared to the level of mtDNA damage in those samples for which information was available, to determine whether the heat shock response is associated with higher or lower levels of mtDNA damage. Figure 65 shows the results for 3 blue whale, 6 fin whale, and 15 sperm whale samples, and as can be seen the level of mtDNA damage was significantly lower in those samples with higher Hsp70 expression (P=0.0063, rho=0.5524, non-parametric Spearman correlation). The level of Hsp70 expression was also compared between the three species, and it was found that although non-significant, the sperm whales had a trend towards a higher level of Hsp70 (Figure 66) (P=0.0690, one-way ANOVA with Bonferroni correction). This may have not been significant due to the low number of blue and fin whale samples available for analysis, as when only the fin and sperm whales were taken into account there was a significant difference between the two species (P=0.0463, unpaired t-test).

Figure 65

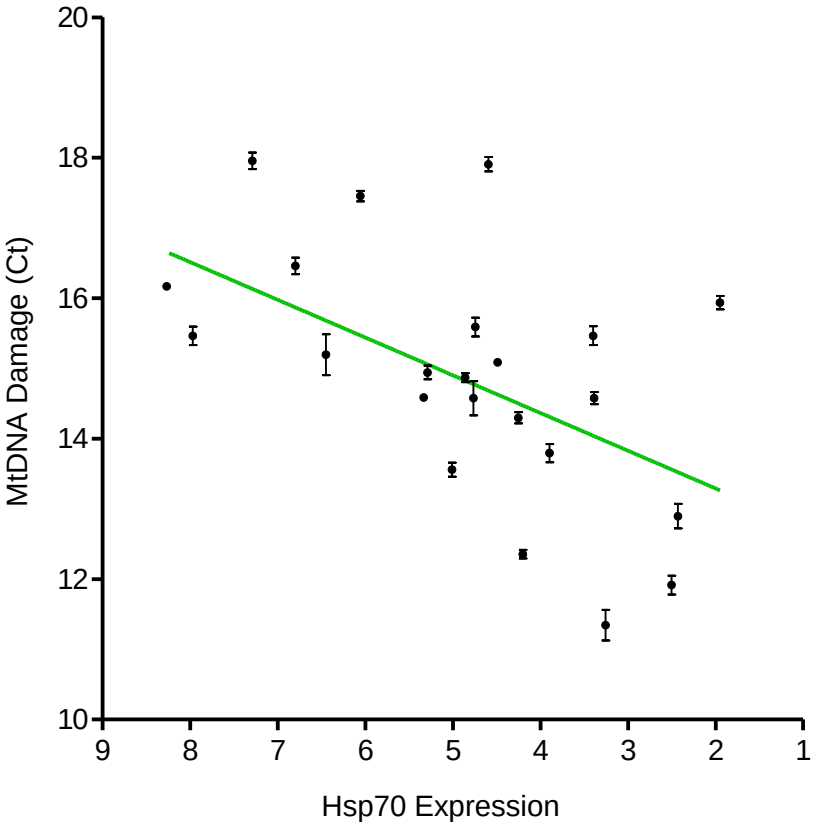

Figure 65. Individual mtDNA damage compared to Hsp70 level. The mtDNA damage (Ct) as determined using the 4.3 kb-product primers was compared to the Hsp70 level for individual whales, for 3 blue whale, 14 sperm whale, and 6 fin whale samples. There was a significant inverse correlation between the level of mtDNA damage and the level of Hsp70 expression (P=0.0063, rho=0.5524, non-parametric Spearman correlation). Hsp70 is given as ΔCt (sample Ct difference from the control), and lower values represent higher levels of expression due to lower Ct values representing higher expression. The green line shows the line of best fit. The error bars show the SEM. At least two qPCR reactions each in triplicate were performed for each sample.

Figure 66

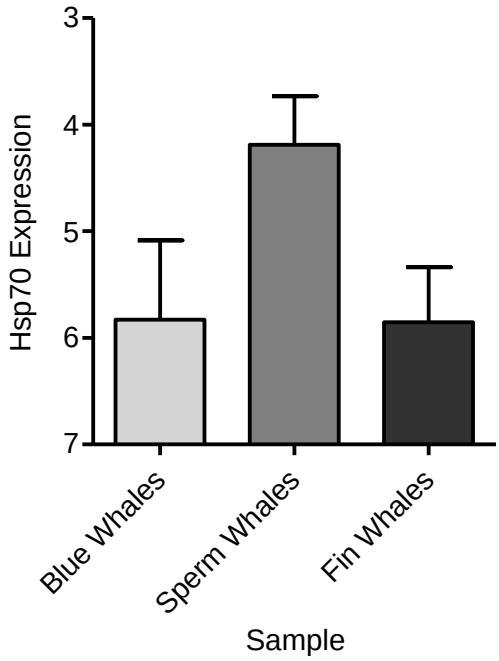

Figure 66. Differences in Hsp70 expression in three different whale species. The Hsp70 level for 3 blue whale, 14 sperm whale, and 6 fin whale samples. There was no significant difference in damage between the three samples (P=0.0690, one-way ANOVA with Bonferroni correction), but the sperm whales were trending towards higher damage. When only the fin and sperm whales were analysed, there was a significant difference in damage (P=0.0463, unpaired t-test). Hsp70 is given as ΔCt, and lower values represent higher levels of damage. The error bars show the SEM.

7.4.12 *MtDNA damage and pigmentation*

The level of mtDNA damage did not correlate with the level of pigmentation present when individual samples from all three species were viewed simultaneously (Figure 67A) (P=0.7633, rho=0.0492, non-parametric Spearman correlation). However, the level of mtDNA damage did correlate with pigmentation when compared within the blue whales alone. Taken as an individual species, the blue whales showed a significant inverse correlation between the level of pigmentation and mtDNA damage (Figure 67B) (P=0.0148, rho=-0.6143, non-parametric Spearman correlation). This was not the case for the sperm whales (Figure 67C) (P=0.9698, rho=0.0107, non-parametric Spearman correlation) or the fin whales (Figure 67D) (P=0.5135, rho=0.2364, non-parametric Spearman correlation), which showed no correlation between individual pigmentation level and individual mtDNA damage.

Figure 67

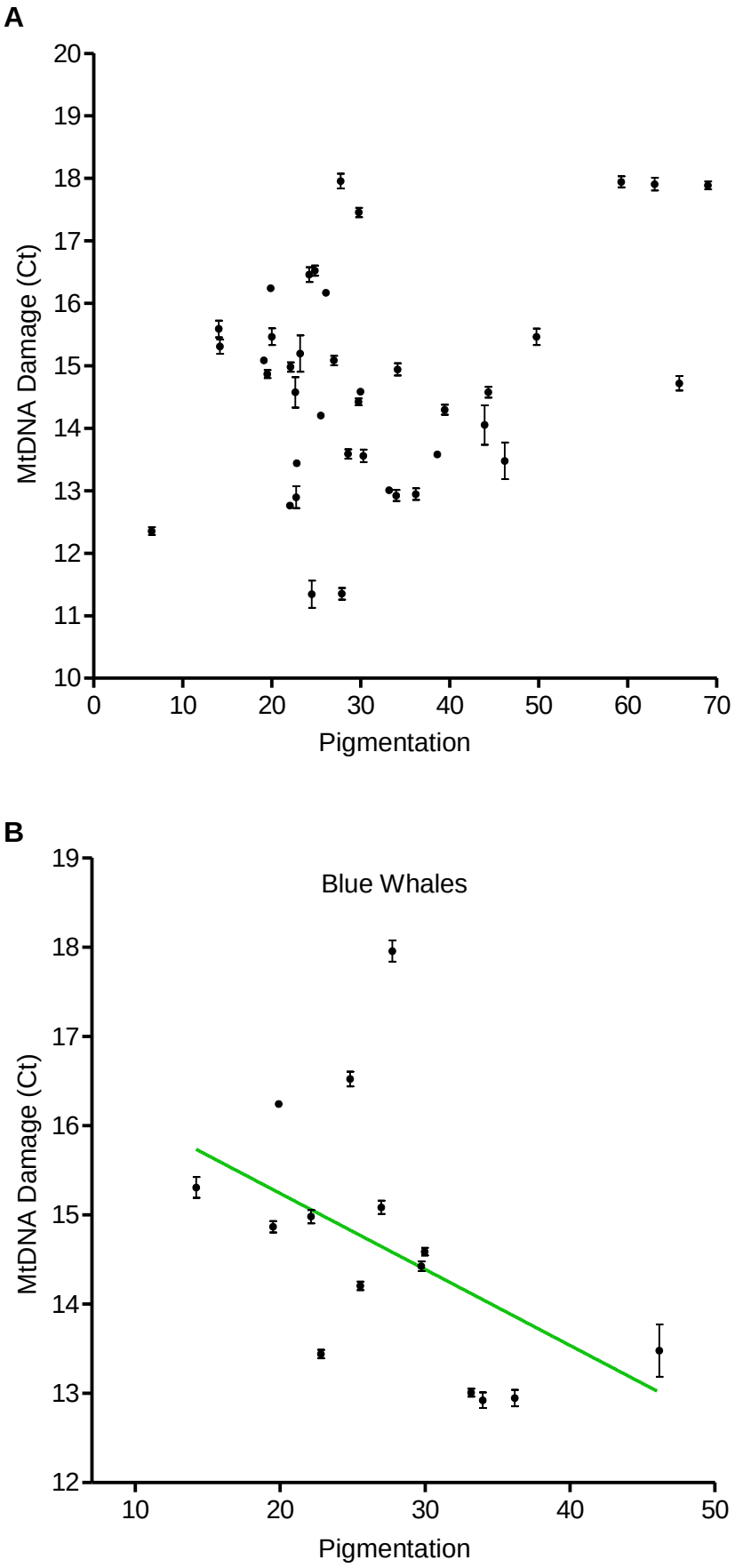
A
MtDNA Damage (Ct)
Pigmentation
B
Blue Whales
MtDNA Damage (Ct)
Pigmentation

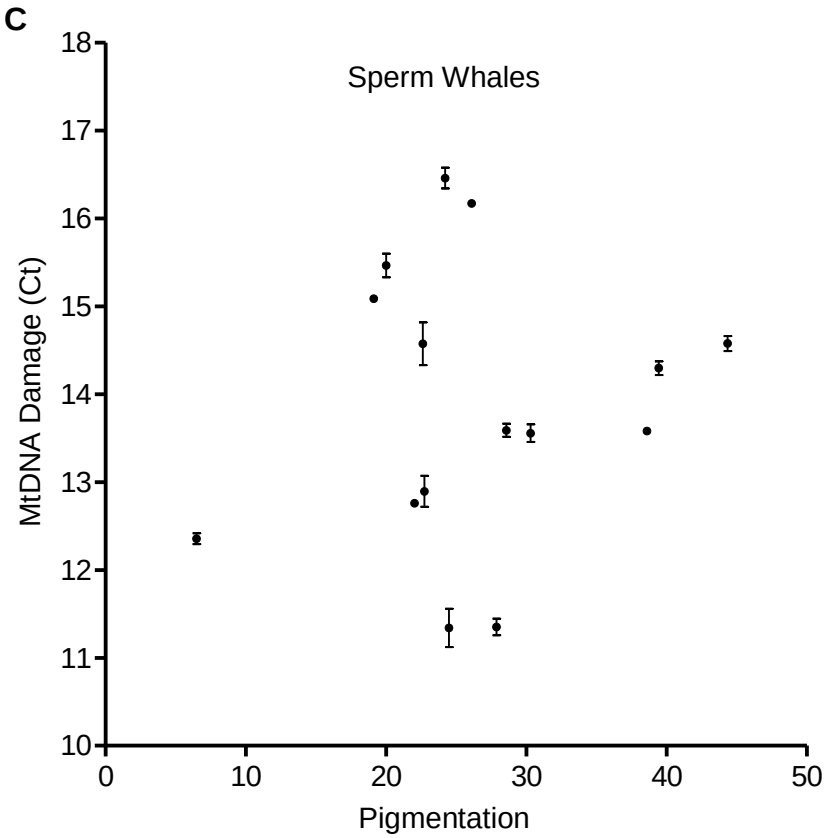
C
Sperm Whales
MtDNA Damage (Ct)
Pigmentation
18
17
16
15
14
13
12
11
10
0
10
20
30
40
50

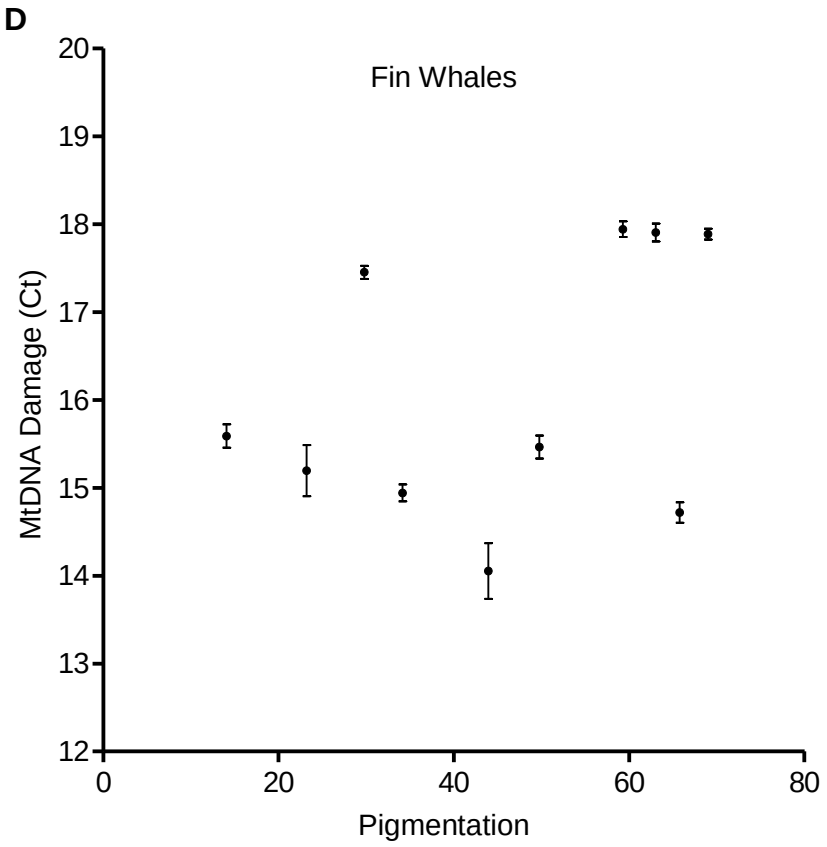
D
Fin Whales
MtDNA Damage (Ct)
Pigmentation
20
19
18
17
16
15
14
13
12
0
20
40
60
80

Figure 67. Individual mtDNA damage compared to individual pigmentation level. A) The mtDNA damage (Ct) as determined using the 4.3 kb-product primers compared to the individual pigmentation level for all three species, for 15 blue whale, 15 sperm whale, and 10 fin whale samples. There was no significant correlation between mtDNA damage and pigmentation (P=0.7633, rho=0.0492, non-parametric Spearman correlation). B) The mtDNA damage compared to the individual pigmentation level for 15 blue whale samples. There was a significant inverse correlation between the level of mtDNA damage and the level of pigmentation (P=0.0148, rho=-0.6143, non-parametric Spearman correlation). The green line shows the line of best fit. C) The mtDNA damage compared to the individual pigmentation level for 15 sperm whale samples. There was no significant correlation between mtDNA damage and pigmentation (P=0.9698, rho=0.0107, non-parametric Spearman correlation). D) The mtDNA damage compared to the individual pigmentation level for 10 fin whale samples. There was no significant correlation between mtDNA damage and pigmentation (P=0.5135, rho=0.2364, non-parametric Spearman correlation). The error bars show the SEM. At least two qPCR reactions each performed in triplicate were used for each sample.

7.4.13 *MtDNA damage and seasonal variation*

In the Gulf of California, Mexico, where the whale samples were obtained, the UV index increases from February to April by approximately 4 UV index points (Lemus-Deschamps *et al.*, 2002). The level of mtDNA damage in whale skin in these 2 months was therefore compared to see if any acute changes in damage were occurring. Unfortunately, the sperm whale samples were all taken in the same month, so were unable to be analysed for differences between months. Although there was no significant difference in damage in the fin whales (Figure 68B) (P=0.2410, unpaired t-test), the blue whales showed a significant decrease in mtDNA damage from February to April (Figure 68A) (P=0.0416, unpaired t-test), despite the increase in UV index. The pigmentation level of the blue whales from February to April was also studied, and it was found that there was a highly significant increase in pigmentation from February to April (Figure 68C) (P=0.0040, unpaired t-test), which was not seen in the fin whales (Figure 68D) (P=0.5100, unpaired t-test).

Figure 68

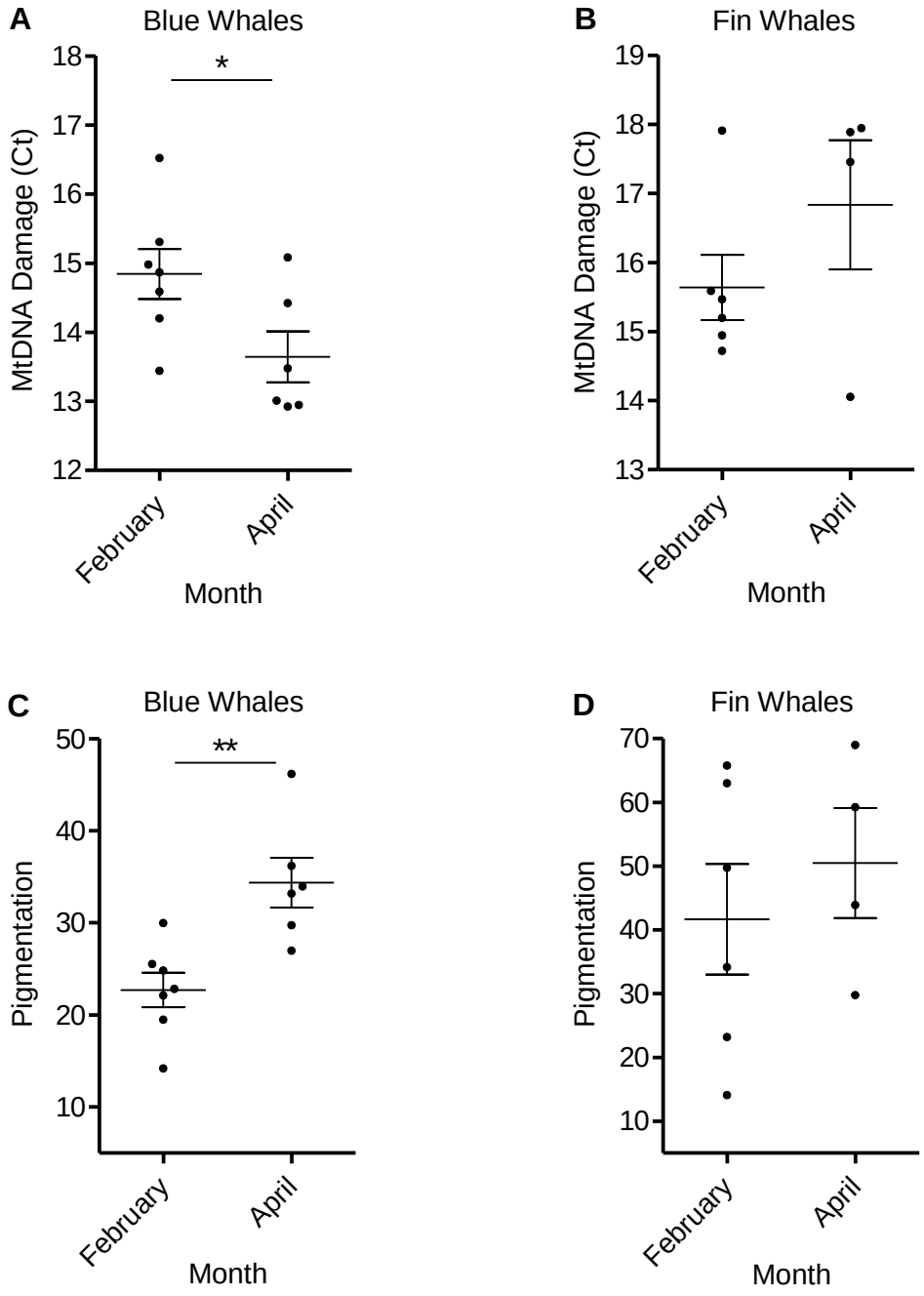

Figure 68. MtDNA damage and pigmentation changes from February to April. A) The mtDNA damage (Ct) as determined using the 4.3 kb-product primers compared to the month for which the individual sample was taken, for 13 blue whale samples. There was a significantly lower level of damage in April compared to February (P=0.0416*, unpaired t-test). B) The mtDNA damage compared to the month for which the individual sample was taken, for 10 fin whale samples. There was no significant change in damage from February to April (P=0.2410, unpaired t-test). At least two qPCR reactions each performed in triplicate were used for each sample. C) The pigmentation level of whales compared to the month for which the individual sample was taken, for 13 blue whale samples. There was a significantly higher level of pigmentation for those samples taken in April (P=0.0040**, unpaired t-test). D) The pigmentation level of whales compared to the month for which the individual sample was taken, for 10 fin whale samples. There was no significant change in pigmentation from February to April (P=0.5100, unpaired t-test). The error bars show the SEM.

7.4.14 *MtDNA damage and increasing age*

The population of blue whales in the Gulf of California have been observed and documented for over 20 years, allowing the minimum age of many of the whale samples to be known. For those whale samples for which the age was known, which included only the blue whales, the age was compared to the mtDNA damage. It was found that a significant correlation existed between the age of the whale and the level of mtDNA damage observed (Figure 69) (P= 0.0279, rho=0.7904, non-parametric Spearman correlation). The age of the individual did not correlate with the pigmentation level of that individual (P=0.3786, rho=-0.3473, non-parametric Spearman correlation) (results not shown), which implied that the increase in mtDNA damage with age was not due to a decrease in pigmentation.

Figure 69

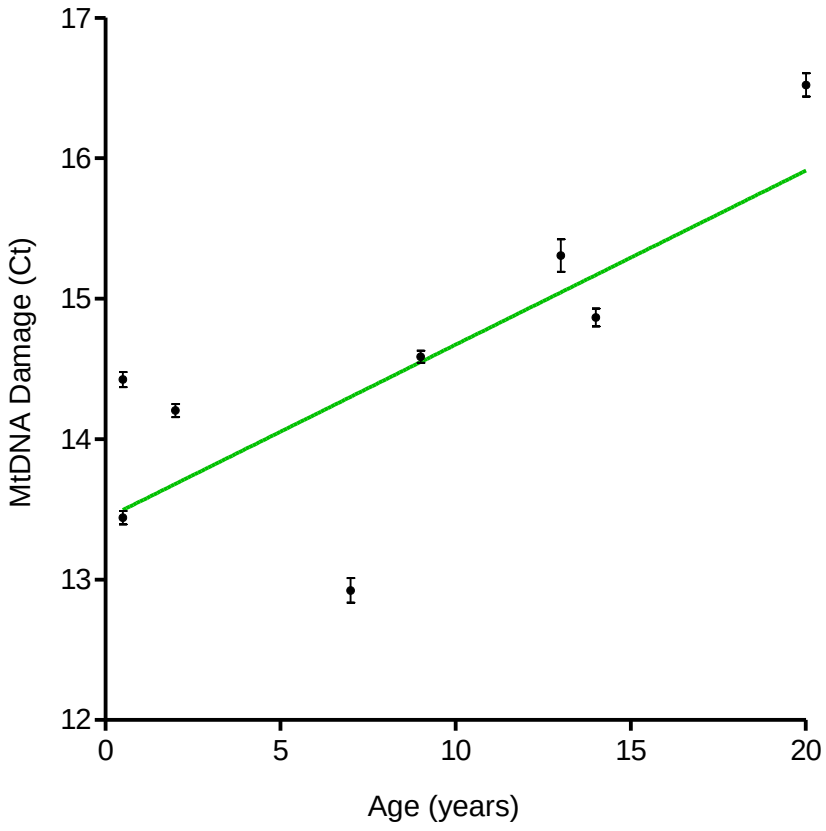

Figure 69. Individual mtDNA damage compared to individual age for blue whale samples. The mtDNA damage (Ct) as determined using the 4.3 kb-product primers compared to the individual age of 8 blue whale samples. There was a significant correlation between the level of mtDNA damage and the age of the whale (P=0.0279, rho=0.7904, non-parametric Spearman correlation). The green line shows the line of best fit. The error bars show the SEM. At least two qPCR reactions each performed in triplicate were used for each sample.

7.5 Discussion

7.5.1 *Successful optimisation of mtDNA damage detection in a previously unstudied taxonomic group*

Real-time qPCR is a technique used previously and reliably to detect UV-induced genetic damage in the mtDNA of humans (Birch-Machin *et al.*, 1998; Ayala-Torres *et al.*, 2000; Ray *et al.*, 2000; Durham *et al.*, 2003; Santos *et al.*, 2006; Swalwell *et al.*, 2012) and a range of laboratory animals including *C. elegans*, mice, and zebrafish (Kalinowski *et al.*, 1992; Hunter *et al.*, 2010; Meyer, 2010). As cetaceans (whales) are a group of animals for which the detection of UV-induced mtDNA damage has not been attempted previously, it was vital to develop and optimise a qPCR technique for the successful detection of damage. In previous studies, damage is typically detected in a large 10 – 15 kb region of the 16.5 kb mtDNA (Hunter *et al.*, 2010; Swalwell *et al.*, 2012) to allow a large probability of damage being encountered. However, multiple sections of smaller lengths (e.g. 11 kb plus 5.5 kb) have also been used to successfully detect UV-induced damage (Ray *et al.*, 2000; Durham *et al.*, 2003), and regions as small as 1 kb and 2.6 kb have also been used successfully (Kalinowski *et al.*, 1992; Eischeid *et al.*, 2009; Hunter *et al.*, 2010). Primer qPCR efficiencies (the amount of sample replication at each cycle, with 100% representing a perfect doubling (Agilent Technologies, 2012)) were low when amplifying sections of 8.5 kb in the present project, which could be problematic if the mtDNA is prevented from amplification due to the primers being unable to function effectively, rather than due to the presence of UV-induced damage. Primers to amplify four regions of 4.4 kb were therefore designed, to improve the efficiency of the reaction due to the lower number of bases required to be replicated. Primers of this size were also shown earlier in the project (Chapter 6) to be able to successfully detect differences in UV-induced mtDNA damage in human skin cells. All four of the primer sets gave similar Ct values per sample for the three species tested, which indicated that there was an evenly distributed spread of damage throughout the genome. This was important to know, as different species could potentially harbour hotspots of damage in different areas throughout their mtDNA genome (Gilbert *et al.*, 2003; Jandova *et al.*, 2012; Zhou *et al.*, 2012). For example, mtDNA sequences that are GC-rich or are palindromic have been shown to be particularly sensitive to mutagenesis caused by ionising radiation (Zhou *et al.*, 2012). As there were

no preferentially damaged areas of the whale mitochondrial genome, this implied that any single 4.4 kb region could be used to determine the general damage throughout the genome.

Based on the successful amplification of blue and fin samples using a section of mtDNA of approximately 4.4 kb, a new species, namely the sperm whale, was introduced. This species was chosen as it has a much higher surface time than the blue or fin whales, and could therefore show potential differences in UV-induced damage or damage responses. A new primer set capable of binding to the mtDNA of all three species was designed to amplify the mtDNA simultaneously to allow for direct comparisons. Due to the sperm whale mitochondrial genome being only 85% similar to that of blue and fin whales (NCBI, 2013) (and the blue and fin whales being only 93% similar themselves), there were limited areas to which 20 bp-long primers could bind with 100% base specificity; however, a single primer set to amplify 4.3 kb was designed, and found to be capable of amplifying the mtDNA of blue whales, sperm whales, and fin whales with high and similar efficiencies.

7.5.2 *UV-induced mtDNA damage is detectable within three different whale species*

UV-induced damage has been detected previously at a cellular level in whale skin (Martinez-Levasseur *et al.*, 2011), but not at a genetic level. In the 15 blue whale, 18 sperm whale, and 10 fin whale samples studied, there were significant differences in mtDNA damage detected, when compared to the least damaged sample for each species. This method of comparison has been used previously when a completely undamaged control was not available (Durham *et al.*, 2003; Birch-Machin, 2006; Hunter *et al.*, 2010), as in the case of this study; whales are wild and free-ranging so it was not possible to acquire a completely undamaged control, for example from a non-exposed region such as the underside of the whale. However, because a spectrum of damage was observed between the different whale samples, it strongly suggested that damage was present and detectable.

7.5.3 *MtDNA damage correlates with known markers of UV-induced damage*

The mtDNA damage levels of samples were compared to other known markers of UV-induced damage, to ensure that the observed mtDNA damage was due to UV, as opposed to other genotoxic factors such as the environmental pollutant benzo[a]pyrene (Begeman and Colucci, 1968), which has been shown previously to induce mtDNA damage detectable by qPCR (Jung *et al.*, 2009). Micro-vesicles are a morphological response to sustained UV exposure in skin to aid in the repair of sun-damaged tissue (Ulrich *et al.*, 2009; Martinez-Levasseur *et al.*, 2011). In this study, individual whales with micro-vesicles present showed the highest amount of mtDNA damage, suggesting that genetic and cellular damage are correlated, and are both caused by UV exposure. Apoptosis is induced in response to UV, as a defensive mechanism to remove damage to prevent potentially carcinogenic mutations from being replicated (Schafer *et al.*, 2010). Whales with apoptotic cells present showed the lowest amount of mtDNA damage. This is in accordance with a previous study on whale skin, which found that the level of apoptosis was increased in response to prolonged UV exposure, and those whales with higher levels of apoptosis had lower levels of UV-induced cellular skin damage (Martinez-Levasseur *et al.*, 2011). Additionally, a previous study on human skin found that there was a significant increase in apoptosis following UV exposure, which was correlated with a reduction in UV-induced cellular and genetic damage (Yamaguchi *et al.*, 2008). These correlations with micro-vesicles and apoptosis imply that the genetic damage observed through this study was caused principally by UV, which is activating damage response mechanisms.

7.5.4 *The level of mtDNA damage varies between different whale species*

When comparing the overall level of mtDNA damage between the blue whales and the fin whales, there was no significant difference observed, despite the much higher level of pigmentation seen in the fin whales. Previous studies have shown that pigment provides protection against UV-induced genetic damage in human skin (Tadokoro *et al.*, 2003; Miyamura *et al.*, 2007; Brenner and Hearing, 2008; Yamaguchi *et al.*, 2008), and fin whales have been shown previously to have lower levels of sun-induced cellular damage (Martinez-Levasseur *et al.*, 2011). However, in the previous study on whale skin

(Martinez-Levasseur *et al.*, 2011), the level of pigmentation correlated positively with the level of apoptosis; this was not the case for the particular samples received for this project, for which the fin whales had similar levels of apoptosis to the blue whales. Therefore the increase in apoptosis usually conferred by melanin (Takeuchi *et al.*, 2004; Yamaguchi *et al.*, 2008) did not appear to be in effect for these particular fin whale samples. Another reason for the high mtDNA damage in the fin whales despite high pigmentation could be that the fin whales are absorbing some of the UV with their high pigmentation levels, however as they spend the majority of the year in the hot climate of Mexico (Bérubé *et al.*, 2002), overall mtDNA damage may still remain high. In contrast, the blue whales spend only 2-4 months per year in the hot climate of Mexico, and spend the remaining time in the cooler area between Alaska and California (Calambokidis *et al.*, 2009). Therefore, despite having lower pigmentation levels, the blue whales are also under lower levels of UV than the fin whales, and therefore have lower mtDNA damage in general.

The blue whales and the sperm whales showed no significant difference in the level of UV-induced mtDNA damage. The particular blue and sperm whales used in this study did not have significantly different levels of pigmentation; however, the sperm whales did have a much higher number of samples with apoptotic cells present. Despite the higher levels of apoptotic protection in the sperm whales, which could be expected to decrease mtDNA damage, there was a similar level of overall damage in the blue and sperm whales. This could be due to the blue whales being exposed to lower levels of UV because of the high surface times of the sperm whales (Whitehead, 2003).

The fin whale samples in this study were found to have a significantly higher level of mtDNA damage than the sperm whale samples. This was despite a higher level of pigmentation in the fin whales, and despite being found in a previous study to have a lower level of UV-induced skin damage (Martinez-Levasseur *et al.*, 2011). This could have again been due to the particular samples received, for which the sperm whales had much higher apoptosis than the fin whales. The high apoptosis in the sperm whale samples could be removing the mtDNA damage (Kulms and Schwarz, 2000; Yamaguchi *et al.*, 2008; Lee *et al.*, 2013), which may explain why this species had lower levels of

mtDNA damage and micro-vesicles. Sperm whale samples were also shown to have higher expression levels of the stress response gene Hsp70, which has been shown previously to be induced in response to UV (Matsuda *et al.*, 2010), to provide photoprotection (Simon *et al.*, 1995; Matsuda *et al.*, 2010). These increased levels of apoptosis and of Hsp70 in the sperm whales may be providing protection, and may suggest that apoptosis and Hsp70 combined provide a higher level of protection than pigmentation alone. This is useful to know in terms of ageing, as therapies to improve stress responses such as these could be beneficial in reducing mtDNA damage, which is thought to play a role in the ageing process (Birch-Machin, 2006).

It could be suggested that the blue whales have not evolved high levels of skin pigmentation, apoptosis, or Hsp70, because they spend the majority of the year in areas with a moderate to low UV index (Bournay and UNEP/GRID-Arendal, 2007). It could also be suggested that the fin whales have evolved higher pigmentation levels as a UV-defensive mechanism, as they spend the majority of the year in an area with a high UV index. As sperm whales have very long surface times, it could be suggested that they have evolved multiple UV-defensive mechanisms (apoptosis and Hsp70) which could be especially efficient at damage removal. Other untested stress response mechanisms in the sperm whales may also be present, which could be adding to the high level of defence and therefore low level of mtDNA damage observed in the sperm whales.

7.5.5 *Higher Hsp70 expression correlates with lower mtDNA damage in three different whale species*

The Hsp70 family of proteins are commonly used as a biomarker for cellular stress (Ogawa *et al.*, 2008). It was found in this project that the level of Hsp70 expression correlated inversely with the level of mtDNA damage when comparing all individuals, suggesting that Hsp70 is playing a role in the reduction of UV-induced genetic damage in all whale skin, as seen in mice and human cells (Niu *et al.*, 2006; Matsuda *et al.*, 2010).

Sperm whales were found to have high levels of both apoptosis and of Hsp70, which was unusual as Hsp70 has been found to suppress apoptosis to allow

protein re-folding instead of cell death (Mosser and Martin, 1992; Beere and Green, 2001). However, other studies have shown that Hsp70 can promote apoptosis when levels of these proteins are high enough (Ran *et al.*, 2004). Therefore, it could be that sperm whales initially induce stress response pathways such as Hsp70, in an attempt to repair any protein damage caused by UV (De la Coba *et al.*, 2009). If this repair is unsuccessful or if the damage becomes too vast, they may be capable of then inducing apoptosis to remove the damage. If this was the case, it could imply that sperm whales are very efficient in both damage repair and removal. Having both of these responses could be necessary for the sperm whales which spend long periods of time at the ocean surface (Whitehead, 2003); therefore the sperm whales may have evolved these mechanisms to counteract the harmful effects of UV. Hsp70 has been shown recently to inhibit the production of melanin in mice (Hoshino *et al.*, 2010), which could explain why the sperm whales had low skin pigmentation.

7.5.6 *Higher pigmentation correlates with lower mtDNA damage within the blue whale species*

When looking within just the blue whale species, it was found that those whales with a higher level of pigmentation had a lower level of mtDNA damage. This correlation was not observed in the sperm whales or fin whales, possibly due to the high levels of other stress responses such as Hsp70 and apoptosis (for the sperm whales), or due to the skin being so dark for the fin whales that slight variations in colour did not affect the genetic damage, as it has been shown in human cells that both medium and darkly pigmented cells provide similar mtDNA protection (Swalwell *et al.*, 2012). The main reason for the inverse correlation between pigmentation and mtDNA damage in the blue whales is likely to be due to the month of sampling; those whales sampled in April were shown to have a lower level of damage than those sampled in February. This is described in more detail below in section 7.5.7.

7.5.7 *Blue whales increase pigmentation levels in response to seasonal UV increases*

The level of pigmentation between animals of the same species can vary dramatically, as seen with humans and other animals (Costin and Hearing, 2007). Research in humans has indicated that as the level of skin pigmentation

increases, the level of UV-induced mtDNA damage decreases (Swalwell *et al.*, 2012). It was observed in the present study that the level of mtDNA damage in the blue whales was decreasing from February to April, despite an increase in the UV index (Martinez-Levasseur *et al.*, 2011). This difference may have been of even higher significance if the same individual whale was able to be sampled from February to April to reduce intra-individual differences. The decrease in UV-induced damage in blue whale skin was in accordance with the previous study on sunburned whales (Martinez-Levasseur *et al.*, 2011), in which it was found that the level of blisters was lower in April compared to February for the blue whales.

When the pigmentation levels were taken into account from February to April, a significant increase in the level of pigmentation was seen for the blue whales, but not the fin whales. The blue whales from the north-east Pacific population studied spend only 2 to 4 months per year in the hot climate of Mexico and spend the remaining time in the cooler area between Alaska and California (Calambokidis *et al.*, 2009); therefore, as the blue whales arrive from cooler regions in February they are suddenly exposed to high UV levels, which continue increasing from February to April (Martinez-Levasseur *et al.*, 2011) (whereas fin whales are in the hot climate year-round). It was proposed that the blue whales may have high mtDNA damage initially due to the sudden exposure to UV, and may be increasing their pigmentation levels long-term from February to April as an acclimatisation response to reduce damage, which is known to happen in humans (Sayre *et al.*, 1981; Costin and Hearing, 2007; Coelho *et al.*, 2009; Miyamura *et al.*, 2011). This 'tanning' response could be a photoprotective mechanism to increase the tolerance to solar radiation after a period of sunlight exposure, and could be possibly being activated by the DNA damage obtained when the blue whales are first exposed to the high levels of UV, which has been shown to happen previously in humans (Eller *et al.*, 1996; Lin and Fisher, 2007). A 'tanning' response has been seen previously in marine life such as hammerhead sharks (Lowe and Goodman-Lowe, 1996) and seabream fish (Adachi *et al.*, 2005), in which it was found that the level of melanin was higher following a period of sun-exposure; however, this study gives evidence for the first time of this response being observed in marine mammals.

The blue whales may have evolved the ability to tan due to the seasonally changing UV conditions which they are exposed to. This has been suggested to also have occurred during early human migration, during which the ability to tan possibly evolved for those humans under seasonally variable conditions (Jablonski and Chaplin, 2012), to allow for increased damage protection during high UV and the ability to produce vitamin D during low UV (Jablonski and Chaplin, 2012). As for the fin whales, it is probable that because they are under high UV levels for the majority of the year and there is little variation in seasonal UV (Lemus-Deschamps *et al.*, 2002; Martinez-Levasseur *et al.*, 2011), they have no need for a tanning response, and are continuously dark-skinned, as happens in humans living in the Tropics (Jablonski and Chaplin, 2010). In order to confirm the tanning response of the blue whales, samples could be taken from the blue whales during the winter months when they have returned to cooler areas, to determine whether the level of pigmentation returns to lower levels once the whales have migrated away from Mexico.

7.5.8 *MtDNA damage is higher in older individual whales*

The age of the blue whales (which were the only species for which the ages were known) correlated significantly with their individual mtDNA damage, which is in accordance with previous results found in humans (Hayakawa *et al.*, 1992; Chomyn and Attardi, 2003; Krishnan *et al.*, 2007). This could suggest that whale skin accumulates mtDNA damage throughout the lifetime of the whale, possibly partially due to UV, and due to intrinsic factors.

The age of the individual whale did not correlate with the level of pigmentation, which implied that the increase in mtDNA damage observed with age was not just due to a decrease in pigmentation. Because mtDNA damage was seen in a 4 kb region for both UV-damaged and chronologically-aged whale skin, it gives evidence that differently UV-exposed whale skin can be used as a reliable model for different ages.

7.6 Summary

Through this chapter, mtDNA damage in whales under various levels of UV stress was examined using qPCR, to give insights as to the effects of mtDNA damage with age, due to the similarities between photo and chronological ageing. A reliable method for mtDNA damage detection was optimised, for a taxonomic group for which this has not been attempted previously. The damage detected using this method correlated with other known markers of UV damage, suggesting UV was responsible. A spectrum of mtDNA damage was observed between the samples, suggesting that differences in mtDNA damage were present, and that all three whale species are indeed susceptible to the damaging effects of UV. This damage was different between the three whale species, which could be due to differently evolved mechanisms of coping with UV-induced stress, from constitutively high pigmentation, to high apoptosis and stress responses, to an ability to tan. Within all whale samples, an increase in Hsp70 expression resulted in decreased mtDNA damage. This could have future therapeutic potentials, with treatments which increase Hsp70 and other stress responses used to potentially reduce mtDNA damage increases observed with age. The level of mtDNA damage was greater with age as well as with increased UV, which demonstrates the use of the optimised method in detecting UV damage as a model for aged skin.

Chapter 8. Discussion

8.1 Overview

For over 50 years it has been speculated that mitochondria may play a key role in the ageing process (Harman, 1972; Hulbert *et al.*, 2007; Barja, 2013). This is due to the mainly correlative results displaying an increase in mtDNA damage, ROS, and mitochondrial dysfunction with age. However, the exact role of the mitochondria in the ageing process remains unknown.

The individual complexes of the mitochondria perform respiration to generate cellular energy, during which ROS are produced as a by-product. The exact role of these mitochondrial complexes in the ageing process is unknown, as some previous studies have shown decreases in complex activities with age, whereas others have shown no change. Complex II of the respiratory chain was chosen to be examined in terms of ageing in the present study, as it is the least studied complex of the respiratory chain, and recent observations have shown that this complex can generate ROS at similar levels as complexes I and III (Guo and Lemire, 2003; Lemarie *et al.*, 2011; Quinlan *et al.*, 2012). This complex has also been shown in previous studies to be associated with the ageing process; for example, mutations in the complex II subunits affecting only the activity of complex II have been shown to decrease the lifespan of nematodes and flies (Hosokawa *et al.*, 1994; Adachi *et al.*, 1998; Ishii *et al.*, 1998; Walker *et al.*, 2006; Tsuda *et al.*, 2007; Huang and Lemire, 2009; Pfeiffer *et al.*, 2011; Wojtovich *et al.*, 2013), which was able to be prevented when complex II respiration was blocked (Pfeiffer *et al.*, 2011). Complex II has also been shown to be lower with age in the skin of naturally aged mice (Velarde *et al.*, 2012), various rat tissues (Sandhu and Kaur, 2003; Kumaran *et al.*, 2004; Cocco *et al.*, 2005; Balietti *et al.*, 2009; Braidy *et al.*, 2011), human muscle (Trounce *et al.*, 1989; Coggan *et al.*, 1992; Boffoli *et al.*, 1994; Short *et al.*, 2005), and human lymphocyte cells (Drouet *et al.*, 1999). However, the activity of complex II in the skin of differently aged humans has not been examined prior to the current study, which was crucial to address as the skin is the largest organ of the body and also provides a barrier to environmental insults, rendering it a very important organ.

The major finding of the present study was the observation that complex II activity decreases in an age-dependant manner in human skin, a finding which

to my knowledge has not been demonstrated previously. This could have been potentially caused by a decrease in the complex II subunits SDHA and SDHB, which also correlated with increasing age. It was observed that the decrease in complex II activity occurred specifically in senescent cells, which could provide the first evidence of a difference in senescent cells from younger individuals and senescent cells from older individuals in terms of mitochondrial complex II activity. Additionally, an increase in mitochondrial dysfunction with age was found not only in human skin, but also in a taxonomic group not previously studied in terms of age-related damage, the whales. In the three whale species studied, it was observed that the level of mtDNA damage increased both with age and with increased UV exposure (as a model for age) using novel primers and a new technique for the detection of age-related mtDNA damage, suggesting that increased mitochondrial damage with age is not just confined to human skin.

8.2 Mitochondrial Complex II Activity Decreases with Age in Human Skin

In the present study it was found that the activity of mitochondrial complex II, but not complex IV, decreased significantly with age in human skin fibroblast cells. This could suggest that a decrease in ETC activity with age is localised to complex II in skin, and is not just a general decrease in overall ETC activity. To confirm this, the activities of complexes I, III, and V with age could be tested in human skin. As complex II has also been shown in previous studies to be decreased with age in human muscle and lymphocyte cells (Trounce *et al.*, 1989; Coggan *et al.*, 1992; Boffoli *et al.*, 1994; Drouet *et al.*, 1999; Short *et al.*, 2005), it could be that older individuals have decreased complex II activity with age throughout the whole body. However, the activity of complex II in other tissues would have to be measured to verify this. The observed decrease in complex II activity in human skin was found to be specific to skin fibroblast cells, possibly due to the higher rate of cellular turnover in skin keratinocyte cells (Iizuka, 1994; Stout *et al.*, 2005), which may prevent the accumulation of damage to complex II. This is the case for mtDNA damage, which does not accumulate as readily in keratinocytes compared to fibroblasts (Krishnan *et al.*, 2004; Harbottle and Birch-Machin, 2006).

The present study confirmed in human skin the previous work on mouse skin (Velarde *et al.*, 2012), demonstrating a decrease in complex II activity, but not complex IV activity, with age. It was initially speculated in the present study that this decrease in complex II activity with age may be due to either a lower activity of complex II per mitochondrial unit, or due to a lower overall abundance of complex II units per mitochondria. This was tested by measuring the expression and protein levels of the individual subunits of complex II, which extends the previous mouse study (Velarde *et al.*, 2012), and it was found that the complex II subunits SDHA and SDHB were also decreased with age; this could suggest that the latter hypothesis is more likely.

It could be speculated that a decrease in complex II activity with age will result in an increase in ROS leakage (Morten *et al.*, 2006; Byun *et al.*, 2008; Quinlan *et al.*, 2012), which may cause damage to cellular components and therefore a decrease in tissue function (Conley *et al.*, 2000; Petersen *et al.*, 2003; Tonkonogi *et al.*, 2003; Short *et al.*, 2005). If this were the case, complex II could be considered causal in the ageing process. It could also be suggested that a decrease in complex II activity with age occurs consequentially of other factors, such as an increase in ROS abundance (Li *et al.*, 1995; Melov *et al.*, 1999; Capel *et al.*, 2005; Morten *et al.*, 2006; Koziel *et al.*, 2011; Velarde *et al.*, 2012) due to lower cellular defence levels with age (Micallef *et al.*, 2007; Krizhanovsky *et al.*, 2008; Rodier and Campisi, 2011; Dutta *et al.*, 2012; Baker and Sedivy, 2013; Viiri *et al.*, 2013). ROS may then affect complex II directly or cause damage to the nDNA-encoded subunits of complex II (Li *et al.*, 1995; Melov *et al.*, 1999; Wallace, 1999; Kumaran *et al.*, 2004; Morten *et al.*, 2006; Velarde *et al.*, 2012). It has been shown previously that increased ROS (generated by SOD-knockout in mice) can result in a decrease in SDHB protein expression and in complex II activity (Morten *et al.*, 2006). ROS may therefore also affect SDHB expression during natural ageing, as it was found in the present study that SDHB decreases with age in both the fibroblasts and the keratinocytes.

8.3 The Age-Related Decrease in Complex II Activity is Specific to Senescent Cells

To further understand the potential reasons behind the age-related decline in complex II activity in human skin fibroblast cells, samples were sorted into senescent and non-senescent cell populations. Senescent cells have been shown to harbour mitochondrial dysfunction (Passos *et al.*, 2007a; Dekker *et al.*, 2009; Moiseeva *et al.*, 2009; Passos *et al.*, 2010; Treiber *et al.*, 2011; Velarde *et al.*, 2012), and it was hypothesised in the present study that senescent cells from older donors may have increased mitochondrial dysfunction than senescent cells from younger donors, which could contribute to the overall complex II activity decrease observed with age. It was found in the present study that this was indeed the case, as there was a significant decline in complex II activity in senescent cells, but not in non-senescent cells, with age. The present study therefore provides the first evidence that senescent cells from older individuals are less efficient in terms of mitochondrial complex II activity than senescent cells from younger individuals. There was no correlation between complex IV activity and age in the senescent or the non-senescent cells, which further validates the finding that complex IV activity is not altered with age in human skin fibroblast cells. As ROS levels are higher in senescent cells (Passos *et al.*, 2007a), it could be that the complex II activity of this cell type is more highly affected with age, as defence mechanisms begin to falter (Micallef *et al.*, 2007; Krizhanovsky *et al.*, 2008; Rodier and Campisi, 2011; Dutta *et al.*, 2012; Baker and Sedivy, 2013; Viiri *et al.*, 2013).

8.4 Complex II as a Potential Target for the Treatment of Ageing

If complex II were found to play a causal role or to exacerbate the ageing process, it could potentially provide a target for treatments of ageing. An enhancement of complex II activity in the brain of aged mice has been observed in past work (Ajith *et al.*, 2009), using an extract from the mushroom *Ganoderma lucidum*, which is commonly used as a medicinal substance in China (Batra *et al.*, 2013). This extract has been shown to extend the lifespan of mice (Nonaka *et al.*, 2006; Steiner, 2013) and *C. elegans* (Chuang *et al.*, 2009). However, whether the life-extending properties of this substance occur solely via complex II is unlikely (Steiner, 2013). Other work has demonstrated that complex II activity is able to be restored in the hearts of aged rats upon long-

term treatment with the drug *N*-acetylcysteine (NAC) (Cocco *et al.*, 2005), however, lifespan was not tested for. In addition, it has been shown previously that an overexpression of SDHA/SDHB subunits in neuronal cells from the brains of Huntington's disease patients restored the usually lowered complex II activity and decreased cellular death (Benchoua *et al.*, 2006).

As only the senescent cells showed a decrease in complex II activity with age, future studies could focus on complex II in senescent cells only as a specific target for age-related treatments. A recent attempt to specifically target senescent cells was performed, using nanotechnology (Agostini *et al.*, 2012). Agostini *et al*., (2012) used nanoparticles to release drugs specifically into senescent cells based on the presence of β-gal, which was successfully performed in yeast. This could allow for future studies to specifically enhance complex II activity in senescent cells of older individuals. This rejuvenation of senescent cells in the elderly may be more beneficial than the complete removal of senescent cells, as this cell type is involved in the prevention of cancerous cell division.

8.5 Complex II Activity is Cell-Type Dependent

The activity of complex II was found to decrease with age in fibroblast cells, but not in keratinocyte cells. It was also found that the fibroblast cells had a significantly higher maximal rate of complex II activity than the keratinocyte cells as shown previously (Hornig-Do *et al.*, 2007), which was suggested to be due to the ROS-generating requirement of keratinocytes for differentiation, at the expense of the maximal complex II activity (Hornig-Do *et al.*, 2007). Differences in maximal complex II activities have also been shown to exist between other cell types (Chretien *et al.*, 1994; Kwong and Sohal, 2000; Benard *et al.*, 2006; Fernández-Vizarra *et al.*, 2011), and it was hypothesised that maximal activities may influence whether or not a change in complex II activity is detectable with age in the particular cell type. It could be speculated that those cells with faster maximal complex II activity rates show noticeable decreases in complex II activity with age, as observed for the fibroblasts and keratinocytes in the present study, and previously in mouse tissues (Kwong and Sohal, 2000; Choksi *et al.*, 2011).

Differences in maximal complex II activity were observed for the cell types tested, which were primary fibroblast cells, primary keratinocyte cells, HDFn cells, HaCaT cells, HepG2 cells, a549 Parental cells, a549 Rho-zero cells, MRC5 cells, and MRC5/hTERT cells. However, no general correlation was found to predict complex II activity, as cells from the same tissue showed differences in complex II activity, and immortal cell types were neither consistency higher or lower in terms of complex II activity compared to non-immortal cells. Future studies could also measure complex II activity in these cell types with age *in vitro*, to determine whether a correlation exists between the overall maximal activity, and whether a decrease in activity with age is detectable.

8.6 The T414G MtDNA Mutation is Higher in Skin Cells from Older Individuals

The level of T414G mtDNA mutation was confirmed in the present study to be at a higher level in older individuals, in human skin fibroblast cells, which is in accordance with previous work (Michikawa *et al.*, 1999; Birket and Birch-Machin, 2007). The T414G mutation, which has been used as a marker of mtDNA damage (Birket and Birch-Machin, 2007; Seibel *et al.*, 2008), was shown in past work not to be preferentially associated with either senescent or non-senescent FACS-sorted populations (Birket *et al.*, 2009). However, whether this mutation is increased in senescent cells alone with age had not been tested before the present study. It was observed in the present work that this mutation was not detectable in senescent or in non-senescent cells following FACS-sorting, possibly due to the lower aged individuals used compared to the previous study (Birket *et al.*, 2009). It was also likely that the mutation was diluted to the point of being non-detectable when only 20% of the sample was analysed. Therefore, this mutation may not be an appropriate marker with which to compare differences in mtDNA damage in FACS-sorted senescent cells with age.

8.7 MtDNA Damage Increases with Age in Whale Skin

The level of mitochondrial dysfunction (in terms of a decrease in complex II activity and an increase in T414G mutation) was shown in the present project to be higher in cells from the skin of older humans, as discussed above. An

increase in mitochondrial damage with age was not restricted to human skin; it was also found in the present study that the level of mtDNA damage increased with both natural age and with increased UV exposure as a model for age, in the skin of a large and previously untested group of animals, the whales. This is in accordance with previous studies on human and laboratory animals, for which mtDNA damage (in the form of mutations rather than strand breaks) has been shown to be increased with both age (Arnheim and Cortopassi, 1992; Cooper *et al.*, 1992; Michikawa *et al.*, 1999; Birket and Birch-Machin, 2007; Meissner *et al.*, 2008; Cui *et al.*, 2012) and UV (Kalinowski *et al.*, 1992; Ray *et al.*, 2000; Durham *et al.*, 2003; Eischeid *et al.*, 2009; Hunter *et al.*, 2010).

8.8 MtDNA Damage Decreases as Hsp70 Increases in Whale Skin

As whales undergo extensive levels of UV exposure due to breathing and other surfacing obligations (Croll *et al.*, 2001; Whitehead, 2003), as well as their long lifespans, and their lack of UV protection from fur or feathers, it is likely that they have developed effective defence mechanisms against UV. It was found in the present study that differences in mtDNA damage exist both between and within the three whale species studied, which could be indicative of different evolutionary response mechanisms for the defence against UV-induced damage. Lower mtDNA damage correlated with increased apoptosis and increased Hsp70 expression across samples from all three species, but did not correlate with pigmentation when all three species were examined. Additionally, the sperm whales were found to have a much lower level of mtDNA damage than the fin whales, despite having a lower pigmentation level. Upon closer inspection, it was observed that the sperm whale samples used in the present study had significantly higher levels of both apoptosis and Hsp70. This could imply that apoptosis and Hsp70 confer higher protection to mtDNA than pigmentation alone.

In terms of therapeutic potentials for human ageing, it could be speculated that improving the Hsp70 stress response may decrease the rate of ageing, resulting in a decrease in mtDNA damage. In humans and laboratory animals, the level of Hsp70 has been shown to decline with age (Heydari *et al.*, 1993; Heydari *et al.*, 1994; Broome *et al.*, 2006; Gagliano *et al.*, 2007; Calderwood *et al.*, 2009; Malyshev, 2013). Previous work has shown that compounds isolated

from the red algae *Porphyra rosengurttii* are able to maintain Hsp70 expression in mice skin exposed to UV (De la Coba *et al.*, 2009), which could possibly be useful for future ageing studies. Past work has also demonstrated that the overexpression of Hsp70 throughout the lifetime of mice results in more effective damage recovery in muscles, as well as lower lipid peroxidation (Broome *et al.*, 2006). Additionally, higher Hsp70 expression has been found in past studies to increase the lifespan of Drosophila (Singh *et al.*, 2007; Malyshev, 2013) and *C. elegans* (Hsu *et al.*, 2003), and in humans it has been demonstrated that centenarians, unlike other older individuals, have similar Hsp70 levels in their lymphocyte cells as those observed in younger individuals (Ambra *et al.*, 2004). Therefore, it could be that the enhancement of Hsp70 may decrease the rate of human ageing, and could be focussed upon in future studies (Calderwood *et al.*, 2009; Malyshev, 2013).

8.9 An Updated Version of the Vicious Cycle Theory of Ageing

It was confirmed in the present study that both mitochondrial dysfunction and mtDNA damage are associated with age, as shown previously in various tissues and species. This was demonstrated in the form of a lower complex II activity with age in human skin, and an increase in mtDNA damage with age in the skin of whales, neither of which has been shown previously. Both of these factors (increased mitochondrial dysfunction and mtDNA damage) agree with the vicious cycle theory of ageing (Bandy and Davison, 1990). Although this theory remains disputed and is unlikely to be the full picture in all cell types (Sanz *et al.*, 2006; Barja, 2013), it presented a useful tool for connecting the three major aspects of mitochondria and ageing. It could be speculated that this cycle is occurring only in specific cell types, such as senescent cells, which were found in the present study to show a decrease in mitochondrial complex II activity with age, whereas the non-senescent cells did not. This may help to explain past controversial results regarding this theory which have attempted to incorporate multiple different cell types. Additionally, an updated version of the vicious cycle may make the theory more valid. As complex II is nuclear-encoded, this could add an additional interacting feature to the cycle, as shown in Figure 70. It was also observed in the present study that senescent cells show a decrease in complex II activity with age, which could indicate that this vicious cycle is taking place predominantly in senescent cells if it is in fact occurring, or is exacerbated

by ROS release from senescent cells (Nelson *et al.*, 2012). ROS may decrease the levels of functional mitochondrial proteins such as the complex II subunits SDHA and SDHB, either directly or via nDNA damage, and cause a lowered activity of this complex, and further ROS release. In addition, this process may be exacerbated by UV from the sun, which can increase ROS or cause DNA damage directly (Schafer *et al.*, 2010).

Figure 70

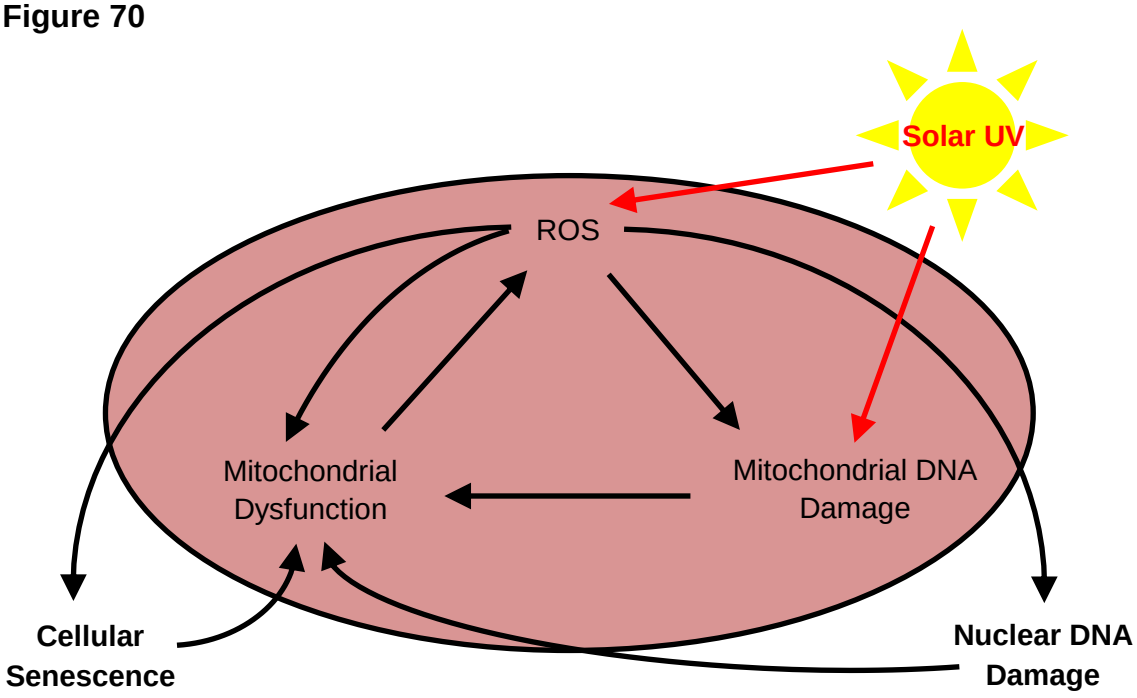

Figure 70. An updated version of the vicious cycle theory of ageing. The vicious cycle theory of ageing suggests that ROS generated during mitochondrial respiration is able to cause damage to mtDNA, which may result in the dysfunctional expression of mitochondrial units, leading to further ROS production in a continuing vicious cycle of increasing damage (Bandy and Davison, 1990; Zdanov *et al.*, 2006; Dlaskova *et al.*, 2008). The traditional vicious cycle theory may be expanded by the observation that complex II is decreased with age, despite being nuclear-encoded. Cellular senescence is also thought to result in mitochondrial dysfunction, as well as being induced and maintained via ROS. In addition, external insults such as solar UV (shown by the red arrows) is thought to enhance ageing, either via an increase in ROS or via mtDNA damage directly. The mitochondrion is shown in pink.

8.10 Future Work

In the present study, the activity of complex II was found to decrease in human skin fibroblast cells with age. This could be indicative of a whole-body decrease in complex II activity; however, the activity of complex II in other tissues from naturally aged individuals would have to be examined in order to confirm or

discard this hypothesis, which could be performed in future work. In addition, the remaining mitochondrial complexes could be studied in human skin and elsewhere in the body, to determine whether the decrease in complex II activity with age was localised to complex II or was observed throughout the respiratory chain. As a decrease in complex II activity with age in human skin may be merely a correlative artefact, future studies could specifically impair complex II activity in laboratory animals (rather than via increased ROS as performed previously (Li *et al.*, 1995; Melov *et al.*, 1999; Morten *et al.*, 2006; Velarde *et al.*, 2012)), to determine the repercussions. If a decrease in complex II activity alone results in the generation of ageing phenotypes, it could be that this complex plays an important causal role in the ageing process.

To confirm that the decrease in complex II activity with age was specific to senescent cells only, future studies could examine the protein and expression levels of SDHA and SDHB in FACS-sorted cells, to see whether any decrease in these subunits with age is occurring, and if so whether this is specific to the senescent cells. If the decrease in complex II activity and its subunits is specific to senescent cells, future therapeutic interventions could focus on this cell type.

In addition to potential future therapeutic interventions to enhance complex II activity in senescent cells with age, treatments focussed on the improvement of the Hsp70 stress response, which was found to be an effective defence mechanism against mtDNA damage in whale skin, could be tested in older animals in future studies to determine whether ageing phenotypes are reduced.

Publications

Papers

Bowman, A., Martinez-Levasseur, L.M., Acevedo-Whitehouse, K., Gendron, D. and Birch-Machin, M.A. (2013) 'The simultaneous detection of mitochondrial DNA damage from sun-exposed skin of three whale species and its association with UV-induced microscopic lesions and apoptosis', *Mitochondrion*, 13(4), pp. 342-9.

Martinez-Levasseur, L.M., Birch-Machin, M.A., Bowman, A., Gendron, D., Weatherhead, E., Knell, R.J. and Acevedo-Whitehouse, K. (2013) 'Whales use distinct strategies to counteract solar ultraviolet radiation', *Scientific Reports*, 3, pp. 2386.

Martinez-Levasseur, L.M., Gendron, D., Knell, R.J., O'Toole, E.A., Singh, M., Bowman, A., Birch-Machin, M.A. and Acevedo-Whitehouse, K. (2014) 'Responses to acute sun exposure in large whales', *McGraw-Hill Education Yearbook of Science and Technology Textbook*. McGraw-Hill Professional.

Anderson*, A., Bowman*, A., Manning, P. and Birch-Machin, M.A. (2014) 'A significant role for human mitochondrial complex II in the production of reactive oxygen species in human skin and its association with ageing', manuscript under preparation for submission, *joint first authors.

Bowman, A. and Birch-Machin, M.A. (2014) 'Mitochondrial DNA as a biosensor of UV exposure in human skin', manuscript submitted to *Springer Methods in Molecular Biology*.

Abstracts

Bowman, A., Martinez-Levasseur, L.M., Acevedo-Whitehouse, K., Gendron, D. and Birch-Machin, M.A. (2012) 'Mitochondrial DNA, a reliable biomarker for measuring the effect of cumulative ultraviolet irradiation exposure in whales (cetaceans)', *British Journal of Dermatology*, 166, pp. e39.

Oyewole, A., Bowman, A., Rogers, T. and Birch-Machin, M.A. (2011) 'The role, mechanism and protective effects of dietary antioxidants in human skin

subjected to inducers of oxidative stress', *British Journal of Dermatology*, 164, pp. 925-926.

Presentations

Bowman, A., Anderson, A. and Birch-Machin, M.A. (2014) 'A significant role for human mitochondrial complex II in the production of reactive oxygen species in human skin and its association with ageing', *British Society for Investigative Dermatology Meeting*, Newcastle, UK (poster presentation).

Bowman, A., Anderson, A. and Birch-Machin, M.A. (2013) 'Mitochondrial electron transport chain activity in different cell lines', *Mitochondria, metabolic regulation and the Biology of Ageing Conference*, Lanzarote, Spain (poster presentation).

Bowman, A., Martinez-Levasseur, L.M., Acevedo-Whitehouse, K., Gendron, D. and Birch-Machin, M.A. (2012) 'Mitochondrial DNA damage detection in sun-exposed whale skin', *North East Postgraduate Conference*, Newcastle, UK (poster presentation).

Bowman, A., Martinez-Levasseur, L.M., Acevedo-Whitehouse, K., Gendron, D. and Birch-Machin, M.A. (2012) 'Mitochondrial DNA, a reliable biomarker for measuring the effect of cumulative ultraviolet irradiation exposure in whales (cetaceans)', *British Society for Investigative Dermatology Meeting*, Exeter, UK (poster presentation).

Bowman, A., Martinez-Levasseur, L.M., Acevedo-Whitehouse, K. and Birch-Machin, M.A. (2011) 'The effects of sun exposure on whale mitochondrial DNA', *North East Postgraduate Conference*, Newcastle, UK (poster presentation).

Bowman, A., Martinez-Levasseur, L.M., Acevedo-Whitehouse, K., Gendron, D. and Birch-Machin, M.A. (2011) 'Mitochondrial DNA, a reliable biomarker for measuring the effect of cumulative UV irradiation exposure in cetaceans', *19th Biennial Conference on the Biology of Marine Mammals*, Florida, USA (poster presentation).

News Articles

A selection of news sources featuring the Bowman *et al*., (2013) and Martinez-Levasseur *et al*., (2013) papers:

Coghlan, A., (2013) 'Whales tan too, basking in the blue', *New Scientist*, 219(2933), pp. 16.

Devlin, H., (2013) 'Whales have to watch out for sunburn', *The Times*, August 31st 2013, pp. 13.

Lee, J.J., (2013) 'How Do Whales Avoid Sunburn? Hint: Some Tan', *National Geographic*, http://news.nationalgeographic.com/news/2013/08/130830-whales-sunburn-ultraviolet-radiation-ocean-animals-science/.

McGrath, M., (2013) "Tanned' whales' sun response gives clues to human ageing', *BBC News*, http://www.bbc.co.uk/news/science-environment-23882667.

References

Abcam (2013) *Fluorescence activated cell sorting of live cells*. Available at: http://www.abcam.com/index.html?pageconfig=resource&rid=12803 (Accessed: 7.10.13).

Ackermann, M. (2008) 'Bacteria as a new model system for aging studies: investigations using light microscopy', *Biotechniques*, 44(4), pp. 564-7.

Adachi, H., Fujiwara, Y. and Ishii, N. (1998) 'Effects of oxygen on protein carbonyl and aging in Caenorhabditis elegans mutants with long (age-1) and short (mev-1) life spans', *J Gerontol A Biol Sci Med Sci. 1998 Jul;53(4):B240-4.*

Adachi, K., Kato, K., Wakamatsu, K., Ito, S., Ishimaru, K., Hirata, T., Murata, O. and Kumai, H. (2005) 'The histological analysis, colorimetric evaluation, and chemical quantification of melanin content in 'suntanned' fish', *Pigment Cell Research*, 18(6), pp. 465-8.

Agilent Technologies, U.S. (2012) 'Introduction to Quantitative PCR', *Methods and Applications Guide*, [Online].

Agostini, A., Mondragon, L., Bernardos, A., Martinez-Manez, R., Marcos, M.D., Sancenon, F., Soto, J., Costero, A., Manguan-Garcia, C., Perona, R., Moreno-Torres, M., Aparicio-Sanchis, R. and Murguia, J.R. (2012) 'Targeted cargo delivery in senescent cells using capped mesoporous silica nanoparticles', *Angew Chem Int Ed Engl*, 51(42), pp. 10556-60.

Ahmed, S., Passos, J.F., Birket, M.J., Beckmann, T., Brings, S., Peters, H., Birch-Machin, M.A., von Zglinicki, T. and Saretzki, G. (2008) 'Telomerase does not counteract telomere shortening but protects mitochondrial function under oxidative stress', *J Cell Sci*, 121(Pt 7), pp. 1046-53.

Ajith, T.A., Sudheesh, N.P., Roshny, D., Abishek, G. and Janardhanan, K.K. (2009) 'Effect of Ganoderma lucidum on the activities of mitochondrial dehydrogenases and complex I and II of electron transport chain in the brain of aged rats', *Exp Gerontol*, 44(3), pp. 219-23.

Akase, T., Nagase, T., Huang, L., Ibuki, A., Minematsu, T., Nakagami, G., Ohta, Y., Shimada, T., Aburada, M., Sugama, J. and Sanada, H. (2012) 'Aging-like

skin changes induced by ultraviolet irradiation in an animal model of metabolic syndrome', *Biological Research for Nursing*, 14(2), pp. 180-7.

Al-Baker, E.A., Oshin, M., Hutchison, C.J. and Kill, I.R. (2005) 'Analysis of UV-induced damage and repair in young and senescent human dermal fibroblasts using the comet assay', *Mechanisms of Ageing and Development*, 126(6–7), pp. 664-672.

Alberts, B., Johnson, A., Lewis, J., Raff, M., Roberts, K. and Walter, P. (2002) *Molecular Biology of the Cell*. 4th edn. Garland Science.

Aldwin, C.M. and Gilmer, D.F. (2013) *Health, Illness, and Optimal Aging: Biological and Psychosocial Perspectives* Springer Publishing Company.

Allen, R.G., Keogh, B.P., Tresini, M., Gerhard, G.S., Volker, C., Pignolo, R.J., Horton, J. and Cristofalo, V.J. (1997) 'Development and age-associated differences in electron transport potential and consequences for oxidant generation', *J Biol Chem. 1997 Oct 3;272(40):24805-12.*

Allsopp, R.C., Chang, E., Kashefi-Aazam, M., Rogaev, E.I., Piatyszek, M.A., Shay, J.W. and Harley, C.B. (1995) 'Telomere shortening is associated with cell division in vitro and in vivo', *Exp Cell Res*, 220(1), pp. 194-200.

Alonso, J.R., Cardellach, F., Casademont, J. and Miro, O. (2004) 'Reversible inhibition of mitochondrial complex IV activity in PBMC following acute smoking', *Eur Respir J*, 23(2), pp. 214-8.

Ambra, R., Mocchegiani, E., Giacconi, R., Canali, R., Rinna, A., Malavolta, M. and Virgili, F. (2004) 'Characterization of the hsp70 response in lymphoblasts from aged and centenarian subjects and differential effects of in vitro zinc supplementation', *Exp Gerontol*, 39(10), pp. 1475-84.

Ames, B.N., Shigenaga, M.K. and Hagen, T.M. (1993) 'Oxidants, antioxidants, and the degenerative diseases of aging', *Proc Natl Acad Sci U S A*, 90(17), pp. 7915-22.

Amundson, S.A., Patterson, A., Do, K.T. and Fornace, A.J., Jr. (2002) 'A nucleotide excision repair master-switch: p53 regulated coordinate induction of global genomic repair genes', *Cancer Biology & Therapy*, 1(2), pp. 145-9.

Andreollo, N.A., Santos, E.F., Araujo, M.R. and Lopes, L.R. (2012) 'Rat's age versus human's age: what is the relationship?', *Arq Bras Cir Dig*, 25(1), pp. 49-51.

Armstrong, L., Saretzki, G., Peters, H., Wappler, I., Evans, J., Hole, N., von Zglinicki, T. and Lako, M. (2005) 'Overexpression of telomerase confers growth advantage, stress resistance, and enhanced differentiation of ESCs toward the hematopoietic lineage', *Stem Cells*, 23(4), pp. 516-29.

Arnheim, N. and Cortopassi, G. (1992) 'Deleterious mitochondrial DNA mutations accumulate in aging human tissues', *Mutat Res*, 275(3-6), pp. 157-67.

Ashrafi, G. and Schwarz, T.L. (2013) 'The pathways of mitophagy for quality control and clearance of mitochondria', *Cell Death Differ*, 20(1), pp. 31-42.

Atzmon, G., Cho, M., Cawthon, R.M., Budagov, T., Katz, M., Yang, X., Siegel, G., Bergman, A., Huffman, D.M., Schechter, C.B., Wright, W.E., Shay, J.W., Barzilai, N., Govindaraju, D.R. and Suh, Y. (2010) 'Evolution in health and medicine Sackler colloquium: Genetic variation in human telomerase is associated with telomere length in Ashkenazi centenarians', *Proceedings of the National Academy of Sciences of the United States of America*, 107 Suppl 1, pp. 1710-7.

Austad, S.N. (1989) 'Life extension by dietary restriction in the bowl and doily spider, Frontinella pyramitela', *Exp Gerontol*, 24(1), pp. 83-92.

Autexier, C. and Lue, N.F. (2006) 'The structure and function of telomerase reverse transcriptase', *Annu Rev Biochem*, 75, pp. 493-517.

Ayala-Torres, S., Chen, Y., Svoboda, T., Rosenblatt, J. and Van Houten, B. (2000) 'Analysis of gene-specific DNA damage and repair using quantitative polymerase chain reaction', *Methods*, 22(2), pp. 135-47.

Ayoub, N.A., McGowen, M.R., Clark, C., Springer, M.S. and Gatesy, J. (2009) 'Evolution and phylogenetic utility of the melanocortin-1 receptor gene (MC1R) in Cetartiodactyla', *Molecular Phylogenetics & Evolution*, 52(2), pp. 550-7.

Bacchetti, S. and Counter, C. (1995) 'Telomeres and telomerase in human cancer (review)', *Int J Oncol*, 7(3), pp. 423-32.

Baker, D.J. and Sedivy, J.M. (2013) 'Probing the depths of cellular senescence', *J Cell Biol*, 202(1), pp. 11-3.

Baker, D.J., Wijshake, T., Tchkonia, T., LeBrasseur, N.K., Childs, B.G., van de Sluis, B., Kirkland, J.L. and van Deursen, J.M. (2011) 'Clearance of p16Ink4a-positive senescent cells delays ageing-associated disorders', *Nature*, 479(7372), pp. 232-6.

Balagopal, P., Rooyackers, O.E., Adey, D.B., Ades, P.A. and Nair, K.S. (1997) 'Effects of aging on in vivo synthesis of skeletal muscle myosin heavy-chain and sarcoplasmic protein in humans', *Am J Physiol*, 273(4 Pt 1), pp. E790-800.

Balietti, M., Fattoretti, P., Giorgetti, B., Casoli, T., Di Stefano, G., Solazzi, M., Platano, D., Aicardi, G. and Bertoni-Freddari, C. (2009) 'A ketogenic diet increases succinic dehydrogenase activity in aging cardiomyocytes', *Ann N Y Acad Sci*, 1171, pp. 377-84.

Bandy, B. and Davison, A.J. (1990) 'Mitochondrial mutations may increase oxidative stress: implications for carcinogenesis and aging?', *Free Radical Biology & Medicine*, 8(6), pp. 523-39.

Baracca, A., Solaini, G., Sgarbi, G., Lenaz, G., Baruzzi, A., Schapira, A.H., Martinuzzi, A. and Carelli, V. (2005) 'Severe impairment of complex I-driven adenosine triphosphate synthesis in leber hereditary optic neuropathy cybrids', *Arch Neurol*, 62(5), pp. 730-6.

Barja, G. (2002) 'Rate of generation of oxidative stress-related damage and animal longevity', *Free Radical Biology & Medicine*, 33(9), pp. 1167-72.

Barja, G. (2013) 'Updating the mitochondrial free radical theory of aging: an integrated view, key aspects, and confounding concepts', *Antioxid Redox Signal*, 19(12), pp. 1420-45.

Barja, G., Cadenas, S., Rojas, C., Perez-Campo, R. and Lopez-Torres, M. (1994) 'Low mitochondrial free radical production per unit O2 consumption can

explain the simultaneous presence of high longevity and high aerobic metabolic rate in birds', *Free Radic Res*, 21(5), pp. 317-27.

Barja, G. and Herrero, A. (1998) 'Localization at complex I and mechanism of the higher free radical production of brain nonsynaptic mitochondria in the short-lived rat than in the longevous pigeon', *J Bioenerg Biomembr*, 30(3), pp. 235-43.

Barja, G. and Herrero, A. (2000) 'Oxidative damage to mitochondrial DNA is inversely related to maximum life span in the heart and brain of mammals', *Faseb j*, 14(2), pp. 312-8.

Barrientos, A. and Ugalde, C. (2013) 'I function, therefore I am: overcoming skepticism about mitochondrial supercomplexes', *Cell Metab*, 18(2), pp. 147-9.

Barritt, J.A., Cohen, J. and Brenner, C.A. (2000) 'Mitochondrial DNA point mutation in human oocytes is associated with maternal age', *Reproductive Biomedicine Online*, 1(3), pp. 96-100.

Bashkatov, A.N., Genina, E.A., Kochubey, V.I. and Tuchin, V.V. (2005) 'Optical properties of human skin, subcutaneous and mucous tissues in the wavelength range from 400 to 2000nm', *Journal of Physics D: Applied Physics*, 38, pp. 2543-2555.

Bass, T.M., Weinkove, D., Houthoofd, K., Gems, D. and Partridge, L. (2007) 'Effects of resveratrol on lifespan in Drosophila melanogaster and Caenorhabditis elegans', *Mech Ageing Dev*, 128(10), pp. 546-52.

Batra, P., Sharma, A.K. and Khajuria, R. (2013) 'Probing Lingzhi or Reishi medicinal mushroom Ganoderma lucidum (higher Basidiomycetes): a bitter mushroom with amazing health benefits', *Int J Med Mushrooms*, 15(2), pp. 127-43.

Baur, J.A., Pearson, K.J., Price, N.L., Jamieson, H.A., Lerin, C., Kalra, A., Prabhu, V.V., Allard, J.S., Lopez-Lluch, G., Lewis, K., Pistell, P.J., Poosala, S., Becker, K.G., Boss, O., Gwinn, D., Wang, M., Ramaswamy, S., Fishbein, K.W., Spencer, R.G., Lakatta, E.G., Le Couteur, D., Shaw, R.J., Navas, P., Puigserver, P., Ingram, D.K., de Cabo, R. and Sinclair, D.A. (2006) 'Resveratrol

improves health and survival of mice on a high-calorie diet', *Nature*, 444(7117), pp. 337-42.

Baur, J.A. and Sinclair, D.A. (2006) 'Therapeutic potential of resveratrol: the in vivo evidence', *Nat Rev Drug Discov*, 5(6), pp. 493-506.

Bech-Thomsen, N. and Wulf, H.C. (1992) 'Sunbathers' application of sunscreen is probably inadequate to obtain the sun protection factor assigned to the preparation', *Photodermatol Photoimmunol Photomed*, 9(6), pp. 242-4.

Beere, H.M. and Green, D.R. (2001) 'Stress management – heat shock protein-70 and the regulation of apoptosis', *Trends in Cell Biology*, 11(1), pp. 6-10.

Begeman, C.R. and Colucci, J.M. (1968) 'Benzo(a)pyrene in gasoline partially persists in automobile exhaust', *Science*, 161(3838), p. 271.

Beleza, S., Santos, A.M., McEvoy, B., Alves, I., Martinho, C., Cameron, E., Shriver, M.D., Parra, E.J. and Rocha, J. (2013) 'The timing of pigmentation lightening in Europeans', *Molecular Biology & Evolution*, 30(1), pp. 24-35.

Bellot, G.L. and Wang, X. (2013) 'Extra-Telomeric Effects of Telomerase (hTERT) in Cell Death', in Rudner, J. (ed.) *Apoptosis*. InTech.

Benard, G., Faustin, B., Passerieux, E., Galinier, A., Rocher, C., Bellance, N., Delage, J.P., Casteilla, L., Letellier, T. and Rossignol, R. (2006) 'Physiological diversity of mitochondrial oxidative phosphorylation', *Am J Physiol Cell Physiol*, 291(6), pp. C1172-82.

Benchoua, A., Trioulier, Y., Zala, D., Gaillard, M.C., Lefort, N., Dufour, N., Saudou, F., Elalouf, J.M., Hirsch, E., Hantraye, P., Deglon, N. and Brouillet, E. (2006) 'Involvement of mitochondrial complex II defects in neuronal death produced by N-terminus fragment of mutated huntingtin', *Mol Biol Cell. 2006 Apr;17(4):1652-63. Epub 2006 Feb 1.*

Bendová, H., Akrman, J., Krejčí, A., Kubáč, L., Jírová, D., Kejlová, K., Kolářová, H., Brabec, M. and Malý, M. (2007) 'In vitro approaches to evaluation of Sun Protection Factor', *Toxicology in Vitro*, 21(7), pp. 1268-1275.

Bensasson, D., Zhang, D.-X., Hartl, D.L. and Hewitt, G.M. (2001) 'Mitochondrial pseudogenes: evolution's misplaced witnesses', *Trends in Ecology & Evolution*, 16(6), pp. 314-321.

Berardi, R.R., Kroon, L.A., McDermott, J.H., Newton, G.D., Oszko, M.A., Popovich, N.G., Remington, T.L., Rollins, C.J., Shimp, L.A. and Tietze, K.J. (2006) *Handbook of Nonprescription Drugs*. APhA Publications.

Berdal, K.G. and Holst-Jensen, A. (2001) *Roundup Ready® soybean event-specific real-time quantitative PCR assay and estimation of the practical detection and quantification limits in GMO analyses*.

Berg, J.M., Tymoczko, J.L. and Stryer, L. (2002) 'The Citric Acid Cycle Is a Source of Biosynthetic Precursors', in *Biochemistry. 5th edition*. New York: W H Freeman.

Berg, J.M., Tymoczko, J.L. and Stryer, L. (2006) *Biochemistry*. 6th edn. W. H. Freeman.

Berg, O.G. and Kurland, C.G. (2000) 'Why mitochondrial genes are most often found in nuclei', *Mol Biol Evol*, 17(6), pp. 951-61.

Bernardes de Jesus, B., Vera, E., Schneeberger, K., Tejera, A.M., Ayuso, E., Bosch, F. and Blasco, M.A. (2012) 'Telomerase gene therapy in adult and old mice delays aging and increases longevity without increasing cancer', *EMBO Mol Med*, 4(8), pp. 691-704.

Berneburg, M., Plettenberg, H., Medve-Konig, K., Pfahlberg, A., Gers-Barlag, H., Gefeller, O. and Krutmann, J. (2004) 'Induction of the photoaging-associated mitochondrial common deletion in vivo in normal human skin', *J Invest Dermatol*, 122(5), pp. 1277-83.

Bernerd, F., Marionnet, C. and Duval, C. (2012) 'Solar ultraviolet radiation induces biological alterations in human skin in vitro: relevance of a well-balanced UVA/UVB protection', *Indian J Dermatol Venereol Leprol*, 78 Suppl 1, pp. S15-23.

Bérubé, M., Urbán, J., Dizon, A.E., Brownell, R.L. and Palsbøll, P.J. (2002) 'Genetic identification of a small and highly isolated population of fin whales

(Balaenoptera physalus) in the Sea of Cortez, México ', *Conservation Genetics*, 3(2), pp. 183-190.

Best, B.P. (2009) 'Nuclear DNA damage as a direct cause of aging', *Rejuvenation Res*, 12(3), pp. 199-208.

Bienert, G.P., Schjoerring, J.K. and Jahn, T.P. (2006) 'Membrane transport of hydrogen peroxide', *Biochim Biophys Acta*, 1758(8), pp. 994-1003.

Birch-Machin, M.A. (2006) 'The role of mitochondria in ageing and carcinogenesis', *Clinical & Experimental Dermatology*, 31(4), pp. 548-52.

Birch-Machin, M.A., Briggs, H.L., Saborido, A.A., Bindoff, L.A. and Turnbull, D.M. (1994) 'An evaluation of the measurement of the activities of complexes I-IV in the respiratory chain of human skeletal muscle mitochondria', *Biochem Med Metab Biol*, 51(1), pp. 35-42.

Birch-Machin, M.A. and Swalwell, H. (2010) 'How mitochondria record the effects of UV exposure and oxidative stress using human skin as a model tissue', *Mutagenesis*, 25(2), pp. 101-7.

Birch-Machin, M.A., Tindall, M., Turner, R., Haldane, F. and Rees, J.L. (1998) 'Mitochondrial DNA deletions in human skin reflect photo- rather than chronologic aging', *Journal of Investigative Dermatology*, 110(2), pp. 149-52.

Birch-Machin, M.A. and Turnbull, D.M. (2001) 'Assaying mitochondrial respiratory complex activity in mitochondria isolated from human cells and tissues', *Methods Cell Biol. 2001;65:97-117.*

Birket, M.J. and Birch-Machin, M.A. (2007) 'Ultraviolet radiation exposure accelerates the accumulation of the aging-dependent T414G mitochondrial DNA mutation in human skin', *Aging Cell*, 6(4), pp. 557-64.

Birket, M.J., Passos, J.F., von Zglinicki, T. and Birch-Machin, M.A. (2009) 'The relationship between the aging- and photo-dependent T414G mitochondrial DNA mutation with cellular senescence and reactive oxygen species production in cultured skin fibroblasts', *Journal of Investigative Dermatology*, 129(6), pp. 1361-6.

Blagosklonny, M.V. (2010) 'Why the disposable soma theory cannot explain why women live longer and why we age', *Aging (Albany NY)*, 2(12), pp. 884-7.

Blaustein, A.R., Romansic, J.M., Kiesecker, J.M. and Hatch, A.C. (2003) 'Ultraviolet radiation, toxic chemicals and amphibian population declines ', *Diversity and distributions*, 9, pp. 123–140.

Bleier, L. and Dröse, S. (2013) 'Superoxide generation by complex III: From mechanistic rationales to functional consequences', *Biochimica et Biophysica Acta (BBA) - Bioenergetics*, 1827(11–12), pp. 1320-1331.

Bodnar, A.G., Ouellette, M., Frolkis, M., Holt, S.E., Chiu, C.P., Morin, G.B., Harley, C.B., Shay, J.W., Lichtsteiner, S. and Wright, W.E. (1998) 'Extension of life-span by introduction of telomerase into normal human cells', *Science*, 279(5349), pp. 349-52.

Boehm, A.M., Khalturin, K., Anton-Erxleben, F., Hemmrich, G., Klostermeier, U.C., Lopez-Quintero, J.A., Oberg, H.H., Puchert, M., Rosenstiel, P., Wittlieb, J. and Bosch, T.C. (2012) 'FoxO is a critical regulator of stem cell maintenance in immortal Hydra', *Proc Natl Acad Sci U S A*, 109(48), pp. 19697-702.

Boffoli, D., Scacco, S.C., Vergari, R., Solarino, G., Santacroce, G. and Papa, S. (1994) 'Decline with age of the respiratory chain activity in human skeletal muscle', *Biochim Biophys Acta*, 1226(1), pp. 73-82.

Boldogh, I.R. and Pon, L.A. (2006) 'Interactions of mitochondria with the actin cytoskeleton', *Biochim Biophys Acta*, 1763(5-6), pp. 450-62.

Bouhours-Nouet, N., May-Panloup, P., Coutant, R., de Casson, F.B., Descamps, P., Douay, O., Reynier, P., Ritz, P., Malthiery, Y. and Simard, G. (2005) 'Maternal smoking is associated with mitochondrial DNA depletion and respiratory chain complex III deficiency in placenta', *Am J Physiol Endocrinol Metab*, 288(1), pp. E171-7.

Boukamp, P., Petrussevska, R.T., Breitkreutz, D., Hornung, J., Markham, A. and Fusenig, N.E. (1988) 'Normal keratinization in a spontaneously immortalized aneuploid human keratinocyte cell line', *J Cell Biol*, 106(3), pp. 761-71.

Bournay, E. and UNEP/GRID-Arendal (2007) *The global solar UV Index*. Available at: http://www.grida.no/graphicslib/detail/the-global-solar-uv-index_1394 (Accessed: 28.8.13).

Braidy, N., Guillemin, G.J., Mansour, H., Chan-Ling, T., Poljak, A. and Grant, R. (2011) 'Age related changes in NAD+ metabolism oxidative stress and Sirt1 activity in wistar rats', *PLoS One*, 6(4), p. e19194.

Brand, M.D., Buckingham, J.A., Esteves, T.C., Green, K., Lambert, A.J., Miwa, S., Murphy, M.P., Pakay, J.L., Talbot, D.A. and Echtay, K.S. (2004) 'Mitochondrial superoxide and aging: uncoupling-protein activity and superoxide production', *Biochem Soc Symp*, (71), pp. 203-13.

Brenner, M. and Hearing, V.J. (2008) 'The protective role of melanin against UV damage in human skin', *Photochemistry & Photobiology*, 84(3), pp. 539-49.

Broome, C.S., Kayani, A.C., Palomero, J., Dillmann, W.H., Mestril, R., Jackson, M.J. and McArdle, A. (2006) 'Effect of lifelong overexpression of HSP70 in skeletal muscle on age-related oxidative stress and adaptation after nondamaging contractile activity', *The FASEB Journal*, 20(9), pp. 1549-1551.

Brudnik, U., Branicki, W., Wojas-Pelc, A. and Kanas, P. (2009) 'The contribution of melanocortin 1 receptor gene polymorphisms and the agouti signalling protein gene 8818A>G polymorphism to cutaneous melanoma and basal cell carcinoma in a Polish population', *Experimental Dermatology*, 18(2), pp. 167-74.

Butow, R.A. and Avadhani, N.G. (2004) 'Mitochondrial signaling: the retrograde response', *Mol Cell*, 14(1), pp. 1-15.

Byun, H.O., Kim, H.Y., Lim, J.J., Seo, Y.H. and Yoon, G. (2008) 'Mitochondrial dysfunction by complex II inhibition delays overall cell cycle progression via reactive oxygen species production', *J Cell Biochem. 2008 Aug 1;104(5):1747-59. doi: 10.1002/jcb.21741.*

Cadenas, E., Boveris, A., Ragan, C.I. and Stoppani, A.O. (1977) 'Production of superoxide radicals and hydrogen peroxide by NADH-ubiquinone reductase and ubiquinol-cytochrome c reductase from beef-heart mitochondria', *Arch Biochem Biophys*, 180(2), pp. 248-57.

Calambokidis, J., Barlow, J., Ford, J.K.B., Chandler, T.E. and Douglas, A.B. (2009) 'Insights into the population structure of blue whales in the Eastern North Pacific from recent sightings and photographic identification', *Marine Mammal Science*, 25(4), pp. 816-832.

Calderwood, S.K., Murshid, A. and Prince, T. (2009) 'The shock of aging: molecular chaperones and the heat shock response in longevity and aging--a mini-review', *Gerontology*, 55(5), pp. 550-8.

Campisi, J. (2005) 'Senescent cells, tumor suppression, and organismal aging: good citizens, bad neighbors', *Cell*, 120(4), pp. 513-22.

Campisi, J. (2013) 'Aging, cellular senescence, and cancer', *Annu Rev Physiol*, 75, pp. 685-705.

Campisi, J. and d'Adda di Fagagna, F. (2007) 'Cellular senescence: when bad things happen to good cells', *Nat Rev Mol Cell Biol*, 8(9), pp. 729-40.

Cancer Research, U.K. (2012) *Skin cancer incidence statistics*. Available at: http://www.cancerresearchuk.org/cancer-info/cancerstats/types/skin/incidence/uk-skin-cancer-incidence-statistics#age (Accessed: 28.8.13).

Capel, F., Rimbert, V., Lioger, D., Diot, A., Rousset, P., Mirand, P.P., Boirie, Y., Morio, B. and Mosoni, L. (2005) 'Due to reverse electron transfer, mitochondrial H2O2 release increases with age in human vastus lateralis muscle although oxidative capacity is preserved', *Mech Ageing Dev*, 126(4), pp. 505-11.

Cardellach, F., Alonso, J.R., Lopez, S., Casademont, J. and Miro, O. (2003) 'Effect of smoking cessation on mitochondrial respiratory chain function', *J Toxicol Clin Toxicol*, 41(3), pp. 223-8.

Cawthon, R.M., Smith, K.R., O'Brien, E., Sivatchenko, A. and Kerber, R.A. (2003) 'Association between telomere length in blood and mortality in people aged 60 years or older', *The Lancet*, 361(9355), pp. 393-395.

Cecarini, V., Gee, J., Fioretti, E., Amici, M., Angeletti, M., Eleuteri, A.M. and Keller, J.N. (2007) 'Protein oxidation and cellular homeostasis: Emphasis on metabolism', *Biochimica et Biophysica Acta*, 1773(2), pp. 93-104.

Chan, S.W., Chevalier, S., Aprikian, A. and Chen, J.Z. (2013) 'Simultaneous quantification of mitochondrial DNA damage and copy number in circulating blood: a sensitive approach to systemic oxidative stress', *Biomed Res Int*, 2013, p. 157547.

Chen, F.G., Zhang, W.J., Bi, D., Liu, W., Wei, X., Chen, F.F., Zhu, L., Cui, L. and Cao, Y. (2007) 'Clonal analysis of nestin(-) vimentin(+) multipotent fibroblasts isolated from human dermis', *J Cell Sci*, 120(Pt 16), pp. 2875-83.

Choksi, K.B., Nuss, J.E., DeFord, J.H. and Papaconstantinou, J. (2011) 'Mitochondrial electron transport chain functions in long-lived Ames dwarf mice', *Aging (Albany NY)*, 3(8), pp. 754-67.

Chomyn, A. and Attardi, G. (2003) 'MtDNA mutations in aging and apoptosis', *Biochemical & Biophysical Research Communications*, 304(3), pp. 519-29.

Chretien, D., Rustin, P., Bourgeron, T., Rotig, A., Saudubray, J.M. and Munnich, A. (1994) 'Reference charts for respiratory chain activities in human tissues', *Clin Chim Acta*, 228(1), pp. 53-70.

Chuang, M.H., Chiou, S.H., Huang, C.H., Yang, W.B. and Wong, C.H. (2009) 'The lifespan-promoting effect of acetic acid and Reishi polysaccharide', *Bioorg Med Chem*, 17(22), pp. 7831-40.

Claus, C., Schonefeld, K., Hubner, D., Chey, S., Reibetanz, U. and Liebert, U.G. (2013) 'Activity increase in respiratory chain complexes by rubella virus with marginal induction of oxidative stress', *J Virol*, 87(15), pp. 8481-92.

Cocco, T., Sgobbo, P., Clemente, M., Lopriore, B., Grattagliano, I., Di Paola, M. and Villani, G. (2005) 'Tissue-specific changes of mitochondrial functions in aged rats: effect of a long-term dietary treatment with N-acetylcysteine', *Free Radic Biol Med. 2005 Mar 15;38(6):796-805.*

Coelho, S.G., Choi, W., Brenner, M., Miyamura, Y., Yamaguchi, Y., Wolber, R., Smuda, C., Batzer, J., Kolbe, L., Ito, S., Wakamatsu, K., Zmudzka, B.Z., Beer, J.Z., Miller, S.A. and Hearing, V.J. (2009) 'Short- and long-term effects of UV radiation on the pigmentation of human skin', *J Investig Dermatol Symp Proc*, 14(1), pp. 32-5.

Coggan, A.R., Spina, R.J., King, D.S., Rogers, M.A., Brown, M., Nemeth, P.M. and Holloszy, J.O. (1992) 'Histochemical and enzymatic comparison of the gastrocnemius muscle of young and elderly men and women', *J Gerontol*, 47(3), pp. B71-6.

Colman, R.J., Anderson, R.M., Johnson, S.C., Kastman, E.K., Kosmatka, K.J., Beasley, T.M., Allison, D.B., Cruzen, C., Simmons, H.A., Kemnitz, J.W. and Weindruch, R. (2009) 'Caloric restriction delays disease onset and mortality in rhesus monkeys', *Science*, 325(5937), pp. 201-4.

Conley, K.E., Jubrias, S.A. and Esselman, P.C. (2000) 'Oxidative capacity and ageing in human muscle', *J Physiol*, 526 Pt 1, pp. 203-10.

Cooper, J.M., Mann, V.M. and Schapira, A.H. (1992) 'Analyses of mitochondrial respiratory chain function and mitochondrial DNA deletion in human skeletal muscle: effect of ageing', *J Neurol Sci*, 113(1), pp. 91-8.

Cortopassi, G.A., Shibata, D., Soong, N.W. and Arnheim, N. (1992) 'A pattern of accumulation of a somatic deletion of mitochondrial DNA in aging human tissues', *Proc Natl Acad Sci U S A*, 89(16), pp. 7370-4.

Cosmedico (2013) *Cosmedico ARIMED B*. Available at: http://www.cosmedico-medizintechnik.de/english/uvb-therapie-lampen.htm (Accessed: 2.9.13).

Costin, G.E. and Hearing, V.J. (2007) 'Human skin pigmentation: melanocytes modulate skin color in response to stress', *FASEB J*, 21(4), pp. 976-94.

Croll, D.A., Acevedo-Gutierrez, A., Tershy, B.R. and Urban-Ramirez, J. (2001) 'The diving behavior of blue and fin whales: is dive duration shorter than expected based on oxygen stores?', *Comparative Biochemistry & Physiology*, Part A, Molecular & Integrative Physiology. 129(4), pp. 797-809.

Croteau, D.L., Stierum, R.H. and Bohr, V.A. (1999) 'Mitochondrial DNA repair pathways', *Mutat Res*, 434(3), pp. 137-48.

Cruciat, C.M., Brunner, S., Baumann, F., Neupert, W. and Stuart, R.A. (2000) 'The cytochrome bc1 and cytochrome c oxidase complexes associate to form a single supracomplex in yeast mitochondria', *J Biol Chem*, 275(24), pp. 18093-8.

Cui, H., Kong, Y. and Zhang, H. (2012) 'Oxidative stress, mitochondrial dysfunction, and aging', *J Signal Transduct*, 2012, p. 646354.

Da Poian, A.T., El-Bacha, T. and Luz, M.R.M.P. (2010) 'Nutrient Utilization in Humans: Metabolism Pathways', *Nature Education* 3(9), p. 11.

Dahms, H.-U. and Lee, J.-S. (2010) 'UV radiation in marine ectotherms: molecular effects and responses', *Aquatic Toxicology*, 97(1), pp. 3-14.

Dameris, M. (2010) 'Depletion of the ozone layer in the 21st century', *Angewandte Chemie. International Ed. in English*, 49(3), pp. 489-91.

Daniels, D.J., Clothier, C., Swan, D.C. and Saretzki, G. (2010) 'Immediate and gradual gene expression changes in telomerase over-expressing fibroblasts', *Biochemical and Biophysical Research Communications*, 399(1), pp. 7-13.

Das, S., Lloyd, J.J., Walshaw, D., Diffey, B.L. and Farr, P.M. (2002) 'Response of psoriasis to sunbed treatment: comparison of conventional ultraviolet A lamps with new higher ultraviolet B-emitting lamps', *Br J Dermatol*, 147(5), pp. 966-72.

Dayal, D., Martin, S.M., Owens, K.M., Aykin-Burns, N., Zhu, Y., Boominathan, A., Pain, D., Limoli, C.L., Goswami, P.C., Domann, F.E. and Spitz, D.R. (2009) 'Mitochondrial complex II dysfunction can contribute significantly to genomic instability after exposure to ionizing radiation', *Radiat Res*, 172(6), pp. 737-45.

De Gruijl, F.R. (1997) 'Health effects from solar UV radiation', *Radiation Protection Dosimetry*, 72, pp. 177–196.

De la Coba, F., Aguilera, J., de Galvez, M.V., Alvarez, M., Gallego, E., Figueroa, F.L. and Herrera, E. (2009) 'Prevention of the ultraviolet effects on clinical and histopathological changes, as well as the heat shock protein-70 expression in mouse skin by topical application of algal UV-absorbing compounds', *Journal of Dermatological Science*, 55(3), pp. 161-9.

Dekker, P., Maier, A.B., van Heemst, D., de Koning-Treurniet, C., Blom, J., Dirks, R.W., Tanke, H.J. and Westendorp, R.G. (2009) 'Stress-induced responses of human skin fibroblasts in vitro reflect human longevity', *Aging Cell*, 8(5), pp. 595-603.

Desler, C., Marcker, M.L., Singh, K.K. and Rasmussen, L.J. (2011) 'The importance of mitochondrial DNA in aging and cancer', *J Aging Res*, 2011, p. 407536.

Diffey, B.L. (2002) 'Sources and measurement of ultraviolet radiation', *Methods*, 28(1), pp. 4-13.

Dillin, A., Hsu, A.L., Arantes-Oliveira, N., Lehrer-Graiwer, J., Hsin, H., Fraser, A.G., Kamath, R.S., Ahringer, J. and Kenyon, C. (2002) 'Rates of behavior and aging specified by mitochondrial function during development', *Science*, 298(5602), pp. 2398-401.

Dimri, G.P., Lee, X., Basile, G., Acosta, M., Scott, G., Roskelley, C., Medrano, E.E., Linskens, M., Rubelj, I., Pereira-Smith, O. and et al. (1995) 'A biomarker that identifies senescent human cells in culture and in aging skin in vivo', *Proc Natl Acad Sci U S A*, 92(20), pp. 9363-7.

Djavaheri-Mergny, M., Marsac, C., Maziere, C., Santus, R., Michel, L., Dubertret, L. and Maziere, J.C. (2001) 'UV-A irradiation induces a decrease in the mitochondrial respiratory activity of human NCTC 2544 keratinocytes', *Free Radic Res*, 34(6), pp. 583-94.

Dlaskova, A., Hlavata, L. and Jezek, P. (2008) 'Oxidative stress caused by blocking of mitochondrial complex I H(+) pumping as a link in aging/disease vicious cycle', *Int J Biochem Cell Biol*, 40(9), pp. 1792-805.

Dobson, G.P. (2003) 'On being the right size: heart design, mitochondrial efficiency and lifespan potential', *Clinical & Experimental Pharmacology & Physiology*, 30(8), pp. 590-7.

Drew, B., Phaneuf, S., Dirks, A., Selman, C., Gredilla, R., Lezza, A., Barja, G. and Leeuwenburgh, C. (2003) 'Effects of aging and caloric restriction on mitochondrial energy production in gastrocnemius muscle and heart', *Am J Physiol Regul Integr Comp Physiol*, 284(2), pp. R474-80.

Driver, C. and Georgeou, A. (2003) 'Variable effects of vitamin E on Drosophila longevity', *Biogerontology*, 4(2), pp. 91-5.

Dröse, S. (2013) 'Differential effects of complex II on mitochondrial ROS production and their relation to cardioprotective pre- and postconditioning', *Biochimica et Biophysica Acta (BBA) - Bioenergetics*, 1827(5), pp. 578-587.

Drouet, M., Lauthier, F., Charmes, J.P., Sauvage, P. and Ratinaud, M.H. (1999) 'Age-associated changes in mitochondrial parameters on peripheral human lymphocytes', *Exp Gerontol*, 34(7), pp. 843-52.

Dudkina, N.V., Sunderhaus, S., Boekema, E.J. and Braun, H.P. (2008) 'The higher level of organization of the oxidative phosphorylation system: mitochondrial supercomplexes', *J Bioenerg Biomembr*, 40(5), pp. 419-24.

Duno, M., Wibrand, F., Baggesen, K., Rosenberg, T., Kjaer, N. and Frederiksen, A.L. (2013) 'A novel mitochondrial mutation m.8989G>C associated with neuropathy, ataxia, retinitis pigmentosa - the NARP syndrome', *Gene*, 515(2), pp. 372-5.

Durham, S.E., Krishnan, K.J., Betts, J. and Birch-Machin, M.A. (2003) 'Mitochondrial DNA damage in non-melanoma skin cancer', *British Journal of Cancer*, 88(1), pp. 90-5.

Durieux, J., Wolff, S. and Dillin, A. (2011) 'The cell-non-autonomous nature of electron transport chain-mediated longevity', *Cell*, 144(1), pp. 79-91.

Dutta, D., Calvani, R., Bernabei, R., Leeuwenburgh, C. and Marzetti, E. (2012) 'Contribution of impaired mitochondrial autophagy to cardiac aging: mechanisms and therapeutic opportunities', *Circ Res*, 110(8), pp. 1125-38.

Efrati, E., Tocco, G., Eritja, R., Wilson, S.H. and Goodman, M.F. (1999) '"Action-at-a-distance" mutagenesis. 8-oxo-7, 8-dihydro-2'-deoxyguanosine causes base substitution errors at neighboring template sites when copied by DNA polymerase beta', *Journal of Biological Chemistry*, 274(22), pp. 15920-6.

Eischeid, A.C. (2011) 'SYTO dyes and EvaGreen outperform SYBR Green in real-time PCR', *BMC Res Notes*, 4, p. 263.

Eischeid, A.C., Meyer, J.N. and Linden, K.G. (2009) 'UV disinfection of adenoviruses: molecular indications of DNA damage efficiency', *Applied & Environmental Microbiology*, 75(1), pp. 23-8.

Eller, M.S., Ostrom, K. and Gilchrest, B.A. (1996) 'DNA damage enhances melanogenesis', *Proc Natl Acad Sci U S A*, 93(3), pp. 1087-92.

Elston, T., Wang, H. and Oster, G. (1998) 'Energy transduction in ATP synthase', *Nature*, 391(6666), pp. 510-3.

Esposito, L.A., Melov, S., Panov, A., Cottrell, B.A. and Wallace, D.C. (1999) 'Mitochondrial disease in mouse results in increased oxidative stress', *Proceedings of the National Academy of Sciences of the United States of America*, 96(9), pp. 4820-5.

Eyer, P., Worek, F., Kiderlen, D., Sinko, G., Stuglin, A., Simeon-Rudolf, V. and Reiner, E. (2003) 'Molar absorption coefficients for the reduced Ellman reagent: reassessment', *Anal Biochem*, 312(2), pp. 224-7.

Fabian, D. and Flatt, T. (2011) 'The Evolution of Aging', *Nature Education Knowledge*, 3(10), p. 9.

Fabrizio, P., Liou, L.L., Moy, V.N., Diaspro, A., Valentine, J.S., Gralla, E.B. and Longo, V.D. (2003) 'SOD2 functions downstream of Sch9 to extend longevity in yeast', *Genetics*, 163(1), pp. 35-46.

Fernández-Vizarra, E., Enríquez, J.A., Pérez-Martos, A., Montoya, J. and Fernández-Silva, P. (2011) 'Tissue-specific differences in mitochondrial activity and biogenesis', *Mitochondrion*, 11(1), pp. 207-213.

Finch, C.E. (2012) 'Evolution of the human lifespan, past, present, and future: phases in the evolution of human life expectancy in relation to the inflammatory load', *Proc Am Philos Soc*, 156(1), pp. 9-44.

Finkel, T. and Holbrook, N.J. (2000) 'Oxidants, oxidative stress and the biology of ageing', *Nature*, 408(6809), pp. 239-47.

Fischer, F., Hamann, A. and Osiewacz, H.D. (2012) 'Mitochondrial quality control: an integrated network of pathways', *Trends Biochem Sci*, 37(7), pp. 284-92.

Flores, S., Gorouhi, F. and Maibach, H.I. (2010) *Textbook of Aging Skin*.

Franco, S., MacKenzie, K.L., Dias, S., Alvarez, S., Rafii, S. and Moore, M.A. (2001) 'Clonal variation in phenotype and life span of human embryonic fibroblasts (MRC-5) transduced with the catalytic component of telomerase (hTERT)', *Exp Cell Res*, 268(1), pp. 14-25.

Frosch, Z.A.K., Dierker, L.C., Rose, J.S. and Waldinger, R.J. (2009) 'Smoking trajectories, health, and mortality across the adult lifespan', *Addictive Behaviors*, 34(8), pp. 701-704.

Gagliano, N., Grizzi, F. and Annoni, G. (2007) 'Mechanisms of aging and liver functions', *Dig Dis*, 25(2), pp. 118-23.

Geng, S., Zhou, S. and Glowacki, J. (2011) 'Age-related decline in osteoblastogenesis and 1alpha-hydroxylase/CYP27B1 in human mesenchymal stem cells: stimulation by parathyroid hormone', *Aging Cell*, 10(6), pp. 962-71.

Gilbert, M.T.P., Willerslev, E., Hansen, A.J., Barnes, I., Rudbeck, L., Lynnerup, N. and Cooper, A. (2003) 'Distribution Patterns of Postmortem Damage in Human Mitochondrial DNA', *The American Journal of Human Genetics*, 72(1), pp. 32-47.

Goffart, S., Von Kleist-Retzow, J.C. and Wiesner, R.J. (2004) 'Regulation of mitochondrial proliferation in the heart: Power-plant failure contributes to cardiac failure in hypertrophy', *Cardiovascular Research*, 64(2), pp. 198-207.

Goldsmith, T.C. (2004) 'Aging as an evolved characteristic - Weismann's theory reconsidered', *Med Hypotheses*, 62(2), pp. 304-8.

Gómez, L.A. and Hagen, T.M. (2012) 'Age-related decline in mitochondrial bioenergetics: Does supercomplex destabilization determine lower oxidative capacity and higher superoxide production?', *Seminars in Cell & Developmental Biology*, 23(7), pp. 758-767.

Gredilla, R., Bohr, V.A. and Stevnsner, T. (2010) 'Mitochondrial DNA repair and association with aging--an update', *Exp Gerontol*, 45(7-8), pp. 478-88.

Greider, C.W. and Blackburn, E.H. (1985) 'Identification of a specific telomere terminal transferase activity in Tetrahymena extracts', *Cell*, 43(2 Pt 1), pp. 405-13.

Guo, J. and Lemire, B.D. (2003) 'The ubiquinone-binding site of the Saccharomyces cerevisiae succinate-ubiquinone oxidoreductase is a source of superoxide', *J Biol Chem. 2003 Nov 28;278(48):47629-35. Epub 2003 Sep 16.*

Haake, A., Scott, G.A. and Holbrook, K.A. (2001) *Structure and function of the skin: Overview of the epidermis and dermis*. Parthenon Publishing Group Ltd.

Hackenbrock, C.R., Chazotte, B. and Gupte, S.S. (1986) 'The random collision model and a critical assessment of diffusion and collision in mitochondrial electron transport', *J Bioenerg Biomembr*, 18(5), pp. 331-68.

Haendeler, J., Drose, S., Buchner, N., Jakob, S., Altschmied, J., Goy, C., Spyridopoulos, I., Zeiher, A.M., Brandt, U. and Dimmeler, S. (2009) 'Mitochondrial telomerase reverse transcriptase binds to and protects mitochondrial DNA and function from damage', *Arterioscler Thromb Vasc Biol*, 29(6), pp. 929-35.

Hagen, T.M., Yowe, D.L., Bartholomew, J.C., Wehr, C.M., Do, K.L., Park, J.Y. and Ames, B.N. (1997) 'Mitochondrial decay in hepatocytes from old rats: membrane potential declines, heterogeneity and oxidants increase', *Proc Natl Acad Sci U S A*, 94(7), pp. 3064-9.

Haigis, M.C., Deng, C.X., Finley, L.W., Kim, H.S. and Gius, D. (2012) 'SIRT3 is a mitochondrial tumor suppressor: a scientific tale that connects aberrant cellular ROS, the Warburg effect, and carcinogenesis', *Cancer Res*, 72(10), pp. 2468-72.

Hamilton, M.L., Van Remmen, H., Drake, J.A., Yang, H., Guo, Z.M., Kewitt, K., Walter, C.A. and Richardson, A. (2001) 'Does oxidative damage to DNA increase with age?', *Proc Natl Acad Sci U S A*, 98(18), pp. 10469-74.

Harbottle, A. and Birch-Machin, M.A. (2006) 'Real-time PCR analysis of a 3895 bp mitochondrial DNA deletion in nonmelanoma skin cancer and its use as a quantitative marker for sunlight exposure in human skin', *British Journal of Cancer*, 94(12), pp. 1887-93.

Harbottle, A., Maki, J., Reguly, B., Wittock, R., Robinson, K., Parr, R. and Birch-Machin, M.A. (2010) 'Real-time polymerase chain reaction analysis of a 3895-

bp mitochondrial DNA deletion in epithelial swabs and its use as a quantitative marker for sunlight exposure in human skin', *British Journal of Dermatology*, 163(6), pp. 1291-5.

Harley, C.B., Futcher, A.B. and Greider, C.W. (1990) 'Telomeres shorten during ageing of human fibroblasts', *Nature*, 345(6274), pp. 458-60.

Harley, C.B., Vaziri, H., Counter, C.M. and Allsopp, R.C. (1992) 'The telomere hypothesis of cellular aging', *Exp Gerontol*, 27(4), pp. 375-82.

Harman, D. (1956) 'Aging: a theory based on free radical and radiation chemistry', *Journal of Gerontology*, 11(3), pp. 298-300.

Harman, D. (1972) 'The biologic clock: the mitochondria?', *Journal of the American Geriatrics Society*, 20(4), pp. 145-7.

Hashiguchi, K. and Zhang-Akiyama, Q.M. (2009) 'Establishment of human cell lines lacking mitochondrial DNA', *Methods Mol Biol*, 554, pp. 383-91.

Hayakawa, M., Hattori, K., Sugiyama, S. and Ozawa, T. (1992) 'Age-associated oxygen damage and mutations in mitochondrial DNA in human hearts', *Biochemical & Biophysical Research Communications*, 189(2), pp. 979-85.

Hayashi, J., Ohta, S., Kagawa, Y., Kondo, H., Kaneda, H., Yonekawa, H., Takai, D. and Miyabayashi, S. (1994) 'Nuclear but not mitochondrial genome involvement in human age-related mitochondrial dysfunction. Functional integrity of mitochondrial DNA from aged subjects', *J Biol Chem. 1994 Mar 4;269(9):6878-83.*

Hayflick, L. (1965) 'THE LIMITED IN VITRO LIFETIME OF HUMAN DIPLOID CELL STRAINS', *Exp Cell Res*, 37, pp. 614-36.

Hayflick, L. and Moorhead, P.S. (1961) 'The serial cultivation of human diploid cell strains', *Exp Cell Res*, 25, pp. 585-621.

Heckman, C.J., Chandler, R., Kloss, J.D., Benson, A., Rooney, D., Munshi, T., Darlow, S.D., Perlis, C., Manne, S.L. and Oslin, D.W. (2013) 'Minimal Erythema Dose (MED) testing', *J Vis Exp*, (75), p. e50175.

Herbig, U., Ferreira, M., Condel, L., Carey, D. and Sedivy, J.M. (2006) 'Cellular senescence in aging primates', *Science*, 311(5765), p. 1257.

Herrero, A. and Barja, G. (1998) 'H2O2 production of heart mitochondria and aging rate are slower in canaries and parakeets than in mice: sites of free radical generation and mechanisms involved', *Mechanisms of Ageing & Development*, 103(2), pp. 133-46.

Hewitt, G., Jurk, D., Marques, F.D., Correia-Melo, C., Hardy, T., Gackowska, A., Anderson, R., Taschuk, M., Mann, J. and Passos, J.F. (2012) 'Telomeres are favoured targets of a persistent DNA damage response in ageing and stress-induced senescence', *Nat Commun*, 3, p. 708.

Heydari, A.R., Takahashi, R., Gutsmann, A., You, S. and Richardson, A. (1994) 'Hsp70 and aging', *Experientia*, 50(11-12), pp. 1092-1098.

Heydari, A.R., Wu, B., Takahashi, R., Strong, R. and Richardson, A. (1993) 'Expression of heat shock protein 70 is altered by age and diet at the level of transcription', *Molecular and Cellular Biology*, 13(5), pp. 2909-2918.

Hirsch, C., Gauss, R. and Sommer, T. (2006) 'Coping with stress: cellular relaxation techniques', *Trends Cell Biol*, 16(12), pp. 657-63.

Hirst, J., King, M.S. and Pryde, K.R. (2008) 'The production of reactive oxygen species by complex I', *Biochem Soc Trans*, 36(Pt 5), pp. 976-80.

Ho, P.W., Ho, J.W., Tse, H.M., So, D.H., Yiu, D.C., Liu, H.F., Chan, K.H., Kung, M.H., Ramsden, D.B. and Ho, S.L. (2012) 'Uncoupling protein-4 (UCP4) increases ATP supply by interacting with mitochondrial Complex II in neuroblastoma cells', *PLoS One*, 7(2), p. e32810.

Hogg, N., Darley-Usmar, V.M., Wilson, M.T. and Moncada, S. (1992) 'Production of hydroxyl radicals from the simultaneous generation of superoxide and nitric oxide', *Biochemical Journal*, 281(Pt 2), pp. 419-24.

Hornig-Do, H.T., von Kleist-Retzow, J.C., Lanz, K., Wickenhauser, C., Kudin, A.P., Kunz, W.S., Wiesner, R.J. and Schauen, M. (2007) 'Human epidermal keratinocytes accumulate superoxide due to low activity of Mn-SOD, leading to mitochondrial functional impairment', *J Invest Dermatol*, 127(5), pp. 1084-93.

Hoshino, T., Matsuda, M., Yamashita, Y., Takehara, M., Fukuya, M., Mineda, K., Maji, D., Ihn, H., Adachi, H., Sobue, G., Funasaka, Y. and Mizushima, T. (2010) 'Suppression of melanin production by expression of HSP70', *J Biol Chem*, 285(17), pp. 13254-63.

Hosokawa, H., Ishii, N., Ishida, H., Ichimori, K., Nakazawa, H. and Suzuki, K. (1994) 'Rapid accumulation of fluorescent material with aging in an oxygen-sensitive mutant mev-1 of Caenorhabditis elegans', *Mech Ageing Dev. 1994 Jun;74(3):161-70.*

Howitz, K.T., Bitterman, K.J., Cohen, H.Y., Lamming, D.W., Lavu, S., Wood, J.G., Zipkin, R.E., Chung, P., Kisielewski, A., Zhang, L.L., Scherer, B. and Sinclair, D.A. (2003) 'Small molecule activators of sirtuins extend Saccharomyces cerevisiae lifespan', *Nature*, 425(6954), pp. 191-6.

Hsu, A.L., Murphy, C.T. and Kenyon, C. (2003) 'Regulation of aging and age-related disease by DAF-16 and heat-shock factor', *Science*, 300(5622), pp. 1142-5.

Huang, J. and Lemire, B.D. (2009) 'Mutations in the C. elegans succinate dehydrogenase iron-sulfur subunit promote superoxide generation and premature aging', *J Mol Biol. 2009 Apr 3;387(3):559-69. doi: 10.1016/j.jmb.2009.02.028. Epub 2009 Feb 20.*

Hudson, E.K., Hogue, B.A., Souza-Pinto, N.C., Croteau, D.L., Anson, R.M., Bohr, V.A. and Hansford, R.G. (1998) 'Age-associated change in mitochondrial DNA damage', *Free Radic Res*, 29(6), pp. 573-9.

Hughes, O.R., Stewart, R., Dimmick, I. and Jones, E.A. (2009) 'A critical appraisal of factors affecting the accuracy of results obtained when using flow cytometry in stem cell investigations: where do you put your gates?', *Cytometry A*, 75(9), pp. 803-10.

Hulbert, A.J., Pamplona, R., Buffenstein, R. and Buttemer, W.A. (2007) 'Life and death: metabolic rate, membrane composition, and life span of animals', *Physiological Reviews*, 87(4), pp. 1175-213.

Hunter, S.E., Jung, D., Di Giulio, R.T. and Meyer, J.N. (2010) 'The QPCR assay for analysis of mitochondrial DNA damage, repair, and relative copy number', *Methods*, 51(4), pp. 444-51.

Hursting, S.D., Lavigne, J.A., Berrigan, D., Perkins, S.N. and Barrett, J.C. (2003) 'Calorie restriction, aging, and cancer prevention: mechanisms of action and applicability to humans', *Annu Rev Med*, 54, pp. 131-52.

Hutter, E., Skovbro, M., Lener, B., Prats, C., Rabol, R., Dela, F. and Jansen-Durr, P. (2007) 'Oxidative stress and mitochondrial impairment can be separated from lipofuscin accumulation in aged human skeletal muscle', *Aging Cell*, 6(2), pp. 245-56.

Ichihashi, M., Ueda, M., Budiyanto, A., Bito, T., Oka, M., Fukunaga, M., Tsuru, K. and Horikawa, T. (2003) 'UV-induced skin damage', *Toxicology*, 189(1-2), pp. 21-39.

Iizuka, H. (1994) 'Epidermal turnover time', *J Dermatol Sci*, 8(3), pp. 215-7.

Imokawa, G. (2008) 'Recent advances in characterizing biological mechanisms underlying UV-induced wrinkles: a pivotal role of fibrobrast-derived elastase', *Archives of Dermatological Research*, 300 Suppl 1, pp. S7-20.

Indran, I.R., Hande, M.P. and Pervaiz, S. (2011) 'hTERT overexpression alleviates intracellular ROS production, improves mitochondrial function, and inhibits ROS-mediated apoptosis in cancer cells', *Cancer Res*, 71(1), pp. 266-76.

Ishii, N., Fujii, M., Hartman, P.S., Tsuda, M., Yasuda, K., Senoo-Matsuda, N., Yanase, S., Ayusawa, D. and Suzuki, K. (1998) 'A mutation in succinate dehydrogenase cytochrome b causes oxidative stress and ageing in nematodes', *Nature. 1998 Aug 13;394(6694):694-7.*

Ishii, N., Senoo-Matsuda, N., Miyake, K., Yasuda, K., Ishii, T., Hartman, P.S. and Furukawa, S. (2004) 'Coenzyme Q10 can prolong C. elegans lifespan by lowering oxidative stress', *Mech Ageing Dev. 2004 Jan;125(1):41-6.*

Ishii, T., Yasuda, K., Akatsuka, A., Hino, O., Hartman, P.S. and Ishii, N. (2005) 'A mutation in the SDHC gene of complex II increases oxidative stress, resulting in apoptosis and tumorigenesis', *Cancer Res. 2005 Jan 1;65(1):203-9.*

Isobe, K., Ito, S., Hosaka, H., Iwamura, Y., Kondo, H., Kagawa, Y. and Hayashi, J.I. (1998) 'Nuclear-recessive mutations of factors involved in mitochondrial translation are responsible for age-related respiration deficiency of human skin fibroblasts', *J Biol Chem. 1998 Feb 20;273(8):4601-6.*

Itahana, K., Campisi, J. and Dimri, G.P. (2007) 'Methods to detect biomarkers of cellular senescence: the senescence-associated beta-galactosidase assay', *Methods Mol Biol*, 371, pp. 21-31.

Itoh, H. and Srere, P.A. (1970) 'A new assay for glutamate-oxaloacetate transaminase', *Anal Biochem*, 35(2), pp. 405-10.

Jablonski, N.G. and Chaplin, G. (2010) 'Colloquium paper: human skin pigmentation as an adaptation to UV radiation', *Proc Natl Acad Sci U S A*, 107 Suppl 2, pp. 8962-8.

Jablonski, N.G. and Chaplin, G. (2012) 'Human skin pigmentation, migration and disease susceptibility', *Philos Trans R Soc Lond B Biol Sci*, 367(1590), pp. 785-92.

Jakob, S. and Haendeler, J. (2007) 'Molecular mechanisms involved in endothelial cell aging: role of telomerase reverse transcriptase', *Z Gerontol Geriatr*, 40(5), pp. 334-8.

Jandova, J., Eshaghian, A., Shi, M., Li, M., King, L.E., Janda, J. and Sligh, J.E. (2012) 'Identification of an mtDNA Mutation Hot Spot in UV-Induced Mouse Skin Tumors Producing Altered Cellular Biochemistry', *J Invest Dermatol*, 132(2), pp. 421-428.

Janeway, K.A., Kim, S.Y., Lodish, M., Nose, V., Rustin, P., Gaal, J., Dahia, P.L., Liegl, B., Ball, E.R., Raygada, M., Lai, A.H., Kelly, L., Hornick, J.L., O'Sullivan, M., de Krijger, R.R., Dinjens, W.N., Demetri, G.D., Antonescu, C.R., Fletcher, J.A., Helman, L. and Stratakis, C.A. (2011) 'Defects in succinate

dehydrogenase in gastrointestinal stromal tumors lacking KIT and PDGFRA mutations', *Proc Natl Acad Sci U S A*, 108(1), pp. 314-8.

Jang, M., Cai, L., Udeani, G.O., Slowing, K.V., Thomas, C.F., Beecher, C.W., Fong, H.H., Farnsworth, N.R., Kinghorn, A.D., Mehta, R.G., Moon, R.C. and Pezzuto, J.M. (1997) 'Cancer chemopreventive activity of resveratrol, a natural product derived from grapes', *Science*, 275(5297), pp. 218-20.

Jang, Y.C., Perez, V.I., Song, W., Lustgarten, M.S., Salmon, A.B., Mele, J., Qi, W., Liu, Y., Liang, H., Chaudhuri, A., Ikeno, Y., Epstein, C.J., Van Remmen, H. and Richardson, A. (2009) 'Overexpression of Mn superoxide dismutase does not increase life span in mice', *J Gerontol A Biol Sci Med Sci*, 64(11), pp. 1114-25.

Jaskelioff, M., Muller, F.L., Paik, J.H., Thomas, E., Jiang, S., Adams, A.C., Sahin, E., Kost-Alimova, M., Protopopov, A., Cadinanos, J., Horner, J.W., Maratos-Flier, E. and Depinho, R.A. (2011) 'Telomerase reactivation reverses tissue degeneration in aged telomerase-deficient mice', *Nature*, 469(7328), pp. 102-6.

Jenkins, G. (2002) 'Molecular mechanisms of skin ageing', *Mechanisms of Ageing and Development*, 123(7), pp. 801-810.

Jonckheere, A.I., Smeitink, J.A. and Rodenburg, R.J. (2012) 'Mitochondrial ATP synthase: architecture, function and pathology', *J Inherit Metab Dis*, 35(2), pp. 211-25.

Jung, D., Cho, Y., Meyer, J.N. and Di Giulio, R.T. (2009) 'The long amplicon quantitative PCR for DNA damage assay as a sensitive method of assessing DNA damage in the environmental model, Atlantic killifish (Fundulus heteroclitus)', *Comparative Biochemistry & Physiology*, Toxicology & Pharmacology: Cbp. 149(2), pp. 182-6.

Kalinowski, D.P., Illenye, S. and Van Houten, B. (1992) 'Analysis of DNA damage and repair in murine leukemia L1210 cells using a quantitative polymerase chain reaction assay', *Nucleic Acids Research*, 20(13), pp. 3485-94.

Kaneko, N., Vierkoetter, A., Kraemer, U., Sugiri, D., Matsui, M., Yamamoto, A., Krutmann, J. and Morita, A. (2012) 'Mitochondrial common deletion mutation and extrinsic skin ageing in German and Japanese women', *Exp Dermatol*, 21 Suppl 1, pp. 26-30.

Kang, T.W., Yevsa, T., Woller, N., Hoenicke, L., Wuestefeld, T., Dauch, D., Hohmeyer, A., Gereke, M., Rudalska, R., Potapova, A., Iken, M., Vucur, M., Weiss, S., Heikenwalder, M., Khan, S., Gil, J., Bruder, D., Manns, M., Schirmacher, P., Tacke, F., Ott, M., Luedde, T., Longerich, T., Kubicka, S. and Zender, L. (2011) 'Senescence surveillance of pre-malignant hepatocytes limits liver cancer development', *Nature*, 479(7374), pp. 547-51.

Kapa Biosystems, U.K. (2013) *KAPA Library Amplification Kits*. Available at: http://www.kapabiosystems.com/products/name/kapa-library-amplification-kits (Accessed: 28.8.13).

Kemnitz, J.W., Weindruch, R., Roecker, E.B., Crawford, K., Kaufman, P.L. and Ershler, W.B. (1993) 'Dietary restriction of adult male rhesus monkeys: design, methodology, and preliminary findings from the first year of study', *J Gerontol*, 48(1), pp. B17-26.

Kennedy, C., ter Huurne, J., Berkhout, M., Gruis, N., Bastiaens, M., Bergman, W., Willemze, R. and Bavinck, J.N. (2001) 'Melanocortin 1 receptor (MC1R) gene variants are associated with an increased risk for cutaneous melanoma which is largely independent of skin type and hair color', *Journal of Investigative Dermatology*, 117(2), pp. 294-300.

Khan, S.A., Sung, K. and Nawaz, M.S. (2011) 'Detection of aacA-aphD, qacEÎ´1, marA, floR, and tetA genes from multidrug-resistant bacteria: Comparative analysis of real-time multiplex PCR assays using EvaGreenÂ® and SYBRÂ® Green I dyes', *Molecular and Cellular Probes*, 25(2â€“3), pp. 78-86.

Khansari, N., Shakiba, Y. and Mahmoudi, M. (2009) 'Chronic inflammation and oxidative stress as a major cause of age-related diseases and cancer', *Recent Pat Inflamm Allergy Drug Discov*, 3(1), pp. 73-80.

Kiesecker, J.M., Blaustein, A.R. and Belden, L.K. (2001) 'Complex causes of amphibian population declines', *Nature*, 410(6829), pp. 681-4.

Kim, N.W., Piatyszek, M.A., Prowse, K.R., Harley, C.B., West, M.D., Ho, P.L., Coviello, G.M., Wright, W.E., Weinrich, S.L. and Shay, J.W. (1994) 'Specific association of human telomerase activity with immortal cells and cancer', *Science*, 266(5193), pp. 2011-5.

Kirby, D. (2012) *Death at SeaWorld: Shamu and the Dark Side of Killer Whales in Captivity* St. Martin's Press.

Kirby, D.M., Thorburn, D.R., Turnbull, D.M. and Taylor, R.W. (2007) 'Biochemical assays of respiratory chain complex activity', *Methods Cell Biol*, 80, pp. 93-119.

Kirkinezos, I.G. and Moraes, C.T. (2001) 'Reactive oxygen species and mitochondrial diseases', *Semin Cell Dev Biol*, 12(6), pp. 449-57.

Kirkwood, T.B. and Austad, S.N. (2000) 'Why do we age?', *Nature*, 408(6809), pp. 233-8.

Kirkwood, T.B.L. (1977) 'Evolution of ageing', *Nature*, 270(5635), pp. 301-304.

Koch, H., Wittern, K.P. and Bergemann, J. (2001) 'In human keratinocytes the Common Deletion reflects donor variabilities rather than chronologic aging and can be induced by ultraviolet A irradiation', *Journal of Investigative Dermatology*, 117(4), pp. 892-7.

Kosmadaki, M.G. and Gilchrest, B.A. (2004) 'The role of telomeres in skin aging/photoaging', *Micron*, 35(3), pp. 155-9.

Kowaltowski, A.J., de Souza-Pinto, N.C., Castilho, R.F. and Vercesi, A.E. (2009) 'Mitochondria and reactive oxygen species', *Free Radic Biol Med*, 47(4), pp. 333-43.

Koziel, R., Greussing, R., Maier, A.B., Declercq, L. and Jansen-Durr, P. (2011) 'Functional interplay between mitochondrial and proteasome activity in skin aging', *J Invest Dermatol*, 131(3), pp. 594-603.

Kraunsoe, R., Boushel, R., Hansen, C.N., Schjerling, P., Qvortrup, K., Stockel, M., Mikines, K.J. and Dela, F. (2010) 'Mitochondrial respiration in subcutaneous and visceral adipose tissue from patients with morbid obesity', *J Physiol*, 588(Pt 12), pp. 2023-32.

Krishnan, K.J., Greaves, L.C., Reeve, A.K. and Turnbull, D. (2007) 'The ageing mitochondrial genome', *Nucleic Acids Research*, 35(22), pp. 7399-405.

Krishnan, K.J., Harbottle, A. and Birch-Machin, M.A. (2004) 'The use of a 3895 bp mitochondrial DNA deletion as a marker for sunlight exposure in human skin', *J Invest Dermatol*, 123(6), pp. 1020-4.

Krizhanovsky, V., Yon, M., Dickins, R.A., Hearn, S., Simon, J., Miething, C., Yee, H., Zender, L. and Lowe, S.W. (2008) 'Senescence of activated stellate cells limits liver fibrosis', *Cell*, 134(4), pp. 657-67.

Krtolica, A. and Campisi, J. (2002) 'Cancer and aging: a model for the cancer promoting effects of the aging stroma', *Int J Biochem Cell Biol*, 34(11), pp. 1401-14.

Krutmann, J. (2003) '[Skin aging]', *Hautarzt*, 54(9), p. 803.

Ku, H.H. and Sohal, R.S. (1993) 'Comparison of mitochondrial pro-oxidant generation and anti-oxidant defenses between rat and pigeon: possible basis of variation in longevity and metabolic potential', *Mech Ageing Dev*, 72(1), pp. 67-76.

Kujoth, G.C., Hiona, A., Pugh, T.D., Someya, S., Panzer, K., Wohlgemuth, S.E., Hofer, T., Seo, A.Y., Sullivan, R., Jobling, W.A., Morrow, J.D., Van Remmen, H., Sedivy, J.M., Yamasoba, T., Tanokura, M., Weindruch, R., Leeuwenburgh, C. and Prolla, T.A. (2005) 'Mitochondrial DNA mutations, oxidative stress, and apoptosis in mammalian aging', *Science*, 309(5733), pp. 481-4.

Kulms, D. and Schwarz, T. (2000) 'Molecular mechanisms of UV-induced apoptosis', *Photodermatol Photoimmunol Photomed*, 16(5), pp. 195-201.

Kumaran, S., Subathra, M., Balu, M. and Panneerselvam, C. (2004) 'Age-associated decreased activities of mitochondrial electron transport chain

complexes in heart and skeletal muscle: role of L-carnitine', *Chem Biol Interact*, 148(1-2), pp. 11-8.

Kunz, W.S. (2003) 'Different metabolic properties of mitochondrial oxidative phosphorylation in different cell types--important implications for mitochondrial cytopathies', *Exp Physiol*, 88(1), pp. 149-54.

Kwong, J.Q., Henning, M.S., Starkov, A.A. and Manfredi, G. (2007) 'The mitochondrial respiratory chain is a modulator of apoptosis', *Journal of Cell Biology*, 179(6), pp. 1163-77.

Kwong, L.K. and Sohal, R.S. (1998) 'Substrate and site specificity of hydrogen peroxide generation in mouse mitochondria', *Arch Biochem Biophys*, 350(1), pp. 118-26.

Kwong, L.K. and Sohal, R.S. (2000) 'Age-related changes in activities of mitochondrial electron transport complexes in various tissues of the mouse', *Arch Biochem Biophys*, 373(1), pp. 16-22.

Lambert, A.J., Boysen, H.M., Buckingham, J.A., Yang, T., Podlutsky, A., Austad, S.N., Kunz, T.H., Buffenstein, R. and Brand, M.D. (2007) 'Low rates of hydrogen peroxide production by isolated heart mitochondria associate with long maximum lifespan in vertebrate homeotherms', *Aging Cell*, 6(5), pp. 607-618.

Lapointe, J., Wang, Y., Bigras, E. and Hekimi, S. (2012) 'The submitochondrial distribution of ubiquinone affects respiration in long-lived Mclk1+/- mice', *J Cell Biol*, 199(2), pp. 215-24.

Lapuente-Brun, E., Moreno-Loshuertos, R., Acin-Perez, R., Latorre-Pellicer, A., Colas, C., Balsa, E., Perales-Clemente, E., Quiros, P.M., Calvo, E., Rodriguez-Hernandez, M.A., Navas, P., Cruz, R., Carracedo, A., Lopez-Otin, C., Perez-Martos, A., Fernandez-Silva, P., Fernandez-Vizarra, E. and Enriquez, J.A. (2013) 'Supercomplex assembly determines electron flux in the mitochondrial electron transport chain', *Science*, 340(6140), pp. 1567-70.

Lawler, D.F., Larson, B.T., Ballam, J.M., Smith, G.K., Biery, D.N., Evans, R.H., Greeley, E.H., Segre, M., Stowe, H.D. and Kealy, R.D. (2008) 'Diet restriction

and ageing in the dog: major observations over two decades', *Br J Nutr*, 99(4), pp. 793-805.

Lawless, C., Jurk, D., Gillespie, C.S., Shanley, D., Saretzki, G., von Zglinicki, T. and Passos, J.F. (2012) 'A stochastic step model of replicative senescence explains ROS production rate in ageing cell populations', *PLoS One*, 7(2), p. 16.

le Maire, M., Champeil, P. and Moller, J.V. (2000) 'Interaction of membrane proteins and lipids with solubilizing detergents', *Biochim Biophys Acta*, 1508(1-2), pp. 86-111.

Lebel, M., Picard, F., Ferland, G. and Gaudreau, P. (2012) 'Drugs, nutrients, and phytoactive principles improving the health span of rodent models of human age-related diseases', *J Gerontol A Biol Sci Med Sci*, 67(2), pp. 140-51.

Lee, B.Y., Han, J.A., Im, J.S., Morrone, A., Johung, K., Goodwin, E.C., Kleijer, W.J., DiMaio, D. and Hwang, E.S. (2006) 'Senescence-associated beta-galactosidase is lysosomal beta-galactosidase', *Aging Cell*, 5(2), pp. 187-95.

Lee, C.-H., Wu, S.-B., Hong, C.-H., Yu, H.-S. and Wei, Y.-H. (2013) 'Molecular Mechanisms of UV-Induced Apoptosis and Its Effects on Skin Residential Cells: The Implication in UV-Based Phototherapy', *International Journal of Molecular Sciences*, 14(3), pp. 6414-6435.

Lee, P.Y., Costumbrado, J., Hsu, C.Y. and Kim, Y.H. (2012) 'Agarose gel electrophoresis for the separation of DNA fragments', *J Vis Exp*, (62).

Lemarie, A., Huc, L., Pazarentzos, E., Mahul-Mellier, A.L. and Grimm, S. (2011) 'Specific disintegration of complex II succinate:ubiquinone oxidoreductase links pH changes to oxidative stress for apoptosis induction', *Cell Death Differ. 2011 Feb;18(2):338-49. doi: 10.1038/cdd.2010.93. Epub 2010 Aug 13.*

Lemus-Deschamps, L., Galindo, I., Solano, R., Elizalde, A.T., Fonseca, J. and (2002) 'Diagnosis of clear sky ultraviolet radiation for Mexico', *Atmosfera*, 15, pp. 165–171.

Lenaz, G., Baracca, A., Carelli, V., D'Aurelio, M., Sgarbi, G. and Solaini, G. (2004) 'Bioenergetics of mitochondrial diseases associated with mtDNA mutations', *Biochim Biophys Acta*, 1658(1-2), pp. 89-94.

Lenaz, G., Bovina, C., Castelluccio, C., Fato, R., Formiggini, G., Genova, M.L., Marchetti, M., Pich, M.M., Pallotti, F., Parenti Castelli, G. and Biagini, G. (1997) 'Mitochondrial complex I defects in aging', *Mol Cell Biochem*, 174(1-2), pp. 329-33.

Lennikov, A., Kitaichi, N., Kase, S., Noda, K., Horie, Y., Nakai, A., Ohno, S. and Ishida, S. (2013) 'Induction of heat shock protein 70 ameliorates ultraviolet-induced photokeratitis in mice', *Int J Mol Sci*, 14(1), pp. 2175-89.

Lesnefsky, E.J., Gudz, T.I., Moghaddas, S., Migita, C.T., Ikeda-Saito, M., Turkaly, P.J. and Hoppel, C.L. (2001) 'Aging decreases electron transport complex III activity in heart interfibrillar mitochondria by alteration of the cytochrome c binding site', *J Mol Cell Cardiol*, 33(1), pp. 37-47.

Levine, A.J. and Puzio-Kuter, A.M. (2010) 'The control of the metabolic switch in cancers by oncogenes and tumor suppressor genes', *Science*, 330(6009), pp. 1340-4.

Li, F., Gong, Q., Dong, H. and Shi, J. (2012) 'Resveratrol, a neuroprotective supplement for Alzheimer's disease', *Curr Pharm Des*, 18(1), pp. 27-33.

Li, L., Yan, Y., Xu, H., Qu, T. and Wang, B. (2011) 'Selection of reference genes for gene expression studies in ultraviolet B-irradiated human skin fibroblasts using quantitative real-time PCR', *BMC Mol Biol*, 12, p. 8.

Li, Y., Huang, T.T., Carlson, E.J., Melov, S., Ursell, P.C., Olson, J.L., Noble, L.J., Yoshimura, M.P., Berger, C., Chan, P.H., Wallace, D.C. and Epstein, C.J. (1995) 'Dilated cardiomyopathy and neonatal lethality in mutant mice lacking manganese superoxide dismutase', *Nat Genet*, 11(4), pp. 376-81.

Lin, J.Y. and Fisher, D.E. (2007) 'Melanocyte biology and skin pigmentation', *Nature*, 445(7130), pp. 843-50.

Livak, K.J. and Schmittgen, T.D. (2001) 'Analysis of relative gene expression data using real-time quantitative PCR and the 2(-Delta Delta C(T)) Method', *Methods*, 25(4), pp. 402-8.

Lois, N. and Forrester, J.V. (2009) *Fundus Autofluorescence*. 1 edn. Lippincott Williams and Wilkins.

Lopez-Lluch, G., Hunt, N., Jones, B., Zhu, M., Jamieson, H., Hilmer, S., Cascajo, M.V., Allard, J., Ingram, D.K., Navas, P. and de Cabo, R. (2006) 'Calorie restriction induces mitochondrial biogenesis and bioenergetic efficiency', *Proc Natl Acad Sci U S A*, 103(6), pp. 1768-73.

Lowe, C. and Goodman-Lowe, G. (1996) 'Suntanning in hammerhead sharks', *Nature*, 383(6602), p. 677.

Lucas, R., McMichael, T., Smith, W. and Armstrong, B. (2006) *Solar ultraviolet radiation: Global burden of disease from solar ultraviolet radiation*.

Lulevich, V., Yang, H.Y., Isseroff, R.R. and Liu, G.Y. (2010) 'Single cell mechanics of keratinocyte cells', *Ultramicroscopy*, 110(12), pp. 1435-42.

Luo, C., Li, Y., Yang, L., Feng, Z., Long, J. and Liu, J. (2013) 'A cigarette component acrolein induces accelerated senescence in human diploid fibroblast IMR-90 cells', *Biogerontology. 2013 Sep 12.*

Maddodi, N., Jayanthy, A. and Setaluri, V. (2012) 'Shining light on skin pigmentation: the darker and the brighter side of effects of UV radiation', *Photochemistry & Photobiology*, 88(5), pp. 1075-82.

Malyshev, I. (2013) *Immunity, Tumors and Aging: The Role of HSP70*.

Maranzana, E., Barbero, G., Falasca, A.I., Lenaz, G. and Genova, M.L. (2013) 'Mitochondrial respiratory supercomplex association limits production of reactive oxygen species from complex I', *Antioxid Redox Signal*, 19(13), pp. 1469-80.

Marchal, J., Pifferi, F. and Aujard, F. (2013) 'Resveratrol in mammals: effects on aging biomarkers, age-related diseases, and life span', *Ann N Y Acad Sci*, 1290, pp. 67-73.

Marchi, S., Giorgi, C., Suski, J.M., Agnoletto, C., Bononi, A., Bonora, M., De Marchi, E., Missiroli, S., Patergnani, S., Poletti, F., Rimessi, A., Duszynski, J., Wieckowski, M.R. and Pinton, P. (2012) 'Mitochondria-ros crosstalk in the control of cell death and aging', *J Signal Transduct*, 2012, p. 329635.

Martin-Ruiz, C., Saretzki, G., Petrie, J., Ladhoff, J., Jeyapalan, J., Wei, W., Sedivy, J. and von Zglinicki, T. (2004) 'Stochastic variation in telomere

shortening rate causes heterogeneity of human fibroblast replicative life span', *J Biol Chem*, 279(17), pp. 17826-33.

Martinez-Levasseur, L.M., Birch-Machin, M.A., Bowman, A., Gendron, D., Weatherhead, E., Knell, R.J. and Acevedo-Whitehouse, K. (2013) 'Whales use distinct strategies to counteract solar ultraviolet radiation', *Sci Rep*, 3, p. 2386.

Martinez-Levasseur, L.M., Gendron, D., Knell, R.J., O'Toole, E.A., Singh, M. and Acevedo-Whitehouse, K. (2011) 'Acute sun damage and photoprotective responses in whales', *Proceedings of the Royal Society of London - Series B: Biological Sciences*, 278(1711), pp. 1581-6.

Masutomi, K., Possemato, R., Wong, J.M., Currier, J.L., Tothova, Z., Manola, J.B., Ganesan, S., Lansdorp, P.M., Collins, K. and Hahn, W.C. (2005) 'The telomerase reverse transcriptase regulates chromatin state and DNA damage responses', *Proc Natl Acad Sci U S A*, 102(23), pp. 8222-7.

Matsuda, M., Hoshino, T., Yamashita, Y., Tanaka, K., Maji, D., Sato, K., Adachi, H., Sobue, G., Ihn, H., Funasaka, Y. and Mizushima, T. (2010) 'Prevention of UVB radiation-induced epidermal damage by expression of heat shock protein 70', *J Biol Chem*, 285(8), pp. 5848-58.

McCay, C.M., Crowell, M.F. and Maynard, L.A. (1935) 'The Effect of Retarded Growth Upon the Length of Life Span and Upon the Ultimate Body Size: One Figure', *The Journal of Nutrition*, 10(1), pp. 63-79.

Mecocci, P., MacGarvey, U., Kaufman, A.E., Koontz, D., Shoffner, J.M., Wallace, D.C. and Beal, M.F. (1993) 'Oxidative damage to mitochondrial DNA shows marked age-dependent increases in human brain', *Ann Neurol*, 34(4), pp. 609-16.

Meissner, C., Bruse, P., Mohamed, S.A., Schulz, A., Warnk, H., Storm, T. and Oehmichen, M. (2008) 'The 4977 bp deletion of mitochondrial DNA in human skeletal muscle, heart and different areas of the brain: a useful biomarker or more?', *Exp Gerontol*, 43(7), pp. 645-52.

Melov, S., Coskun, P., Patel, M., Tuinstra, R., Cottrell, B., Jun, A.S., Zastawny, T.H., Dizdaroglu, M., Goodman, S.I., Huang, T.T., Miziorko, H., Epstein, C.J.

and Wallace, D.C. (1999) 'Mitochondrial disease in superoxide dismutase 2 mutant mice', *Proc Natl Acad Sci U S A*, 96(3), pp. 846-51.

Menshikova, E.V., Ritov, V.B., Fairfull, L., Ferrell, R.E., Kelley, D.E. and Goodpaster, B.H. (2006) 'Effects of exercise on mitochondrial content and function in aging human skeletal muscle', *J Gerontol A Biol Sci Med Sci*, 61(6), pp. 534-40.

Meyer, J.N. (2010) 'QPCR: a tool for analysis of mitochondrial and nuclear DNA damage in ecotoxicology', *Ecotoxicology*, 19(4), pp. 804-11.

Micallef, M., Lexis, L. and Lewandowski, P. (2007) 'Red wine consumption increases antioxidant status and decreases oxidative stress in the circulation of both young and old humans', *Nutr J*, 6, p. 27.

Michikawa, Y., Mazzucchelli, F., Bresolin, N., Scarlato, G. and Attardi, G. (1999) 'Aging-dependent large accumulation of point mutations in the human mtDNA control region for replication', *Science*, 286(5440), pp. 774-9.

Miller, B.F., Robinson, M.M., Bruss, M.D., Hellerstein, M. and Hamilton, K.L. (2012) 'A comprehensive assessment of mitochondrial protein synthesis and cellular proliferation with age and caloric restriction', *Aging Cell*, 11(1), pp. 150-61.

Miller, R.A., Harrison, D.E., Astle, C.M., Baur, J.A., Boyd, A.R., de Cabo, R., Fernandez, E., Flurkey, K., Javors, M.A., Nelson, J.F., Orihuela, C.J., Pletcher, S., Sharp, Z.D., Sinclair, D., Starnes, J.W., Wilkinson, J.E., Nadon, N.L. and Strong, R. (2011) 'Rapamycin, but not resveratrol or simvastatin, extends life span of genetically heterogeneous mice', *J Gerontol A Biol Sci Med Sci*, 66(2), pp. 191-201.

Miro, O., Alonso, J.R., Jarreta, D., Casademont, J., Urbano-Marquez, A. and Cardellach, F. (1999) 'Smoking disturbs mitochondrial respiratory chain function and enhances lipid peroxidation on human circulating lymphocytes', *Carcinogenesis*, 20(7), pp. 1331-6.

Mishima, K., Handa, J.T., Aotaki-Keen, A., Lutty, G.A., Morse, L.S. and Hjelmeland, L.M. (1999) 'Senescence-associated beta-galactosidase

histochemistry for the primate eye', *Invest Ophthalmol Vis Sci*, 40(7), pp. 1590-3.

Miyamura, Y., Coelho, S.G., Schlenz, K., Batzer, J., Smuda, C., Choi, W., Brenner, M., Passeron, T., Zhang, G., Kolbe, L., Wolber, R. and Hearing, V.J. (2011) 'The deceptive nature of UVA tanning versus the modest protective effects of UVB tanning on human skin', *Pigment Cell Melanoma Res*, 24(1), pp. 136-47.

Miyamura, Y., Coelho, S.G., Wolber, R., Miller, S.A., Wakamatsu, K., Zmudzka, B.Z., Ito, S., Smuda, C., Passeron, T., Choi, W., Batzer, J., Yamaguchi, Y., Beer, J.Z. and Hearing, V.J. (2007) 'Regulation of human skin pigmentation and responses to ultraviolet radiation', *Pigment Cell Research*, 20(1), pp. 2-13.

Moiseeva, O., Bourdeau, V., Roux, A., Deschenes-Simard, X. and Ferbeyre, G. (2009) 'Mitochondrial dysfunction contributes to oncogene-induced senescence', *Mol Cell Biol*, 29(16), pp. 4495-507.

Mondello, C., Bottone, M.G., Noriki, S., Soldani, C., Pellicciari, C. and Scovassi, A.I. (2006) 'Oxidative stress response in telomerase-immortalized fibroblasts from a centenarian', *Ann N Y Acad Sci*, 1091, pp. 94-101.

Montagna, W., Kligman, A.M. and Carlisle, K.S. (1992) *Atlas of Normal Human Skin*. 1 edn. Springer Publishing Company.

Morbey, Y.E., Brassil, C.E. and Hendry, A.P. (2005) 'Rapid senescence in pacific salmon', *Am Nat*, 166(5), pp. 556-68.

Moreno-Sanchez, R., Hernandez-Esquivel, L., Rivero-Segura, N.A., Marin-Hernandez, A., Neuzil, J., Ralph, S.J. and Rodriguez-Enriquez, S. (2013) 'Reactive oxygen species are generated by the respiratory complex II--evidence for lack of contribution of the reverse electron flow in complex I', *Febs j*, 280(3), pp. 927-38.

Morley, A.A. and Trainor, K.J. (2001) 'Lack of an effect of vitamin E on lifespan of mice', *Biogerontology*, 2(2), pp. 109-12.

Morris, J.P., Thatje, S. and Hauton, C. (2013) 'The use of stress-70 proteins in physiology: a re-appraisal', *Mol Ecol*, 22(6), pp. 1494-502.

Morten, K.J., Ackrell, B.A. and Melov, S. (2006) 'Mitochondrial reactive oxygen species in mice lacking superoxide dismutase 2: attenuation via antioxidant treatment', *J Biol Chem*, 281(6), pp. 3354-9.

Mosser, D.D. and Martin, L.H. (1992) 'Induced thermotolerance to apoptosis in a human T lymphocyte cell line', *J Cell Physiol*, 151(3), pp. 561-70.

Mott, J.L., Zhang, D., Stevens, M., Chang, S., Denniger, G. and Zassenhaus, H.P. (2001) 'Oxidative stress is not an obligate mediator of disease provoked by mitochondrial DNA mutations', *Mutat Res*, 474(1-2), pp. 35-45.

Mouton, M. and Botha, A. (2012) *Cutaneous Lesions in Cetaceans: An Indicator of Ecosystem Status?* InTech.

Mraz, M., Malinova, K., Mayer, J. and Pospisilova, S. (2009) 'MicroRNA isolation and stability in stored RNA samples', *Biochemical and Biophysical Research Communications*, 390(1), pp. 1-4.

Muramatsu, T., Tada, H., Kobayashi, N., Yamji, M., Shirai, T. and Ohnishi, T. (1992) 'Induction of the 72-kD heat shock protein in organ-cultured normal human skin', *J Invest Dermatol*, 98(5), pp. 786-90.

Murphy, M.P. (2009) 'How mitochondria produce reactive oxygen species', *Biochem J*, 417(1), pp. 1-13.

Muscari, C., Caldarera, C.M. and Guarnieri, C. (1990) 'Age-dependent production of mitochondrial hydrogen peroxide, lipid peroxides and fluorescent pigments in the rat heart', *Basic Res Cardiol*, 85(2), pp. 172-8.

Nachman, M.W., Hoekstra, H.E. and D'Agostino, S.L. (2003) 'The genetic basis of adaptive melanism in pocket mice', *Proceedings of the National Academy of Sciences of the United States of America*, 100(9), pp. 5268-73.

Nair, K.S. (2005) 'Aging muscle', *Am J Clin Nutr*, 81(5), pp. 953-63.

Nakamura, A.J., Chiang, Y.J., Hathcock, K.S., Horikawa, I., Sedelnikova, O.A., Hodes, R.J. and Bonner, W.M. (2008) 'Both telomeric and non-telomeric DNA damage are determinants of mammalian cellular senescence', *Epigenetics Chromatin*, 1(1), p. 6.

Nakaseko, H., Kobayashi, M., Akita, Y., Tamada, Y. and Matsumoto, Y. (2003) 'Histological changes and involvement of apoptosis after photodynamic therapy for actinic keratoses', *British Journal of Dermatology*, 148(1), pp. 122-127.

Nass, M.M. and Nass, S. (1963) 'INTRAMITOCHONDRIAL FIBERS WITH DNA CHARACTERISTICS. I. FIXATION AND ELECTRON STAINING REACTIONS', *J Cell Biol*, 19, pp. 593-611.

Navarro, A., Gomez, C., Sanchez-Pino, M.-J., Gonzalez, H., Bandez, M.J., Boveris, A.D. and Boveris, A. (2005) 'Vitamin E at high doses improves survival, neurological performance, and brain mitochondrial function in aging male mice', *American Journal of Physiology - Regulatory Integrative & Comparative Physiology*, 289(5), pp. R1392-9.

Naylor, E.C., Watson, R.E.B. and Sherratt, M.J. (2011) 'Molecular aspects of skin ageing', *Maturitas*, 69(3), pp. 249-56.

Naylor, R.M., Baker, D.J. and van Deursen, J.M. (2013) 'Senescent cells: a novel therapeutic target for aging and age-related diseases', *Clin Pharmacol Ther*, 93(1), pp. 105-16.

NCBI (2013) *National Center for Biotechnology Information*. Available at: http://www.ncbi.nlm.nih.gov/ (Accessed: 28.8.13).

Nelson, G., Wordsworth, J., Wang, C., Jurk, D., Lawless, C., Martin-Ruiz, C. and von Zglinicki, T. (2012) 'A senescent cell bystander effect: senescence-induced senescence', *Aging Cell*, 11(2), pp. 345-9.

Newman, P.A. and McKenzie, R. (2011) 'UV impacts avoided by the Montreal Protocol', *Photochemical & Photobiological Sciences*, 10, pp. 1152-60.

Niemitz, E.L., DeBaun, M.R., Fallon, J., Murakami, K., Kugoh, H., Oshimura, M. and Feinberg, A.P. (2004) 'Microdeletion of LIT1 in familial Beckwith-Wiedemann syndrome', *American Journal of Human Genetics*, 75(5), pp. 844-9.

Nishimori, Y., Edwards, C., Pearse, A., Matsumoto, K., Kawai, M. and Marks, R. (2001) 'Degenerative alterations of dermal collagen fiber bundles in photodamaged human skin and UV-irradiated hairless mouse skin: possible

effect on decreasing skin mechanical properties and appearance of wrinkles', *Journal of Investigative Dermatology*, 117(6), pp. 1458-63.

Niu, P., Liu, L., Gong, Z., Tan, H., Wang, F., Yuan, J., Feng, Y., Wei, Q., Tanguay, R.M. and Wu, T. (2006) 'Overexpressed heat shock protein 70 protects cells against DNA damage caused by ultraviolet C in a dose-dependent manner', *Cell Stress Chaperones*, 11(2), pp. 162-9.

Nonaka, Y., Shibata, H., Nakai, M., Kurihara, H., Ishibashi, H., Kiso, Y., Tanaka, T., Yamaguchi, H. and Abe, S. (2006) 'Anti-tumor activities of the antlered form of Ganoderma lucidum in allogeneic and syngeneic tumor-bearing mice', *Biosci Biotechnol Biochem*, 70(9), pp. 2028-34.

Noonan, F.P., Dudek, J., Merlino, G. and De Fabo, E.C. (2003) 'Animal models of melanoma: an HGF/SF transgenic mouse model may facilitate experimental access to UV initiating events', *Pigment Cell Research*, 16, pp. 16-25.

Noppe, G., Dekker, P., de Koning-Treurniet, C., Blom, J., van Heemst, D., Dirks, R.W., Tanke, H.J., Westendorp, R.G. and Maier, A.B. (2009) 'Rapid flow cytometric method for measuring senescence associated beta-galactosidase activity in human fibroblasts', *Cytometry A*, 75(11), pp. 910-6.

Norgen (2010) 'Beta-Gal Staining Kit'. 7.10.13. Available at: http://norgenbiotek.com/product_resources/gal_staining_kit_gal_staining_kit__protocol_37000_1313.pdf.

O'Brien, T.W. (2003) 'Properties of human mitochondrial ribosomes', *IUBMB Life*, 55(9), pp. 505-13.

Ogawa, F., Shimizu, K., Hara, T., Muroi, E., Hasegawa, M., Takehara, K. and Sato, S. (2008) 'Serum levels of heat shock protein 70, a biomarker of cellular stress, are elevated in patients with systemic sclerosis: association with fibrosis and vascular damage', *Clin Exp Rheumatol*, 26(4), pp. 659-62.

Olovnikov, A.M. (1973) 'A theory of marginotomy. The incomplete copying of template margin in enzymic synthesis of polynucleotides and biological significance of the phenomenon', *J Theor Biol*, 41(1), pp. 181-90.

Osborne, T.B., Mendel, L.B. and Ferry, E.L. (1917) 'THE EFFECT OF RETARDATION OF GROWTH UPON THE BREEDING PERIOD AND DURATION OF LIFE OF RATS', *Science*, 45(1160), pp. 294-5.

Ostojic, J., Panozzo, C., Lasserre, J.P., Nouet, C., Courtin, F., Blancard, C., di Rago, J.P. and Dujardin, G. (2013) 'The Energetic State of Mitochondria Modulates Complex III Biogenesis through the ATP-Dependent Activity of Bcs1', *Cell Metab*, 18(4), pp. 567-577.

Paffenbarger, R.S., Jr., Hyde, R.T., Wing, A.L., Lee, I.M., Jung, D.L. and Kampert, J.B. (1993) 'The association of changes in physical-activity level and other lifestyle characteristics with mortality among men', *N Engl J Med*, 328(8), pp. 538-45.

Parihar, M.S. and Brewer, G.J. (2007) 'Simultaneous age-related depolarization of mitochondrial membrane potential and increased mitochondrial reactive oxygen species production correlate with age-related glutamate excitotoxicity in rat hippocampal neurons', *J Neurosci Res*, 85(5), pp. 1018-32.

Park, S.J., Ahmad, F., Philp, A., Baar, K., Williams, T., Luo, H., Ke, H., Rehmann, H., Taussig, R., Brown, A.L., Kim, M.K., Beaven, M.A., Burgin, A.B., Manganiello, V. and Chung, J.H. (2012) 'Resveratrol ameliorates aging-related metabolic phenotypes by inhibiting cAMP phosphodiesterases', *Cell*, 148(3), pp. 421-33.

Passos, J.F., Nelson, G., Wang, C., Richter, T., Simillion, C., Proctor, C.J., Miwa, S., Olijslagers, S., Hallinan, J., Wipat, A., Saretzki, G., Rudolph, K.L., Kirkwood, T.B. and von Zglinicki, T. (2010) 'Feedback between p21 and reactive oxygen production is necessary for cell senescence', *Mol Syst Biol*, 6, p. 347.

Passos, J.F., Saretzki, G., Ahmed, S., Nelson, G., Richter, T., Peters, H., Wappler, I., Birket, M.J., Harold, G., Schaeuble, K., Birch-Machin, M.A., Kirkwood, T.B. and von Zglinicki, T. (2007a) 'Mitochondrial dysfunction accounts for the stochastic heterogeneity in telomere-dependent senescence', *PLoS Biol*, 5(5), p. e110.

Passos, J.F., Saretzki, G. and von Zglinicki, T. (2007b) 'DNA damage in telomeres and mitochondria during cellular senescence: is there a connection?', *Nucleic Acids Res*, 35(22), pp. 7505-13.

Passos, J.F. and von Zglinicki, T. (2007) 'Methods for cell sorting of young and senescent cells', *Methods Mol Biol. 2007;371:33-44.*

Passos, J.F. and Zglinicki, T. (2012) 'Mitochondrial dysfunction and cell senescence--skin deep into mammalian aging', *Aging (Albany NY)*, 4(2), pp. 74-5.

Paz, M.L., Gonzalez Maglio, D.H., Weill, F.S., Bustamante, J. and Leoni, J. (2008) 'Mitochondrial dysfunction and cellular stress progression after ultraviolet B irradiation in human keratinocytes', *Photodermatology, Photoimmunology & Photomedicine*, 24(3), pp. 115-22.

Pearl, R. (1928) *The rate of living*. University of London Press.

Pearson, K.J., Baur, J.A., Lewis, K.N., Peshkin, L., Price, N.L., Labinskyy, N., Swindell, W.R., Kamara, D., Minor, R.K., Perez, E., Jamieson, H.A., Zhang, Y., Dunn, S.R., Sharma, K., Pleshko, N., Woollett, L.A., Csiszar, A., Ikeno, Y., Le Couteur, D., Elliott, P.J., Becker, K.G., Navas, P., Ingram, D.K., Wolf, N.S., Ungvari, Z., Sinclair, D.A. and de Cabo, R. (2008) 'Resveratrol delays age-related deterioration and mimics transcriptional aspects of dietary restriction without extending life span', *Cell Metab*, 8(2), pp. 157-68.

Perez, V.I., Van Remmen, H., Bokov, A., Epstein, C.J., Vijg, J. and Richardson, A. (2009) 'The overexpression of major antioxidant enzymes does not extend the lifespan of mice', *Aging Cell*, 8(1), pp. 73-5.

Petersen, K.F., Befroy, D., Dufour, S., Dziura, J., Ariyan, C., Rothman, D.L., DiPietro, L., Cline, G.W. and Shulman, G.I. (2003) 'Mitochondrial dysfunction in the elderly: possible role in insulin resistance', *Science*, 300(5622), pp. 1140-2.

Pfeiffer, M., Kayzer, E.B., Yang, X., Abramson, E., Kenaston, M.A., Lago, C.U., Lo, H.H., Sedensky, M.M., Lunceford, A., Clarke, C.F., Wu, S.J., McLeod, C., Finkel, T., Morgan, P.G. and Mills, E.M. (2011) 'Caenorhabditis elegans UCP4

protein controls complex II-mediated oxidative phosphorylation through succinate transport', *J Biol Chem*, 286(43), pp. 37712-20.

Pinney, D.O., Stephens, D.F. and Pope, L.S. (1972) 'Lifetime effects of winter supplemental feed level and age at first parturition on range beef cows', *J Anim Sci*, 34(6), pp. 1067-74.

Purschke, M., Laubach, H.J., Anderson, R.R. and Manstein, D. (2010) 'Thermal injury causes DNA damage and lethality in unheated surrounding cells: active thermal bystander effect', *J Invest Dermatol*, 130(1), pp. 86-92.

Purves, W.K., Orians, G.H. and Heller, H.C. (1994) *Life: The Science of Biology* 4th edn. Sinauer Associates Inc

Quan, T., He, T., Shao, Y., Lin, L., Kang, S., Voorhees, J.J. and Fisher, G.J. (2006) 'Elevated cysteine-rich 61 mediates aberrant collagen homeostasis in chronologically aged and photoaged human skin', *American Journal of Pathology*, 169(2), pp. 482-90.

Quinlan, C.L., Orr, A.L., Perevoshchikova, I.V., Treberg, J.R., Ackrell, B.A. and Brand, M.D. (2012) 'Mitochondrial complex II can generate reactive oxygen species at high rates in both the forward and reverse reactions', *J Biol Chem. 2012 Aug 3;287(32):27255-64. doi: 10.1074/jbc.M112.374629. Epub 2012 Jun 11.*

Ran, R., Lu, A., Zhang, L., Tang, Y., Zhu, H., Xu, H., Feng, Y., Han, C., Zhou, G., Rigby, A.C. and Sharp, F.R. (2004) 'Hsp70 promotes TNF-mediated apoptosis by binding IKK gamma and impairing NF-kappa B survival signaling', *Genes Dev*, 18(12), pp. 1466-81.

Rass, K. and Reichrath, J. (2008) *Sunlight, Vitamin D and Skin Cancer*

Ray, A.J., Turner, R., Nikaido, O., Rees, J.L. and Birch-Machin, M.A. (2000) 'The spectrum of mitochondrial DNA deletions is a ubiquitous marker of ultraviolet radiation exposure in human skin', *Journal of Investigative Dermatology*, 115(4), pp. 674-9.

Rebbaa, A., Zheng, X., Chu, F. and Mirkin, B.L. (2006) 'The role of histone acetylation versus DNA damage in drug-induced senescence and apoptosis', *Cell Death Differ*, 13(11), pp. 1960-7.

Redout, E.M., Wagner, M.J., Zuidwijk, M.J., Boer, C., Musters, R.J., van Hardeveld, C., Paulus, W.J. and Simonides, W.S. (2007) 'Right-ventricular failure is associated with increased mitochondrial complex II activity and production of reactive oxygen species', *Cardiovasc Res*, 75(4), pp. 770-81.

Rees, J.L. (2004) 'The genetics of sun sensitivity in humans', *American Journal of Human Genetics*, 75(5), pp. 739-51.

Reimann, V., Kramer, U., Sugiri, D., Schroeder, P., Hoffmann, B., Medve-Koenigs, K., Jockel, K.-H., Ranft, U. and Krutmann, J. (2007) 'Sunbed Use Induces the Photoaging-Associated Mitochondrial Common Deletion', *J Invest Dermatol*, 128(5), pp. 1294-1297.

Rhein, V., Baysang, G., Rao, S., Meier, F., Bonert, A., Muller-Spahn, F. and Eckert, A. (2009) 'Amyloid-beta leads to impaired cellular respiration, energy production and mitochondrial electron chain complex activities in human neuroblastoma cells', *Cell Mol Neurobiol*, 29(6-7), pp. 1063-71.

Richter, C., Park, J.W. and Ames, B.N. (1988) 'Normal oxidative damage to mitochondrial and nuclear DNA is extensive', *Proc Natl Acad Sci U S A*, 85(17), pp. 6465-7.

Rodier, F. and Campisi, J. (2011) 'Four faces of cellular senescence', *J Cell Biol*, 192(4), pp. 547-56.

Rodier, F., Kim, S.H., Nijjar, T., Yaswen, P. and Campisi, J. (2005) 'Cancer and aging: the importance of telomeres in genome maintenance', *Int J Biochem Cell Biol*, 37(5), pp. 977-90.

Rodley, C.D., Grand, R.S., Gehlen, L.R., Greyling, G., Jones, M.B. and O'Sullivan, J.M. (2012) 'Mitochondrial-nuclear DNA interactions contribute to the regulation of nuclear transcript levels as part of the inter-organelle communication system', *PLoS One*, 7(1), p. e30943.

Ronquist, G., Andersson, A., Bendsoe, N. and Falck, B. (2003) 'Human epidermal energy metabolism is functionally anaerobic', *Exp Dermatol*, 12(5), pp. 572-9.

Rooyackers, O.E., Adey, D.B., Ades, P.A. and Nair, K.S. (1996) 'Effect of age on in vivo rates of mitochondrial protein synthesis in human skeletal muscle', *Proc Natl Acad Sci U S A*, 93(26), pp. 15364-9.

Rossi, D.J., Jamieson, C.H. and Weissman, I.L. (2008) 'Stems cells and the pathways to aging and cancer', *Cell*, 132(4), pp. 681-96.

Rossignol, R., Faustin, B., Rocher, C., Malgat, M., Mazat, J.-P. and Letellier, T. (2003) 'Mitochondrial threshold effects', *Biochemical Journal*, 370(Pt 3), pp. 751-62.

Rouault, T.A. (2012) 'Biogenesis of iron-sulfur clusters in mammalian cells: new insights and relevance to human disease', *Dis Model Mech*, 5(2), pp. 155-64.

Royal Geographical Society (2013) *Spearman's Rank Correlation Coefficient – Excel Guide*. Available at: http://www.rgs.org/NR/rdonlyres/4844E3AB-B36D-4B14-8A20-3A3C28FAC087/0/OASpearmansRankExcelGuidePDF.pdf (Accessed: 10.9.13).

Rozen, S. and Skaletsky, H. (2000) 'Primer3 on the WWW for general users and for biologist programmers', *Methods in Molecular Biology*, 132, pp. 365-86.

Rufini, A., Tucci, P., Celardo, I. and Melino, G. (2013) 'Senescence and aging: the critical roles of p53', *Oncogene*.

Sachdeva, S. (2009) 'Fitzpatrick skin typing: applications in dermatology', *Indian J Dermatol Venereol Leprol*, 75(1), pp. 93-6.

Sahin, E., Colla, S., Liesa, M., Moslehi, J., Muller, F.L., Guo, M., Cooper, M., Kotton, D., Fabian, A.J., Walkey, C., Maser, R.S., Tonon, G., Foerster, F., Xiong, R., Wang, Y.A., Shukla, S.A., Jaskelioff, M., Martin, E.S., Heffernan, T.P., Protopopov, A., Ivanova, E., Mahoney, J.E., Kost-Alimova, M., Perry, S.R., Bronson, R., Liao, R., Mulligan, R., Shirihai, O.S., Chin, L. and DePinho, R.A. (2011) 'Telomere dysfunction induces metabolic and mitochondrial compromise', *Nature*, 470(7334), pp. 359-65.

Salvi, S.M., Akhtar, S. and Currie, Z. (2006) 'Ageing changes in the eye', *Postgrad Med J*, 82(971), pp. 581-7.

Sandhu, S.K. and Kaur, G. (2003) 'Mitochondrial electron transport chain complexes in aging rat brain and lymphocytes', *Biogerontology*, 4(1), pp. 19-29.

Santos, J.H., Mandavilli, B.S. and Van Houten, B. (2002) 'Measuring oxidative mtDNA damage and repair using quantitative PCR', *Methods in Molecular Biology*, 197, pp. 159-76.

Santos, J.H., Meyer, J.N., Mandavilli, B.S. and Van Houten, B. (2006) 'Quantitative PCR-based measurement of nuclear and mitochondrial DNA damage and repair in mammalian cells', *Methods in Molecular Biology*, 314, pp. 183-99.

Santos, J.H., Meyer, J.N., Skorvaga, M., Annab, L.A. and Van Houten, B. (2004) 'Mitochondrial hTERT exacerbates free-radical-mediated mtDNA damage', *Aging Cell*, 3(6), pp. 399-411.

Sanz, A., Caro, P., Gomez, J. and Barja, G. (2006) 'Testing the vicious cycle theory of mitochondrial ROS production: effects of H2O2 and cumene hydroperoxide treatment on heart mitochondria', *J Bioenerg Biomembr*, 38(2), pp. 121-7.

Saretzki, G. (2009) 'Telomerase, mitochondria and oxidative stress', *Experimental Gerontology*, 44(8), pp. 485-492.

Saretzki, G., Petersen, S., Petersen, I., Kolble, K. and von Zglinicki, T. (2002) 'hTERT gene dosage correlates with telomerase activity in human lung cancer cell lines', *Cancer Lett*, 176(1), pp. 81-91.

Sawada, M. and Carlson, J.C. (1987) 'Changes in superoxide radical and lipid peroxide formation in the brain, heart and liver during the lifetime of the rat', *Mechanisms of Ageing and Development*, 41(1–2), pp. 125-137.

Sawada, M., Sester, U. and Carlson, J.C. (1992) 'Superoxide radical formation and associated biochemical alterations in the plasma membrane of brain, heart, and liver during the lifetime of the rat', *J Cell Biochem*, 48(3), pp. 296-304.

Sayre, R.M., Desrochers, D.L., Wilson, C.J. and Marlowe, E. (1981) 'Skin type, minimal erythema dose (MED), and sunlight acclimatization', *Journal of the American Academy of Dermatology*, 5, pp. 439-443.

Schafer, M., Dutsch, S., auf dem Keller, U., Navid, F., Schwarz, A., Johnson, D.A., Johnson, J.A. and Werner, S. (2010) 'Nrf2 establishes a glutathione-mediated gradient of UVB cytoprotection in the epidermis', *Genes & Development*, 24(10), pp. 1045-58.

Schagger, H. and Pfeiffer, K. (2000) 'Supercomplexes in the respiratory chains of yeast and mammalian mitochondria', *Embo j*, 19(8), pp. 1777-83.

Scheffler, I.E. (2007) *Mitochondria*. 2 edn. Wiley-Liss.

Schneider, C.A., Rasband, W.S. and Eliceiri, K.W. (2012) 'NIH Image to ImageJ: 25 years of image analysis', *Nat Meth*, 9(7), pp. 671-675.

Schock, G. (2012) 'Pyrosequencing in genotyping and epigenetic studies' Qiagen. 7.10.13. Available at: http://cgs.hku.hk/portal/files/GRC/Events/Seminars/2012/20120328/pyrosequencing%20in%20genotyping%20%20epigentic%20studies.pdf.

Schriner, S.E., Linford, N.J., Martin, G.M., Treuting, P., Ogburn, C.E., Emond, M., Coskun, P.E., Ladiges, W., Wolf, N., Van Remmen, H., Wallace, D.C. and Rabinovitch, P.S. (2005) 'Extension of murine life span by overexpression of catalase targeted to mitochondria', *Science*, 308(5730), pp. 1909-11.

Schroeder, P., Gremmel, T., Berneburg, M. and Krutmann, J. (2008) 'Partial depletion of mitochondrial DNA from human skin fibroblasts induces a gene expression profile reminiscent of photoaged skin', *J Invest Dermatol*, 128(9), pp. 2297-303.

Schuch, A.P. and Menck, C.F.M. (2010) 'The genotoxic effects of DNA lesions induced by artificial UV-radiation and sunlight', *Journal of Photochemistry & Photobiology*, B - Biology. 99(3), pp. 111-6.

Searcy, D.G. (2003) 'Metabolic integration during the evolutionary origin of mitochondria', *Cell Research*, 13(4), pp. 229-38.

Seibel, P., Di Nunno, C., Kukat, C., Schafer, I., Del Bo, R., Bordoni, A., Comi, G.P., Schon, A., Capuano, F., Latorre, D. and Villani, G. (2008) 'Cosegregation of novel mitochondrial 16S rRNA gene mutations with the age-associated T414G variant in human cybrids', *Nucleic Acids Res. 2008 Oct;36(18):5872-81. doi: 10.1093/nar/gkn592. Epub 2008 Sep 16.*

Seidlmayer, L., Blatter, L.A. and Dedkova, E.N. (2011) '20 Increased activity of mitochondrial complex II in rabbit heart failure is associated with reactive oxygen species generation and impaired excitation-contraction coupling', *Heart*, 97(24), p. e8.

Selman, C., McLaren, J.S., Mayer, C., Duncan, J.S., Collins, A.R., Duthie, G.G., Redman, P. and Speakman, J.R. (2008) 'Lifelong alpha-tocopherol supplementation increases the median life span of C57BL/6 mice in the cold but has only minor effects on oxidative damage', *Rejuvenation Res*, 11(1), pp. 83-96.

Seo, M.-Y., Chung, S.-Y., Choi, W.-K., Seo, Y.-K., Jung, S.-H., Park, J.-M., Seo, M.-J., Park, J.-K., Kim, J.-W. and Park, C.-S. (2009) 'Anti-aging effect of rice wine in cultured human fibroblasts and keratinocytes', *Journal of Bioscience & Bioengineering*, 107(3), pp. 266-71.

Serrano, M., Lin, A.W., McCurrach, M.E., Beach, D. and Lowe, S.W. (1997) 'Oncogenic ras provokes premature cell senescence associated with accumulation of p53 and p16INK4a', *Cell*, 88(5), pp. 593-602.

Sharma, G.G., Gupta, A., Wang, H., Scherthan, H., Dhar, S., Gandhi, V., Iliakis, G., Shay, J.W., Young, C.S. and Pandita, T.K. (2003) 'hTERT associates with human telomeres and enhances genomic stability and DNA repair', *Oncogene*, 22(1), pp. 131-46.

Shi, Y., Pulliam, D.A., Liu, Y., Hamilton, R.T., Jernigan, A.L., Bhattacharya, A., Sloane, L.B., Qi, W., Chaudhuri, A., Buffenstein, R., Ungvari, Z., Austad, S.N. and Van Remmen, H. (2013) 'Reduced mitochondrial ROS, enhanced antioxidant defense, and distinct age-related changes in oxidative damage in muscles of long-lived Peromyscus leucopus', *Am J Physiol Regul Integr Comp Physiol*, 304(5), pp. R343-55.

Shigenaga, M.K., Hagen, T.M. and Ames, B.N. (1994a) 'Oxidative damage and mitochondrial decay in aging', *Proc Natl Acad Sci U S A*, 91(23), pp. 10771-8.

Shigenaga, M.K., Hagen, T.M. and Ames, B.N. (1994b) 'Oxidative damage and mitochondrial decay in aging', *Proceedings of the National Academy of Sciences of the United States of America*, 91(23), pp. 10771-10778.

Shindo, Y., Witt, E., Han, D., Epstein, W. and Packer, L. (1994) 'Enzymic and non-enzymic antioxidants in epidermis and dermis of human skin', *J Invest Dermatol*, 102(1), pp. 122-4.

Short, K.R., Bigelow, M.L., Kahl, J., Singh, R., Coenen-Schimke, J., Raghavakaimal, S. and Nair, K.S. (2005) 'Decline in skeletal muscle mitochondrial function with aging in humans', *Proc Natl Acad Sci U S A*, 102(15), pp. 5618-23.

Shuman, S. and Glickman, M.S. (2007) 'Bacterial DNA repair by non-homologous end joining', *Nat Rev Microbiol*, 5(11), pp. 852-61.

Siebels, I. and Drose, S. (2013) 'Q-site inhibitor induced ROS production of mitochondrial complex II is attenuated by TCA cycle dicarboxylates', *Biochim Biophys Acta*, 1827(10), pp. 1156-64.

Simon, M.M., Reikerstorfer, A., Schwarz, A., Krone, C., Luger, T.A., Jaattela, M. and Schwarz, T. (1995) 'Heat shock protein 70 overexpression affects the response to ultraviolet light in murine fibroblasts. Evidence for increased cell viability and suppression of cytokine release', *J Clin Invest*, 95(3), pp. 926-33.

Singh, R., Kolvraa, S. and Rattan, S.I. (2007) 'Genetics of human longevity with emphasis on the relevance of HSP70 as candidate genes', *Front Biosci*, 12, pp. 4504-13.

Sinha, R.P. and Hader, D.P. (2002) 'UV-induced DNA damage and repair: a review', *Photochemical & Photobiological Sciences*, 1(4), pp. 225-36.

Slane, B.G., Aykin-Burns, N., Smith, B.J., Kalen, A.L., Goswami, P.C., Domann, F.E. and Spitz, D.R. (2006) 'Mutation of succinate dehydrogenase subunit C results in increased O2.-, oxidative stress, and genomic instability', *Cancer Res. 2006 Aug 1;66(15):7615-20.*

Smeitink, J.A., Loeffen, J.L., Triepels, R.H., Smeets, R.J., Trijbels, J.M. and van den Heuvel, L.P. (1998) 'Nuclear genes of human complex I of the mitochondrial electron transport chain: state of the art', *Hum Mol Genet*, 7(10), pp. 1573-9.

Smith, M.C., Goddard, E.T., Perusina Lanfranca, M. and Davido, D.J. (2013) 'hTERT extends the life of human fibroblasts without compromising type I interferon signaling', *PLoS One. 2013;8(3):e58233. doi: 10.1371/journal.pone.0058233. Epub 2013 Mar 5.*

Sohal, R.S. and Sohal, B.H. (1991) 'Hydrogen peroxide release by mitochondria increases during aging', *Mech Ageing Dev*, 57(2), pp. 187-202.

Solomon, S. (2004) 'The hole truth', *Nature*, 427(6972), pp. 289-91.

Sood, A., Salih, S., Roh, D., Lacharme-Lora, L., Parry, M., Hardiman, B., Keehan, R., Grummer, R., Winterhager, E., Gokhale, P.J., Andrews, P.W., Abbott, C., Forbes, K., Westwood, M., Aplin, J.D., Ingham, E., Papageorgiou, I., Berry, M., Liu, J., Dick, A.D., Garland, R.J., Williams, N., Singh, R., Simon, A.K., Lewis, M., Ham, J., Roger, L., Baird, D.M., Crompton, L.A., Caldwell, M.A., Swalwell, H., Birch-Machin, M., Lopez-Castejon, G., Randall, A., Lin, H., Suleiman, M.S., Evans, W.H., Newson, R. and Case, C.P. (2011) 'Signalling of DNA damage and cytokines across cell barriers exposed to nanoparticles depends on barrier thickness', *Nat Nanotechnol*, 6(12), pp. 824-33.

Speakman, J.R. (2005) 'Body size, energy metabolism and lifespan', *J Exp Biol*, 208(Pt 9), pp. 1717-30.

Spradbrow, P.B., Samuel, J.L., Kelly, W.R. and Wood, A.L. (1987) 'Skin cancer and papillomaviruses in cattle', *Journal of Comparative Pathology*, 97(4), pp. 469-79.

Stefanatos, R. and Sanz, A. (2011) 'Mitochondrial complex I: A central regulator of the aging process', *Cell Cycle*, 10(10), pp. 1528-32.

Steiner, E. (2013) 'How Reishi Combats Aging ', *Life Extension Magazine*.

Stout, G.J., Westdijk, D., Calkhoven, D.M., Pijper, O., Backendorf, C.M., Willemze, R., Mullenders, L.H. and de Gruijl, F.R. (2005) 'Epidermal transit of

replication-arrested, undifferentiated keratinocytes in UV-exposed XPC mice: an alternative to in situ apoptosis', *Proc Natl Acad Sci U S A. 2005 Dec 27;102(52):18980-5. Epub 2005 Dec 19.*

Strong, R., Miller, R.A., Astle, C.M., Baur, J.A., de Cabo, R., Fernandez, E., Guo, W., Javors, M., Kirkland, J.L., Nelson, J.F., Sinclair, D.A., Teter, B., Williams, D., Zaveri, N., Nadon, N.L. and Harrison, D.E. (2013) 'Evaluation of resveratrol, green tea extract, curcumin, oxaloacetic acid, and medium-chain triglyceride oil on life span of genetically heterogeneous mice', *J Gerontol A Biol Sci Med Sci*, 68(1), pp. 6-16.

Swalwell, H., Latimer, J., Haywood, R.M. and Birch-Machin, M.A. (2012) 'Investigating the role of melanin in UVA/UVB- and hydrogen peroxide-induced cellular and mitochondrial ROS production and mitochondrial DNA damage in human melanoma cells', *Free Radical Biology and Medicine*, 52, pp. 626-34.

Tadokoro, T., Kobayashi, N., Zmudzka, B.Z., Ito, S., Wakamatsu, K., Yamaguchi, Y., Korossy, K.S., Miller, S.A., Beer, J.Z. and Hearing, V.J. (2003) 'UV-induced DNA damage and melanin content in human skin differing in racial/ethnic origin', *FASEB Journal*, 17(9), pp. 1177-9.

Takeuchi, S., Zhang, W., Wakamatsu, K., Ito, S., Hearing, V.J., Kraemer, K.H. and Brash, D.E. (2004) 'Melanin acts as a potent UVB photosensitizer to cause an atypical mode of cell death in murine skin', *Proceedings of the National Academy of Sciences of the United States of America*, 101(42), pp. 15076-81.

Tatarkova, Z., Kuka, S., Racay, P., Lehotsky, J., Dobrota, D., Mistuna, D. and Kaplan, P. (2011) 'Effects of aging on activities of mitochondrial electron transport chain complexes and oxidative damage in rat heart', *Physiol Res. 2011;60(2):281-9. Epub 2010 Nov 29.*

Tedetti, M. and Sempere, R. (2006) 'Penetration of ultraviolet radiation in the marine environment. A review', *Photochemistry & Photobiology*, 82(2), pp. 389-97.

Terzibasi, E., Valenzano, D.R. and Cellerino, A. (2007) 'The short-lived fish Nothobranchius furzeri as a new model system for aging studies', *Exp Gerontol*, 42(1-2), pp. 81-9.

Tinker, S.W. (1988) *Whales of the World*. Bess Pr Inc

Tomás-Loba, A., Flores, I., Fernández-Marcos, P.J., Cayuela, M.L., Maraver, A., Tejera, A., Borrás, C., Matheu, A., Klatt, P., Flores, J.M., Viña, J., Serrano, M. and Blasco, M.A. (2008) 'Telomerase Reverse Transcriptase Delays Aging in Cancer-Resistant Mice', *Cell*, 135(4), pp. 609-622.

Tome-Carneiro, J., Larrosa, M., Gonzalez-Sarrias, A., Tomas-Barberan, F.A., Garcia-Conesa, M.T. and Espin, J.C. (2013) 'Resveratrol and clinical trials: the crossroad from in vitro studies to human evidence', *Curr Pharm Des*, 19(34), pp. 6064-93.

Tonkonogi, M., Fernstrom, M., Walsh, B., Ji, L.L., Rooyackers, O., Hammarqvist, F., Wernerman, J. and Sahlin, K. (2003) 'Reduced oxidative power but unchanged antioxidative capacity in skeletal muscle from aged humans', *Pflugers Arch*, 446(2), pp. 261-9.

Tornaletti, S. and Pfeifer, G.P. (1996) 'UV damage and repair mechanisms in mammalian cells', *Bioessays*, 18(3), pp. 221-8.

Treiber, N., Maity, P., Singh, K., Kohn, M., Keist, A.F., Ferchiu, F., Sante, L., Frese, S., Bloch, W., Kreppel, F., Kochanek, S., Sindrilaru, A., Iben, S., Hogel, J., Ohnmacht, M., Claes, L.E., Ignatius, A., Chung, J.H., Lee, M.J., Kamenisch, Y., Berneburg, M., Nikolaus, T., Braunstein, K., Sperfeld, A.D., Ludolph, A.C., Briviba, K., Wlaschek, M., Florin, L., Angel, P. and Scharffetter-Kochanek, K. (2011) 'Accelerated aging phenotype in mice with conditional deficiency for mitochondrial superoxide dismutase in the connective tissue', *Aging Cell*, 10(2), pp. 239-54.

Trifunovic, A., Hansson, A., Wredenberg, A., Rovio, A.T., Dufour, E., Khvorostov, I., Spelbrink, J.N., Wibom, R., Jacobs, H.T. and Larsson, N.-G. (2005) 'Somatic mtDNA mutations cause aging phenotypes without affecting reactive oxygen species production', *Proceedings of the National Academy of Sciences of the United States of America*, 102(50), pp. 17993-8.

Trounce, I., Byrne, E. and Marzuki, S. (1989) 'Decline in skeletal muscle mitochondrial respiratory chain function: possible factor in ageing', *Lancet*, 1(8639), pp. 637-9.

Tsuda, M., Sugiura, T., Ishii, T., Ishii, N. and Aigaki, T. (2007) 'A mev-1-like dominant-negative SdhC increases oxidative stress and reduces lifespan in Drosophila', *Biochem Biophys Res Commun. 2007 Nov 16;363(2):342-6. Epub 2007 Sep 5.*

Tulah, A.S. and Birch-Machin, M.A. (2013) 'Stressed out mitochondria: the role of mitochondria in ageing and cancer focussing on strategies and opportunities in human skin', *Mitochondrion*, 13(5), pp. 444-53.

Turrens, J.F., Alexandre, A. and Lehninger, A.L. (1985) 'Ubisemiquinone is the electron donor for superoxide formation by complex III of heart mitochondria', *Arch Biochem Biophys*, 237(2), pp. 408-14.

Twig, G., Elorza, A., Molina, A.J., Mohamed, H., Wikstrom, J.D., Walzer, G., Stiles, L., Haigh, S.E., Katz, S., Las, G., Alroy, J., Wu, M., Py, B.F., Yuan, J., Deeney, J.T., Corkey, B.E. and Shirihai, O.S. (2008) 'Fission and selective fusion govern mitochondrial segregation and elimination by autophagy', *Embo j*, 27(2), pp. 433-46.

Ulrich, M., Ruter, C., Astner, S., Sterry, W., Lange-Asschenfeldt, B., Stockfleth, E. and Rowert-Huber, J. (2009) 'Comparison of UV-induced skin changes in sun-exposed vs. sun-protected skin- preliminary evaluation by reflectance confocal microscopy', *British Journal of Dermatology*, 161 Suppl 3, pp. 46-53.

Vage, D.I., Lu, D., Klungland, H., Lien, S., Adalsteinsson, S. and Cone, R.D. (1997) 'A non-epistatic interaction of agouti and extension in the fox, Vulpes vulpes', *Nature Genetics*, 15(3), pp. 311-5.

Vander Heiden, M.G., Cantley, L.C. and Thompson, C.B. (2009) 'Understanding the Warburg effect: the metabolic requirements of cell proliferation', *Science*, 324(5930), pp. 1029-33.

Velarde, M.C., Flynn, J.M., Day, N.U., Melov, S. and Campisi, J. (2012) 'Mitochondrial oxidative stress caused by Sod2 deficiency promotes cellular senescence and aging phenotypes in the skin', *Aging (Albany NY). 2012 Jan;4(1):3-12.*

Verge, B., Alonso, Y., Valero, J., Miralles, C., Vilella, E. and Martorell, L. (2011) 'Mitochondrial DNA (mtDNA) and schizophrenia', *Eur Psychiatry*, 26(1), pp. 45-56.

Viiri, J., Amadio, M., Marchesi, N., Hyttinen, J.M., Kivinen, N., Sironen, R., Rilla, K., Akhtar, S., Provenzani, A., D'Agostino, V.G., Govoni, S., Pascale, A., Agostini, H., Petrovski, G., Salminen, A. and Kaarniranta, K. (2013) 'Autophagy activation clears ELAVL1/HuR-mediated accumulation of SQSTM1/p62 during proteasomal inhibition in human retinal pigment epithelial cells', *PLoS One*, 8(7), p. e69563.

Voss, M.W., Nagamatsu, L.S., Liu-Ambrose, T. and Kramer, A.F. (2011) 'Exercise, brain, and cognition across the life span', *J Appl Physiol (1985)*, 111(5), pp. 1505-13.

Walker, D.W., Hajek, P., Muffat, J., Knoepfle, D., Cornelison, S., Attardi, G. and Benzer, S. (2006) 'Hypersensitivity to oxygen and shortened lifespan in a Drosophila mitochondrial complex II mutant', *Proc Natl Acad Sci U S A*, 103(44), pp. 16382-7.

Wallace, D.C. (1992) 'Mitochondrial genetics: a paradigm for aging and degenerative diseases?', *Science*, 256(5057), pp. 628-32.

Wallace, D.C. (1999) 'Mitochondrial diseases in man and mouse', *Science*, 283(5407), pp. 1482-8.

Wallace, D.C. (2010) 'Mitochondrial DNA mutations in disease and aging', *Environ Mol Mutagen*, 51(5), pp. 440-50.

Waterhouse, N.J. (2003) 'The cellular energy crisis: mitochondria and cell death', *Medicine & Science in Sports & Exercise*, 35(1), pp. 105-10.

Watson, J.D. (1972) 'Origin of concatemeric T7 DNA', *Nat New Biol*, 239(94), pp. 197-201.

Weber, T.P. and Piersma, T. (1996) 'Basal Metabolic Rate and the Mass of Tissues Differing in Metabolic Scope: Migration-Related Covariation between Individual Knots Calidris canutus', *Journal of Avian Biology*, 27(3), pp. 215-224.

Weismann, A. (1882) *Ueber die Dauer des Lebens; Ein Vortrag*. Jena : G. Fischer

Whitaker-Menezes, D., Martinez-Outschoorn, U.E., Flomenberg, N., Birbe, R.C., Witkiewicz, A.K., Howell, A., Pavlides, S., Tsirigos, A., Ertel, A., Pestell, R.G., Broda, P., Minetti, C., Lisanti, M.P. and Sotgia, F. (2011) 'Hyperactivation of oxidative mitochondrial metabolism in epithelial cancer cells in situ: visualizing the therapeutic effects of metformin in tumor tissue', *Cell Cycle*, 10(23), pp. 4047-64.

Whitehead, H. (2003) *Sperm whales: social evolution in the ocean*. University Of Chicago Press.

Wiegand, G. and Remington, S.J. (1986) 'Citrate synthase: structure, control, and mechanism', *Annu Rev Biophys Biophys Chem*, 15, pp. 97-117.

Willcox, B.J., Willcox, D.C., Todoriki, H., Fujiyoshi, A., Yano, K., He, Q., Curb, J.D. and Suzuki, M. (2007) 'Caloric restriction, the traditional Okinawan diet, and healthy aging: the diet of the world's longest-lived people and its potential impact on morbidity and life span', *Ann N Y Acad Sci*, 1114, pp. 434-55.

Williams, G.C. (1957) 'Pleiotropy, Natural Selection, and the Evolution of Senescence', *Evolution*, 11(4), pp. 398-411.

Williams, K., Irwin, D.A., Jones, D.G. and Murphy, K.M. (2010) 'Dramatic Loss of Ube3A Expression during Aging of the Mammalian Cortex', *Front Aging Neurosci*, 2, p. 18.

Wilson, A., Shehadeh, L.A., Yu, H. and Webster, K.A. (2010) 'Age-related molecular genetic changes of murine bone marrow mesenchymal stem cells', *BMC Genomics. 2010 Apr 7;11:229. doi: 10.1186/1471-2164-11-229.*

WMO-UNEP (2011) *Scientific Assessment of Ozone Depletion: 2010*. Geneva, Switzerland.

Wojtovich, A.P., Smith, C.O., Haynes, C.M., Nehrke, K.W. and Brookes, P.S. (2013) 'Physiological consequences of complex II inhibition for aging, disease, and the mKATP channel', *Biochim Biophys Acta. 2013 May;1827(5):598-611. doi: 10.1016/j.bbabio.2012.12.007. Epub 2013 Jan 2.*

World Health Organisation, W.H.O. (2006) *Exposure to Artificial UV Radiation and Skin Cancer*.

World Health Organisation, W.H.O. (2011) *What are the public health implications of global ageing?* Available at: http://www.who.int/features/qa/42/en/index.html (Accessed: 2.11.13).

World Health Organisation, W.H.O. (2013) *UV Index*. Available at: http://www.who.int/uv/intersunprogramme/activities/uv_index/en/ (Accessed: 28.8.13).

Wu, J.Q., Kosten, T.R. and Zhang, X.Y. (2013) 'Free radicals, antioxidant defense systems, and schizophrenia', *Prog Neuropsychopharmacol Biol Psychiatry*, 46, pp. 200-6.

Yakes, F.M. and Van Houten, B. (1997) 'Mitochondrial DNA damage is more extensive and persists longer than nuclear DNA damage in human cells following oxidative stress', *Proc Natl Acad Sci U S A*, 94(2), pp. 514-9.

Yamaguchi, Y., Beer, J.Z. and Hearing, V.J. (2008) 'Melanin mediated apoptosis of epidermal cells damaged by ultraviolet radiation: factors influencing the incidence of skin cancer', *Archives of Dermatological Research*, 300 Suppl 1, pp. S43-50.

Yamaguchi, Y., Takahashi, K., Zmudzka, B.Z., Kornhauser, A., Miller, S.A., Tadokoro, T., Berens, W., Beer, J.Z. and Hearing, V.J. (2006) 'Human skin responses to UV radiation: pigment in the upper epidermis protects against DNA damage in the lower epidermis and facilitates apoptosis', *FASEB Journal*, 20(9), pp. 1486-8.

Yang, J.H., Lee, H.C. and Wei, Y.H. (1995) 'Photoageing-associated mitochondrial DNA length mutations in human skin', *Arch Dermatol Res*, 287(7), pp. 641-8.

Yen, M.Y., Lee, H.C., Liu, J.H. and Wei, Y.H. (1996) 'Compensatory elevation of complex II activity in Leber's hereditary optic neuropathy', *Br J Ophthalmol*, 80(1), pp. 78-81.

Yoon, Y.S., Byun, H.O., Cho, H., Kim, B.K. and Yoon, G. (2003) 'Complex II defect via down-regulation of iron-sulfur subunit induces mitochondrial dysfunction and cell cycle delay in iron chelation-induced senescence-associated growth arrest', *J Biol Chem*, 278(51), pp. 51577-86.

Yoon, Y.S., Cho, H., Lee, J.H. and Yoon, G. (2004) 'Mitochondrial dysfunction via disruption of complex II activity during iron chelation-induced senescence-like growth arrest of Chang cells', *Ann N Y Acad Sci*, 1011, pp. 123-32.

Yoon, Y.S., Lee, J.H., Hwang, S.C., Choi, K.S. and Yoon, G. (2005) 'TGF beta1 induces prolonged mitochondrial ROS generation through decreased complex IV activity with senescent arrest in Mv1Lu cells', *Oncogene. 2005 Mar 10;24(11):1895-903.*

Youle, R.J. and van der Bliek, A.M. (2012) 'Mitochondrial fission, fusion, and stress', *Science*, 337(6098), pp. 1062-5.

Zdanov, S., Remacle, J. and Toussaint, O. (2006) 'Establishment of H2O2-induced premature senescence in human fibroblasts concomitant with increased cellular production of H2O2', *Ann N Y Acad Sci*, 1067, pp. 210-6.

Zhang, J., Block, E.R. and Patel, J.M. (2002) 'Down-regulation of mitochondrial cytochrome c oxidase in senescent porcine pulmonary artery endothelial cells', *Mech Ageing Dev*, 123(10), pp. 1363-74.

Zhang, Y., Ikeno, Y., Qi, W., Chaudhuri, A., Li, Y., Bokov, A., Thorpe, S.R., Baynes, J.W., Epstein, C., Richardson, A. and Van Remmen, H. (2009) 'Mice deficient in both Mn superoxide dismutase and glutathione peroxidase-1 have increased oxidative damage and a greater incidence of pathology but no reduction in longevity', *J Gerontol A Biol Sci Med Sci*, 64(12), pp. 1212-20.

Zheng, W. (2012) 'Multiplex Detection of Oxidative Phosphorylation (OXPHOS) as a Mechanistic Indicator for Mitochondrial Health and Toxicity' Millipore, E. Available at: http://www.millipore.com/techpublications/tech1/an1102en00.

Zhou, X., Liu, X., Zhang, X., Zhou, R., He, Y., Li, Q., Wang, Z. and Zhang, H. (2012) 'Non-randomized mtDNA damage after ionizing radiation via charge transport', *Sci. Rep.*, 2.

Zhu, H., Fu, W. and Mattson, M.P. (2000) 'The catalytic subunit of telomerase protects neurons against amyloid beta-peptide-induced apoptosis', *J Neurochem*, 75(1), pp. 117-24.

Appendix

Table 13

Sample	Age	Sex	Race	Anatomical Site
S485F	6	Male	Caucasian	Foreskin
S499F	20	Male	Caucasian	Foreskin
S420F	21	Male	Caucasian	Foreskin
S538F	29	Male	Caucasian	Foreskin
S544F	30	Male	Caucasian	Foreskin
S539F	31	Male	Caucasian	Foreskin
S490F	32	Male	Caucasian	Foreskin
S537F	34	Male	Caucasian	Foreskin
S554F	34	Male	Caucasian	Foreskin
S497F	37	Male	Caucasian	Foreskin
S563F	42	Male	Caucasian	Foreskin
S550F	43	Male	Caucasian	Foreskin
S482F	45	Male	Caucasian	Foreskin
S533F	45	Male	Caucasian	Foreskin
S483F	46	Male	Caucasian	Foreskin
S498F	48	Male	Caucasian	Foreskin
S536F	51	Male	Caucasian	Foreskin
S564F	54	Male	Caucasian	Foreskin
S534F	56	Male	Caucasian	Foreskin
S540F	62	Male	Caucasian	Foreskin
S549F	62	Male	Caucasian	Foreskin
S421F	64	Male	Caucasian	Foreskin
S423F	65	Male	Caucasian	Foreskin
S557F	65	Male	Caucasian	Foreskin
S541F	66	Male	Caucasian	Foreskin
S436F	71	Male	Caucasian	Foreskin
S484F	72	Male	Caucasian	Foreskin

Table 13. Donor information for the human skin fibroblast samples. The names of the skin samples are given, as well as the age, sex, race, and anatomical site of each donor, for the fibroblast cell samples. Unfortunately, information regarding the lifestyle of the individual donors such as smoking, exercise levels, and diet, as well as information regarding disease, was not available.

Table 14

Sample	Age	Sex	Race	Anatomical Site
S614F	18	Male	Caucasian	Foreskin
S615F	18	Male	Caucasian	Foreskin
S591F	19	Male	Caucasian	Foreskin
S547F	20	Male	Caucasian	Foreskin
S601F	22	Male	Caucasian	Foreskin
S617F	24	Male	Caucasian	Foreskin
S689F	26	Male	Caucasian	Foreskin
S702F	26	Male	Caucasian	Foreskin
S537F	34	Male	Caucasian	Foreskin
S583F	39	Male	Caucasian	Foreskin
S607F	40	Male	Caucasian	Foreskin
S528F	44	Male	Caucasian	Foreskin
S593F	44	Male	Caucasian	Foreskin
S496F	46	Male	Caucasian	Foreskin
S536F	51	Male	Caucasian	Foreskin
S552F	51	Male	Caucasian	Foreskin
S683F	53	Male	Caucasian	Foreskin
S534F	56	Male	Caucasian	Foreskin
S535F	58	Male	Caucasian	Foreskin
S602F	61	Male	Caucasian	Foreskin
S549F	62	Male	Caucasian	Foreskin
S599F	63	Male	Caucasian	Foreskin
S557F	65	Male	Caucasian	Foreskin
S624F	77	Male	Caucasian	Foreskin
S597F	79	Male	Caucasian	Foreskin
S531F	80	Male	Caucasian	Foreskin

Table 14. Donor information for the human skin keratinocyte samples. The names of the skin samples, as well as the age, sex, race, and anatomical site of each donor, are given for the keratinocyte cell samples.

Table 15

Cell Name	Cell Type	Disease	Age	Sex	Anatomical Site
HDFn	Fibroblast	Normal	Neonatal	Male	Foreskin
HaCaT	Keratinocyte	Distant periphery of a Melanoma	62 years old	Male	Back
HepG2	Epithelial	Hepatocellular Carcinoma	15 years old	Male	Liver
a549 Parental	Epithelial	Adenocarcinoma	58 years old	Male	Lung
a549 Rho-zero	Epithelial	Adenocarcinoma	58 years old	Male	Lung
MRC5	Fibroblast	Normal	14 weeks gestation	Male	Lung
MRC5/hTERT	Fibroblast	Normal	14 weeks gestation	Male	Lung

Table 15. Details on the cell lines used. The cell type and disease status of each cell line is given, as well as information regarding the age and sex of the donor, and the anatomical site from which the sample was taken. All cell lines were derived from humans.